2015

The biological treatment of wastewater: mathematical models

Asma Olyan M. Alharbi
University of Wollongong

The biological treatment of wastewater: Mathematical Models

Asma Olyan M Alharbi

A thesis presented for the degree of

Doctor of Philosophy

School of Mathematics and Applied Statistics

University of Wollongong

Australia

2015

Supervisors: A/PR Mark Nelson, A/PR Annette Worthy

and A/PR Harvinder Sidhu (UNSW)

Abstract

The activated sludge process is one of the major aerobic processes used in the biological treatment of wastewater. A significant drawback of this process is the production of excess sludge, the disposal of which can account for 50-60% of the running costs of a plant. Thus there is a growing interest in methods that reduce the volume and mass of excess sludge produced as part of biological wastewater treatment processes. In practice a target value is often set for the sludge content inside the bioreactor. If the sludge content is higher than the target value, the process is stopped and the reactor is cleaned. This is undesirable as it increases running costs.

In chapter 2 we investigate a simple model for the activated sludge process in which the influent contains a mixture of soluble and biodegradable particulate substrate. Within the bioreactor the biodegradable particulate substrate is hydrolyzed to form soluble substrate. The soluble organics are used for energy and growth by the biomass. Biomass decay produces soluble substrate in addition to inert material. We use steady-state analysis to investigate how the amount of sludge formed depends upon the residence time and the use of a settling unit. We show that when the steady-state sludge content is plotted as a function of the residence time that there are five generic response diagrams, depending upon the value of the effective recycle parameter. Four of them are desirable because the sludge content is below the target value if the residence time is higher than some critical value that is not 'too large' in practice.

In chapter 3 we investigate how the volume and mass of excess sludge produced by the activated sludge process can be reduced by coupling the bioreactor used in the process to a sludge disintegration unit.

In chapter 4 a seemingly minor modification is made to the model in chapter 2.

Instead of biomass decay producing soluble substrate and inert material it produces slowly biodegradable substrate and non-biodegradable particulates. We use steady-state analysis to investigate how the amount of sludge formed depends upon the residence time and the use of a settling unit. We show that when the steady-state sludge content is plotted as a function of the residence time that there are three generic response diagrams, depending upon the value of the effective recycle parameter. In *particular*, the seemingly minor change has had a pronounced effect on the behavior of the model. Unlike the model investigated in chapter 2 we find that in *practice* excessive sludge formation is inevitable.

In chapter 5 we investigate how increasing the decay rate effected the behavior of models one and two. We find that this is not an effective way to reduce sludge formation.

In the final chapter we summarize the results of the thesis and include recommendations for future research.

Certification

I, Asma Olyan M Alharbi, declare that this thesis, submitted in partial fulfilment of the requirements for the award of Doctor of Philosophy, in the School of Mathematics and Applied Statistics, University of Wollongong, is wholly my own work unless otherwise referenced or acknowledged. The document has not been submitted for qualifications at any other academic institution.

Asma Olyan M Alharbi

2015

Dedications

I lovingly dedicate this thesis to my parents for their endless inspiration and love through all my walks of life.

The most special thanks and gratitude go to my beloved husband for his essential support and continued encouragement.

This work is also dedicated to my princes Ammar and Mohammed and my beautiful princess Sereen who have made me stronger, better and more fulfilled than I could have ever imagined. I love you to the moon and back.

Acknowledgments

In the name of Allah, the Most Gracious, the Most Merciful.

First and foremost, I would like to kneel down in gratitude to Almighty God for giving me the ability to complete this thesis despite all difficulties, as well as guidance in conducting this research study.

As an endeavor of this magnitude is never accomplished individually, I would like to acknowledge many kind people around me who have contributed and supported me complete this important career step.

My sincere acknowledgment, great respect and appreciation go to my supervisor Associate professor Mark Nelson for his countless hours of assistance, guidance and patience during this educational journey. Without his knowledge, advice and unselfish help, I could never finish my doctoral work in University of Wollongong. My gratitude will never be enough to repay him for giving me the opportunity to become one of his student.

I would like to extend my deep thanks to my co-supervisors Associate Professor Annette Worthy and Associate Professor Harvinder Sidhu for their generous support and advice.

I want to express my deepest appreciation to my mother Setah and my father Olyan for their constant prayer and unconditional support.

I also would like to extend my great gratitude and infinite love to my wonderful husband Abdurahim who supported me each step of the way. I sincerely appreciate all of your unfailing support, sacrifices and all love you selflessly give me.

Very special thanks go to my dear children Ammar, Sereen and Mohammed for their understanding and long patience. Your love supported me during the difficult time. My heartfelt appreciation goes to my brothers and sisters who really encourage me throughout my study.

Last but not least, I would like to thank all my friends for their support and encouragement.

Finally, I thank the Ministry of Education in Saudi Arabia for the awarding of a PhD scholarship.

List of Publications

Journal Article

[1] **A.O.M. Alharbi**, M.I. Nelson, A.L. Worthy, and H.S. Sidhu. Sludge formation in the activated sludge process with a sludge disintegration unit. *Australian and New Zealand Industrial and Applied Mathematics Journal*, **55**:348-367, 2014. http://journal.austms.org.au/ojs/index.php/ANZIAMJ/article/view/7803.

Refereed Conference Papers

[1] **A.O.M. Alharbi**, M.I. Nelson, A.L. Worthy, and H.S. Sidhu. Sludge Formation In The Activated Sludge Process: Mathematical Analysis. *In Proceedings of the Australian Chemical Engineering Conference*, 1-7, 2013. http://ro.uow.edu.au/cgi/viewcontent.cgi?article=2657&context=eispapers.

[2] **A.O.M. Alharbi**, M.I. Nelson, A.L. Worthy, and H.S. Sidhu. Sludge Formation In The Activated Sludge Process: Mathematical Analysis. *In Proceedings of the Australian Chemical Engineering Conference*, 2014. http://ro.uow.edu.au/cgi/viewcontent.cgi?article=2657&context=eispapers.

There were five hundred papers presented at this conference. We were one of a handful of presenters invited to submit a paper to a special issue of a journal.

[3] **A.O.M. Alharbi**, M.I. Nelson, A.L. Worthy, and H.S. Sidhu. Analysis of an activated sludge model in which dead biomass is recycled into slowly biodegradable particulate substrate. Submitted to *Asia-Pacific Journal of Chemical Engineering*, 2014.

Table of Contents

The advantages of the activated sludge process include its high quality performance and its ability to remove nitrogen and phosphorus. The disadvantages include its difficulty to operate and frequent failure due to sludge bulking or the loss of nitrifying ability[9, page 5]. In addition, compared to other biological processes that are used in wastewater treatment, the activated sludge process is more expensive to operate because it requires more energy[9, page 5].

The first models for bioreactors were developed in the 1960s [51, 52, 80]. These models assume that there is one limiting substrate, one limiting microorganism and one rate-limiting biochemical reaction. Such models are easy to calibrate and often provide useful insights into process behavior; accordingly they remain widely used. Furthermore, they are often more suitable to use in control schemes than more detailed models. A very recent example of the use of such a model is the development of a simple dynamic model of a submerged membrane bioreactor which uses the traditional one component model [81].

Chung and Neethling [23] extended the basic model in two ways. Firstly, they introduced a slowly biodegradable substrate component which is hydrolysed to produce small soluble organic materials. Secondly, they allowed a fraction of the dead biomass to be recycled back into the soluble substrate pool. They calibrated their model against experimental steady-state data and used it to estimate the fraction of the total volatile suspended solids that was due to biomass. They investigated how this fraction varied as a function of the sludge age.

Larger models have been developed, such as the IWA Activated Sludge models [43, 56, 78]. These models have been extended to model processes in membrane bioreactors [34, 74].

Recent developments in the mathematical modeling of the activated sludge process are reviewed in [42, 67].

A process model was presented in [16] to simulate the dynamic behaviour of a pilot-scale process for the anaerobic two-stage digestion of sewage sludge. This model was

implemented to support experimental investigations into the anaerobic two-stage digestion process. This model is a derivative of the IWA Anaerobic Digestion Model No.1 (ADM1), which has been developed by the IWA task group for mathematical modelling of anaerobic processes [16].

The basic model remains attractive because it is easy to calibrate and apply. It remains widely used to estimate the effluent concentration from the activated sludge process, however it does not model sludge formation. The model of Chung and Neethling includes sludge formation [23]. We use this model as the basis for the work reported in this thesis. In particular we investigate how the amount of sludge formed is affected by the operation of the settling unit.

1.2 Literature review

1.2.1 History: Introducing the Monod model

It is important to have a grounded knowledge of the various mathematical models that have been developed and devised in the field of enzyme kinetics and biological processes for the research presented in this thesis. Population dynamics, an enormous field, can be regarded as a generic name to portray such processes. Hence, the term population dynamics is used frequently throughout this particular chapter.

One of the most basic mathematical models, which replicates population growth by a simple exponential function, is the Malthusian model [13, 57]. This model has limitations in that it does not, for instance, cater for a decrease in nutrients for a given population (and therefore a slow down in population growth). Consequently other models have been derived [11, 13]. In 1838, Verhulst published 'A Note on the Low of Population Growth' which included the logistic, or Verhulst, model in which the growth of a population is constrained [13, 96]. This model was inspired by Quetelet who published 'A Treatise on Man and the Development of his Faculties'. Quetelet suggested that populations do not grow geometrically over a long period

of time because of certain obstacles such as hunger and epidemics [13].

Further model improvements have been developed to suit the requirement of physical population dynamics models (or biological process). One of these model improvements is the Monod model. This model describes the relationships between the microbial growth rate and the concentration of a limiting nutrient or food supply [21, 66, 68]. The Monod model was first investigated and derived by the French biologist Jacques Monod in 1942 [77], who received a Nobel Prize for his work in microbiological processes in 1965 [54]. In 1949 Monod [66] gave a detailed account of the growth of genetically homogeneous bacterial using a quantitative approach by analysing experimental data. He examined the positive phases of growth, rather than including death and mutations or selections of a culture. Through his model Monod brought together a relationship between the concentrations of microbiological organism and the material or substance that the organisms live on [21, 66]. Hence, the Monod model can describe the growth of bacterial cultures.

The specific growth rate for the Monod model is

$$\mu(S) = \frac{\mu_m S}{K_s + S}, \tag{1.1}$$

where μ_m is the maximum specific growth rate, S is the concentration of biodegradable solids (later known as substrate) and K_s (the most difficult constant to obtain from experiments [62]) is the Monod constant or saturation constant. This is the substrate concentration at which the specific growth rate is half the maximum specific growth rate.

The assumption of this model is that the growth rate depends on the amount of available nutrients. This leads to, at least, a coupled system of two differential equations, one for the population of microorganisms and the other for the concentration of nutrients [93]. It is assumed that the reaction mixture is will mixed.

A Monod model for the microbial growth of microorganisms, where microbes and nutrients reside in water or a liquid phase, and where there is only one nutrient is

given by:

$$\frac{d}{dt}(C_i) = T_i(C_M, C_N),$$

where $C_i = M, N$ are the mass concentration of reactant i per unit volume of the liquid phase (M and N are the microbes ("tiny organisms including yeasts, mold and bacteria" [36])), and $T_i, (i = M, N)$ are the total rate at which species i is produced through reactions and sources [93]. The rate of microbial growth is given by the Monod equation [93]:

$$\mu(C_i) = \frac{\mu_m C_i}{K_s + C_i}, \quad i = M, N, \tag{1.2}$$

Assuming that the microbial death rate is proportional to the size of the population the final form of the governing system of differential equations is given by:

$$\frac{dC_M}{dt} = \frac{\mu_m C_N}{K_s + C_N} C_M - k_r C_M, \tag{1.3}$$

$$\frac{dC_N}{dt} = -\frac{1}{Y} \frac{\mu_m C_N}{K_s + C_N} C_M, \tag{1.4}$$

where k_r is the first-order endogenous decay rate and Y is the yield coefficient [93]. The first term on the right hand side of equation (1.3) represents the growth of species C_M upon the nutrients C_N. The second term on the right hand side of equation (1.3) represents the decay of the microorganisms. The first term on the right hand side of equation (1.4) represents the depletion of the nutrients because the microorganisms are eating them.

By far the most widely used approach, the Monod model is versatile and robust enough to be studied in environmental engineering processes by quantitative, numerical and experimental means. It has been used to model activated sludge process for wastewater treatment [3, 18, 23, 29, 39, 71, 72], global warming [90], and air pollution models such as for acid rain [46]. The dynamics between the microorganisms

and the degradable solids in a well-stirred, well-aerated, bioreactor with a membrane reactor were analysed in [71]. There are also detailed works reviewing the hydrolysis and fermentation stages of organic matter entering an anaerobic water treatment plant [29]. Another area of important environmental engineering concern is the pollution of soil through chemicals such as petroleum [79], polynuclear aromatic hydrocarbons [47], lead [14], pesticides [21] radioactive waste [91, 101], and heavy metals [12]. Chemical leaching of pesticides in soil was examined in [21] so as to account and predict the diffusion of poisons into the environment [92].

The basic model was analyzed in [71] for a continuous flow bioreactor and membrane reactor models. Figure (1.2) shows the biochemistry of the biochemical process when substrate (S) is consumed by biomass which produce products (P, not shown) and biomass (X_b). The latter produce unspecified matter (not shown) by death (k_d). Unused substrate, microorganisms, and the product flow out of the reactor.

$$\mathrm{S} \xrightarrow{\mu(S)} X_b \xrightarrow{k_d}$$

Figure 1.2: Schematic diagram of the biochemical process in the basic model.

The Monod model has the same form as the Michaelis-Menten equation [63].

$$\upsilon = \frac{V_{\max}\,[S]}{K_m + [S]},$$

where υ is a reaction rate for the substrate [S], $V_{\max}$ is the maximum rate achieved by the system and the Michaelis constant K_m is the substrate concentration at which the reaction rate is half of $V_{\max}$. However, the Monod equation is considered to be an empirical model whereas Michaelis-Menten equation has been derived theoretically [54, 63].

1.3 Terminology

To allow a discussion on the developments in this area we first introduce some terminology. This is done in the following subsections.

1.3.1 Chemical oxygen demand

Biological oxygen demand (BOD) and chemical oxygen demand (COD) are the mostly widely used parameters for characterizing the organic carbon content in wastewaters. The chemical oxygen demand parameter is perhaps the most widely used. It is defined as the amount of oxygen consumed in the oxidation of organic compounds [49]. Although COD does not differentiate between biodegradable organic and non biodegradable compounds, this is no longer considered a drawback as new experimental techniques now enable the separate experimental identification of these fractions [78, page 21].

1.3.2 Sludge

Sludge is defined as the combination of microorganisms and solid particles which settle in the bottom of the settling unit. It is knowing as activated sludge because the microorganisms entrapped within it break down organic matter into carbon dioxide, water, and other compounds.

1.3.3 The volatile suspended solids

The volatile suspended solids are the solids which are lost if dried sludge is ignited. They represent the solid organic carbon content in the sludge. This parameter is important because it directly gives the amount of active biomass in the sample, whereas the total suspended solids includes inorganic matter and particulates. The volatile suspended solids gives an approximation of carbon content of sludge. High volatile suspended solids means more sludge content. Membrane reactor produce

less sludge than the conventional activated sludge process, however sludge must still be removed to maintain appropriate levels of biomass within the reactor [73]. At high values of the volatile suspended solids the performance of the membrane may deteriorate [20, 53, 100]. This reduction is because of poor oxygenation, which increases aeration cost, and extensive membrane fouling, which requires replacement and a frequent cleaning of the membrane [99].

In this thesis we specify a target value for the volatile suspended solids.

$$\mathrm{VSS_t} = 12000\,\mathrm{mg\,l^{-1}}.$$

This value is a typical target value used in the activated sludge process [102].

1.3.4 Anaerobic vs Aerobic Processes

1.3.4.1 Anaerobic Processes

The anaerobic digestion process is used to treat agricultural, municipal and industrial wastes. It is not only an effective process for environmental depollution but also produces renewable energy in the form of biogas of which the main component is methane [86]. The anaerobic process breaks down biodegradable material by microorganisms in the absence of oxygen [33]. In many wastewater treatment plants anaerobic digestion is used to stabilize large fractions of organic matter entering the plant [29].

The emission of landfill gas into the atmosphere comes from wastewater materials such as wastewater sludge and agriculture and municipal solid wastes. These emissions can be reduced by anaerobic digestion, so as to produce a methane and carbon dioxide rich biogas suitable for energy production; reducing the need to use fossil fuels [29]. As a result anaerobic digestion provides a renewable energy source, making it cost effective [29].

It is acknowledged that animal confinement facilities can move towards energy self

sufficiency and stabilize the large quantities of organic wastes that they produce by employing mixed swine waste digesters which are thought to be among the most economically attractive [27]. The Monod model was used in [48] to describe the anaerobic kinetics of animal wastes (e.g. swine) and dairy wastes products.

1.3.4.2 Phases of Anaerobic Processes

Anaerobic digestion has four key biological and chemical stages:

- Hydrolysis. This breaks down degradable solids to produce smaller soluble molecules [29].
- Acidogenesis. This corresponds to the conversion of easily fermentable sugar to acetic acid [64].
- Acetogenesis. Acetogenic bacteria are capable of the oxidative decomposition of melanoidins [88]. Anaerobic acetogenesis of food waste is a feasible alternative to biogas generation [10].
- Methanogenesis. This is the biological production of methane mediated by the reduction of carbon dioxide and the fermentation of acetate and methylamines [35]. Methanogenesis can be used to describe the decarboxylation of this acid into methane and carbon dioxide [64].

1.3.4.3 Acid Phase Digestion

The anaerobic process consists of bacteria which are either acid or methane formers. The methane formers convert acids into methane. Acid Phase Digestion (APD) is an increase in the destruction of volatile solids and a corresponding increase in the gas production from anaerobic digestion [15]. The acid phase also has hydrolysis and fermentation processes in its overall model [29]. Thus the overall process is that organic solids hydrolysis to give soluble products which ferment to acids.

1.3.4.4 Aerobic Processes

An aerobic process happens when microorganisms breakdown organic contaminants in the presence of oxygen [55, 87].

Aerobic bacteria, called aerobes, degrade many organic contaminants under aerobic conditions, as they have an oxygen based metabolism. Cellular respiration is an example of aerobic digestion that happens when aerobes use oxygen to oxidize substrates such as sugars and fats in order to obtain energy [105]. For example in the cytoplasm of the aerobes, glucose molecules are first broken down into two smaller molecules. Aerobic respiration then takes place when these smaller molecules enter into a mitochondrion that found in large numbers in most cells, it is here that the biochemical processes of respiration and energy production occur.

Recently, the aerobic digestion of activated sludge has been utilized in some wastewater treatment plants as an alternative to the more traditional anaerobic digestion [37, 38]. There are many advantages associated with aerobic digestion such as high efficiency (i.e. a complete depletion of solids, no pungent gases, rapid biodegradability [84]), wide ranging with many applications [68], a lower capital investment [37] and fewer operational problems [37]. In addition, aerobic digestion has impact resistance and strong adaptability [55]. For instance, a short detention time of about 15 days at a temperature of 20 degree centigrade is usually sufficient to produce sludge that can be easily dewatered [37], whereas anaerobic digestion needs a detention time of 22 days at a temperature of 15 to 45 degree centigrade [95].

There are some doubts about using aerobic digestion for primary sludge. It is often stated that the treatment is an expensive alternative, although there is no persuasive economic analysis supporting this statement [37]. In fact aerobic digestion can be a more economical alternative than anaerobic digestion, as shown in a case study of substrate containing primary solids in raw sewage [44] .

The aerobic processes can be used in the follow-up treatment of an anaerobic process. For example in dealing with auto manufacturing wastewater, such a two-step

process removed 81% of the Chemical Oxygen Demand (COD) of the influent [55]. Some examples of aerobic treatment systems are the conventional activated sludge (CAS) and membrane bioreactor (MBR). The CAS process is widely used for treating low strength wastewater (< 1000 mg COD/L) such as in municipal wastewater systems [75].

1.3.4.5 Substrate and Biomass

Degradable solids break down to produce smaller soluble molecules, that is, substrates. Biomass is produced by microbial growth on these substrates. Many studies link substrate degradation with the growth of biomass. An example of this is the hydrolysis and fermentation of substrate and accompanying growth of biomass during the acid phase of anaerobic digestion [29]. The state of a continuous flow bioreactor can be describe in terms of the variables that comprise the microorganism and a growth limiting substrate [71]. A model for the transport of substrate and biomass has been studied in a porous medium, whereby it accounts for the transport, growth and decay of biomass suspended in both water and biofilm phases [94]. In addition, substrate degradation has been investigated under certain operational and environmental parameters [hydraulic retention time (HRT), solids retention time (SRT), pH, and reactor configuration] during the acid-phase digestion of municipal primary sludge [32]. In [32] the pathways of substrate degradation has three stages which are hydrolysis, fermentation and anaerobic degradation. The material and methods used in [32] are: feed source and characteristics, reactor configuration and operation, analytical procedures, effect of hydraulic retention time (HRT) and effect of solids retention time (SRT), effect of pH and product formation.

1.3.5 Experiments

The problem of designing experiments for the Monod model was discussed in [26]. To obtain robust and efficient designs for parameter estimation, uniform designs and maximin optimal designs are considered. In particular standardized maximin D- and E-optimal designs are found and compared with uniform designs which are usually utilised in these microbiological models [26].

Atrazine fat in soil mini-columns was studied in [21]. It was found that first-order degradation models do not describe the fate of atrazine in soil. It was modelled using Monod kinetics, indicating that the growth of an atrazine degrading biomass occurs when atrazine is present [21].

1.4 Variations of the Monod Model

Some limitations of the Monod model are described in [77] where the authors reviewed microbiological processes. There are many offshoots of the Monod model equations (1.3) and (1.4) that have been used to describe limiting conditions of reaction free energy for bacterial respiration in energy-limited environments. One limitation is the deviations of the specific growth rate $\mu(S)$ at low substrate concentration [82] from that predicted by the Monod model. A number of structured models have been presented as alternatives to describe the hyperbolic curve nature of population or microbial growth. However, these models have their own disadvantages. Thus there is no single 'correct' model. There are various types of specific growth models. An example is the Modified Monod model, which expresses the influence of the initial substrate concentration on the growth rate [1, 65],

$$\mu(S) = \frac{\mu_{\max} S}{K_s S_0 + S},$$

where S_0 is the initial substrate concentration.

The Monod model is an increasing fraction of the substrate concentration; the more

substrate available, the quicker the microorganisms grow [72]. Substrate inhibition is common in many processes such as aerobic fermentation processes, the biological treatment of industrial wastewaters and wastes, and when the substrate is toxic to the microorganism.

For systems subject to substrate inhibition the specific growth rate is an increasing function at low values of the substrate concentration and it is a decreasing function at high values of the substrate concentration.

$$\frac{d\mu}{dS} > 0 \quad \text{if} \quad S < S_{\text{cr}}, \tag{1.5}$$

$$\frac{d\mu}{dS} < 0 \quad \text{if} \quad S > S_{\text{cr}}, \tag{1.6}$$

where "S_{cr} is the value of the substrate concentration at which substrate inhibition 'sets in', i.e. the transition point at which the specific growth rate changes from an increasing function of the substrate concentration to a decreasing function of the substrate concentration" [72].

A common modification to the Monod model to represent growth kinetics subject to substrate inhibition is Andrews model [8].

$$\mu(S) = \frac{\mu_m S}{K_s + S + S^2/K_I},$$

where K_I is the inhibition constant.

Substrate inhibition by glucose on biomass and pediocin production in cultures of Pediococcus acidilactici on a residual medium was investigated in [98].

The Tessier model [1, 50], formulates the specific growth rate as,

$$\mu(S) = \mu_{\max}\left(1 - \exp\left[\frac{-S}{K_s}\right]\right).$$

A fundamental analysis of continuous flow bioreactor and membrane reactor models with Tessier kinetics was reported in[70]. Some examples of experimental systems

governed by Tessier kinetics are given in [40, 61, 83, 89, 104].

The Contois model allows the specific growth rate to depend upon the biomass concentration[1, 24],

$$\mu(S, X) = \frac{\mu_{\max} S}{K_X X + S},$$

where K_X is the Contois kinetic constant and X is the biomass concentration. In this model as the biomass increases the specific growth rate decreases, due to an increasing obstruction to substrate uptake. The authors in [2] investigated the performance of a continuous stirred tank bioreactor with a growth rate that is assumed to follow the Contois model.

1.5 Mathematics

A simple model was proposed for the solubilization process during the acid phase of anaerobic digestion, the acid phase has both hydrolysis and fermentation processes occurring in series as shown in Figure 1.3. In the first process degradable particulates (F) are hydrolyzed (k_h) to soluble substrates (S). In the second process the soluble substrates (S) are consumed ($\hat{\mu}S$) to produce acid phase products (P) and biomass (X). The biomass subsequently decay (k_d) to give unspecified matter (U) [29].

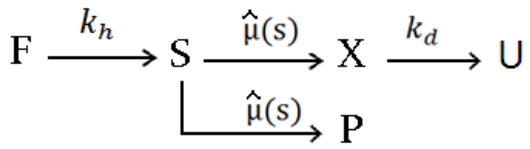

Figure 1.3: Schematic diagram of the acid phase fermentation of particulates [29].

Monod's equation was used to express the bacterial growth rate at constant temperature and pH in the acid phase model.

The parameters of the Monod model for recombinant fermentation have been esti-

mation in [22] using hybrid differential evolution. The model profiles based on the initial concentration of glucose were found to give a satisfactory fit to the experimental observations [22]. The stabilization and robustness of a chemostat model were analysed in [60] via a Lyapunov approach. The author studied a two species chemostat model with one limiting substrate by designing feedback controllers so that an equilibrium with arbitrary prescribed species concentrations becomes globally asymptotically stable. A mathematical model concerning a chemostat with impulsive state feedback control was developed in [41] to investigate the periodicity of bioprocess. The authors estimated the position of the periodic solution of order one and discussed the existence of periodic solution of order two [41]. A mathematical model for immune cell interactions via specific, dose-dependent cytokine production rates of cell populations was developed in [97]. This describes the criteria required for normal and pathological immune system responses and suggests that various stable levels which manifest themselves in different disease phenotypes can be found by alterations in the cytokine production rates.

1.5.1 Applications of the Monod model

The use of the Monod model in applications covers a broad spectrum that includes the activated sludge model for sewage treatment. In [64] the model was tested in batch cultures for the simulation of anaerobic digestion with pea bleaching wastewaters and a synthetic substrate containing sucrose and organic acid. The model satisfactorily represented methane production under very different operational conditions [64].

The Monod equation has been used effectively in many aspects. For instance, a continuous flow bioreactor [71], cascade reactors-in-series [68], simultaneous degradation of chlorophenol mixtures [28] and multi-stage bioreactors [17]. Further, when there are simultaneous limitations of substrates and nutrients, dual or multiple Monod models can be used [54]. In addition, modelling microbiological processes

in petroleum and environmental biotechnologies can use mixed Monod-based and constraint-based approaches [54, 77]. However, the Monod model and its variations do have shortcomings in modelling processes. For instance, dynamic physiological responses to changing environments are not well described by the Monod model [45, 54].

1.6 Summary

In sections 1.2 and 1.3 we described some of the mathematical models that have been developed in the field of enzyme kinetics and bioprocess engineering. The relationships between microbial growth rates and the concentration of a limiting nutrient or food supply are often defined by the Monod model. We described a simple model of enzyme and substrate interaction in section 1.2. We described the commonly used variations of the Monod Model in section 1.4. We described the use of the Monod model on some mathematical model and applications in 1.5.

1.7 Outline of the thesis

The aim of this thesis is to undertake studies of the activated sludge process using the Monod type model as the basic design.
Other than the mathematical analysis of these works, there are a variety of reasons and motivations to undertake studies in bioreactors.

- To better understand the modeling aspects of biological processes.
- To make improvements in gaining knowledge about such processes.
- To obtain an understanding of such processes that can be adapted to other environmental applications.

The main aims of this thesis are to:

- Find the steady-state solutions representing the washout and no-washout branches. The washout branch corresponds to process failure due to removal of all the biomass. The no-washout branch is when biomass is present in the system.
- Determine the stability of the steady-state solutions.
- Investigate how the chemical oxygen demand and the total volatile suspended solids depend upon the residence time and the operation of a settling unit.

In this thesis the model used is an extension of the basic model discussed in section 1.2. In chapter 2 we analyse an extension of the standard model which adds an insoluble substrate and allows for a fraction of dead biomass to be recycled into the pool of insoluble substrate. This allows a more realistic depiction of the biochemical processes than the standard model. It is also the simplest model that can be used to investigate sludge production in the activated sludge process. It has the advantage over the IWA models [43, 56, 78] that it is amenable to mathematical analysis, rather than relying on numerical simulations. In particular we study how the sludge response diagram, which shows the steady-state sludge content as a function of the residence time, changes as the effective recycle parameter, which characterizes the operation of the recycle unit, is varied.

We find the steady-state solutions and determine their stability as a function of process parameters. These are used to calculate the steady-state chemical oxygen demand and the steady-state volatile suspended solids inside the reactor as a function of the residence time. We investigate the circumstances under which it is possible to operate the reactor at, or below, a target value for the volatile suspended solids.

The process begins when the biodegradable particulate substrate (X_s) is hydrolyzed into a soluble substrate (S). The rate at which this happens is given by the hydrolysis rate of insoluble organic compounds (k_h). In the next step the biomass (X_b) feed upon the soluble substrate to produce more biomass. Finally, when the biomass

die they are converted into a mixture of inert material (X_i) and soluble substrate. This model is due to Chung and Neethling [23]. Figure 1.4 gives an overview of the process.

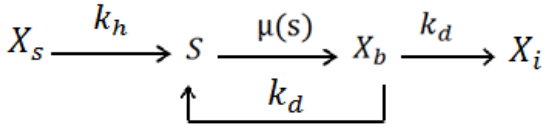

Figure 1.4: Overview of biochemical processes used in chapter 2 (model one).

We extend the process model from chapter 2 in chapter 3 by investigating how a sludge disintegration unit (SDU) can be used to control the amount of sludge within the bioreactor. The flow rate entering the bioreactor is F, we assume that the flow rate going from the bioreactor to the sludge disintegration unit is DF where D is a sludge disintegration factor.

The biochemical processes in the sludge disintegration unit are shown in figure 1.5.

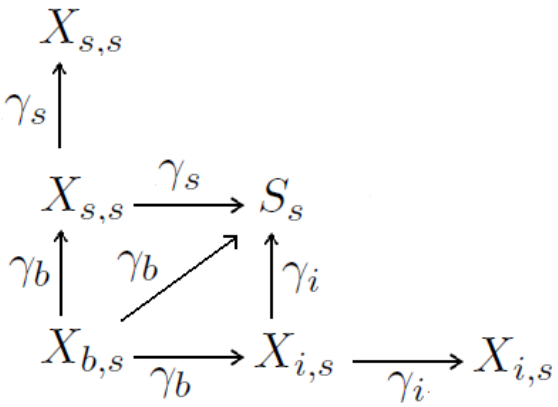

Figure 1.5: Schematic diagram of biochemical processes occurring in a sludge disintegration unit (chapter 3).

There are three biochemical processes. In the first reaction biomass ($X_{b,s}$) is disintegrated into non-biodegradable particulate ($X_{i,s}$), biodegradable particulate substrate ($X_{s,s}$) and soluble substrate (S_s). In the second process the biodegradable particulate substrate ($X_{s,s}$) is disintegrated into soluble substrate (S_s) and biodegradable particulate substrate ($X_{s,s}$). The last process is when the non-biodegradable

particulate ($X_{i,s}$) is disintegrated into the soluble substrate (S_s) and further non-biodegradable particulates ($X_{i,s}$).

In principle we have different values for the three disintegration rates in the sludge disintegration unit. However to simplify we assume that the value of the disintegration rates are the same (γ) for all processes.

We find the steady-state solutions and determine their stability as a function of the residence time. We find that as the value of the disintegration rate (γ) increases the amount of sludge in the bioreactor decreases. Two forms of behaviour are found as the disintegration rate is increased. The transition between the two types is governed by the value of the volatile suspended solids when the residence time is infinity. This value is independent of the disintegration rate (γ).

A very important finding from this chapter is that for a fixed value of the effective recycle parameter (R^*), which governs the behaviour of the settling unit, there is a critical value of the sludge disintegration factor (D). If the sludge disintegration factor is greater than the critical value ($D>D_{\text{cr}}$) then the volatile suspended solids is below the target value ($\text{VSS}^*<\text{VSS}^*_t$) if the residence time is larger than some critical value.

In chapter 4 we change one of the assumptions in the Chung and Neethling model. Namely instead of a fraction of the dead biomass being recycled into the pool of soluble substrate we assume that it is instead recycled into the pool of particulate substrate.

The biochemical process is shown in figure 1.6.

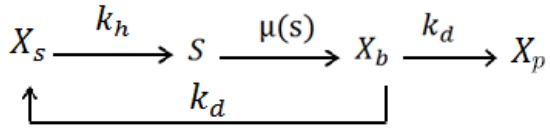

Figure 1.6: Overview of biochemical processes used in chapter 4 (model two).

We find the steady-state solutions and determine their stability as a function of

process parameters. These are used to calculate the steady-state chemical oxygen demand and the steady-state volatile suspended solids as a function of the residence time. We use the steady-state results to investigate the circumstances under which it is possible to operate the reactor at, or below, a target value for the volatile suspended solids. Where appropriate we discuss where the results of these models agree and differ.

If we compare model one in chapter 2 and model two in chapter 4 we find that this small change in the assumptions results in a large change in the behaviour of the reactor. In model one when the biomass produces slowly biodegradable substrate, the volatile suspended solids in practice is below the target value when the effective recycle parameter is smaller than some critical. however, in practice for model two the volatile suspended solids is always above the target value.

In chapter 5 we re-investigate models one and two. We consider what happens if we increase the biomass decay coefficient inside the main reactor. Thus we investigate how changing the value of the biomass decay coefficient (k_d^*) effects both the chemical oxygen demand and the sludge formation within a bioreactor.

We finish in chapter 6 with a conclusion and propose some problems for future work.

Chapter 2

Simple extension of the standard model (model one)

2.1 Introduction

The basic models for the activated sludge process were developed in the 1960s [51, 52, 80]. These models assume that there is one limiting substrate, one limiting microorganism and one rate-limiting biochemical reaction.

In this chapter we analyse a model due to Chung and Neethling [23]. Chung and Neethling [23] extended the basic model in two ways. Firstly, they introduced a slowly biodegradable substrate component which is hydrolysed to produce small soluble organic materials. Secondly, they allowed a fraction of the dead biomass to be recycled back into the soluble substrate pool. They calibrated their model against experimental steady-state data and used it to estimate the fraction of the total volatile suspended solids that was due to biomass. They investigated how this fraction varied as a function of the sludge age. They only investigated their model using numerical methods.

In this chapter we analyse their model in detail. In particular by finding the steady-state solutions of the model we investigate how the 'sludge response diagram', which

shows the steady-state sludge content as a function of the residence time, changes as the effective recycle parameter, which characterizes the operation of the recycle unit, is varied.

We use our steady-state results to establish conditions under which it is *guaranteed* that the steady-state sludge content is *always* higher than a target value. This is very undesirable.

Some of the results from this chapter have been published in a refereed conference proceeding [4].

2.2 Biochemistry

2.2.1 Microbial reactions

In this section the biochemistry of the model is discussed. An overview of the biochemical processes is shown in Figure 2.1. In this figure X_b is the concentration of biomass, X_i is the concentration of non-biodegradable particulate material, X_s is the concentration of biodegradable particulate substrate, S is the concentration of soluble substrate, $\mu(s)$ is the specific growth rate, k_d is the death coefficient, and k_h is the hydrolysis rate of biodegradable particulate substrate (X_s).

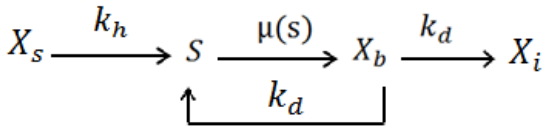

Figure 2.1: Overview of the biochemical processes model one.

Figure 2.1 contains three processes. In the first step biodegradable particulate substrate is made soluble. In the second step biomass feed upon the soluble substrate to produce more biomass. Finally, when the biomass die they are converted into a mixture of inert material (X_i) and soluble substrate (S).

We now describe the three biological processes in the model in more detail.

1. The hydrolysis of biologically degradable particulate organic solids (X_s) to smaller soluble substrate (S).

$$cX_s \xrightarrow{k_h} (c\alpha_h)S, \tag{2.1}$$

where α_h is the yield factor for hydrolysis of insoluble organic compounds. The dimensions of the parameter α_h ($|S||X|^{-1}$) reflect the change from one substance (insoluble substrate) to a second substance (soluble substrate).

2. The soluble organic materials (S) are used as substrates for energy and growth by the biomass (X_b).

$$aS \xrightarrow{\mu(s)} a\alpha_g X_b, \tag{2.2}$$

where α_g is the yield factor for growth of biomass. As above, the dimensions of α_g ($|S||X|^{-1}$) reflect the changes from one substance to another with different units.

3. The decay of biomass, or endogenous respiration, adds to the pool of soluble substrate (S) in addition to producing an inert residue (X_i).

$$bX_b \xrightarrow{k_d} f_i bX_i + f_s \alpha_s bS, \tag{2.3}$$

where f_i is the fraction of dead biomass converted to inert material, f_s is the fraction of dead biomass converted to soluble substrate and α_s is the yield factor for conversion of dead biomass to soluble substrate, which again reflects the possibility that the units of X_b and S differ.

It is assumed that after death the biomass is converted either into inert residue or soluble substrate. Thus the sum of the fraction of inert residue and the

fraction of soluble substrate must be one,

$$f_i + f_s = 1.$$

The sequence of biological reactions (2.2) – (2.3) converts substrate through biomass back to substrate. Mass conservation imposes the restriction that

$$0 < f_s \alpha_g \alpha_s \leq 1.$$

To show that this is true consider an experiment carried out in a batch reactor in which (a) units of substrate is consumed to produce $(a\alpha_g)$ units of biomass (reaction 2, (2.2)). The biomass dies to give $(f_s \alpha_s a \alpha_g)$ units of substrate and $(f_i a \alpha_g)$ units of inert residue (reaction 3, (2.3)). This process is illustrated below.

$$aS \xrightarrow{\mu(s)} a\alpha_g X_b \xrightarrow{k_d} (a\alpha_g) f_s \alpha_s S + (a\alpha_g) f_i X_i.$$

Thus the amount of substrate produced from the consumption of (a) units of substrate is $(a f_s \alpha_g \alpha_s)$ units of substrate. Hence conservation of mass imposes the restriction that

$$f_s \alpha_g \alpha_s \leq 1. \tag{2.4}$$

Inequality (2.4) is true regardless of the units that soluble substrate (S) and the other species (X_j) are measured in. If all components are measured in the same units the following additional inequalities must hold

$$\alpha_g \leq 1,$$

$$f_s \alpha_s \leq 1.$$

This biochemical model was originally proposed by Chung and Neethling [23].

2.2.2 Chemical oxygen demand

In our model the COD of the wastewater is given by

$$\text{COD} = S + \alpha_h X_s,$$

where α_h is a conversion factor that is required because the units of soluble substrate (S) differ from that of biodegradable particulate substrate (X_s).

In this chapter we follow Chung and Neethling [23]. The units of soluble substrate (S) are mg COD l^{-1} and the units of biodegradable particulate substrate (X_s) are mg VSS l^{-1}. It's a non trivial task to convert these units into the chemical oxygen demand.

Note, in this chapter we do not use the chemical oxygen demand because the units of soluble substrate is $|S|$ which is different from the units of biodegradable particulate substrate $|X_s|$.

2.2.3 The volatile suspended solids

In the extended model, reactions (2.1)-(2.3), the volatile suspended solids (VSS) are given by

$$\text{VSS} = X_b + X_i + X_s.$$

The target value (a maximum desirable value) of the volatile suspended solids for the safety of membrane filtration is

$$\text{VSS} = 12000 \text{ mg } \text{l}^{-1} [102].$$

2.3 Equations

In this section we write down the model equations for the concentration of microorganisms, biodegradable particulates, inert material, and soluble substrate within a well-stirred, well-aerated, bioreactor. The assumption that the reactor is well stirred means that the substrate is instantaneously and homogeneously mixed with the reactor contents. The assumption that the reactor is well-aerated means that oxygen is not a rate-limiting substance. We also assume that the flow through the bioreactor is sufficiently fast so that cell growth does not occur on the walls of the reactors, i.e. there is no biofilm on the reactor walls, and that operating conditions such as the pH and temperature are automatically controlled so as to remain constant.
For a reactor employing recycle, we further assume that substrate utilisation only occurs in the reactor, i.e. there is no reaction in either the settling tank or the return line, and that the recycle rate is constant.

2.3.1 The dimensional model

The conservation of mass equations are
The rate of change of soluble substrate

$$V\frac{dS}{dt} = F(S_0 - S) + V\alpha_h k_h X_s + V f_s \alpha_s k_d X_b - \frac{V X_b \mu(S)}{\alpha_g}. \tag{2.5}$$

The rate of change of biomass

$$V\frac{dX_b}{dt} = F(X_{b,0} - X_b) + RF(C-1)X_b + V X_b \mu(S) - V k_d X_b. \tag{2.6}$$

Non-biodegradable particulate material

$$V\frac{dX_i}{dt} = F(X_{i,0} - X_i) + RF(C-1)X_i + V f_i k_d X_b. \tag{2.7}$$

The rate of change of biodegradable particulate substrate.

$$V\frac{dX_s}{dt} = F(X_{s,0} - X_s) + RF(C-1)X_s - Vk_hX_s. \tag{2.8}$$

The specific growth rate is given by

$$\mu(S) = \frac{\mu_m S}{K_s + S}. \tag{2.9}$$

The residence time is defined by

$$\tau = \frac{V}{F}. \tag{2.10}$$

The chemical demand oxygen

$$\text{COD} = S + \alpha_h X_s. \tag{2.11}$$

Total Volatile Suspended Solids (VSS)

$$X_t = X_b + X_i + X_s. \tag{2.12}$$

Note that we have assumed that the settling unit is equally effective at concentrating the biological component (X_b) and the particulates (X_s and X_i). In the following we denote the units of soluble substrate concentration by $|S|$ and the units of biomass, non-biodegradable particulate material and biodegradable particulate substrate concentration by $|X|$.

In these equations C is the recycle concentration factor (–), the value of this factor depends on the settling unit design operation. F is the bioreactor flow rate ($\text{dm}^3\ \text{hr}^{-1}$), K_s is the Monod constant $|S|$, R is the recycle ratio based on volumetric flow rates(–), S is the substrate concentration within the bioreactor $|S|$, S_0 is

the concentration of substrate flowing into the reactor $|S|$, V is the volume of the bioreactor (dm^3), X_b is the concentration of biomass $|X|$, X_i is the concentration of of non-biodegradable particulate material $|X|$, X_s is the concentration of biodegradable particulate substrate $|X|$, $X_{j,0}(j = b, i, s)$ is a feed concentration flowing into the reactor $|X|$, X_t is total volatile suspended solids $|X|$, k_h is the hydrolysis rate of insoluble organic compounds (hr^{-1}), k_d is the death coefficient (hr^{-1}), f_s is the fraction of dead biomass converted to soluble substrate (–), f_i is the fraction of dead biomass converted to inert material (–), t is time (hr^{-1}), α_h is the yield factor for hydrolysis of insoluble organic compounds ($|S||X|^{-1}$), α_g is the yield factor for growth of biomass ($|X||S|^{-1}$), α_s is the yield factor for conversion of dead biomass to soluble substrate ($|S||X|^{-1}$), $\mu(S)$ is the specific growth rate model (hr^{-1}), μ_m is the maximum specific growth rate (hr^{-1}), and τ is the residence time (hr).

Note that we can assume that $C \geq 1$, as otherwise recycle leads to a decrease in performance of the bioreactor. For a specific wastewater, a given biological community, and a particular set of environmental conditions, the parameters K_s, k_d, α_h, α_g, α_s and μ_m are fixed. The parameters that can be varied are S_0, $X_{j,0}(j = b, i, s)$, and τ.

In the standard model [71] the components X_i and X_s are not included and it is further assumed that $f_s = 0$.

Typical parameter values for the model are stated in appendix A.3.

2.3.2 The dimensionless model

By introducing dimensionless variables for concentrations of the substrate [$S^* = S/K_s$], microorganism and particulates [$X_j^* = X_j/(\alpha_g K_s)$] $(j = b, i, s)$ and time [$t^* = \mu_m t$] the dimensional model, equations (2.5)-(2.8), can be written in the dimensionless

form

$$\frac{dS^*}{dt^*} = \frac{1}{\tau^*}(S_0^* - S^*) + \alpha_{g,h} k_h^* X_s^* + f_s \alpha_{g,s} k_d^* X_b^* - \frac{S^* X_b^*}{1+S^*}, \tag{2.13}$$

$$\frac{dX_b^*}{dt^*} = \frac{1}{\tau^*}(X_{b,0}^* - X_b^*) + \frac{R^*}{\tau^*} X_b^* + \frac{X_b^* S^*}{1+S^*} - k_d^* X_b^*, \tag{2.14}$$

$$\frac{dX_i^*}{dt^*} = \frac{1}{\tau^*}(X_{i,0}^* - X_i^*) + \frac{R^*}{\tau^*} X_i^* + f_i k_d^* X_b^*, \tag{2.15}$$

$$\frac{dX_s^*}{dt^*} = \frac{1}{\tau^*}(X_{s,0}^* - X_s^*) + \frac{R^*}{\tau^*} X_s^* - k_h^* X_s^*. \tag{2.16}$$

The chemical oxygen demand COD*

$$\mathrm{COD}^* = S^* + \alpha_{g,h} X_s^*. \tag{2.17}$$

Total Volatile Suspended Solids VSS*

$$\mathrm{VSS}^* = X_b^* + X_i^* + X_s^*. \tag{2.18}$$

The parameter groups are: the effective recycle parameter [$R^* = (C\text{-}1)R$], the dimensionless substrate concentration in the feed [$S_0^* = S_0/K_s$], a dimensionless concentration in the feed [$X_{0,j}^* = X_{j,0}/(\alpha_g K_s)$] ($j = b, i, s$), the dimensionless residence time [$\tau^* = V\mu_m/F$], the dimensionless decay rate [$k_d^* = k_d/\mu_m$], the dimensionless hydrolysis rate of insoluble organic compounds [$k_h^* = k_h/\mu_m$], and two combined yield factors [$\alpha_{g,h} = \alpha_g \alpha_h$] and [$\alpha_{g,s} = \alpha_g \alpha_s$].

The cases $R^* = 0$, $0 < R^* < 1$ and $R^* = 1$ represent a flow reactor without recycle, a flow reactor with non-idealised recycle, and a flow reactor with idealised recycle, respectively [71].

From now on we assume that the growth medium fed into the bioreactor is sterile, i.e. there are no microorganisms in the influent ($X_{b,0} = X_{b,0}^* = 0$). Furthermore, we assume that the concentration of soluble substrate in the feed nonzero ($S_0^* > 0$), and that the concentration of biodegradable particulate substrate ($X_{s,0}^* > 0$). Note that

if the biodegradable particulate substrate is equal to zero, the model reduces to the standard substrate-cellmass model, which has been widely studied [51, 52, 71, 80]. Note that inequality (2.4) becomes

$$0<f_s\alpha_{g,s}\leq 1. \tag{2.19}$$

Note that the target value (a maximum desirable value) for volatile suspended solid becomes

$$\mathrm{VSS}_{\mathrm{t}}^{*}=\frac{\mathrm{VSS}_{\mathrm{t}}}{\alpha_g k_s}=\frac{12000}{\alpha_g k_s}=77.071. \tag{2.20}$$

Typical dimensionless parameter values are stated in appendix B.2 of this chapter.

2.3.3 Model simplification

The model consists of four differential equations (2.13)-(2.16). In this section we show that the model reduces to a planar system.

2.3.3.1 The equation for the biodegradable particulate substrate

We write the initial condition for the variable of the biodegradable particulate substrate (X_s^*) as

$$X_s^*(0)=X_{s,i}^*.$$

Equation (2.16) is a linear first order differential equation. Solving equation (2.16), we have

$$X_s^*=\frac{B}{A}+\left(X_{s,i}^*-\frac{B}{A}\right)e^{-At^*},$$

where the coefficients are

$$A = \frac{1 - R^* + k_h^* \tau^*}{\tau^*},$$
$$B = \frac{X_{s,0}^*}{\tau^*}.$$

In the limit of large time we have

$$X_{s,\infty}^* = \lim_{t^* \to \infty} X_s^* = \frac{B}{A} = \frac{X_{s,0}^*}{1 - R^* + k_h^* \tau^*}. \tag{2.21}$$

Note in the limit of infinite residence time we have $X_{s,\infty}^* = 0$.

We are not interested in the start-up of the reactor, only its long-term operation. Consequently from now on, we replace the variable X_s^* in equation (2.13) by its steady state value and drop equation (2.16) from the model. Expression (2.21) is used latter to calculate the steady state value for the dimensionless volatile suspended solid (VSS*).

2.3.3.2 The equation for the non-biodegradable particulate material

Note that the variable of the non-biodegradable particulate material (X_i^*) does not appear in either equation (2.13) or (2.14) and therefore decouples from the model. We write the initial condition for the variable X_i^* in the form

$$X_i^*(0) = X_{i,i}^*.$$

Equation (2.15) is a linear non-autonomous first order differential equation.

The formal solution of equation (2.15) is given by

$$X_i^* = \frac{E}{D} + F e^{-Dt^*} + G e^{-Dt^*} \int e^{Dt^*} X_b^*(t) dt,$$

where the coefficients are

$$E = \frac{X^*_{i,0}}{\tau^*}, \quad D = \frac{1 - R^*}{\tau^*}, \quad G = f_i k^*_d,$$

and F is an integration constant determined by the initial condition.

In the limit of large time we have

$$X^*_{i,\infty} = \lim_{t^* \to \infty} X^*_i = \frac{X^*_{i,0}}{1 - R^*} + \frac{f_i k^*_d X^*_b \tau^*}{1 - R^*}.$$

The steady state value for the non-biodegradable particulate material ($X^*_{i,\infty}$) is best obtained directly from equation (2.15). This value for the steady-state is used later to calculate the dimensionless volatile suspended solids (VSS*).

2.3.3.3 The planar system

In the limit of large time the system (2.13) – (2.16) reduces to the planar system

$$\frac{dS^*}{dt^*} = \frac{1}{\tau^*}(S^*_0 - S^*) + \alpha_{g,h} k^*_h X^*_{s,\infty} + f_s \alpha_{g,s} k^*_d X^*_b - \frac{S^* X^*_b}{1 + S^*}, \tag{2.22}$$

$$\frac{dX^*_b}{dt^*} = \frac{1}{\tau^*}(R^* - 1)X^*_b + \frac{X^*_b S^*}{1 + S^*} - k^*_d X^*_b, \tag{2.23}$$

$$\text{COD}^* = S^* + \alpha_{g,h} X^*_s, \tag{2.24}$$

$$\text{VSS}^* = \left(1 + \frac{f_i k^*_d \tau^*}{1 - R^*}\right) X^*_b + \frac{X^*_{i,0}}{1 - R^*} + \frac{X^*_{s,0}}{1 - R^* + k^*_h \tau^*}. \tag{2.25}$$

Note that when the two middle terms in the right hand side of equation (2.22) are zero the model simplifies to the standard model considered in [71]. This happens when either $\alpha_s = 0 \quad (\Rightarrow \alpha_{g,s} = 0)$ or $f_s = 0$ and either $k^*_h = 0$ or $\alpha_h = 0 \quad (\Rightarrow \alpha_{g,h} = 0)$.

2.4 Results

In section 2.4.1 we discus some global properties of the solution of the system (2.22)−(2.23). In section 2.4.2 the steady-state solution branches are given and the condition for the no-washout solution branch to be physically meaningful is identified. In section 2.4.3 the stability of the steady state solutions is determined. In section 2.4.4 asymptotic solutions are stated. In section 2.4.5 steady-state diagrams for the case when there is no recycle ($R^* = 0$) are discussed. In section 2.4.6 and 2.4.7 the steady-state results are used to calculate the chemical oxygen demand and the volatile suspended solids respectively when a settling unit is used ($0<R^* \leq 1$).

2.4.1 Global behaviour

In section 2.4.1.1 we show that there is a positively invariant region which is exponentially attracting. Then in section 2.4.1.2 we show that if the dimensionless decay rate is too large ($k_d^* \geq 1$), then the biomass must die out ($\lim_{t^*\to\infty} X_b^*(t^*) = 0$). This bound is slightly improved by using properties of the invariant region established in 2.4.1.1. In section 2.4.1.3 we construct an improved invariant region which leads to an improved bound on the death coefficient (k_d^*) which is valid under certain specified conditions.

2.4.1.1 A positively invariant region

In this section we first show that the variable concentrations (S^* and X_b^*) can not become negative. We then construct a (positively) invariant region which is exponentially attracting for all (physically meaningful) initial conditions. In particular, we show that the region (I^*) bounded by

$$0 \leq S^*,$$

$$0 \leq X_b^*,$$

$$S^* + X_b^* \leq \frac{\hat{S}_0^*}{1 - R^*},$$

is (positively) invariant, where

$$\begin{aligned} \hat{S}_0^* &= S_0^* + \alpha_{g,h} k_h^* X_{s,\infty}^* \tau^*, \\ &= S_0^* + \frac{\alpha_{g,h} k_h^* X_{s,0}^* \tau^*}{1 - R^* + k_h^* \tau^*}. \end{aligned} \tag{2.26}$$

As concentrations have to be positive, it is reasonable to expect that the first two statements are true. In the absence of a settling unit the third statement is reasonable. If we put $R^* = 0$ in the planar model (2.22)-(2.23) then the differential equations "tell us" that if we consume one unit of scaled substrate we then produce one unit of scaled microorganisms. It is now intuitive that the amount of substrate plus the amount of microorganisms leaving the reactor must be less than the amount of substrate flowing into the reactor. (These quantities would be equal if the biomass did not die, i.e. when k_d^*=0).

To show that the substrate concentration is non-negative, consider the value for the derivative $\frac{dS^*}{dt^*}$ when $S^* = 0$. We have

$$\left.\frac{dS^*}{dt^*}\right|_{S^*=0} = \frac{S_0^*}{\tau^*} + \alpha_{g,h} k_h^* X_{s,\infty}^* + f_s \alpha_{g,s} k_d^* X_b^* \quad > 0,$$

as by assumption the biomass concentration is non-negative ($0 \leq X_b^*$) and the feed concentration and residence times are strictly positive. Thus when $S^* = 0$ the derivative is positive. This means that if the soluble substrate concentration is zero then the soluble substrate concentration is increasing, so it can not become negative. The above inequality further shows that the substrate concentration is strictly positive for t^*>0, i.e. it can not be reduced to zero.

We now consider what happens when the biomass concentration is zero. We have

$$\frac{dX_b^*}{dt^*}\Big|_{X_b^*=0} = 0.$$

This shows that the line $X_b^* = 0$ is invariant.

To establish the third inequality we let

$$Z(t^*) = S^*(t^*) + X_b^*(t^*).$$

Then

$$\begin{aligned}
\frac{dZ^*}{dt^*} &= \frac{dS^*}{dt^*} + \frac{dX_b^*}{dt^*}, \\
&= \frac{1}{\tau^*}(S_0^* - S^*) - \frac{(1-R^*)}{\tau^*}X_b^* + \alpha_{g,h}k_h^*X_{s,\infty}^* - (1 - f_s\alpha_{g,s})k_d^*X_b^*, \\
&\leq \frac{1}{\tau^*}S_0^* - \frac{1}{\tau^*}S^* - \frac{(1-R^*)}{\tau^*}X_b^* + \alpha_{g,h}k_h^*X_{s,\infty}^*.
\end{aligned}$$

The last line is true as we have shown that $X_b^* \geq 0$ and by equation (2.19) we have $0 \leq 1 - f_s\alpha_{g,s}$.

We rewrite the last line as

$$\begin{aligned}
\frac{dZ^*}{dt^*} &\leq \frac{S_0^* + \alpha_{g,h}k_h^*X_{s,\infty}^*\tau^*}{\tau^*} - \frac{(1-R^*)}{\tau^*}(S^* + X_b^*) - \frac{R^*S^*}{\tau^*}, \\
&\leq \frac{1}{\tau^*}\hat{S}_0^* - \frac{(1-R^*)}{\tau^*}Z, \quad \text{as we have shown that } S^*{>}0,
\end{aligned}$$

where

$$\begin{aligned}
\hat{S}_0^* &= S_0^* + \alpha_{g,h}k_h^*X_{s,\infty}^*\tau^*, \\
&= S_0^* + \frac{\alpha_{g,h}k_h^*X_{s,0}^*\tau^*}{1 - R^* + k_h^*\tau^*},
\end{aligned}$$

substituting for the steady state value of X_s^* using equation (2.21).

The solution of the differential equation

$$\frac{dZ_1^*}{dt^*} = \frac{1}{\tau^*}\hat{S}_0^* - \frac{(1-R^*)}{\tau^*}(Z_1^*), \quad Z_1^*(0) = S^*(0) + X_b^*(0),$$

is

$$Z_1^*(t^*) = \frac{B}{A} + \left(Z_{1,i}^* - \frac{B}{A}\right) e^{-At^*},$$

where $A = \frac{1-R^*}{\tau^*}$ and $B = \frac{\hat{S}_0^*}{\tau^*}$.

Note that as $\frac{dZ^*}{dt^*} \leq \frac{dZ_1^*}{dt^*}$ and $Z^*(0) \leq Z_1^*(0)$ it follows $Z^*(t^*) \leq Z_1^*(t^*)$. Hence [25]

$$Z(t^*) = S^*(t^*) + X_b^*(t^*) \leq \frac{B}{A} + \left(Z_{1,i}^* - \frac{B}{A}\right) e^{-At^*}. \tag{2.27}$$

By taking the limit as $t^* \to \infty$ we deduce that

$$Z^* \leq \frac{\hat{S}_0^*}{1-R^*}. \tag{2.28}$$

There are two things to notice from inequality (2.27).

Firstly, suppose that the initial condition is inside the invariant region, i.e.

$$0 \leq S^*(0) + X_b^*(0) \leq \frac{\hat{S}_0^*}{1-R^*}.$$

Equation (2.27) immediately implies that

$$Z(t^*) = X_b^*(t^*) + S^*(t^*) \leq \frac{\hat{S}_0^*}{1-R^*},$$

i.e. the solution remains in the invariant region.

Secondly, suppose that the initial condition is outside the invariant region, i.e.

$$S^*(0) + X_b^*(0) > \frac{\hat{S}_0^*}{1 - R^*}.$$

Then (2.27) implies that in the limit that $t^* \to \infty$ we have

$$Z(t^*) = X_b^*(t^*) + S^*(t^*) \leq \frac{\hat{S}_0^*}{1 - R^*},$$

i.e. the solution has entered the invariant region.

For $0 \leq R^* \leq 1$ the invariant region is shown in figure 2.2.

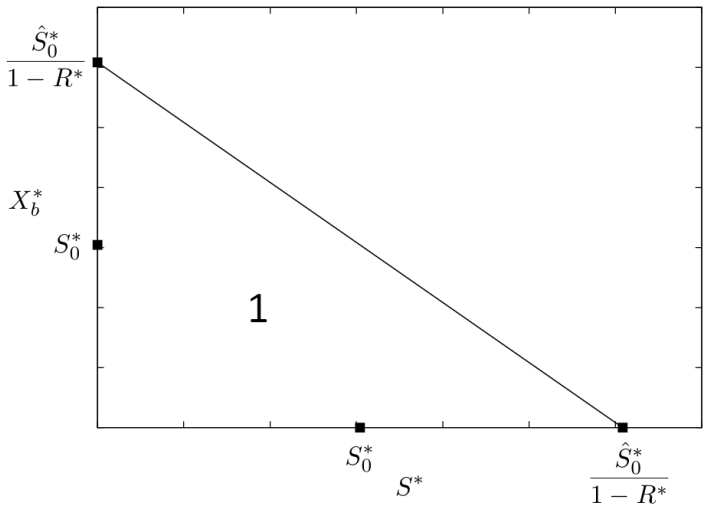

Figure 2.2: The invariant region I^* (1) in the $S^* - X_b^*$ plane for $0 \leq R^* \leq 1$.

2.4.1.2 Global stability for large decay rate

In this section we show that if

$$k_d^* \geq \frac{S_0^* + \alpha_{g,h} k_h^* X_s^* \tau^*}{1 - R^* + S_0^* + \alpha_{g,h} k_h^* X_s^* \tau^*}, \tag{2.29}$$

then

$$\lim_{t^*\to\infty} X_b^*(t^*) = 0, \tag{2.30}$$

i.e. the biomass is guaranteed to die out if the decay rate is too large.

We first show that if $k_d^* \geq 1$ that the biomass must die out. Recall equation (2.23)

$$\frac{dX_b^*}{dt^*} = X_b^* \left[\frac{R^* - 1}{\tau^*} + \frac{S^*}{1 + S^*} - k_d^* \right]. \tag{2.31}$$

If $(k_d^* \geq 1 > \frac{S^*}{1+S^*})$, then we obtain

$$\frac{dX_b^*}{dt^*} \leq \frac{(R^* - 1)}{\tau^*} X_b^*.$$

For $0 \leq R^* < 1$, it follows that

$$X_b^* \leq X_b^*(0) \exp\left[\left(\frac{R^* - 1}{\tau^*} \right) t^* \right],$$

where $X_b^*(0)$ is the initial value of X_b^*. This inequality shows that when $0 \leq R^* < 1$ and $k_d^* \geq 1$

$$\lim_{t^*\to\infty} X_b^* = 0,$$

i.e. the biomass dies out. When $R^* = 1$ we require $k_d^* > 1$.

When the biomass die out $(X_b^* \to 0)$ it follows that the substrate concentration converges to the feed concentration $(S^* \to S_0^*)$.

The steady state solution with $[(S^*, X_b^*) = (S_0^*, 0)]$ is known as the washout solution.

From now on in this chapter we assume that

$$k_d^* < 1. \tag{2.32}$$

In establishing the bound (2.32) we did not use our knowledge of the invariant region. We can improve the bound (2.32) slightly, by using the fact that all solutions enter the invariant region.

Inside the invariant region we have

$$\begin{aligned} &S^*(t^*) + X_b^*(t^*) \leq \frac{\hat{S}_0^*}{1-R^*}, \\ &\Rightarrow S^*(t^*) \leq \frac{\hat{S}_0^*}{1-R^*}, \\ &\Rightarrow \frac{S^*(t^*)}{1+S^*(t^*)} \leq \frac{\frac{\hat{S}_0^*}{1-R^*}}{1+\frac{\hat{S}_0^*}{1-R^*}} = \frac{\hat{S}_0^*}{1-R^*+\hat{S}_0^*}. \end{aligned}$$

Using the same method as before we immediately deduce that the washout solution is globally stable if

$$\begin{aligned} k_d^* \geq k_{\mathrm{d,cr}}^* &= \frac{\hat{S}_0^*}{1-R^*+\hat{S}_0^*}, \\ &= \frac{S_0^*(1-R^*) + (S_0^* + \alpha_{g,h} X_{s,0}^*) k_h^* \tau^*}{(1-R^*)[1-R^*+S_0^*] + (1-R^*+S_0^*+\alpha_{g,h}X_{s,0}^*)k_h^*\tau^*}. \end{aligned} \tag{2.33}$$

The parameter $k_{\mathrm{d,cr}}^*$ is an increasing function of the residence time.

$$\frac{dk_{\mathrm{d,cr}}^*}{d\tau^*} = \frac{\alpha_{g,h} X_{s,0}^* k_h^* (1-R^*)^2}{[(1-R^*)[1-R^*+S_0^*] + (1-R^*+S_0^*+\alpha_{g,h}X_{s,0}^*)k_h^*\tau^*]^2} > 0. \tag{2.34}$$

Now we take the limit $\tau^* \to \infty$ to deduce that $\lim_{t\to\infty} X_b^*(t^*) = 0$ when

$$k_d^* \geq k_{\mathrm{d,cr1}}^*(\tau^* = \infty) = \frac{(S_0^* + \alpha_{g,h}X_{s,0}^*)k_h^*\tau^*}{(1-R^*+S_0^*+\alpha_{g,h}X_{s,0}^*)k_h^*\tau^*} = \frac{S_0^* + \alpha_{g,h}X_{s,0}^*}{1-R^*+S_0^*+\alpha_{g,h}X_{s,0}^*}. \tag{2.35}$$

Note, this bound (2.32) provides no additional information when there is perfect recycle ($R^* = 1$) as then $k_{\mathrm{d,cr1}}^* = 1$.

Note that equation (2.35) can be written as

$$k^*_{\mathrm{d,cr1}} = \frac{\mathrm{COD}^*_{\mathrm{in}}}{1 - R^* + \mathrm{COD}^*_{\mathrm{in}}}, \tag{2.36}$$

where $\mathrm{COD}^*_{\mathrm{in}}$ is the chemical oxygen demand in the inflow.

Note that the value $k^*_{\mathrm{d,cr}}(\tau^* = \infty)$ is an increasing function of the effective recycle ratio (R^*). This means that a microbial species that dies out in the absence of recycle ($R^* = 0$) might be able to survive in the presence of recycle. The use of such a species in the activated sludge process is highly undesirable.

If the decay rate is smaller than the critical value $k^*_{\mathrm{d,cr}}$ then there is a critical value of the residence time (τ^*_+). If the residence time is smaller than the critical value ($\tau^*<\tau^*_+$) then the washout solution, i.e. $(S^*, X^*_b) = (S^*_0, 0)$, is globally stable.

The biomass will die out, from equation (2.31), when

$$\frac{R^* - 1}{\tau^*} + \frac{S^*}{1 + S^*} - k^*_d<0. \tag{2.37}$$

From (2.33) we have

$$\frac{S^*}{1 + S^*} \leq \frac{S^*_0(1 - R^* + k^*_h\tau^*) + \alpha_{g,h}k^*_hX^*_{s,0}\tau^*}{(1 - R^* + S^*_0)(1 - R^* + k^*_h\tau^*) + \alpha_{g,h}k^*_hX^*_{s,0}\tau^*}. \tag{2.38}$$

Substituting inequality (2.37) into inequality (2.38) we obtain

$$Q(\tau^*) = a\tau^{2*} + b\tau^* + c<0, \quad \text{and the coefficients are} \tag{2.39}$$

$$a = [(S^*_0 + \alpha_{g,h}X^*_{s,0}) - (1 + S^*_0 + \alpha_{g,h}X^*_{s,0})k^*_d]k^*_h, \tag{2.40}$$

$$b = -(1 - R^*)[(1 + S^*_0)(k^*_h + k^*_d) + k^*_h\alpha_{g,h}X^*_{s,0} - S^*_0], \tag{2.41}$$

$$c = -(1 - R^*)^2(1 + S^*_0)<0. \tag{2.42}$$

It follows from the analysis in appendix A.1 that the inequality (2.39) is always true when

$$\begin{aligned} a &= [(S_0^* + \alpha_g X_{s,0}^*) - (1 + S_0^* + \alpha_{g,h} X_{s,0}^*) k_d^*] k_h^* \leq 0, \\ \Rightarrow k_d^* &\geq \frac{\mathrm{COD}_{\mathrm{in}}^*}{1 + \mathrm{COD}_{\mathrm{in}}^*}. \end{aligned} \tag{2.43}$$

When $a>0$, the inequality (2.39) is true when $\tau_+^* > \tau^*$, where

$$\tau_+^* = (1 - R^*)\tau_{\mathrm{cr}}^*(R^* = 0), \tag{2.44}$$

where

$$\begin{aligned} \tau_{\mathrm{cr}}^*(R^* = 0) &= \frac{b^* + \sqrt{b^{*2} + 4ac^*}}{2a}, \\ b^* &= (1 + S_0^*)(k_h^* + k_d^*) + k_h^* \alpha_g X_{s,0}^* - S_0^*, \\ c^* &= (1 + S_0^*). \end{aligned}$$

Here we have a gap because the results in the appendix show that the no-washout branch is not meaningful when

$$k_d^* > \frac{\mathrm{COD}_{\mathrm{in}}^*}{1 + \mathrm{COD}_{\mathrm{in}}^*}.$$

However, we have only shown that the washout branch is globally stable when

$$k_d^* > \frac{\mathrm{COD}_{\mathrm{in}}^*}{1 - R^* + \mathrm{COD}_{\mathrm{in}}^*} > \frac{\mathrm{COD}_{\mathrm{in}}^*}{1 + \mathrm{COD}_{\mathrm{in}}^*}.$$

This suggests that the washout solution is globally stable if

$$k_d^* < \frac{\mathrm{COD}_{\mathrm{in}}^*}{1 + \mathrm{COD}_{\mathrm{in}}^*}.$$

In the next section we show that this is indeed the case.

2.4.1.3 Revising the (positively) invariant region

In this section we obtain conditions under which the the (positively) invariant region (R^*) can be made smaller. This leads to an improved bound on the critical value of the decay $k^*_{\mathrm{d,cr}}$.

In equation (2.22) consider the expression

$$\left(f_s\alpha_{g,s}k_d^* - \frac{S^*}{1+S^*}\right)X_b^*.$$

We would like to know when this is negative. This happens when

$$\begin{aligned}
&f_s\alpha_{g,s}k_d^*(1+S^*) - S^* < 0,\\
&\Rightarrow (1 - f_s\alpha_{g,s}k_d^*)S^* > f_s\alpha_{g,s}k_d^*,\\
&\Rightarrow S^* > \frac{f_s\alpha_{g,s}k_d^*}{1 - f_s\alpha_{g,s}k_d^*} = b_{\mathrm{cr}}.
\end{aligned}$$

Note that we have the bound $0 < f_s\alpha_{g,s} \leq 1$ from equation (2.19) and $k_d^* < 1$ from equation (2.32).

The differential equation for the substrate is

$$\frac{dS^*}{dt^*} = \frac{1}{\tau^*}(\hat{S}_0^* - S^*) + \left[f_s\alpha_{g,s}k_d^* - \frac{S^*}{1+S^*}\right]X_b^*.$$

Now suppose that $S^* \geq \hat{S}_0^* > b_{\mathrm{cr}}$. Then

$$\frac{S^*}{1+S^*} \geq f_s\alpha_{g,s}k_d^*.$$

Hence

$$\begin{aligned}
&\frac{dS^*}{dt^*} \leq \frac{1}{\tau^*}(\hat{S}_0^* - S^*),\\
&\Rightarrow S^*(t^*) \leq \hat{S}_0^* + \left(S^*(0) - \hat{S}_0^*\right)\exp\left[-\frac{1}{\tau^*}\cdot t^*\right],
\end{aligned}$$

where $S^*(0)$ is the initial value of S^*.

We now take the limit $t^* \to \infty$ to deduce that

$$S^* \leq \hat{S}_0^*.$$

This shows that when $\hat{S}_0^* > b_{\text{cr}}$ that the region $S^* \leq \hat{S}_0^*$ is exponentially attracting and (positively) invariant.

In this case the invariant region I^* established in section 2.4.1.1 can be improved to the region (I_{new}^*) given by

$$0 \leq S^* \leq \hat{S}_0^*,$$
$$0 \leq X_b^* \leq \frac{\hat{S}_0^*}{1-R^*} - S^*,$$

which is shown in figure 2.3. Note that when there is no recycle the invariant regions, I^* and I_{new}^* are identical.

Using typical values for the parameters given in appendix B.2, we find that $b_{\text{cr}} = 0.0023$ and $S_0^* = 1.996$. Thus for typical parameter values we have $\hat{S}_0^* \geq S_0^* > b_{\text{cr}}$.

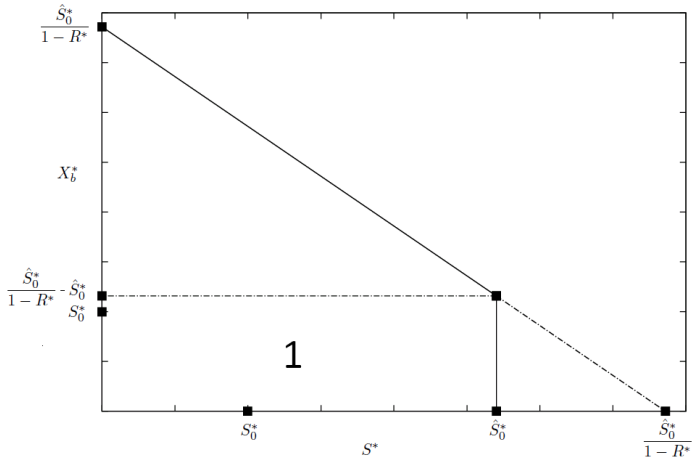

Figure 2.3: The improved invariant region (I_{new}^*), denoted as region 1 for $0 \leq I^* < 1$ when $\hat{S}_0^* > b_{\text{cr}}$.

Repeating the argument from section 2.4.1.2 we deduce that if $\hat{S}_0^* > b_{\text{cr}}$ then $\lim_{\tau^* \to \infty} X_b^*(t^*) = 0$ if

$$k_d^* > \frac{\hat{S}_0^*}{1 + \hat{S}_0^*}.$$

Substituting (2.26) for $\hat{S}_0^*$ we have

$$k_d^* > k_{\text{d,cr2}}^* = \frac{S_0^*(1 - R^* + k_h^* \tau^*) + \alpha_{g,h} k_h^* X_{s,0}^* \tau^*}{(1 - R^*)\left(S_0^* + 1\right) + \tau^* k_h^* \left(\alpha_{g,h} X_{s,0}^* + S_0^* + 1\right)},$$
$$\frac{dk_{\text{d,cr2}}^*}{d\tau^*} = \frac{\alpha_{g,h} X_{s,0}^* k_h^* (1 - R^*)}{[(1 - R^*)[1 + S_0^*] + (1 + S_0^* + \alpha_{g,h} X_{s,0}^*) k_h^* \tau^*]^2} > 0.$$

Taking the limit $\tau^* \to \infty$ we deduce that if $\hat{S}_0^* > b_{\text{cr}}$ then

$$\lim_{t \to \infty} X_b^*(t^*) = 0,$$

when

$$k_d^* \geq k_{\text{d,cr2}}^* = \frac{(S_0^* + \alpha_{g,h} X_{s,0}^*) k_h^* \tau^*}{(1 + S_0^* + \alpha_{g,h} X_{s,0}^*) k_h^* \tau^*} = \frac{S_0^* + \alpha_{g,h} X_{s,0}^*}{1 + S_0^* + \alpha_{g,h} X_{s,0}^*},$$
$$= \frac{\text{COD}_{\text{in}}^*}{1 + \text{COD}_{\text{in}}^*}.$$

Note that this bound is independent of the effective recycle parameter, compare with equation (2.35).

Thus if $S^* \geq \hat{S}_0^* > b_{\text{cr}}$ is true then the critical value of the death coefficient is given by

$$k_d^* = \frac{\text{COD}_{\text{in}}^*}{1 + \text{COD}_{\text{in}}^*},$$

as suggested at the end of the last section.

Note that the requirement

$$\hat{S}_0^* > b_{\mathrm{cr}} = \frac{f_s \alpha_{g,s} k_d^*}{1 - f_s \alpha_{g,s} k_d^*},$$

requires

$$\begin{aligned} & S_0^* + \frac{\alpha_{g,h} k_h^* X_{s,0}^* \tau^*}{1 - R^* + k_h^* \tau^*} > \frac{f_s \alpha_{g,s} k_d^*}{1 - f_s \alpha_{g,s} k_d^*}, \\ & \Rightarrow k_d^* < \frac{S_0^* (1 - R^*) + (S_0^* + \alpha_{g,h} X_{s,0}^*) k_h^* \tau^*}{\left[(1 + S_0^*)(1 - R^*) + (S_0^* + \alpha_{g,h} X_{s,0}^*) k_h^* \tau^* \right] f_s \alpha_{g,s}}. \end{aligned} \tag{2.45}$$

Let

$$Y = \frac{S_0^* (1 - R^*) + (S_0^* + \alpha_{g,h} X_{s,0}^*) k_h^* \tau^*}{\left[(1 + S_0^*)(1 - R^*) + (S_0^* + \alpha_{g,h} X_{s,0}^*) k_h^* \tau^* \right] f_s \alpha_{g,s}}.$$

Then

$$\frac{dY}{d\tau^*} = \frac{B_Y (C_Y + D_Y \tau^*) - D_Y (A_Y + B_Y \tau^*)}{(C_Y + D_Y \tau^*)^2} > 0,$$

where

$$\begin{aligned} A_Y &= S_0^* (1 - R^*), \\ B_Y &= (S_0^* + \alpha_{g,h} X_{s,0}^*) k_h^*, \end{aligned}$$

$$\begin{aligned} C_Y &= (1 + S_0^*)(1 - R^*) f_s \alpha_{g,s}, \\ D_Y &= (1 + S_0^* + \alpha_{g,h} X_{s,0}^*) k_h^* f_s \alpha_{g,s}. \end{aligned}$$

We have

$$Y_{\min} = Y(\tau^* = 0) = \frac{S_0^* (1 - R^*)}{(1 + S_0^*)(1 - R^*) f_s \alpha_{g,s}}.$$

So (2.45) is always true if

$$k_d^*<k_{\mathrm{d,cr3}}^* = \frac{S_0^*}{(1+S_0^*)f_s\alpha_{g,s}}. \tag{2.46}$$

Therefore, $\lim_{\tau^*\to\infty} X_b^* = 0$ if

$$k_{\mathrm{d,cr2}}^* = \frac{\mathrm{COD}_{\mathrm{in}}^*}{1+\mathrm{COD}_{\mathrm{in}}^*} \leq k_d^*<k_{\mathrm{d,cr3}}^* = \frac{S_0^*}{(1+S_0^*)f_s\alpha_{g,s}}. \tag{2.47}$$

For typical parameter values we have

$$k_{\mathrm{d,cr3}}^* = 19.5618.$$

2.4.2 Steady-state solution branches

The steady-state solutions are found by putting the derivative equal to zero in equations (2.13) (2.16) and then solving the resulting system of the equations.

The steady-state solutions are given by washout branch.

$$(S^*, X_b^*, X_i^*, X_s^*) = \left(S_W^*, 0, X_{i,\infty}^*, X_{s,\infty}^*\right), \tag{2.48}$$

$$S_w^* = \hat{S}_0^* = S_0^* + \frac{\alpha_{g,h}k_h^*X_{s,0}^*\tau^*}{1-R^*+k_h^*\tau^*}, \tag{2.49}$$

$$X_{i,\infty}^* = \frac{X_{i,0}^*}{1-R^*}, \tag{2.50}$$

$$X_{s,\infty}^* = \frac{X_{s,0}^*}{1-R^*+k_h^*\tau^*}, \tag{2.51}$$

$$\mathrm{COD}_w^* = S_0^* + \frac{(1+k_h^*\tau^*)\alpha_{g,h}X_{s,0}^*}{1-R^*+k_h^*\tau^*}, \tag{2.52}$$

$$\mathrm{VSS}_w^* = \frac{X_{i,0}^*}{1-R^*} + \frac{X_{s,0}^*}{1-R^*+k_h^*\tau^*}. \tag{2.53}$$

Washout branch corresponds to process failure due to removal of all the biomass. The washout value for the soluble substrate (S_w^*) is different from that in the earlier model [71] because it now depends upon the residence time, whereas in [71] it is

a constant ($S_w^* = S_0^*$). The latter case occurs when either $k_h^* = 0$, or $\alpha_{g,h} = 0$. The washout value (S_w^*) is an increasing function of the residence time τ^*. It has a minimum value

$$\lim_{\tau^* \to 0} S_w^* = S_0^*,$$

and a maximum value

$$\lim_{\tau^* \to \infty} S_w^* = S_0^* + \alpha_{g,h}^* k_h^* X_{s,0}^*.$$

Later on, it is useful to know that

$$\begin{aligned} S_w^* &= \frac{S_0^*(1 - R^* + k_h^*\tau^*) + \alpha_{g,h} k_h^* X_{s,0}^* \tau^*}{1 - R^* + k_h^*\tau^*}, \\ \Rightarrow \frac{S_w^*}{1 + S_w^*} &= \frac{S_0^*(1 - R^*) + (S_0^* + \alpha_{g,h} X_{s,0}^*) k_h^* \tau^*}{(1 + S_0^*)(1 - R^*) + (1 + S_0^* + \alpha_{g,h} X_{s,0}^*) k_h^* \tau^*}. \end{aligned} \tag{2.54}$$

No-washout branch.

$$(S^*, X_b^*, X_i^*, X_s^*) = \left(S_{\mathrm{nw}}^*, X_{\mathrm{b,nw}}^*, X_{i,\infty}^*, X_{s,\infty}^*\right), \tag{2.55}$$

$$S_{\mathrm{nw}}^* = \frac{1 - R^* + k_d^*\tau^*}{(1 - k_d^*)\tau^* - 1 + R^*}, \tag{2.56}$$

$$X_{\mathrm{b,nw}}^* = \frac{(1 + S_{\mathrm{nw}}^*)(S_{\mathrm{w}}^* - S_{\mathrm{nw}}^*)}{(S_{\mathrm{nw}}^* - (1 + S_{\mathrm{nw}}^*) f_s \alpha_{g,s} k_d^*)\tau^*}, \tag{2.57}$$

$$X_{i,\infty}^* = \frac{X_{i,0}^*}{1 - R^*} + \frac{f_i k_d^* X_{\mathrm{b,nw}}^* \tau^*}{1 - R^*}, \tag{2.58}$$

$$X_{s,\infty}^* = \frac{X_{s,0}^*}{1 - R^* + k_h^*\tau^*}, \tag{2.59}$$

$$\mathrm{COD}_{\mathrm{nw}}^* = \frac{1 - R^* + k_d^*\tau^*}{(1 - k_d^*)\tau^* - 1 + R^*} + \frac{\alpha_{g,h} X_{s,0}^*}{1 - R^* + k_h^*\tau^*}, \tag{2.60}$$

$$\mathrm{VSS}_{\mathrm{nw}}^* = \left(1 + \frac{f_i k_d^* \tau^*}{1 - R^*}\right) X_{\mathrm{b,nw}}^* + \frac{X_{i,0}^*}{1 - R^*} + \frac{X_{s,0}^*}{1 - R^* + k_h^*\tau^*}. \tag{2.61}$$

The value for the substrate concentration along the no-washout branch (S_{nw}^*) is identical to that in the standard model [71]. It is interesting to observe that although

a fraction of the dead biomass is converted into soluble substrate that this process does not contribute to the steady state soluble substrate concentration.

The no-washout branch is physically meaningful only when the substrate and cell-mass concentrations are positive ($S^* \geq 0, X_b^* \geq 0$). The condition for this to hold are identified in appendix A.2.

Differentiating equation (2.56) with respect to the recycle parameter we obtain

$$\frac{dS_{\text{nw}}^*}{dR^*} = \frac{-\tau^*}{[(1-k_d^*)\tau^* - 1 + R^*]^2} < 0. \tag{2.62}$$

Hence the substrate concentration is a decreasing function of the effective recycle parameter (R^*).

Differentiating equation (2.56) with respect to the residence time we obtain

$$\frac{dS_{\text{nw}}^*}{d\tau^*} = \frac{R^* - 1}{[(1-k_d^*)\tau^* - 1 + R^*]^2}. \tag{2.63}$$

This equation has a vertical asymptote when

$$\tau^* = \frac{1-R^*}{1-k_d^*} = \tau_{\text{pm},1}^*.$$

In the limit of infinite residence time, the soluble substrate is independent of the effective recycle parameter.

$$S_{\text{nw}}^* \lim_{\tau^* \to \infty} (\tau^*, R^*) = \frac{k_d^*}{1-k_d^*}. \tag{2.64}$$

These results (equations (2.62), (2.63) and (2.64)) for the soluble substrate are the same with the basic model and our model in section 4.4.1.

The substrate concentration along the no-washout branch is always physically meaningful when $\tau^* > \tau_+^* > \tau_{\text{pm},1}^*$ (see appendix A.1.1).

When the substrate concentration along the no-washout branch is physically meaningful it is a strictly monotonically decreasing function of the residence time, i.e. the

lowest effluent concentration is obtained at an infinite residence time.

For a flow reactor with idealized recycle or an idealized membrane reactor ($R^* = 1$), the substrate concentration is independent of the residence time and is given by

$$S^*_{\mathrm{nw}}(R^* = 1) = \frac{k^*_{\mathrm{d}}}{1 - k^*_{\mathrm{d}}}. \tag{2.65}$$

Differentiating equation (2.60) with respect to the residence time we obtain

$$\frac{d\mathrm{COD}^*_{\mathrm{nw}}}{d\tau^*} = -\left(\frac{1 - R^*}{[(1 - k^*_d)\tau^* - 1 + R^*]^2} + \frac{\alpha_{g,h} X^*_{s,0} k^*_h}{[1 - R^* + k^*_h \tau^*]^2}\right) <0. \tag{2.66}$$

By comparing equations (2.48) – (2.53) with equation (2.56) – (2.61) we see that the washout branch and the no-washout branch are identical when

$$\begin{aligned} & S^*_w = S^*_{\mathrm{nw}}, \\ & \Rightarrow S^*_0 + \frac{\alpha_{g,h} k^*_h X^*_{s,0} \tau^*}{1 - R^* + k^*_h \tau^*} = \frac{1 - R^* + k^*_d \tau^*}{(1 - k^*_d)\tau^* - 1 + R^*}. \end{aligned}$$

This intersection point corresponds to a trans-critical bifurcation.

After some algebra we find that this is true when the residence time satisfies a quadratic equation $Q(\tau^*) = 0$, where

$$Q(\tau^*) = a\tau^{2*} + b\tau^* + c, \quad \text{and the coefficients are} \tag{2.67}$$

$$a = [(S^*_0 + \alpha_{g,h} X^*_{s,0}) - (1 + S^*_0 + \alpha_{g,h} X^*_{s,0}) k^*_d] k^*_h, \tag{2.68}$$

$$b = -(1 - R^*)[(1 + S^*_0)(k^*_h + k^*_d) + k^*_h \alpha_{g,h} X^*_{s,0} - S^*_0], \tag{2.69}$$

$$c = -(1 - R^*)^2 (1 + S^*_0) <0. \tag{2.70}$$

It follows from the analysis in appendix A.2 that that trans-critical bifurcation point is physically meaningful only when $a>0$ and is given by

$$\tau_{+}^{*} = (1 - R^{*})\tau_{\mathrm{cr}}^{*}(R^{*} = 0), \tag{2.71}$$

where

$$\begin{aligned} \tau_{\mathrm{cr}}^{*}(R^{*} = 0) &= \frac{b^{*} + \sqrt{b^{*2} + 4ac^{*}}}{2a}, \\ b^{*} &= (1 + S_{0}^{*})(k_{h}^{*} + k_{d}^{*}) + k_{h}^{*}\alpha_{g,h}X_{s,0}^{*} - S_{0}^{*}, \\ c^{*} &= (1 + S_{0}^{*}). \end{aligned} \tag{2.72}$$

The condition $a>0$ is

$$k_{d}^{*} < \frac{S_{0}^{*} + \alpha_{g,h}X_{s,0}^{*}}{1 + S_{0}^{*} + \alpha_{g,h}X_{s,0}^{*}} = \frac{\mathrm{COD}_{\mathrm{in}}^{*}}{1 + \mathrm{COD}_{\mathrm{in}}^{*}}. \tag{2.73}$$

The expression for the critical value of the decay rate only depends upon the value of the chemical oxygen demand flow in the feed. However, the expression for the critical value of the residence time depends upon how the chemical oxygen demand is partitioned into its components, as shown in the expressions for the coefficients of b^{*} and c^{*}.

When the no-washout branch is not physically meaningful then the only stable steady state is the washout solution. In this circumstance process failure must occur.

2.4.3 Stability of the steady-state solutions

The Jacobian matrix of system (2.22) and (2.23) is given by

$$J(S^*, X^*) = \begin{pmatrix} -\frac{1}{\tau^*} - \frac{X_b^*}{(1+S^*)^2} & f_s k_d^* \alpha_{g,s} - \frac{S^*}{1+S^*} \\ \\ \frac{X_b^*}{(1+S^*)^2} & -\frac{1}{\tau^*} + \frac{R^*}{\tau^*} + \frac{S^*}{1+S^*} - k_d^* \end{pmatrix}.$$

2.4.3.1 Stability of the washout solution

The Jacobian matrix evaluated at the washout steady state solution is given by

$$J(S_w^*, 0) = \begin{pmatrix} -\frac{1}{\tau^*} & f_s k_d^* \alpha_{g,s} - \frac{S_w^*}{1+S_w^*} \\ \\ 0 & -\frac{1}{\tau^*} + \frac{R^*}{\tau^*} + \frac{S_w^*}{1+S_w^*} - k_d^* \end{pmatrix}.$$

The eigenvalues of this matrix are

$$\begin{aligned} \lambda_1 &= -\frac{1}{\tau^*} < 0, \\ \lambda_2 &= \frac{R^* - 1}{\tau^*} + \frac{S_w^*}{1 + S_w^*} - k_d^*. \end{aligned}$$

Recall that $0 \leq R^* \leq 1$. The stability of the washout branch depends upon the sign of λ_2.

Note that, the washout steady-state is always stable when

$$\begin{aligned} & k_d^* \geq 1, \\ & \Rightarrow \frac{k_d}{\mu_m} \geq 1, \\ & \Rightarrow k_d \geq \mu_m. \end{aligned}$$

This makes sense because it says that the washout steady state is always stable if the death rate is greater than, or equal to, the maximum growth rate. Note that we showed in section 2.4.1.2 that when $k_d^* \geq 1$ then the washout solution is globally stable.

We now show that there is a critical value ($k_{\mathrm{d,cr},\infty}^*$) such that the washout branch is

always stable when $k^*_{\mathrm{d,cr},\infty}<k^*_d \leq 1$. The eigenvalue λ_2 is always negative when

$$k^*_d>k^*_{\mathrm{d,cr}} = \frac{S^*_w}{1+S^*_w} = \frac{S^*_0(1-R^*)+(S^*_0+\alpha_{g,h}X^*_{s,0})k^*_h\tau^*}{(1+S^*_0)(1-R^*)+(1+S^*_0+\alpha_{g,h}X^*_{s,0})k^*_h\tau^*}.$$

Note that

$$\frac{dk^*_{\mathrm{d,cr}}}{d\tau^*} = \frac{\alpha_{g,h}X^*_{s,0}k^*_h(1-R^*)}{[(1+S^*_0)(1-R^*)+(1+S^*_0+\alpha_{g,h}X^*_{s,0})k^*_h\tau^*]^2}>0.$$

Thus $k^*_{\mathrm{d,cr}}$ has a minimum value $S^*_0/(1+S^*_0)$ when $(\tau^*=0)$ and a maximum value $(k^*_{\mathrm{d,cr},\infty})$

$$\begin{aligned} k^*_{\mathrm{d,cr},\infty} &= \lim_{\tau^*\to\infty}\frac{S^*_0(1-R^*)+(S^*_0+\alpha_{g,h}X^*_{s,0})k^*_h\tau^*}{(1+S^*_0)(1-R^*)+(1+S^*_0+\alpha_{g,h}X^*_{s,0})k^*_h\tau^*}, \\ k^*_{\mathrm{d,cr},\infty} &= \frac{S^*_0+\alpha_{g,h}X^*_{s,0}}{1+S^*_0+\alpha_{g,h}X^*_{s,0}}, \\ &= \frac{\mathrm{COD}^*_{\mathrm{in}}}{1+\mathrm{COD}^*_{\mathrm{in}}}. \end{aligned} \tag{2.74}$$

Thus if $k^*_d>k^*_{\mathrm{d,cr},\infty}$ then the washout branch is always stable.

We now consider the case $k^*_d<k^*_{\mathrm{d,cr},\infty}$ and show that there is a critical value of the residence time, τ^*_{cr}, such that if $\tau^*<\tau^*_{\mathrm{cr}}$ then the washout solution is locally stable. We have

$$\lambda_2 = \frac{R^*-1}{\tau^*}+\frac{S^*_w}{1+S^*_w}-k^*_d = \frac{-Q(\tau^*)}{B},$$

and

$$B = [(R^*-1)(1+S^*_0)-(1+S^*_0+\alpha_{g,h}X^*_{s,0})k^*_h\tau^*]\tau^*<0,$$

where $Q(\tau^*)$ is defined by equation (2.67). The denominator B is always negative. Hence the problem of establishing $\lambda_2<0$ reduces to determining when $-Q(\tau^*)$ is positive i.e. when the quadratic $A = Q(\tau^*)$ is negative.

We only need to consider the case

$$k_d^* < \frac{S_0^* + \alpha_{g,h} X_{s,0}^*}{1 + S_0^* + \alpha_{g,h} X_{s,0}^*} = k_{\mathrm{d,cr},\infty}^*.$$

This condition implies that the coefficient a is positive ($a>0$). Then the graph of the quadratic function $Q(\tau^*)$ is shown in appendix A.2 in figure A.1. Therefore the inequality $Q(\tau^*)>0$ is only true if $0<\tau^*<\tau_+^*$.

2.4.3.2 Stability of the no-washout solution

The Jacobian matrix for the no-washout branch is given by

$$J(S_{\mathrm{nw}}^*, X_{\mathrm{b,nw}}^*) = \begin{pmatrix} -\frac{1}{\tau^*} - \frac{X_{\mathrm{b,nw}}^*}{(1+S^*)^2} & f_s k_d^* \alpha_{g,s} - \frac{S_{\mathrm{nw}}^*}{1+S_{\mathrm{nw}}^*} \\ \\ \frac{\hat{X}_{\mathrm{b,nw}}^*}{(1+S_{\mathrm{nw}}^*)^2} & 0 \end{pmatrix}.$$

This solution branch is stable if det $J>0$ and trace $J<0$.

We have

$$\text{trace } J = -\frac{1}{\tau^*} - \frac{X_{\mathrm{b,nw}}^*}{(1+S_{\mathrm{nw}}^*)^2}.$$

When the no-washout branch is physically meaningful then trace $J<0$.

We have

$$\det J = -\left[\frac{X_{\mathrm{b,nw}}^*}{(1+S_{\mathrm{nw}}^*)^2}\left(f_s k_d^* \alpha_{g,s} - \frac{S_{\mathrm{nw}}^*}{1+S_{\mathrm{nw}}^*}\right)\right].$$

When the no-washout branch is physically meaningful the condition for det J>0 is

$$f_s k_d^* \alpha_{g,s} < \frac{S_{\mathrm{nw}}^*}{1 + S_{\mathrm{nw}}^*},$$

After some algebra this implies

$$\tau^* > \frac{R^* - 1}{(1 - f_s \alpha_{g,s}) k_d^*}. \tag{2.75}$$

Equation (2.75) is always true as the left-hand side is positive whilst the right hand side is strictly non-positive.

It therefore follows that det J>0 and trace J<0 wheneverX^*>0 and S^*>0 . Thus the no-washout branch is stable whenever it is physically meaningful.

2.4.4 Asymptotic solutions

In this section we obtain asymptotic solutions for large residence time approximations ($\tau_{\mathrm{cr}}^* \gg 1$) and asymptotic approximations when residence time is slightly larger than the critical value ($\tau^* - \tau_{\mathrm{cr}}^* \ll 1$).

2.4.4.1 Large residence time approximations

At large residence times, we have

$$S_{\mathrm{nw}}^* \approx \frac{k_d^*}{1 - k_d^*} + \frac{(1 - R^*)}{(1 - k_d^*)^2} \cdot \frac{1}{\tau^*} + O\left(\frac{1}{\tau^{*2}}\right), \tag{2.76}$$

$$X_{\mathrm{b,nw}}^* \approx a_0 \cdot \frac{1}{\tau^*} + O\left(\frac{1}{\tau^{*2}}\right), \tag{2.77}$$

$$X_i^* \approx \frac{X_{i,0}^*}{1 - R^*} + \frac{f_i k_d^*}{1 - R^*} a_0 + \frac{f_i k_d^*}{1 - R^*} \cdot \frac{a_1}{\tau^*} + O\left(\frac{1}{\tau^{*2}}\right), \tag{2.78}$$

$$X_s^* \approx \frac{X_{s,0}^*}{k_h^*} \cdot \frac{1}{\tau^*} + O\left(\frac{1}{\tau^{*2}}\right), \tag{2.79}$$

$$\mathrm{COD}_{\mathrm{nw}}^* \approx \frac{k_d^*}{1 - k_d^*} + \left[\frac{(1 - R^*)}{(1 - k_d^*)^2} + \frac{\alpha_{g,h} X_{s,0}^*}{k_h^*}\right] \cdot \frac{1}{\tau^*} + O\left(\frac{1}{\tau^{*2}}\right), \tag{2.80}$$

$$\mathrm{VSS}^*_{\mathrm{nw}} \approx \frac{X^*_{i,0}}{1-R^*} + \frac{f_i k^*_d}{1-R^*} a_0 + \left(a_0 + \frac{f_i k^*_d}{1-R^*} \cdot a_1 + \frac{X^*_{s,0}}{k^*_h} \right) \cdot \frac{1}{\tau^*} + O\left(\frac{1}{\tau^{*2}} \right), \tag{2.81}$$

where

$$a_0 = \frac{S^*_0(1-k^*_d) - k^*_d + \alpha_{g,h} X^*_{s,0}(1-k^*_d)}{k^*_d(1-k^*_d)(1-f_s\alpha_{g,s})} > 0.$$

(Recall that from (2.19) and (A.5) we have $(1-f_s\alpha_{g,s})>0$ and $S^*_0(1-k^*_d)-k^*_d>0$.)

$$\begin{aligned}
a_1 &= \frac{(1-R^*)}{k^*_d(1-f_s\alpha_{g,s})}(B-A-C),\\
A &= \frac{\alpha_{g,h}X^*_{s,0}}{k^*_h} + \frac{1}{(1-k^*_d)^2},\\
B &= \frac{(S^*_0+\alpha_{g,h}X^*_{s,0})(1-k^*_d)-k^*_d}{(1-k^*_d)^2},\\
C &= \frac{\left[(S^*_0+\alpha_{g,h}X^*_{s,0})(1-k^*_d)-k^*_d\right](1-f_s\alpha_{g,s}k^*_d)}{k^*_d(1-k^*_d)^2(1-f_s\alpha_{g,s})}.
\end{aligned}$$

It is useful to note that the coefficient a_0 can be written as

$$a_0 = \frac{\mathrm{COD}^*_{\mathrm{in}}(1-k^*_d) - k^*_d}{k^*_d(1-k^*_d)(1-f_s\alpha_{g,s})}, \tag{2.82}$$

where

$$\mathrm{COD}^*_{\mathrm{in}} = S^*_0 + \alpha_{g,h} X^*_{s,0}.$$

For the default parameter values we have $a_0 = 153.86$.

At sufficiently large value of residence time the biomass concentration ($X^*_{\mathrm{b,nw}}$) is independent of the value of the effective recycle factor (R^*). The case $k^*_d = 1$ is not allowed in the asymptotic formula, because when this is true then the no-washout branch is not physically meaningful.

It is important to note that the effluent concentration can not be reduced below the

limiting value

$$\lim_{t^*\to\infty} S^*_{\mathrm{nw}} = \frac{k^*_d}{1-k^*_d} > 0.$$

2.4.4.2 Asymptotic approximations when $(\tau^* - \tau^*_{\mathbf{cr}} \ll 1)$

The asymptotic solutions for residence time that are slightly larger than criticality are

$$S^*_{\mathrm{nw}} \approx \frac{1-R^*+\tau^*_{\mathrm{cr}}\,k^*_d}{R^*-1+(1-k^*_d)\,\tau^*_{\mathrm{cr}}} + \frac{R^*-1}{\left(R^*-1+\tau^*_{\mathrm{cr}}-k^*_d\tau^*_{\mathrm{cr}}\right)^2}\cdot\epsilon, \tag{2.83}$$

$$X^*_{\mathrm{b,nw}} \approx a_2\cdot\epsilon, \tag{2.84}$$

$$X^*_i \approx \frac{1}{1-R^*}\left(X^*_{i,0} + f_i k^*_d a_3\cdot\epsilon\right), \tag{2.85}$$

$$X^*_s \approx \frac{1}{1-R^*+k_h\tau^*_{\mathrm{cr}}}\left(X^*_{s,0} + \frac{k^*_h X^*_{s,0}}{(R^*-1-k^*_h\tau^*_{\mathrm{cr}})}\cdot\epsilon\right), \tag{2.86}$$

$$\begin{aligned}\mathrm{COD}^*_{\mathrm{nw}} \approx{}& \frac{1-R^*+\tau^*_{\mathrm{cr}}\,k^*_d}{R^*-1+(1-k^*_d)\,\tau^*_{\mathrm{cr}}} + \frac{X^*_{s,0}}{1-R^*+k_h\tau^*_{\mathrm{cr}}}\\ &+\left[\frac{R^*-1}{\left(R^*-1+\tau^*_{\mathrm{cr}}-k^*_d\tau^*_{\mathrm{cr}}\right)^2} + \frac{k^*_h X^*_{s,0}}{(R^*-1-k^*_h\tau^*_{\mathrm{cr}})}\right]\cdot\epsilon,\end{aligned} \tag{2.87}$$

$$\begin{aligned}\mathrm{VSS}^*_{\mathrm{nw}} \approx{}& \frac{X^*_{i,0}}{1-R^*} + \frac{X^*_{s,0}}{1-R^*+k^*_h\tau^*_{\mathrm{cr}}}\\ &+\left(\frac{k^*_h X^*_{s,0}}{(-1+R^*-k^*_h\tau^*_{\mathrm{cr}})\,(1-R^*+k^*_h\tau^*_{\mathrm{cr}})} + \left(1+\frac{f_i k^*_d}{1-R^*}\right)a_2\right)\epsilon,\end{aligned} \tag{2.88}$$

$$\epsilon = \tau^* - \tau^*_{\mathrm{cr}}, \tag{2.89}$$

where

$$a_2 = G\left(\frac{A_\epsilon B_\epsilon D_\epsilon - C_\epsilon}{H_\epsilon\tau^*_{\mathrm{cr}}} + \frac{C_\epsilon E_\epsilon}{I_\epsilon}\right),$$

and

$$a_3 = \left(A_\epsilon B_\epsilon F_\epsilon + C_\epsilon E_\epsilon\tau^*_{\mathrm{cr}}\right)\left(\frac{f_i k^*_d G_\epsilon}{(1-R^*)I_\epsilon}\right).$$

The coefficients in these formula are

$$
\begin{aligned}
A_\epsilon &= \frac{\tau^*_{\rm cr}}{R^* - 1 + (1 - k^*_d)\,\tau^*_{\rm cr}},\\
B_\epsilon &= (1 - R^*)\left(\frac{k^*_h \alpha_{g,h} X^*_{s,0}}{(1 - R^* + k^*_h \tau^*_{\rm cr})^2} + \frac{1}{(R^* - 1 + (1 - k^*_d)\tau^*_{\rm cr})^2}\right),\\
C_\epsilon &= k^*_h\left[(k^*_d - 1)(S^*_0 + \alpha_{g,h} X^*_{s,0}) + k^*_d\right]{\tau^*_{\rm cr}}^2 + (1 - R^*)[k^*_h(1 + S^*_0 + \alpha_{g,h} X^*_{s,0})\\
&\quad + S^*_0(1 - k^*_d) + k^*_d]\tau^*_{\rm cr} + (1 - R^*)^2(1 + S^*_0),\\
D_\epsilon &= (R^* - 1 - k^*_h \tau^*_{\rm cr})\,(R^* - 1 + (1 - k^*_d)\tau^*_{\rm cr})^2\,,\\
E_\epsilon &= \frac{(R^* - 1)(1 - f_s \alpha_{g,s} k^*_d)}{(R^* - 1 + (1 - k^*_d)\tau^*_{\rm cr})^2},\\
F_\epsilon &= (R^* - 1 + (f_s \alpha_{g,s} - 1) k^*_d \tau^*_{\rm cr})\,(R^* - 1 - k^*_h \tau^*_{\rm cr})\,(R^* - 1 + (1 - k^*_d)\tau^*_{\rm cr})\,,\\
G_\epsilon &= \frac{1}{1 - R^* + (1 - f_s \alpha_{g,s}) k^*_d \tau^*_{\rm cr}},\\
H_\epsilon &= (R^* - 1 - k^*_h \tau^*_{\rm cr})\,(R^* - 1 + (1 - k^*_d)\tau^*_{\rm cr})\,,\\
I_\epsilon &= (R^* - 1 + (f_s \alpha_{g,s} - 1) k^*_d \tau^*_{\rm cr})\,(R^* - 1 - k^*_h \tau^*_{\rm cr})\,.
\end{aligned}
$$

The asymptotic solutions (2.86)-(2.83) are plotted against the exact solutions in figure 2.4. These figures show that the asymptotic solutions are only valid in a small region near the washout point.

2.4.5 Steady-state diagram

Figure 2.5 shows steady state diagrams for the four state variables in the model. In figure 2.5(a) the soluble substrate increases along the washout branch, as it is clear from equation (2.49) as additional soluble substrate is produced by the hydrolysis of the insoluble substrate and there is no biomass to consume it. After the transcritical bifurcation the soluble substrate is a decreasing function of the residence time as shown in equation (2.63). From equation (2.76) we know that in the limit when the residence time approaches infinity the soluble substrate concentration approaches the limiting value $S^* = k^*_d/(1 - k^*_d)$.

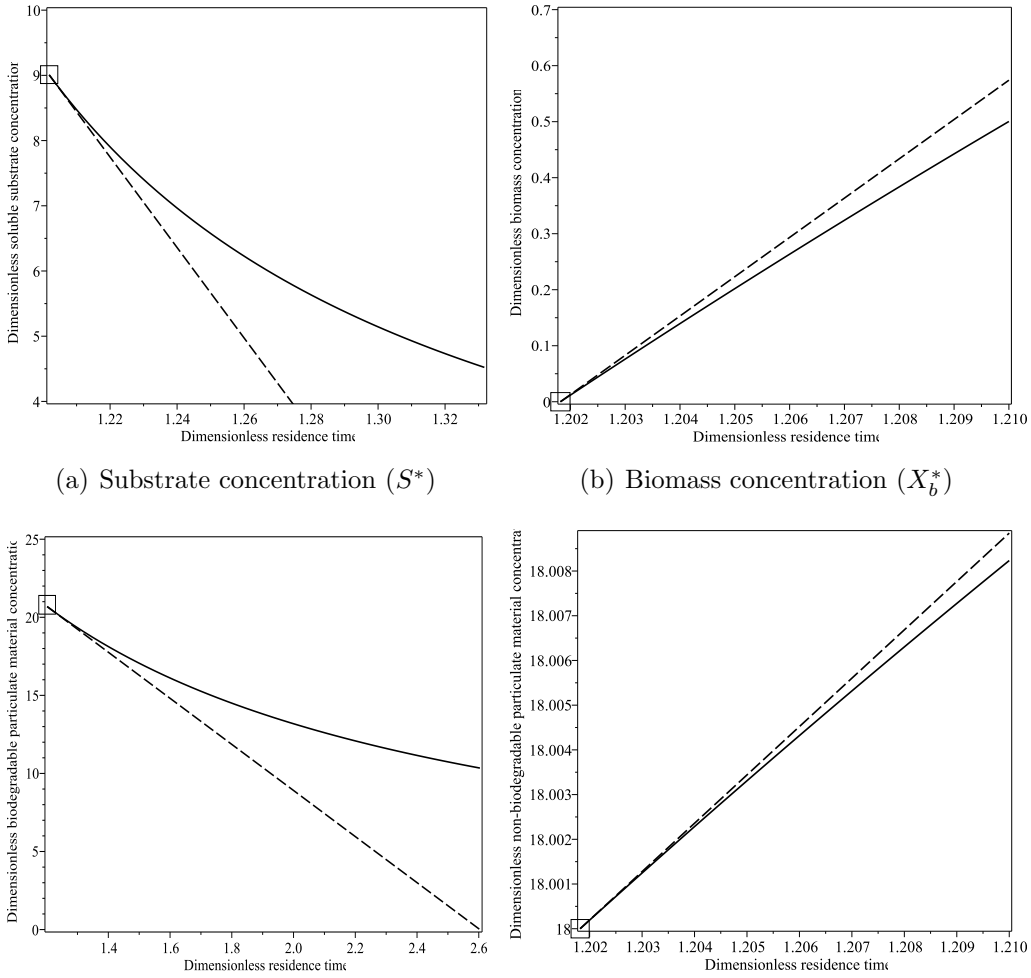

(a) Substrate concentration (S^*)

(b) Biomass concentration (X_b^*)

(c) Biodegradable substrate concentration (X_s^*)

(d) Inert concentration X_i^*

Figure 2.4: Asymptotic solutions near the trans-critical bifurcation ($\tau_{\text{cr}}^* = 1.2018$). The line shows the exact steady state value and the dash line shows the asymptotic value.

Figure 2.5(b) shows that the biomass is zero along the washout branch. After the trans-critical bifurcation it increases sharply to a maximum vale ($X_b^* = 7.5128$) when $\tau_{\text{max}}^* = 2.9459$, thereafter there is a gradual decreasing along the no-washout branch. From equation (2.77) we know that in the limit when the residence time approaches infinity the biomass concentration approaches the limiting value $X_b^* = 0$. Figure 2.5(c) shows that the insoluble substrate concentration decreases exponentially with the residence time towards the limiting value zero.

Figure 2.5(d) shows that along the washout branch the inert fraction is equal to

the influent value.

After the trans-critical bifurcation it increases. Along the no-washout branch the steady-state biomass concentration is non-zero. Consequently there is a contribution to the pool of inert material through the decay of biomass. From equation (2.78) we know that in the limit when the residence time approaches infinity the inert concentration approaches the limiting value $(X^*_{i,0} + f_i k^*_d a_0)/(1 - R^*)$. This has two components the first component due to the inflow and the second component due to the death of biomass.

2.4.6 The chemical oxygen demand

Figure 2.6 shows the chemical oxygen demand as a function of the residence time when there is no recycle ($R^* = 0$).

When there is no recycle the chemical oxygen demand is constant along the washout branch ($\tau^* < \tau^*_{\mathrm{cr}} = 1.2018$).

$$\mathrm{COD}^*_w = S^*_0 + \frac{(1 + k^*_h \tau^*)\alpha_{g,h} X^*_{s,0}}{1 - R^* + k^*_h \tau^*},$$

$$\mathrm{COD}^*_w(R^* = 0) = S^*_0 + \alpha_{g,h} X^*_{s,0} = \mathrm{COD}^*_{\mathrm{in}} = 10.1788.$$

Along the no-washout branch the chemical oxygen demand is a decreasing function of the residence time, as shown by equation (2.66). From equation (2.80) it has limiting value when the residence time approaches infinity ($\tau^* \to \infty$) given by

$$\lim_{\tau^* \to \infty} \mathrm{COD}^*_{\mathrm{nw}} = \frac{k^*_d}{1 - k^*_d} = 0.0732. \tag{2.90}$$

The efficiency at which the chemical oxygen demand is removed is defined by

$$E_{\mathrm{COD}^*} = \frac{\mathrm{COD}^*_{\mathrm{in}} - \mathrm{COD}^*_{\mathrm{out}}}{\mathrm{COD}^*_{\mathrm{in}}}.$$

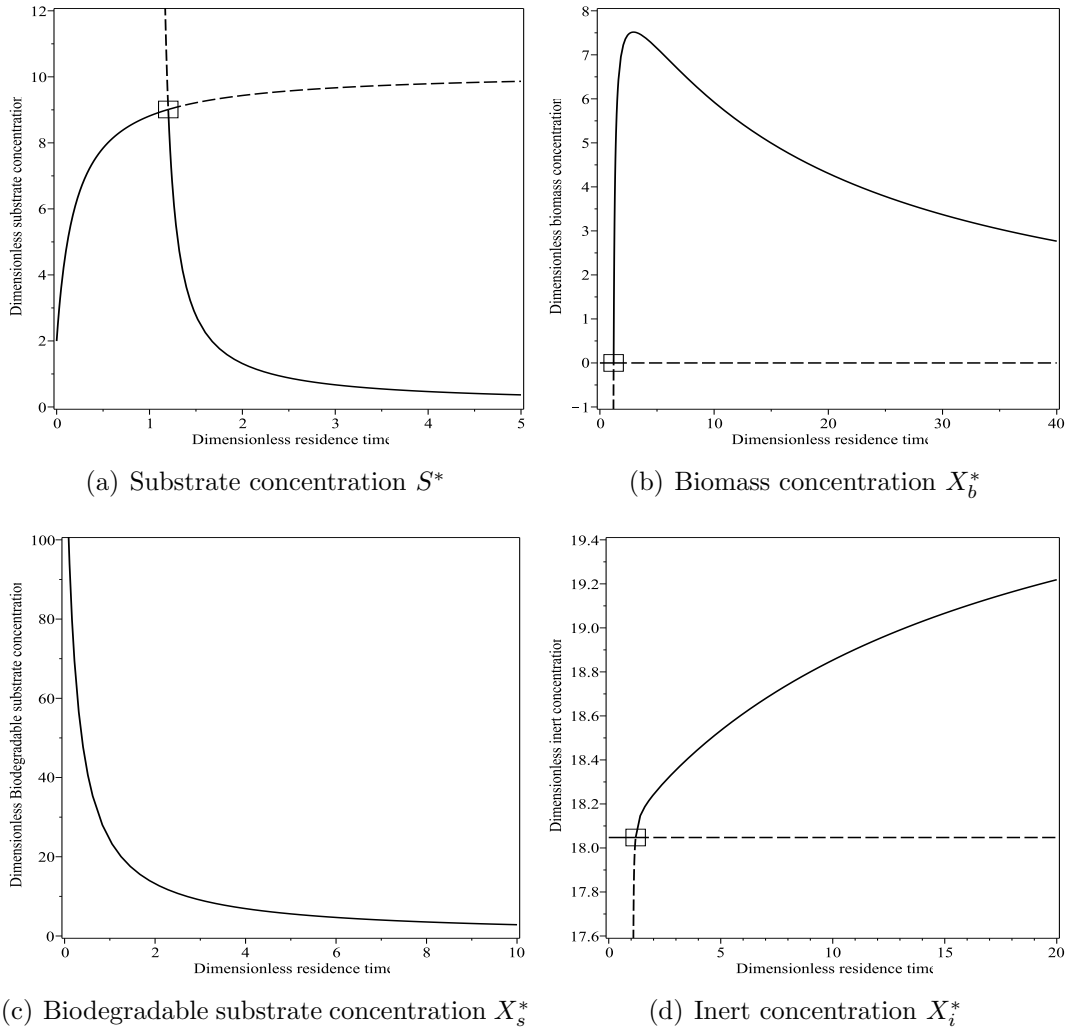

(a) Substrate concentration S^*

(b) Biomass concentration X_b^*

(c) Biodegradable substrate concentration X_s^*

(d) Inert concentration X_i^*

Figure 2.5: Steady-state diagrams showing the variation of dimensionless substrate concentration (S^*), biomass concentration (X_b^*), biodegradable substrate concentration (X_s^*) and inert concentration (X_i^*) as a function of the dimensionless residence time (τ^*). The solid line is stable and the dashed is unstable. The box denotes the location of the trans-critical bifurcation. Parameter value $R^* = 0$.

From equation (2.90) the efficiency can not be increased over the limiting value

$$E_{\mathrm{COD}^*_{\mathrm{nw}}}(\tau^* = \infty) = 0.9928.$$

This means that it is impossible to remove more that 99.28% of the chemical oxygen demand flowing into the reactor.

When $E_{\mathrm{COD}^*} = 0.90$, the chemical oxygen demand in the effluent has been reduced

to 90% of the value in the influent. The required value of the residence time is τ^*=3.4131 (15.5 days). On figure 2.6 the residence time requested to obtain the target value $E_{\mathrm{COD}^*} = 0.9$ is indicated by the horizontal line.

In order to reduce the chemical oxygen demand in the effluent to 1% of the value in the influent ($E_{\mathrm{COD}^*} = 0.99$) the required value of the residence time is τ^*=97.0394 (441.1 days).

In general, suppose that we fix a target value for the chemical oxygen demand (COD_t^*). Then equating this value with the steady state expression (2.60) and rearranging we find that the required value of the residence time is a root of the quadratic equation.

$$Q(\tau_{\mathrm{COD}}^*) = a_{\mathrm{COD}}\tau^{*2} + b_{\mathrm{COD}}\tau^* + c_{\mathrm{COD}}, \tag{2.91}$$

where

$$\begin{aligned}
a_{\mathrm{COD}} &= \left(k_d^*\left(1+\mathrm{COD}^*{}_t\right) - \mathrm{COD}^*{}_t\right)k_h^*,\\
b_{\mathrm{COD}} &= (1-R^*)\left[\left(k_d^*+k_h^*\right)\left(1+\mathrm{COD}^*{}_t\right) - \mathrm{COD}^*{}_t\right] + \alpha_{g,h}X_{s,0}^*\left(1-k_d^*\right),\\
c_{\mathrm{COD}} &= (1-R^*)\left[(1-R^*)\left(1+\mathrm{COD}^*{}_t\right) - \alpha_{g,h}X_{s,0}^*\right].
\end{aligned}$$

The coefficient a_{COD} is negative because we have

$$\begin{aligned}
\mathrm{COD}_{\mathrm{in}}^* > \mathrm{COD}_t^* > \mathrm{COD}_{\mathrm{out}}^*(\tau^*=\infty) &= \frac{k_d^*}{1-k_d^*},\\
\Rightarrow \mathrm{COD}_t^* &> \frac{k_d^*}{1-k_d^*},\\
\Rightarrow 1+\mathrm{COD}_t^* &> \frac{1}{1-k_d^*},
\end{aligned}$$

$$\begin{aligned}
\Rightarrow (1+\mathrm{COD}_t^*)k_d^* &> \frac{k_d^*}{1-k_d^*},\\
\Rightarrow (1+\mathrm{COD}_t^*)k_d^* - \mathrm{COD}_t^* &< 0.
\end{aligned}$$

A root of equation (2.91) is only physically meaningful if it is larger than the washout value (τ^*_{cr}). For the cases $E_{\mathrm{COD}^*} = 0.90$ and $E_{\mathrm{COD}^*} = 0.99$ considered previously the second root was positive but smaller than the critical value and therefore it is not physically meaningful. These values were $\tau^* = 0.4102$ when $E_{\mathrm{COD}^*} = 0.90$ and $\tau^* = 0.5432$ when $E_{\mathrm{COD}^*} = 0.99$.

We can see graphically that when the target value is between two limiting values [$\mathrm{COD}^*(\tau^* = \infty) < \mathrm{COD}^*(\tau^*) < \mathrm{COD}^*(\tau^* = \tau^*_{\mathrm{cr}})$] that equation (2.92) has a unique physically meaningful solution.

The physically meaningful is given by

$$\tau^*_{\mathrm{COD}^*} = \frac{-b_{\mathrm{COD}^*} - \sqrt{b^2_{\mathrm{COD}^*} - 4a_{\mathrm{COD}^*}c_{\mathrm{COD}^*}}}{2a_{\mathrm{COD}^*}} > \tau^*_{\mathrm{cr}}. \tag{2.92}$$

(The negative root is required as $a_{\mathrm{COD}} < 0$.)

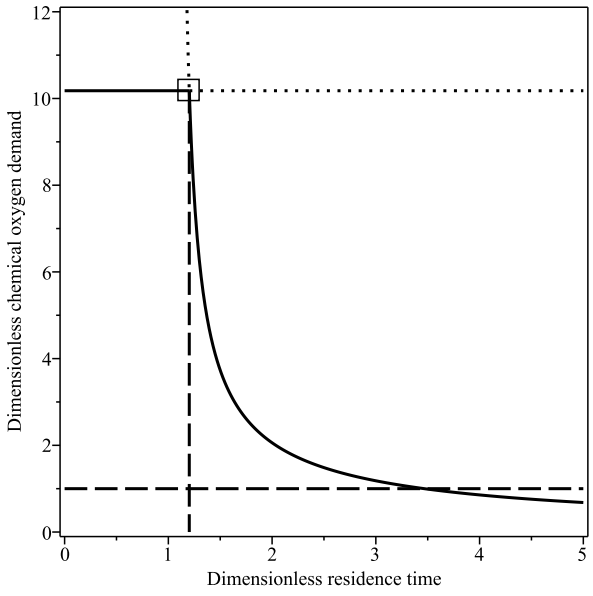

Figure 2.6: Steady state diagram for the dimensionless chemical oxygen demand. Parameter value $R^* = 0$. The horizontal line correspond to a chemical oxygen demand removal efficiency of 90%.

2.4.7 The volatile suspended solids

2.4.7.1 The case $R^* = 0$

Figure 2.7 shows a steady state diagram for the volatile suspended solids as a function of the residence time when there is no recycle ($R^* = 0$). Along the washout branch ($0<\tau^*<\tau^*_{\rm cr}$) we have

$$\mathrm{VSS}^*_w = \frac{X^*_{i,0}}{1-R^*} + \frac{X^*_{s,0}}{1-R^*+k^*_h\tau^*},$$

$$\mathrm{VSS}^*_w(R^*=0) = X^*_{i,0} + \frac{X^*_{s,0}}{1+k^*_h\tau^*}, \tag{2.93}$$

which is a decreasing function of the residence time. The volatile suspended solid is decreasing because insoluble substrate is converted to soluble substrate by hydrolysis. Its maximum value is when the residence time is zero. For the case of no recycle ($R^* = 0$) we have.

$$\mathrm{VSS}^*_{w,\max} = X^*_{i,0} + X^*_{s,0} = 163.1332.$$

When there is no settling unit ($R^* = 0$) the volatile suspended solids at the trans-critical bifurcation $\tau^*_{\rm cr} = 1.2018$ has decreased to the value $\mathrm{VSS}^*_w = 38.7474$.

After the trans-critical bifurcation the volatile suspended solids is given by

$$\mathrm{VSS}^*_{\rm nw} = \left(1+\frac{f_i k^*_d\tau^*}{1-R^*}\right)X^*_{\rm b,nw} + \frac{X^*_{i,0}}{1-R^*} + \frac{X^*_{s,0}}{1-R^*+k^*_h\tau^*}, \tag{2.94}$$

where the value for $X^*_{\rm b,nw}$ is given by equation (2.57).

The volatile suspended solids increases to a local maximum $\mathrm{VSS}^*_{\rm nw,max} = 40.1413$ when $\tau^* = 1.2396$. Thereafter it decreases toward its limiting value.

From equation (2.81) the limiting value when the residence time is infinity is given

by

$$\mathrm{VSS}^* \approx \frac{X^*_{i,0}}{1-R^*} + \frac{f_i k^*_d}{1-R^*} a_0 = X^*_{i,0} + f_i k^*_d a_0 = 56.9313,$$

where a_0=153.8593 from equation (2.82).

From equation (2.20) the target value of the volatile suspended solids is

$$\mathrm{VSS}^*_t = \frac{\mathrm{VSS}_t}{\alpha_g k_s} = \frac{12000}{\alpha_g k_s} = 77.0713.$$

From figure 2.7 we can see that there is one intersection point where the volatile suspended solids is equal to the target value and this is on the washout branch. When this happens the value of the residence time at the intersection point is found from equation (2.93). We have

$$\begin{aligned} \tau^*_{i,w} &= \frac{(1-R^*)\left[X^*_{i,0} + X^*_{s,0} - \mathrm{VSS}^*_t\ (1-R^*)\right]}{\left[\mathrm{VSS}^*_t\ (1-R^*) - X^*_{i,0}\right] k^*_h}, \\ &= 0.2916. \end{aligned} \tag{2.95}$$

For these particular parameter values we see that along the no-washout branch the volatile suspended solids is always below the target value. As westwater plants always operates along the no-washout branch we have the desirable situation that the sludge content is always below the target value.

2.4.7.2 The case $R^*>0$

From figure 2.7 we can see that by varying the location of the target line, there are five generic cases of behavior for how the target value intersects the volatile suspended solids curve.

Case one is when the target value is larger than the maximum value along the

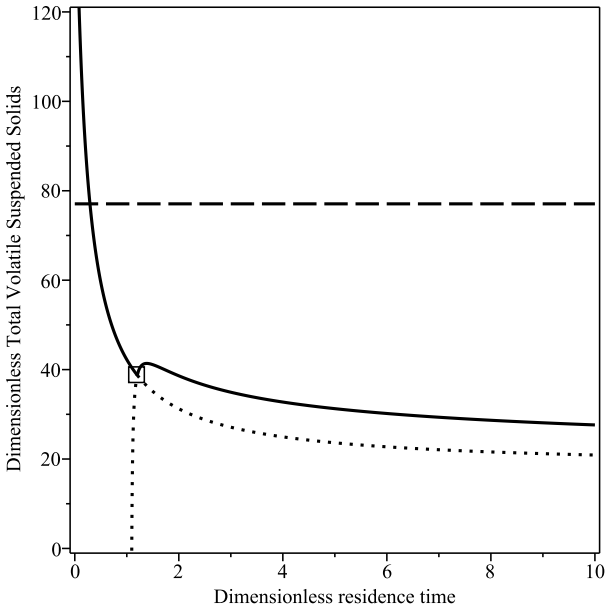

Figure 2.7: Steady state diagram for the dimensionless volatile suspended solids (case two). Parameter value $R^* = 0, \tau^*_{\text{cr}} = 1.2018$. The horizontal line denotes the target value of the dimensionless volatile suspended solids ($\text{VSS}^*_t = 77.0713$). The solid line is stable and the dotted is unstable.

washout branch, from equation (2.93) this is when $\text{VSS}^*_t > \frac{1}{1-R^*}(X^*_{i,0} + X^*_{s,0})$. In this case there are no intersection point as the volatile suspended solids are below the target value for all residence times. This is not realistic. (Technically, we also require the target value to be larger that the maximum value along the no-washout branch).

Case two is when the target value is larger than the maximum value of the volatile suspended solids along the no-washout branch but smaller than the maximum value along the washout branch. This is shown in figure 2.7. In this case there is only one intersection point, which is on the washout branch and the value of the residence time at this point is given by equation (2.95). This is a good case to have because the concentration of volatile suspended solids at any point on the no-washout branch is below the target value.

Case three occurs when the target value is between the volatile suspended solids concentration at the trans-critical bifurcation and the maximum value of the concentration of volatile suspended solids along the no-washout branch. This shown in

figure 2.8(a). In this case there are three intersection points; one intersection point along the washout branch and two intersection points along the no-washout branch. The target value is larger than the steady-state volatile suspended solids value if the residence time is between the intersection point on the washout branch and the first intersection point on the no-washout branch or larger than the second intersection point on the washout branch. In practice a wastewater treatment plant would be operated with the residence time larger than the second intersection point on the washout branch.

Case four is when the target value is larger than the asymptotic value along the no-washout branch (when the residence time approaches infinity) but smaller than the volatile suspended solids at the trans-critical bifurcation. This case is illustrated in figure 2.8(b). In this case there is one intersection point which is along the no-washout branch. In operating an activated sludge plant we require the residence time to be larger than the critical value.

Case five is when the target value is smaller than the value at both the trans-critical bifurcation and the limiting value when the residence time approaches infinity. This is shown in figure 2.8(c). In this case there are no intersection points. This case is very undesirable because it means that we can never reduce the volatile suspended solids below the target value.

There are two non-generic cases when we have two intersection points. These happen when the target value of the volatile suspended solid is either exactly equal to the maximum value along the washout branch or exactly equal to the value at the trans-critical bifurcation.

There is one non-generic case when we have one intersection point when the volatile suspended solids at infinite residence time is equal to the target value.

The location of the different regions as a fraction of the effective recycle parameter is shown in table 2.1. The calculation of the transition values is explained in the discussion section.

R^*	Case
$0 < R^* < R^*_{2,3} = 0.4631$	Case two
$R^*_{2,3} < R^* < R^*_{3,4} = 0.4972$	Case three
$R^*_{3,4} < R^* < R^*_{4,5} = 0.7387$	Case four
$R^*_{4,5} < R^*$	Case five

Table 2.1: The generic behavior of the reactor as a function of the effective recycle parameter.

2.5 Discussion ($R^* \neq 0$)

In this section we investigate the effect of the effective recycle parameter upon the performance of the reactor.

2.5.1 The chemical oxygen demand

Figure 2.9(a) shows the value of the residence time required to achieve a chemical oxygen demand efficiency of 10% ($E^*_{\text{COD}} = 0.90$) as a function of the value of the effective recycle parameter. The value of the residence time (τ^*) decreases by 50.75% from 3.4131 (15.5 days), when there is no recycle ($R^* = 0$), to 1.7320 (7.9 days), when the effective recycle parameter takes its maximum value ($R^* = 1$).

Figure 2.9(b) shows the value of the residence time required to achieve the chemical oxygen demand efficiency of 1% ($E^*_{\text{COD}} = 0.99$) as a function of the value of the effective recycle parameter. The value of the residence time(τ^*) decreases by 58.50% from 97.0394 (441.1 days), when there is no recycle ($R^* = 0$), to 56.7727 (258.1 days), when the effective recycle parameter takes its maximum value ($R^* = 1$).

In both cases the use of a settling unit has the potential to significantly decrease the required the residence time.

Note that the limiting value $R^* = 1$ is not physically meaningful because the concentration of volatile suspended solids approaches infinity, equation (2.61), even though

the chemical oxygen demand is finite.

2.5.2 The volatile suspended solids

In this section we explore in greater detail the effect of the effective recycle parameter (R^*) upon the value of the residence time at when the volatile suspended solids concentration is equal to the target value.

2.5.2.1 Intersection points on the washout branch

We start by noting that the value of the residence time when the target value is reached on the washout branch is given by equation (2.95). The value of the residence time given by this equation is physically meaningful if the target value is lower than the maximum value along the washout branch, which is found by substituting $\tau^* = 0$ into equation (2.93), and greater than the value at the washout branch, which is found by substituting $\tau^* = \tau^*_{\text{cr}}$ in equation (2.93). It is not physically meaningful when the intersection point is either negative or larger than the washout value.

2.5.2.2 Intersection point on the no-washout branch

We now investigate when there is an intersection point along the no-washout branch. This happens when

$$\text{VSS}^*_{\text{nw}} = \left(1 + \frac{f_i k^*_d \tau^*}{1 - R^*}\right) X^*_b + \frac{X^*_{i,0}}{1 - R^*} + \frac{X^*_{s,0}}{1 - R^* + k^*_h \tau^*} = \text{VSS}^*_{\text{t}}. \tag{2.96}$$

Rearranging equation (2.96) and using equations (2.49), (2.56) and (2.57) to substitute for the biomass concentration (X^*_b) the intersection point is found to solve the cubic equation

$$a_{\text{VSS}} \tau^{*3} + b_{\text{VSS}} \tau^{*2} + c_{\text{VSS}} \tau^* + d_{\text{VSS}} = 0, \tag{2.97}$$

where the coefficients are

$$\begin{aligned}
a_{\mathrm{VSS}^*} &= -k_h^* f_i k_d^* \left[\left(\alpha_{g,h} X_{s,0}^* + S_0^*\right)\left(1-k_d^*\right) - k_d^*\right] \\
&\quad + k_d^*\left(1 - f_s\alpha_{g,s}\right)\left(1-k_d^*\right)\left[-X_{i,0}^* k_h^* + \mathrm{VSS}_t^*\, k_h^*\left(1-R^*\right)\right] \\
&= 17.4256 - 23.5900 R^*, \\
b_{\mathrm{VSS}^*} &= -(1-R^*)\left\{-\left[\left(k_d^*+k_h^*\right)\left(S_0^*+1\right) + k_h^*\alpha_{g,h}X_{s,0}^* - S_0^*\right] f_i k_d^*\right. \\
&\quad + k_h^*\left[\left(\alpha_{g,h}X_{s,0}^* + S_0^*\right)\left(1-k_d^*\right) - k_d^*\right] \\
&\quad - \left(1 - 2\,k_d^* + f_s\alpha_{g,s}k_d^*\right)\left[-X_{i,0}^* k_h + \mathrm{VSS}_t^* k_h^*\left(1-R^*\right)\right] \\
&\quad \left. + k_d^*\left(1-f_s\alpha_{g,s}\right)\left(1-k_d^*\right)\left[X_{i,0}^* + X_{s,0}^* - \mathrm{VSS}_t^*\left(1-R^*\right)\right]\right\} \\
&= 338.5591 R^{*2} - 542.5998 R^* + 204.0408, \\
c_{\mathrm{VSS}^*} &= (1-R^*)^2\left[\left(S_0^*+1\right) f_i k_d^* + \left(k_d^*+k_h^*\right)\left(S_0^*+1\right) + k_h^*\alpha_{g,h}X_{s,0}^* - S_0^* + X_{i,0}^* k_h^*\right. \\
&\quad \left. -\mathrm{VSS}_t^* k_h^*\left(1-R^*\right) - \left(1-2\,k_d^*+f_s\alpha_{g,s}k_d^*\right)\left(X_{i,0}^* + X_{s,0}^* - \mathrm{VSS}_t^*\left(1-R^*\right)\right)\right] \\
&= 318.5883 R^{*3} - 952.7099 R^{*2} + 949.6549 R^* - 315.5333,
\end{aligned}$$

$$\begin{aligned}
d_{\mathrm{VSS}^*} &= -\left(1-R^*\right)^3\left[-S_0^* - 1 - X_{i,0}^* - X_{s,0}^* + \mathrm{VSS}_t^*\left(1-R^*\right)\right] \\
&= -77.0713 R^{*4} + 142.1560 R^{*3} + 35.9598 R^{*2} - 190.1024 R^* + 89.0579.
\end{aligned}$$

For a given value of the effective recycle parameter, R^*, equation (2.97) is readily solved to find the corresponding values for the intersection points. These values are only physically meaningful if they are larger than the value of the residence time at the trans-critical bifurcation point (τ_{cr}^*).

Information regarding the location of all intersection points is summarized in figure 2.10. In this figure the dotted line is the critical value for the residence time (τ_{cr}^*), it is a linearly decreasing function of the effective recycle parameter-as shown by equation (2.71). The dash line is the intersection point along the washout branch equation is given by (2.95). This is only physically meaningful when it is lower than the dotted line. The solid line is the intersection point along the no-washout branch

equation, found from equation (2.97). These are only physically meaningful when they are higher than dotted line.

For example when R^*=0 there is one physically meaningful intersection point which is on the washout branch ($\tau^*_{i,w}$=0.2916). The corresponding steady-state digram is shown in figure 2.7. When R^*=0.48 there are three physically meaningful intersection points, one along the washout branch and two intersection points along the no-washout branch ($\tau^*_{i,w}$=0.5809, $\tau^*_{\mathrm{i,nw1}}$=0.6433, $\tau^*_{\mathrm{i,nw2}}$=0.8901). The corresponding steady-state digram is shown in figure 2.8(a). When R^*=0.6 there is only one physically meaningful intersection point along the no-washout branch ($\tau^*_{\mathrm{i,nw}}$=2.1478). The corresponding steady-state digram is shown in figure 2.8(b). When R^*=0.8 there are no physically meaningful intersection points. The corresponding steady-state digram is shown in figure 2.8(c). Table 2.2 shows all the intersection points, including the physically non-meaningful points.

R^*	τ^*_{cr}	$\tau^*_{i,w}$	$\tau^*_{\mathrm{i,nw}}$
0	1.2018	0.2916	0.3772, 1.0327, -13.1192
0.48	0.6249	0.5809	0.6433, 0.8901, -5.0725
0.6	0.4807	0.8281	0.4543, 2.1478, -2.7127
0.8	0.2404	-2.2439	0.2211, -0.4169, -9.0415

Table 2.2: Different values of the effective recycle parameter, value of the critical value of the residence time and the intersection points along the washout and the no-washout branch.

2.5.2.3 The transition from case two to case three ($R^*_{2,3}$=0.4631).

Case two (figure 2.7) happens when there is one intersection point along the washout branch. Case three (figure 2.8(a)) happens when there are three intersection points, one along the washout branch and two along the no-washout branch. The transition from case two to case three occurs when the target value is equal to the maximum value of the volatile suspended solids along the no-washout branch (VSS_t =

$\text{VSS}_{\text{nw,max}}$). In figure 2.10(a) two limit points are visible along the curve of intersection points for the no-washout branch. These are found by solving the equations

$$\tau^*_{\text{i,nw}} = 0 \quad \text{and} \quad \frac{d}{d\tau^*}\tau^*_{\text{i,nw}} = 0,$$

subject to

$$\frac{d^2}{d\tau^{*2}}\tau^*_{\text{i,nw}} \neq 0 \quad \text{and} \quad \frac{d}{dR^*}\tau^*_{\text{i,nw}} \neq 0.$$

The location of these limit points are (R^*, τ^*)=(1,0), (0.2371,0.6582) and (0.4631,0.7424). If the effective recycle parameter is between 0 and 0.2371 then there are no physically meaningful intersection points along the no-washout branch because their value is lower than the trans-critical bifurcation. Over this range only the intersection point on the no-washout branch is physically meaningful. The volatile suspended solids steady-state diagram is case two. If the effective recycle parameter is between 0.2371 and 0.4631 there are no positive intersection points on the no-washout branch. There is one intersection point on the washout branch and the volatile suspended solids steady-state diagram remains case two.

If the effective recycle parameter is slightly higher than 0.4631 then there are three physically meaningful intersection points: one intersection point along the washout branch and two intersection points along the no-washout branch. The volatile suspended solids steady-state diagram is case four.

2.5.2.4 The transition from case three to case four ($R^*_{3,4}$=0.4972).

As discussed in the previous section case three (figure 2.8(a)) happens when there are three intersection points, one along the washout branch and two along the no-washout branch. Case four (figure 2.8(b)) happens when there is one intersection point along the no-washout branch. The transition occurs when the value of the volatile suspended solids at the trans-critical bifurcation is equal to the target value

$(\text{VSS}^*(\tau^*_{\text{cr}}) = \text{VSS}^*_t)$.

Note that from equation (2.71) the value of the residence time at the trans-critical bifurcation is a linearly decreasing function of the effective recycle parameter ($\frac{d\tau^*_+}{dR^*}<0$). It has a minimum value 0 when $R^* = 1$.

Figure 2.11 shows the volatile suspended solids concentration at the trans-critical bifurcation as a function of of the effective recycle parameter. When the effective recycle ratio is sufficiently small (large) the value of the volatile suspended solids at the intersection point is below (above) the critical value. The intersection point at $R^* = R^*_{3,4} \approx 0.4972$ denotes the transition from case three to case four. The figure shows that when the effective recycle parameter is small, the increase in the volatile suspended solids is small but as the effective recycle parameter approaches one then the increase is dramatic (exponential).

From (2.71) the value of the residence time at the trans-critical bifurcation is given by

$$\tau^*_+ = (1 - R^*)\tau^*_{\text{cr}}(R^* = 0), \tag{2.98}$$

where

$$\begin{aligned}
\tau^*_{\text{cr}}(R^* = 0) &= \frac{b^* + \sqrt{b^{*2} + 4ac^*}}{2a}, \\
a &= [(S^*_0 + \alpha_g X^*_{s,0}) - (1 + S^*_0 + \alpha_g X^*_{s,0})k^*_d]k^*_h, \\
b^* &= (1 + S^*_0)(k^*_h + k^*_d) + k^*_h \alpha_g X^*_{s,0} - S^*_0, \\
c^* &= (1 + S^*_0).
\end{aligned}$$

To draw figure 2.11, we fixed the value for the effective recycle parameter and then calculated the value of the trans-critical bifurcation using equation (2.98). This value is then substituted into equation (2.93) to determine the corresponding value for the volatile suspended solids. Equating equation (2.93) to the target value and

using equation (2.98) we find that the transition happens when

$$(1 - R^*_{3,4}) \left\{ \mathrm{VSS}^*_t (1 - R^*_{3,4}) \left[1 + k^*_h \tau^*_{\mathrm{cr}} (R^* = 0) \right] - (X^*_{i,0} + X^*_{s,0}) \left[1 + k^*_h \tau^*_{\mathrm{cr}} (R^* = 0) \right] \right\},$$

$$\Rightarrow R^*_{3,4} = 1 \quad \text{or}$$
$$\Rightarrow R^*_{3,4} = \frac{(\mathrm{VSS}^*_t - X^*_{i,0}) \left[1 + k^*_h \tau^*_{\mathrm{cr}} (R^* = 0) \right] + X^*_{s,0}}{\mathrm{VSS}^*_t \left[1 + k^*_h \tau^*_{\mathrm{cr}} (R^* = 0) \right]} = 0.4972.$$

Note that the solution $R^*_{3,4} = 1$ is invalid because equation (2.93) is not defined for this value.

If the effective recycle parameter is smaller than the critical value of the effective recycle parameter ($R^* < R^*_{3,4}$) then the volatile suspended solids at the trans-critical bifurcation is smaller than the target value. Therefore there is an intersection point on the no-washout branch. The volatile suspended solids steady-state diagram will be either case two or case three. If the effective recycle parameter is larger than the critical value ($R^* > R^*_{3,4}$) then the volatile suspended solids at the trans-critical bifurcation is larger than the target value. Therefore if there is an intersection point it is along the no-washout branch. The intersection points along the no-washout branch are physically meaningful if they are larger than the value of the trans-critical bifurcation. The volatile suspended solids steady-state diagram will be either case four or case five. If the effective recycle parameter is between 0.4972 and 0.7387 there are two intersection points on the no-washout branch but only one is physically meaningful.

2.5.2.5 The transition from case four to case five ($R^*_{4,5}$=0.7387).

Case four (figure 2.8(b)) happens when there is one physically meaningful intersection point along the no-washout branch. Case five (figure 2.8(c)) happens when there is no intersection point. The transition from case four to case five occurs when

the target value is equal to the asymptotic value of the volatile suspended solids in the limit as the residence time approaches infinity. In table 2.1 we stated that this transition occurred when $R^*_{4,5} = 0.7387$

Figure 2.10 also shows that when the effective recycle parameter is larger than the critical value $R^*_{4,5} = 0.7387$ there is no physically meaningful intersection point on the no-washout branch. The intersection point on the washout branch is not physically meaningful because it is larger than the trans-critical bifurcation.

Setting the leading term of the asymptotic solution for the volatile suspended solids at large residence time (2.81) equal to the target value we find that

$$R^*_1 = 1 \quad \text{and} \tag{2.99}$$

$$R^*_{4,5} = \frac{(1-k^*_d)[(1-f_s\alpha_{g,s})(\mathrm{VSS}^*_t - X^*_{i,0}) - \mathrm{COD}^*_{\mathrm{in}} f_i] + f_i k^*_d}{(1-k^*_d)[1-f_s\alpha_{g,s}]\mathrm{VSS}^*_t} = 0.7387, \tag{2.100}$$

where the coefficient a_0 is given by equation (2.82).

Differentiating equation (2.100) with respect to the chemical oxygen demand in the feed we obtain

$$\frac{dR^*_{4,5}}{d\mathrm{COD}^*_{\mathrm{in}}} = -\frac{f_i}{(1-f_s\alpha_{g,s})\mathrm{VSS}^*_t} < 0. \tag{2.101}$$

When the effective recycle parameter is smaller than the critical value ($R^* < R^*_{4,5}$) then the asymptotic value of the volatile suspended solids is below the target value $\mathrm{VSS}^*(\tau^* = \infty) < \mathrm{VSS}^*_{\mathrm{t}}$. In this case there is at least one intersection point along the no-washout branch.

When the effective recycle parameter is larger than the critical value ($R^* > R^*_{4,5}$) then the asymptotic value of the volatile suspended solids is larger than the target value $\mathrm{VSS}^*(\tau^* = \infty) > \mathrm{VSS}^*_{\mathrm{t}}$.

Therefore the volatile suspended solids is always larger than the target value.

Note that there is also a vertical asymptote for the intersection along the no-washout branch. Of course this asymptote is not of physical interest since the intersection

points on the washout branch occurs for values of the residence time higher than that at the trans-critical bifurcation.

From equation (2.95) we have a valid asymptote when

$$\begin{aligned} &\mathrm{VSS}_t^* \ (1 - R^*) - X_{i,0}^* k_h^* = 0, \\ &\Rightarrow R^* = R_{\mathrm{wcr},\infty}^* = \frac{\mathrm{VSS}_t^* - X_{i,0}^*}{\mathrm{VSS}_t^*} = 0.7658. \end{aligned}$$

2.5.2.6 Summary of transitions

Figure 2.12 shows the transitions from case two to case three, case three to case four, and from case four to case five. Figure 2.12(a) shows the transition point from case two to case three ($R_{2,3}^*$=0.4631) and the transition from case three to case four ($R_{3,4}^*$=0.4972). Figure 2.12(b) shows the transition point from case four to case five ($R_{4,5}^*$=0.7387).

2.5.2.7 The effect of partitioning the chemical oxygen demand

In section 2.5.2.5 we fond that if the effective recycle parameter is larger than a critical value of the effective recycle parameter (R^*>$R_{4,5}^*$) then the volatile suspended solids at infinity is larger than the target value. Therefore there is no physically meaningful intersection point on the no-washout branch.

Suppose that the chemical oxygen demand in the feed is fixed. Does the critical value of the effective recycle parameter for the transition from case four to case five $R_{4,5}^*$ depend upon how the chemical oxygen demand is partitioned into the components S_0^* and $X_{s,0}^*$? Examining equations (2.82) and (2.100) we see that the critical value of the effective recycle parameter depends *only* upon the total chemical oxygen demand in the influent not the individual components (S_0^* and $X_{s,0}^*$). This result makes sense because at large residence time almost all of the insoluble substrate is

converted to the soluble substrate, equation (2.59).

Figure 2.13 shows that the effective recycle parameter $R^*_{4,5}$ is a decreasing function of the chemical oxygen demand $\mathrm{COD}^*_{\mathrm{in}}$, as shown by equation (2.101). Cases one to four happen when the chemical oxygen demand is smaller than $\mathrm{COD}^*_{\mathrm{in}}$ and when the chemical oxygen demand is bigger than $\mathrm{COD}^*_{\mathrm{in}}$ case five happens.

Substituting equation (2.82) into equation (2.100) we have $\mathrm{COD}^*_{\mathrm{in}}(R^*_{4,5} = 0)$ =285.1343. If the chemical oxygen demand in the feed is higher than 285.1343 then the volatile suspended solids for any value of the residence time is always larger than the target value. In other words, if the feed is too polluted it is impossible to reduce the volatile suspended solids below the target value even though it is possible to reduce the chemical oxygen demand to the limiting value $k^*_d/(1 - k^*_d)$.

2.5.2.8 Model simplification

If we assume that there is no inert material flowing in the feed ($X^*_{i,0} = 0$), which is a common assumption in mathematical modeling, then from equation (2.100) we have

$$R^*_{4,5} = \frac{\mathrm{VSS}^*_{\mathrm{t}} - f_i k^*_d a_0}{\mathrm{VSS}^*_{\mathrm{t}}} = 0.9728.$$

Even if no inert material flows into the reactor it is generated inside the reactor by the decay of biomass.

Note that in the basic model the degradation products from biomass decay are ignored. This corresponds to setting ($f_i = 0$). In this case ($R^*_{4,5} = 1$).

Removal of inert material from the feed stream prior to entering the activated sludge process significantly increases the value of the effective recycle parameter in the transition from case five to case four.

2.5.2.9 The effect of changing COD^*_{in}

In the previous two sections we investigate the effect of changing the effective recycle ratio (R^*) whilst the value for the chemical oxygen demand in the feed (COD^*_{in}) was fixed. In this section we change the value of the chemical oxygen demand in the feed (COD^*_{in}) to investigate how this effects the behavior. We write

$$\begin{aligned} S^*_0 &= AS^*_{0,\text{old}}, \\ X^*_{s,0} &= AX^*_{\text{s,0,old}}, \\ \text{COD}^*_{\text{in}} &= A\text{COD}^*_{\text{in,old}}, \end{aligned} \tag{2.102}$$

where $S^*_{0,\text{old}}$ and $X^*_{\text{s,0,old}}$ are the values for the soluble and insoluble substrate used in the previous section i.e. $S^*_{0,\text{old}}$=1.9961 and $X^*_{\text{s,0,old}}$=145.0857. The value of A is $0<A\leq 1$. We first note that as the chemical oxygen demand in the feed (COD^*_{in}) is decreased there is a critical value below which the washout branch is stable for all values of the residence time.

To find this critical value we substitute equation (2.102) into equation (2.73) and rearrange to obtain

$$A_{\text{cr}} = \frac{1}{\text{COD}^*_{\text{in,old}}}\left(\frac{k^*_d}{1-k^*_d}\right) = 0.0072.$$

This means that if $\text{COD}^*_{\text{in}} \leq A_{\text{cr}}\text{COD}^*_{\text{in,old}}$=0.0072(0.9105)=0.0066 then process failure occurs. We now investigate where the different volatile suspended solids steady-state solution digrams occur as a function as the effective recycle ratio (R^*) and the value of the chemical oxygen demand in the feed (though the parameter A).

The dotted vertical line in figure 2.14 represents the value A_{cr}, below which process failure automatically occurs. Line 1 in figure 2.14 shows where the volatile suspended solids on the washout branch at zero residence time is equal to the target value of the volatile suspended solids ($\text{VSS}^*_{\text{w}}(\tau^*=0)=\text{VSS}^*_{\text{t}}$). The line marks

the transition from case one, where there are no intersection points and the volatile suspended solids is smaller than the target value as shown in figure 2.15(a), to case two, where there is one intersection point along the washout branch as shown in figure 2.15(b).

Using equation (2.53) when the residence time is zero we obtain the formula for the transition from case one to case two:

$$A_{12} = \frac{\mathrm{VSS}^*_{\mathrm{t}}(1 - R^*) - X^*_{i,0}}{X^*_{\mathrm{s},0,\mathrm{old}}}.$$

Line 2 in figure 2.14 shows the transition where the target value of the volatile suspended solids is equal to the maximum value of the volatile suspended solids along the no-washout branch ($\mathrm{VSS}^*_{\mathrm{nw}} = \mathrm{VSS}^*_{\mathrm{t}}$). The line marks the transition from case two, where there is one intersection point along the washout branch, as shown in figure 2.15(b), to case three, where there are three intersection points; one along the washout branch and two along the no-washout branch as shown in figure 2.15(c).

To find this transition, A_{23}, we write $G = \mathrm{VSS}^*_{\mathrm{nw}} - \mathrm{VSS}^*_{\mathrm{t}}$ and solve the system of equation $G = 0$ and $\frac{dG}{d\tau^*}$=0.

Line 3 in figure 2.14 shows the transition where the concentration of volatile suspended solids along the no-washout branch at the critical value of the residence time is equal to the target value $\mathrm{VSS}^*_{\mathrm{nw}}(\tau^* = \tau^*_{\mathrm{cr}}) = \mathrm{VSS}^*_{\mathrm{t}}$. This line makes the transition from case three, where there are three intersection points (one along the washout and two along the no-washout branch) as shown in figure 2.15(c), to case four, where there is one intersection point along the no-washout branch, as shown in figure 2.15(d).

To find this transition we equate equation (2.53) to the target value and set the residence time equal to the critical value, equation (2.72). We obtain the formula

for the transition from case three to four:

$$A_{34} = \frac{[(1 - R^*)\mathrm{VSS}_{\mathrm{t}}^* - X_{i,0}^*]\{1 + k_h^* \tau_{\mathrm{cr}}^*(R^* = 0)\}}{X_{s,0}^*}.$$

Line 4 in figure 2.14 shows the transition where the volatile suspended solids along the no-washout branch at infinite residence time is equal to the target value of the volatile suspended solids ($\mathrm{VSS}_{\mathrm{nw}}^*(\tau^* = \infty) = \mathrm{VSS}_{\mathrm{t}}^*$). The line marks the transition from case four, where there is one intersection point along the no-washout branch as shown in figure 2.15(d), to case five, where there are no intersection points as shown in figure 2.15(e).

To find this transition we set equation (2.81) equal to the target value. We obtain the transition from case four to five:

$$A_{45} = \frac{(1 - k_d^*)[(1 - R^*)\mathrm{VSS}_{\mathrm{t}}^* - X_{i,0}^*]\{1 - \alpha_{g,s} f_s\} + f_i k_d^*}{f_i(1 - k_d^*)[S_0^* + \alpha_{g,h} X_{s,0}^*]}. \tag{2.103}$$

In this model regions one and two are the best, because either the volatile suspended solids is always below the target value (region one) or it is always below the target value for any residence time below the critical value (region two). If these regions existed in practice, there would be no problem with sludge formation in the activated sludge process.

In regions three and four there is a critical value for the residence time, if the residence time is larger than the critical value then the volatile suspended solids is always below the target value; this is good as values for the critical value are low.

In regions five there is no value for the residence time where the volatile suspended solids is below the target value, this undesirable.

Therefore the main question of practical important from this model is how to increase the transition value from region four to region five (A_{45}).

We can write equation (2.103) as

$$\mathrm{COD}^*_{\mathrm{in}} = A_{45}(S^*_0 + \alpha_{g,h} X^*_{s,0}).$$

The best possible case is when this transition occurs when R^*=1. This gives

$$\begin{aligned}
[\mathrm{COD}^*_{\mathrm{in}}]\mathrm{best} &= \frac{(1-k^*_d)[(1-R^*)\mathrm{VSS}^*_{\mathrm{t}} - X^*_{i,0}]\{1-\alpha_{g,s}f_s\} + f_i k^*_d}{f_i(1-k^*_d)}, \\
&= \frac{k^*_d}{1-k^*_d} - \frac{-(1-\alpha_{g,s}f_s)X^*_{i,0}]}{f_i}, \\
&\leq \frac{k^*_d}{1-k^*_d} = 0.0732.
\end{aligned}$$

However, if

$$[\mathrm{COD}^*_{\mathrm{in}}]\mathrm{best} \leq \frac{k^*_d}{1-k^*_d}.$$

process failure is guaranteed.

Thus, in practice, for any reasonable value of the chemical oxygen demand in the flow, we know that $0 \leq R^*_{4,5} < 1$. Thus excessive sludge formation must happen if the effective recycle parameter is too high. This motivates our investigation in the next chapter can we use a sludge disintegration unit to reduce sludge formation so as to allow the operation of a settling unit with high values of the effective recycle parameter, ideally with R^*=1.

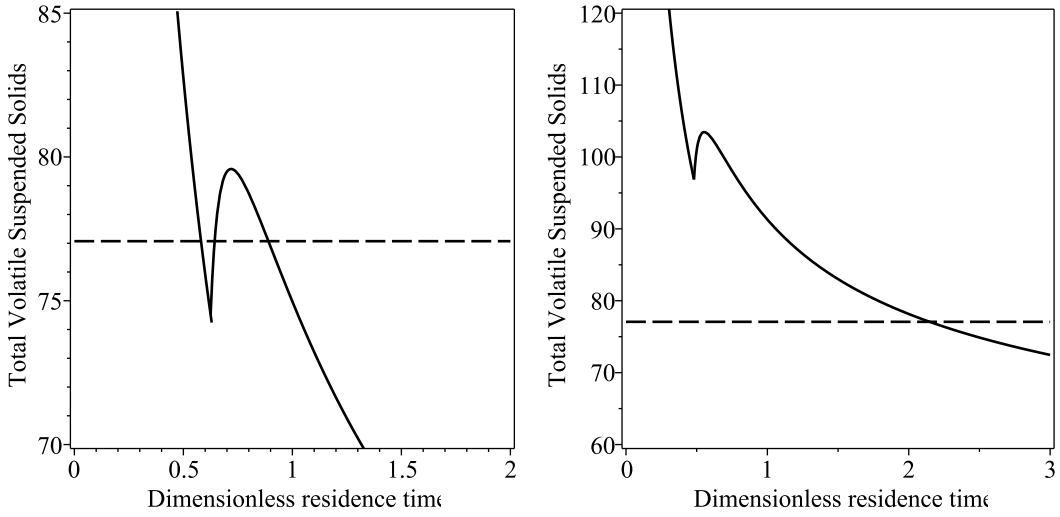

(a) $R^* = 0.48, \tau_{\text{cr}}^* = 0.6249$ (b) $R^* = 0.6, \tau_{\text{cr}}^* = 0.4807$

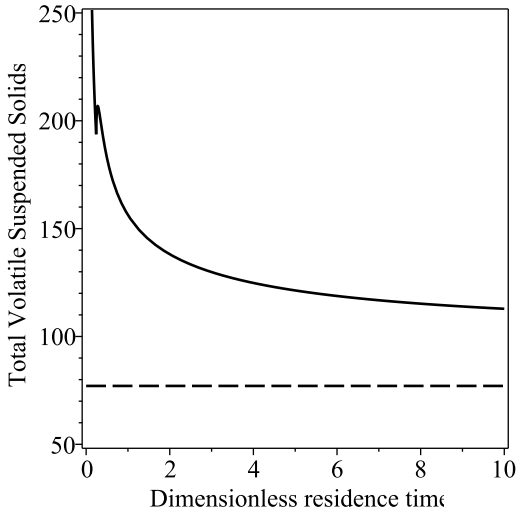

(c) $R^* = 0.8, \tau_{\text{cr}}^* = 0.2404$

Figure 2.8: Steady state diagrams for the dimensionless volatile suspended solids. Parameter values R^*=0.48, 0.6, 0.8 giving τ_{cr}^*=0.6249, 0.4807, 0.2404 respectively. The horizontal line denotes the target value of the dimensionless volatile suspended solids ($\text{VSS}_{\text{t}}^* = 77.0713$). The figures correspond to cases three to five respectively.

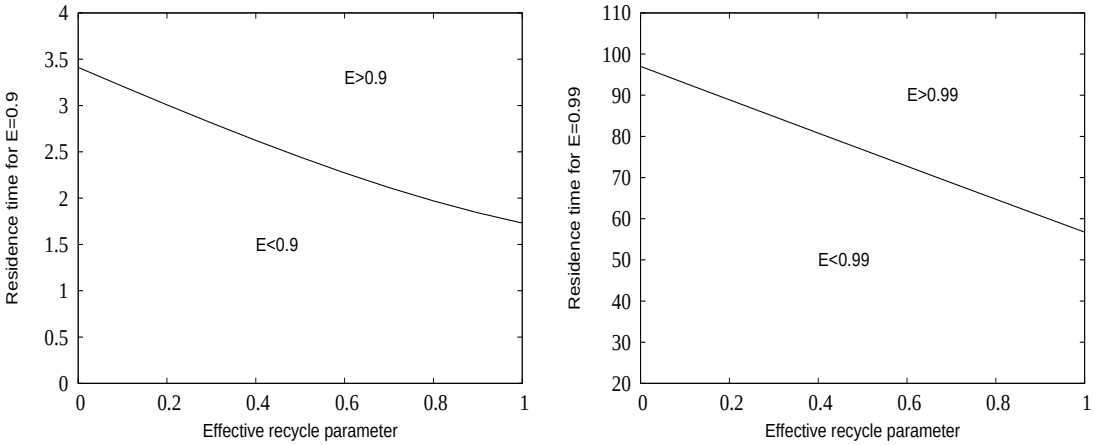

(a) E = 0.9 (b) E = 0.99

Figure 2.9: The residence time required to achieve the chemical oxygen demand efficiency $E = 0.9$ and $E = 0.99$ as a function of the effective recycle parameter (R^*).

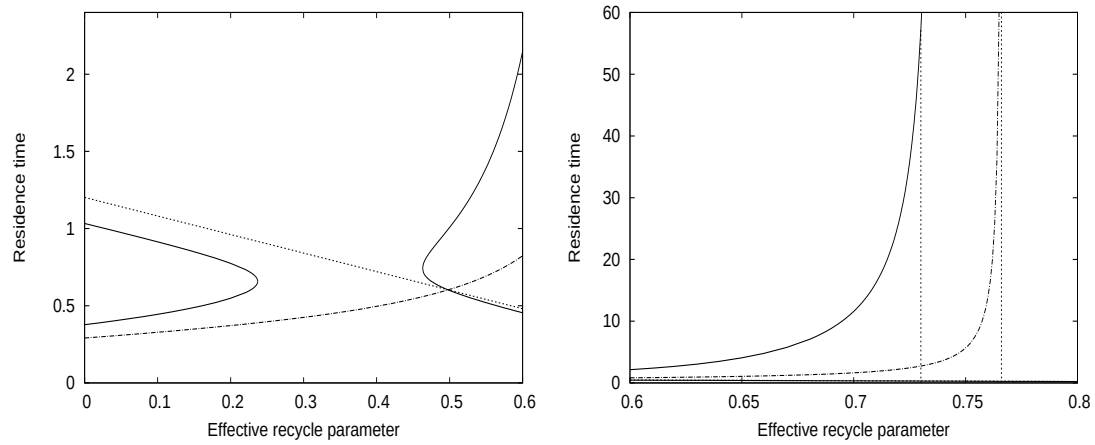

(a) $0 \leq R^* \leq 0.6$ (b) $0.6 \leq R^* \leq 0.8$

Figure 2.10: The values of the residence time where the the volatile suspended solids concentration is equal to the target value as a function of the effective recycle parameter. The dotted line is the critical value for the residence time, the dash line is the intersection point along the washout branch and the solid line is the intersection point along the no-washout branch equation.

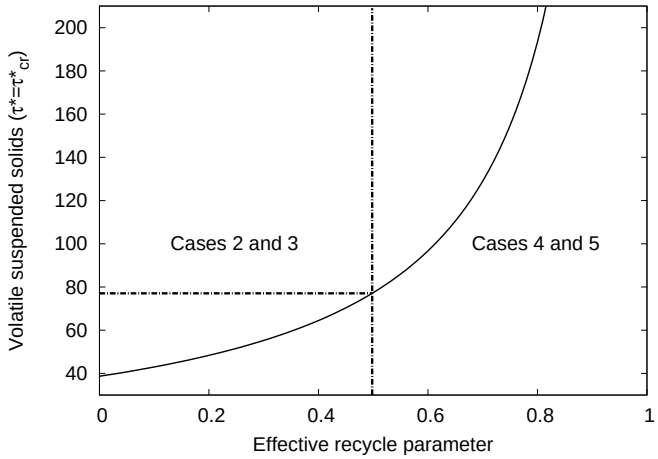

Figure 2.11: The volatile suspended solids concentration at the trans-critical bifurcation as a function of of the effective recycle parameter (R^*). When $R^* = R^*_{3,4} = 0.4972$, the volatile suspended solids is equal to the the target value ($\text{VSS}^*_t = 77.0713$).

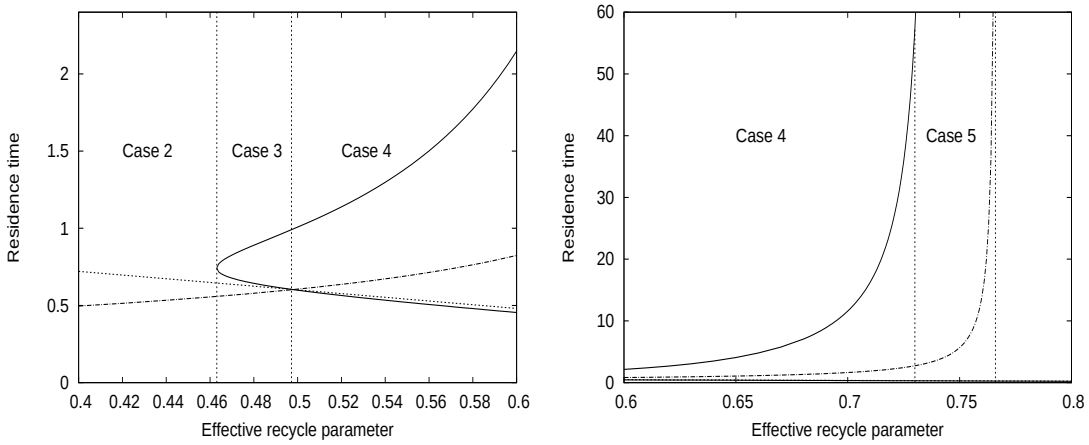

(a) $0.4 \leq R^* \leq 0.6$ (b) $0.6 \leq R^* \leq 0.8$

Figure 2.12: The values of the residence time where the the volatile suspended solids concentration is equal to the target value ($\text{VSS}^* = \text{VSS}^*_t$) as a function of the effective recycle parameter (R^*). The dotted line is the critical value for the residence time, the dash line is the intersection point along the washout branch and the solid line is the intersection point along the no-washout branch equation.

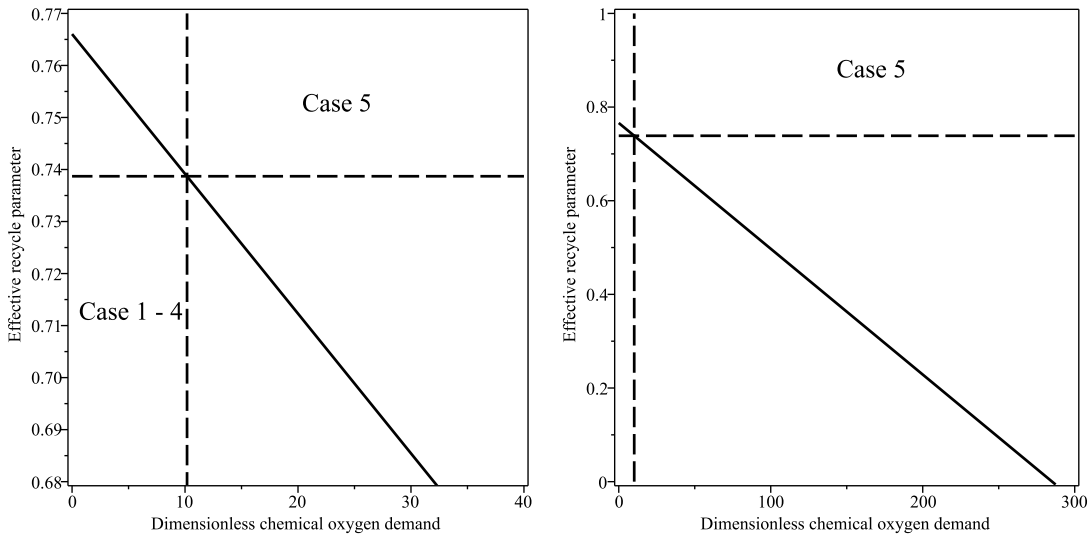

(a) 0 <COD< 40. (b) 0 <COD< 300.

Figure 2.13: The effective recycle parameter $R^*_{4,5}$ as a function of the chemical oxygen demand $\mathrm{COD}_{\mathrm{in}}$.

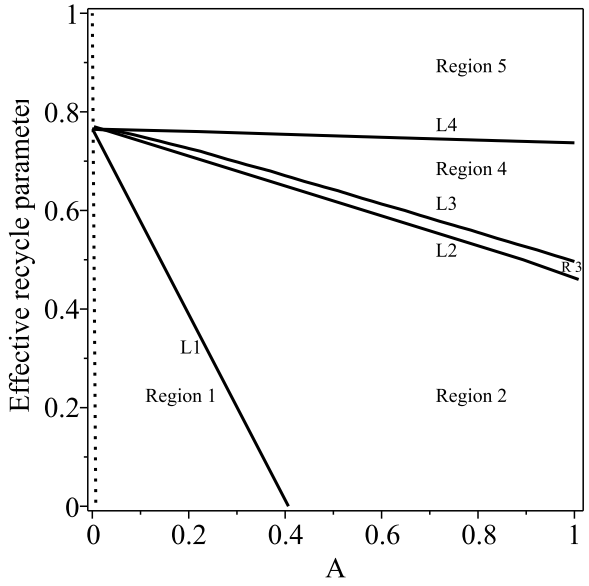

Figure 2.14: The location of the volatile suspended solids steady-state digrams in the effective recycle Parameter chemical oxygen demand parameter plane, where $\mathrm{COD}^*_{\mathrm{in}} = A\mathrm{COD}^*_{\mathrm{in,old}}$. The dotted line represent the minimum value A=0.0072.

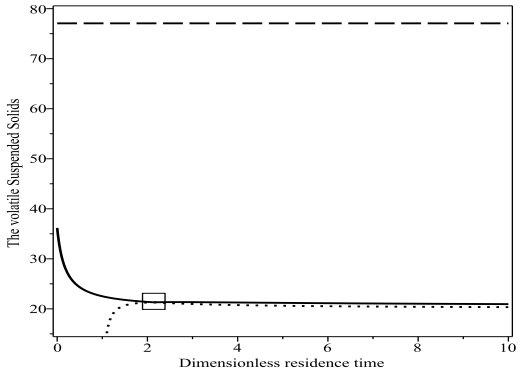

(a) Case one. Parameter values: R^*=0.1 and A=0.1.

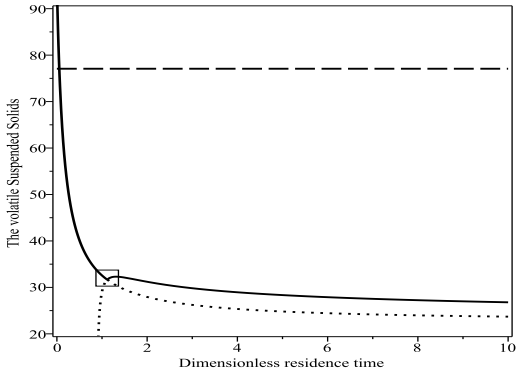

(b) Case two. Parameter values: R^*=0.2 and A=0.4.

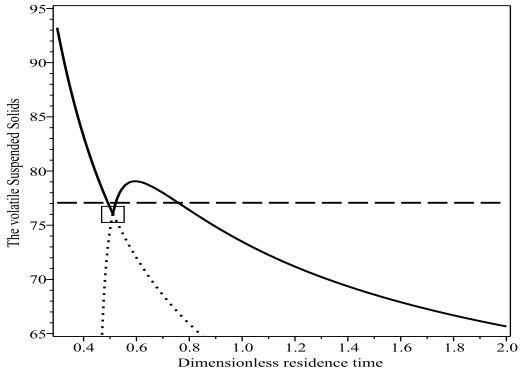

(c) Case three. Parameter values: R^*=0.6 and A=0.63.

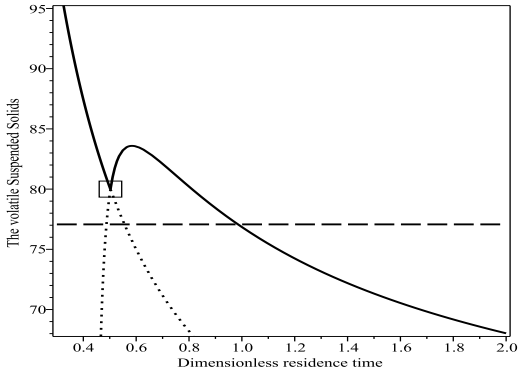

(d) Case four. Parameter values: R^*=0.6 and A=0.7.

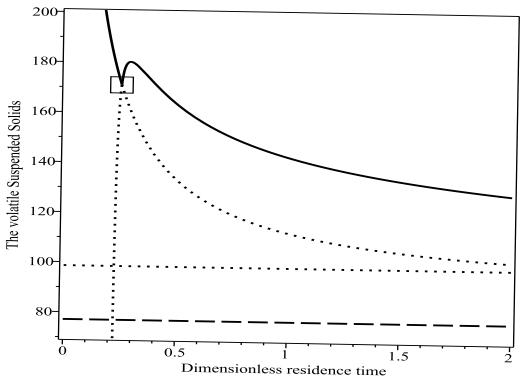

(e) Case 5. Parameter values: R^*=0.8 and A=0.8.

Figure 2.15: Steady-state diagrams showing the volatile suspended solids as a function of the dimensionless residence time (τ^*). The box denotes the location of the trans-critical bifurcation. The solid and dotted lines represent stable and unstable solutions respectively.The horizontal dash line denotes the target value of the volatile suspended solids and the horizontal dotted line denotes the asymptotic value.

2.6 Conclusion

In this chapter we extended the basic activated sludge model [71] to include additional biochemistry. The additional biochemistry has two components. Firstly, insoluble substrate is included which is hydrolyzed to give soluble substrate. Secondly, the products of biomass decay are included. This gives an inert fraction and a soluble substrate fraction. This model has four equations, rather than two in the basic model, because we now have equations for the inert material and the biodegradable substrate.

In addition to being produced as a product of biomass decay, inert material may also flow into the reactor.

Initially we established some general mathematical results. Firstly, we reduced the model from four equations to two equations. We then constructed a positively invariant region and showed that it is also exponentially attracting. We showed that if the decay rate is sufficiently high ($k_d^* \geq 1$), then the biomass must die out ($X_b^*(t^*) \to 0$), which means that the washout solution is globally asymptoticly stable. For practical applications we can assume that ($k_d^*<1$).

We found two steady state solutions corresponding to washout and no-washout branches. The washout branch corresponds to process failure and has to be avoided. In appendix A.2 we proved that the no-washout branch is only physically meaningful when

$$k_d^*<k_{\mathrm{d,cr}}^* = \frac{S_0^* + \alpha_{g,h} X_{s,0}^*}{S_0^* + \alpha_{g,h} X_{s,0}^* + 1} = \frac{\mathrm{COD}_{\mathrm{in}}^*}{1 + \mathrm{COD}_{\mathrm{in}}^*}<1, \tag{2.104}$$

and

$$\tau^*>\tau_+^* = (1 - R^*) \left[\frac{b^* + \sqrt{b^{*2} + 4ac^*}}{2a} \right] >0. \tag{2.105}$$

When the no-washout branch is not physically meaningful, we showed the washout solution is locally stable. We showed that when the no-washout branch is physically meaningful then it is locally stable and the washout branch is not stable.

We showed that for high values of the residence time ($\tau^* \gg 1$), the steady state effluent concentration can not be reduced below a limiting value ($S^* = k_d^*/(1+k_d^*)$). We investigated the chemical oxygen demand and show that it is a decreasing function of the residence time and it is also a decreasing function of the effective recycle parameter.

When we investigate the volatile suspended solids as a function of the residence time for different values of the effective recycle ratio we find that there are five generic cases. The cases one to four are all good. In case one we can operate the reactor at any residence time and we are guaranteed that the steady-state volatile suspended solids will be lower than the target value. In cases two to four there is a critical value of the residence time. If we operate the reactor at any value of the residence time greater than this value we are guaranteed that the steady-state volatile suspended solids will be lower than the target value, Case five is undesirable because for any value of the residence time the steady-state volatile suspended solids is greater than the target value. When this happens it means that we must stop operating the plant to remove the sludge, this increasing the cost of running the plant.

Some of the results from this chapter have been published in a refereed conference proceeding [4].

Chapter 3

Addition of Sludge Disintegration Unit to the extension of the standard model

3.1 Introduction

In the previous chapter we examined an extension of the basic model containing four components which are soluble substrate, biomass, non-biodegradable particulate material and biodegradable particulate substrate. We investigated how the operation of the settling unit influences the amount of sludge formed in the bioreactor. We found that when the recycle ratio is sufficiently high that the volatile suspended solids is always above the target value. In this chapter we extend our model by investigating how a sludge disintegration unit (SDU) can be used to control the amount of sludge within the bioreactor.

Some of the results from this chapter have been published [7].

3.2 Biochemistry

The biochemistry inside the bioreactor is identical to the previous chapter.

3.2.1 Biochemical reactions (sludge disintegration)

In this section the biochemistry inside the sludge disintegration unit is discussed. An overview of the sludge disintegration processes is shown in Figure 3.1 (This figure is identical to figure 1.5, it is included here for clarity). In this figure $X_{b,s}$ is the concentration of biomass within the sludge disintegration unit, $X_{i,s}$ is the concentration of non-biodegradable particulate material within the sludge disintegration unit, $X_{s,s}$ is the concentration of biodegradable particulate substrate within the sludge disintegration unit, S_s is the concentration of soluble substrate within the sludge disintegration unit, γ_b is the disintegration rate of biomass within the sludge disintegration unit, γ_i is the disintegration rate of non-biodegradable particulates within the sludge disintegration unit and γ_s is the disintegration rate of slowly biodegradable particulates within the sludge disintegration unit.

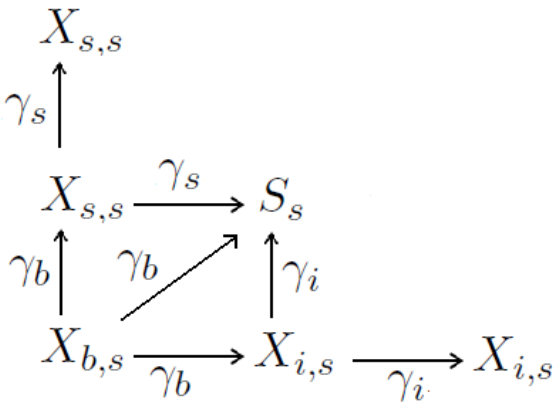

Figure 3.1: Overview of biochemical processes inside the sludge disintegration unit.

Inside the sludge disintegration unit three disintegration processes occur.

1. One concentration unit of biomass ($X_{b,s}$) is disintegrated into f_i concentration units of non-biodegradable particulate ($X_{i,s}$), $(1-\alpha-f_i)$ concentration units of biodegradable particulate substrate ($X_{s,s}$) and α concentration units of soluble substrate (S_s).

$$X_{b,s} \xrightarrow{\gamma_b} f_{p,s}X_{i,s} + (1-\alpha-f_{p,s})X_{s,s} + \alpha\alpha_s S_s, \tag{3.1}$$

where

$$0 \leq \alpha \leq 1 - f_{p,s}. \tag{3.2}$$

In reaction (3.1) α is the solubilization efficiency of the sludge disintegration unit, $f_{p,s}$ is the fraction of dead biomass converted to inert material by disintegration and γ_b is the disintegration rate of biomass within the sludge disintegration unit.

We note that in the original model (without the SDU) we have a term which models the decay of biomass as follows

$$X_b \xrightarrow{k_d} f_i X_i + f_s \alpha_s S,$$
$$f_i + f_s = 1.$$

The largest amount of soluble substrate that can be produced is when f_s=1 i.e. α_s. We argue that the largest amount of soluble substrate produced by the disintegration of biomass in reaction (3.1) must similarly be α_s.

2. Sludge disintegration reaction two is analogous to the hydrolysis of biodegradable particulate substrate. It states that one unit of biodegradable particulate substrate ($X_{s,s}$) is converted into α units of soluble substrate (S_s) and $(1-\alpha)$ units of biodegradable particulate substrate ($X_{s,s}$).

$$X_{s,s} \xrightarrow{\gamma_s} \alpha\alpha_h S_s + (1-\alpha)X_{s,s}. \tag{3.3}$$

We note that in the original model (without the SDU) we have a term which models the production of soluble substrate through the hydrolysis of biologi-

cally degradable particulate organic solids as follows

$$X_s \xrightarrow{k_h} \alpha_h S.$$

We argue that the largest amount of soluble substrate produced by the disintegration of biodegradable particulate organic solids must similarly be α_h.

3. Sludge disintegration reaction three states that inside the sludge disintegration unit one unit of non-biodegradable particulate substrate ($X_{i,s}$) is disintegrated into β_i units of soluble substrate (S_s) and $(1-\beta_i)$ units of non-biodegradable particulate substrate ($X_{i,s}$),

$$X_{i,s} \xrightarrow{\gamma_i} \beta_i \alpha_{SDU} S_s + (1-\beta_i) X_{i,s}. \tag{3.4}$$

In reaction (3.4) β_i is the conversion efficiency from non-biodegradable particulates to readily biodegradable (soluble) substrate.

For numerical simulations we argue that it would be unrealistic for the value of α_{SDU} to be larger than either α_s and α_h. We take α_{SDU}=max$(\alpha_h, \alpha_s) = \alpha_s$.

3.2.2 Chemical demand oxygen in the sludge disintegration unit

As in the previous chapter the COD in the sludge disintegration unit is defined by

$$\text{COD}_s = S_s + \alpha_h X_{s,s}.$$

3.2.3 The volatile suspended solids in the sludge disintegration unit

The volatile suspended solids was defined in the previous chapter. The volatile suspended solids in the sludge disintegration unit (VSS_s) is given by

$$\mathrm{VSS}_s = X_{b,s} + X_{i,s} + X_{s,s}.$$

The target value of the volatile suspended solids in the sludge disintegration unit is [102]

$$\mathrm{VSS}_{\mathrm{st}} = 12000\,\mathrm{mg\,l^{-1}}.$$

We aim to be below the target value.

3.3 Equations

In this section we write down the model equations for the concentration of microorganisms, particulates, inert material, and substrate within a well-stirred, well-aerated, bioreactor and a sludge disintegration unit.

3.3.1 The dimensional model

The model equations are

Equations in the bioreactor

Concentration of soluble substrate

$$V\frac{dS}{dt} = F(S_0 - S) + DF(S_s - S) + V\alpha_h k_h X_s + V f_s \alpha_s k_d X_b - \frac{V X_b \mu(S)}{\alpha_g}. \quad (3.5)$$

Concentration of biomass

$$V\frac{dX_b}{dt} = F(X_{b,0} - X_b) + RF(C-1)X_b + DF(X_{b,s} - X_b) + VX_b\mu(S) - Vk_dX_b. \tag{3.6}$$

Concentration of non-biodegradable particulate material

$$V\frac{dX_i}{dt} = F(X_{i,0} - X_i) + RF(C-1)X_i + DF(X_{i,s} - X_i) + Vf_ik_dX_b. \tag{3.7}$$

Concentration of biodegradable particulate substrate

$$V\frac{dX_s}{dt} = F(X_{s,0} - X_s) + RF(C-1)X_s + DF(X_{s,s} - X_s) - Vk_hX_s. \tag{3.8}$$

The specific growth rate is given by

$$\mu(S) = \frac{\mu_m S}{K_s + S}. \tag{3.9}$$

The residence time is defined by

$$\tau = \frac{V}{F}. \tag{3.10}$$

The chemical demand oxygen inside the bioreactor

$$\text{COD} = S + \alpha_h X_s. \tag{3.11}$$

Total Volatile Suspended Solids (VSS) inside the bioreactor

$$X_t = X_b + X_i + X_s. \tag{3.12}$$

Equations in the sludge disintegration unit

When $\chi = 0$ we assume that the disintegration process is accruing much quicker

than the biochemical process so that we can ignore the biochemical process.

When $\chi = 1$ we assume that the disintegration process and the biochemical process are included which is more realistic for sufficiently 'low' values of the disintegration rates $(\gamma_b, \gamma_i, \gamma_s)$.

In our analysis we always take $\chi = 0$.

Concentration of soluble substrate

$$V_s \frac{dS_s}{dt} = DF(S - S_s) + V_s \alpha \alpha_s \gamma_b X_{b,s} + V_s \alpha \alpha_h \gamma_s X_{s,s} + V_s \beta_i \alpha_{SDU} \gamma_i X_{i,s} + \chi V_s \left[\alpha_h k_h X_{s,s} + f_s \alpha_s k_d X_{b,s} - \frac{X_{b,s} \mu(S_s)}{\alpha_g} \right]. \tag{3.13}$$

Concentration of biomass

$$V_s \frac{dX_{b,s}}{dt} = DF(X_b - X_{b,s}) - V_s \gamma_b X_{b,s} + \chi V_s \left[X_{b,s} \mu(S_s) - k_d X_{b,s} \right]. \tag{3.14}$$

Concentration of non-biodegradable particulate material

$$V_s \frac{dX_{i,s}}{dt} = DF(X_i - X_{i,s}) + V_s f_{p,s} \gamma_b X_{b,s} - V_s \beta_i \gamma_i X_{i,s} + \chi V_s \left[f_i k_d X_{b,s} \right]. \tag{3.15}$$

Concentration of biodegradable particulate substrate

$$V_s \frac{dX_{s,s}}{dt} = DF(X_s - X_{s,s}) + V_s (1 - \alpha - f_{p,s}) \gamma_b X_{b,s} - V_s \alpha \gamma_s X_{s,s} - \chi V_s \left[k_h X_{s,s} \right]. \tag{3.16}$$

The specific growth rate is given by

$$\mu(S_s) = \frac{\mu_m S_s}{K_s + S_s}. \tag{3.17}$$

The residence time is defined by

$$\tau_s = \frac{V_s}{F}. \tag{3.18}$$

The chemical demand oxygen inside the sludge disintegration uni

$$\mathrm{COD}_s = S_s + \alpha_h X_{s,s}. \tag{3.19}$$

Total Volatile Suspended Solids (VSS_s) inside the sludge disintegration unit

$$X_{t,s} = X_{b,s} + X_{i,s} + X_{s,s}. \tag{3.20}$$

Note that we can assume that $C \geq 1$, as otherwise recycle leads to a decrease in performance of the bioreactor.

For a specific wastewater, a given biological community, and a particular set of environmental conditions, the parameters K_s, k_d, α_h, α_g, α_s and μ_m are fixed. The parameters that can be varied are S_0, $X_{j,0}(j = b, i, s)$, and τ.

All the parameters in the dimensional model are defined in table 3.1.

Abbreviation	Explanation	Unit
D	Sludge disintegration factor	(–)
C	The recycle concentration factor	(–)
F	Flow rate through bioreactor	($\mathrm{dm}^3\ \mathrm{hr}^{-1}$)
K_s	Monod constant	($\mathrm{g\ dm}^{-3}$)
R	Recycle ratio based on volumetric flow rates	(–)
S	Substrate concentration within the bioreactor	($\lvert S \rvert$)
S_s	Substrate concentration in the sludge integration unit	($\lvert S \rvert$)
S_0	Concentration of substrate flowing into the reactor	($\lvert S \rvert$)

V	Volume of the bioreactor	(dm^3)
V_s	Volume of the sludge integration unit	(dm^3)
X_b	Concentration of biomass	($\|X\|$)
$X_{b,s}$	Concentration of biomass in the sludge integration unit	($\|X\|$)
X_i	Concentration of of non-biodegradable particulate material	($\|X\|$)
$X_{i,s}$	Concentration of non-biodegradable particulate material in the sludge integration unit	($\|X\|$)
X_s	Concentration of biodegradable particulate substrate	($\|X\|$)
$X_{s,s}$	Concentration of biodegradable particulate substrate in the sludge integration unit	($\|X\|$)
$X_{j,0}(j = b, i, s)$	Concentration flowing into the reactor	($\|X\|$)
X_t	Total biomass	($\|X\|$)
$X_{t,s}$	Total biomass in the sludge integration unit	($\|X\|$)
k_h	Hydrolysis rate of insoluble organic compounds	(hr^{-1})
k_d	Death coefficient	(hr^{-1})
f_s	The fraction of dead biomass converted to soluble substrate	(–)
f_i	The fraction of dead biomass converted to inert material	(–)
$f_{p,s}$	Fraction of dead biomass converted to inert material in the sludge integration unit	(–)
t	Time	(hr^{-1})

γ_b	Disintegration rate of biomass within the sludge disintegration unit	(hr^{-1})
γ_i	Disintegration rate of non-biodegradable particulates within the sludge disintegration unit	(hr^{-1})
γ_s	Disintegration rate of slowly biodegradable particulates within the sludge disintegration unit	(hr^{-1})
β_i	Conversion efficiency from non-biodegradable particulates to readily biodegradable (soluble) substrate,	(–)
α_h	Yield factor for hydrolysis of insoluble organic compounds	($\|S\|\|X\|^{-1}$)
α_g	Yield factor for growth of biomass	($\|S\|\|X\|^{-1}$)
α_s	Yield factor for conversion of dead biomass to soluble substrate	($\|S\|\|X\|^{-1}$)
α	Solubilization efficiency of the sludge integration unit	(–)
α_{SDU}	Yield factor for conversion of inert material to soluble substrate	($\|S\|\|X\|^{-1}$)
$\mu(S)$	Specific growth rate model	(hr^{-1})
$\mu(S_s)$	Specific growth rate model in the sludge integration unit	(hr^{-1})
μ_m	Maximum specific growth rate	(hr^{-1})
τ	Residence time	(hr)
τ_s	Residence time in the sludge disintegration unit	(hr)

χ	Modelling parameter for the sludge integration unit	(–)

Table 3.1: The definitions of the parameters.

3.3.2 The dimensionless model

By introducing dimensionless variables for concentrations of the substrate [S^* =S/K_s, S_0^* =$S_0/K_s, S_s^*$ =S_s/K_s], microorganism and particulates [X_j^* =$X_j/(\alpha_g K_s), X_{j,0}^*$ =$X_{j,0}/(\alpha_g K_s), X_{j,s}^*$ =$X_{j,s}/(\alpha_g K_s)$] ($j = b, i, s$), time [t^*=$\mu_m t$], and parameters $\alpha_{\mathrm{gSDU}} = \alpha_g \alpha_{SDU}$, $\alpha_{g,h} = \alpha_h \alpha_g$, $\alpha_{g,s} = \alpha_s \alpha_g$, $\gamma_j^* = \gamma_j/\mu_m (j = b, i, s)$, $k_h^* = k_h/\mu_m$, $k_d^* = k_d/\mu_m$, $\tau^* = V\mu_m/F$ and $V^* = V/V_s$, the dimensional model equations can be written in dimensionless form.

Equations in the bioreactor

$$\frac{dS^*}{dt^*} = \frac{1}{\tau^*}(S_0^* - S^*) + \frac{D}{\tau^*}(S_s^* - S^*) + \alpha_{g,h} k_h^* X_s^* + f_s \alpha_{g,s} k_d^* X_b^* - \frac{S^* X_b^*}{1 + S^*}, \tag{3.21}$$

$$\frac{dX_b^*}{dt^*} = \frac{1}{\tau^*}(X_{b,0}^* - X_b^*) + \frac{R^*}{\tau^*} X_b^* + \frac{D}{\tau^*}(X_{b,s}^* - X_b^*) + \frac{X_b^* S^*}{1 + S^*} - k_d^* X_b^*, \tag{3.22}$$

$$\frac{dX_i^*}{dt^*} = \frac{1}{\tau^*}(X_{i,0}^* - X_i^*) + \frac{R^*}{\tau^*} X_i^* + \frac{D}{\tau^*}(X_{i,s}^* - X_i^*) + f_i k_d^* X_b^*, \tag{3.23}$$

$$\frac{dX_s^*}{dt^*} = \frac{1}{\tau^*}(X_{s,0}^* - X_s^*) + \frac{R^*}{\tau^*} X_s^* + \frac{D}{\tau^*}(X_{s,s}^* - X_s^*) - k_h^* X_s^*. \tag{3.24}$$

The chemical oxygen demand COD^* inside the bioreactor

$$\mathrm{COD}^* = S^* + \alpha_{g,h} X_s^*. \tag{3.25}$$

Total Volatile Suspended Solids VSS* inside the bioreactor

$$X_t^* = X_b^* + X_i^* + X_s^*. \tag{3.26}$$

The effective recycle parameter is given by [$R^* = (C\text{-}1)R$].

The cases $R^* = 0$, $0<R^*<1$ and $R^* = 1$ represent a flow reactor without recycle, a flow reactor with non-idealized recycle, and a flow reactor with idealized recycle, respectively.

From now on we assume that the growth medium fed into the bioreactor is sterile, i.e. there are no microorganisms in the influent ($X_{b,0} = X_{b,0}^* = 0$).

Note that the target value for volatile suspended solid becomes

$$\mathrm{VSS}_{\mathrm{t}}^* = \frac{\mathrm{VSS}_{\mathrm{t}}}{\alpha_g k_s} = \frac{12000}{\alpha_g k_s} = 77.071. \tag{3.27}$$

Equations in the sludge disintegration unit

$$\begin{aligned}\frac{dS_s^*}{dt^*} &= \frac{DV^*}{\tau^*}(S^* - S_s^*) + \alpha\alpha_{g,s}\gamma_b^* X_{b,s}^* + \alpha\alpha_{g,h}\gamma_s^* X_{s,s}^* + \beta_i\alpha\alpha_{\mathrm{g,SDU}}\gamma_i^* X_{i,s}^* \\ &\quad + \chi\left[\alpha_{g,h}k_h^* X_{s,s}^* + f_s\alpha_{g,s}k_d^* X_{b,s}^* - \frac{S_s^* X_{b,s}^*}{1+S_s^*}\right], \qquad (3.28)\\ \frac{dX_{b,s}^*}{dt^*} &= \frac{DV^*}{\tau^*}(X_b^* - X_{b,s}^*) - \gamma_b^* X_{b,s}^* + \chi\left[\frac{X_{b,s}^* S_s^*}{1+S_s^*} - k_d^* X_{b,s}^*\right], \qquad (3.29)\\ \frac{dX_{i,s}^*}{dt^*} &= \frac{DV^*}{\tau^*}(X_i^* - X_{i,s}^*) + f_{p,s}\gamma_b^* X_{b,s}^* - \beta_i\gamma_i^* X_{i,s}^* + \chi\left[f_i k_d^* X_{b,s}^*\right], \qquad (3.30)\end{aligned}$$

$$\begin{aligned}\frac{dX_{s,s}^*}{dt^*} &= \frac{DV^*}{\tau^*}(X_s^* - X_{s,s}^*) + (1-\alpha-f_{p,s})\gamma_b^* X_{b,s}^* - \alpha\gamma_s^* X_{s,s}^* \\ &\quad - \chi\left[k_h^* X_{s,s}^*\right]. \qquad (3.31)\end{aligned}$$

The chemical oxygen demand COD$_s^*$ inside the sludge disintegration unit

$$\mathrm{COD}_s^* = S_s^* + \alpha_{g,h} X_{s,s}^*. \tag{3.32}$$

Total Volatile Suspended Solids VSS_s^* inside the sludge disintegration unit

$$X_{t,s}^* = X_{b,s}^* + X_{i,s}^* + X_{s,s}^*. \tag{3.33}$$

3.3.3 Model simplification when $D = 0$

When $D = 0$, i.e. there is no sludge disintegration unit, we have the same model that we examined in the previous chapter.

3.3.4 Model simplification for a fast sludge disintegration unit

We assume ($\chi = 0$) which means that the sludge disintegration reactions are faster than the biochemical process.

The model equations in the sludge disintegration unit become

$$\frac{dS_s^*}{dt^*} = \frac{DV^*}{\tau^*}(S^* - S_s^*) + \alpha\alpha_{g,s}\gamma_b^* X_{b,s}^* + \alpha\alpha_{g,h}\gamma_s^* X_{s,s}^* + \beta_i\alpha\alpha_{\mathrm{g,SDU}}\gamma_i^* X_{i,s}^*, \tag{3.34}$$

$$\frac{dX_{b,s}^*}{dt^*} = \frac{DV^*}{\tau^*}(X_b^* - X_{b,s}^*) - \gamma_b^* X_{b,s}^*, \tag{3.35}$$

$$\frac{dX_{i,s}^*}{dt^*} = \frac{DV^*}{\tau^*}(X_i^* - X_{i,s}^*) + f_{p,s}\gamma_b^* X_{b,s}^* - \beta_i\gamma_i^* X_{i,s}^*, \tag{3.36}$$

$$\frac{dX_{s,s}^*}{dt^*} = \frac{DV^*}{\tau^*}(X_s^* - X_{s,s}^*) + (1 - \alpha - f_{p,s})\gamma_b^* X_{b,s}^* - \alpha\gamma_s^* X_{s,s}^*. \tag{3.37}$$

We assume that the sludge disintegration unit is at steady state. Webelieve that it is a reasonable approximation to assume that the sludge disintegration unit is at steady-state because the processes occurring in the sludge disintegration unit are much quicker than the biochemical reactions. In the limiting case they occur 'infinitely quickly'. This assumption could be investigated in future work.

The steady-state solutions in the sludge disintegration unit are given by

$$\begin{aligned} S_s^* &= S^* + \left[\frac{\alpha_{g,s}\gamma_b^* X_{b,s}^* + \alpha_{g,h}\gamma_s^* X_{s,s}^* + \beta_i \alpha_{\mathrm{g,SDU}}\gamma_i^* X_{i,s}^*}{DV^*}\right]\alpha\tau^*, \\ &= S^* + \left[\frac{\gamma_b^*}{P}\left(\alpha_{g,s} + \frac{\alpha_{g,h}\gamma_s^*(1-\alpha-f_{p,s})\tau^*}{H} + \frac{\beta_i\alpha_{\mathrm{g,SDU}}\gamma_i^* f_{p,s}\tau^*}{G}\right)X_b^*\right. \\ &\quad \left. + \left(\frac{\alpha_{g,h}\gamma_s^* X_s^*}{H} + \frac{\beta_i\alpha_{\mathrm{g,SDU}}\gamma_i^* X_i^*}{G}\right)\right]\alpha\tau^*, \end{aligned} \tag{3.38}$$

$$X_{b,s}^* = \frac{DV^*}{P}X_b^*, \tag{3.39}$$

$$\begin{aligned} X_{i,s}^* &= \frac{1}{G}(DV^* X_i^* + f_{p,s}\gamma_b^* X_{b,s}^*\tau^*), \\ &= \frac{DV^*}{GP}\left(PX_i^* + f_{p,s}\gamma_b^* X_b^*\tau^*\right), \end{aligned} \tag{3.40}$$

$$\begin{aligned} X_{s,s}^* &= \frac{1}{H}\left[DV^* X_s^* + (1-\alpha-f_{p,s})\gamma_b^* X_{b,s}^*\tau^*\right], \\ &= \frac{DV^*}{PH}\left[PX_s^* + (1-\alpha-f_{p,s})\gamma_b^* X_b^*\tau^*\right]. \end{aligned} \tag{3.41}$$

where

$$G = DV^* + \beta_i\gamma_i^*\tau^* > 0, \tag{3.42}$$

$$H = DV^* + \alpha\gamma_s^*\tau^* > 0, \tag{3.43}$$

$$P = DV^* + \gamma_b^*\tau^* > 0. \tag{3.44}$$

Note, in the equations (3.40) and (3.41) we have X_b^*, the concentration of biomass in the *bioreactor*, whereas in equation (3.39) we have $X_{b,s}^*$, the concentration in the *sludge disintegration unit*.

Substituting (3.38)-(3.41) into (3.21)-(3.24) we obtain the reduced model for the bioreactor

$$\begin{aligned} \frac{dS^*}{dt^*} &= \frac{S_0^* - S^*}{\tau^*} + \left\{\frac{D\alpha\gamma_b^*}{P}\left[\alpha_{g,s} + \frac{\alpha_{g,h}\gamma_s^*(1-\alpha-f_{p,s})\tau^*}{H} + \frac{\beta_i\alpha_{\mathrm{g,SDU}}\gamma_i^* f_{p,s}\tau^*}{G}\right]\right. \\ &\quad \left. + f_s\alpha_{g,s}k_d^*\tau^* - \frac{S^*}{1+S^*}\right\}X_b^* + D\alpha\left[\frac{\alpha_{g,h}\gamma_s^* X_s^*}{H} + \frac{\beta_i\alpha_{\mathrm{g,SDU}}\gamma_i^* X_i^*}{G}\right] + \alpha_{g,h}k_h^* X_s^*, \end{aligned} \tag{3.45}$$

$$\frac{dX_b^*}{dt^*} = \left[\frac{R^*-1}{\tau^*} - \frac{D\gamma_b^*}{P} + \frac{S^*}{1+S^*} - k_d^*\right] X_b^*, \tag{3.46}$$

$$\frac{dX_i^*}{dt^*} = \frac{X_{i,0}^*}{\tau^*} + \left[R^* - 1 - \frac{D\beta_i\gamma_i^*\tau^*}{G}\right]\frac{X_i^*}{\tau^*} + \left[\frac{D^2V^*f_{p,s}\gamma_b^*}{PG} + f_i k_d^*\right] X_b^*, \tag{3.47}$$

$$\frac{dX_s^*}{dt^*} = \frac{X_{s,0}^*}{\tau^*} + \left[R^* - 1 - k_h^*\tau^* - \frac{D\alpha\gamma_s^*\tau^*}{H}\right]\frac{X_s^*}{\tau^*} + \left[\frac{D^2V^*(1-\alpha-f_{p,s})\gamma_b^*}{PH}\right] X_b^*. \tag{3.48}$$

3.4 Results (general case)

In this section we investigate the general case in which the value for the three disintegration reactions $(\gamma_{\mathrm{b}}^*, \gamma_{\mathrm{i}}^*, \gamma_{\mathrm{s}}^*)$ are independent.

3.4.1 Washout solution $(X_{\mathbf{b}}^* = X_{\mathbf{b,s}}^* = 0)$

From equations (3.45) – (3.48) the washout steady-state solutions of the bioreactor are given by

$$S_w^* = S_0^* + \frac{(D\alpha\alpha_{\mathrm{g,h}}\gamma_{\mathrm{s}}^* + A)X_{\mathrm{s},0}^*\tau^*}{C} + \frac{D\alpha\alpha_{\mathrm{g,SDU}}\gamma_{\mathrm{i}}^*\beta_{\mathrm{i}}X_{\mathrm{i},0}^*\tau^*}{F} > 0, \tag{3.49}$$

$$X_{\mathrm{bw}}^* = 0, \tag{3.50}$$

$$X_{\mathrm{iw}}^* = \frac{G}{F}X_{\mathrm{i},0}^* > 0, \tag{3.51}$$

$$X_{\mathrm{sw}}^* = \frac{H}{C}X_{\mathrm{s},0}^* > 0, \tag{3.52}$$

$$\mathrm{COD}_w^* = S_0^* + \frac{(D\alpha\alpha_{\mathrm{g,h}}\gamma_{\mathrm{s}}^* + A)X_{\mathrm{s},0}^*\tau^*}{C} + \frac{D\alpha\alpha_{\mathrm{g,SDU}}\gamma_{\mathrm{i}}^*\beta_{\mathrm{i}}X_{\mathrm{i},0}^*\tau^*}{F} + \alpha_{\mathrm{g,h}}\frac{H}{C}X_{\mathrm{s},0}^*, \tag{3.53}$$

$$\mathrm{VSS}_w^* = \frac{G}{F}X_{\mathrm{i},0}^* + \frac{H}{C}X_{\mathrm{s},0}^*, \tag{3.54}$$

where

$$A = H\alpha_{\mathrm{g,h}}k_h^* > 0, \tag{3.55}$$

$$C = H(1 - R^* + k_h^*\tau^*) + D\alpha\gamma_{\mathrm{s}}^*\tau^* > 0, \tag{3.56}$$

$$F = G(1 - R^*) + D\gamma_{\mathrm{i}}^*\beta_{\mathrm{i}}\tau^* > 0. \tag{3.57}$$

The coefficients G and H are defined in equations (3.42) and (3.43) respectively. Substituting (3.49)-(3.52) into (3.38)-(3.41) we obtain the steady-state solutions inside the sludge disintegration unit

$$\begin{aligned} S_{\mathrm{sw}}^* = S_0^* + \frac{(D\alpha\alpha_{\mathrm{g,h}}\gamma_{\mathrm{s}}^* + A)X_{\mathrm{s,0}}^*\tau^*}{C} + \frac{D\alpha\alpha_{\mathrm{g,SDU}}\gamma_{\mathrm{i}}^*\beta_{\mathrm{i}}X_{\mathrm{i,0}}^*\tau^*}{F} \\ + \left(\frac{\alpha_{\mathrm{g,h}}\gamma_{\mathrm{s}}^*X_{\mathrm{s,0}}^*}{C} + \frac{\beta_{\mathrm{i}}\alpha_{\mathrm{g,SDU}}\gamma_{\mathrm{i}}^*X_{\mathrm{i,0}}^*}{F}\right)\alpha\tau^*, \end{aligned} \tag{3.58}$$

$$X_{\mathrm{b,sw}}^* = 0, \tag{3.59}$$

$$X_{\mathrm{i,sw}}^* = \frac{DV^*}{F}X_{\mathrm{i,0}}^*, \tag{3.60}$$

$$X_{\mathrm{s,sw}}^* = \frac{DV^*}{C}X_{\mathrm{s,0}}^*. \tag{3.61}$$

The coefficients C and F are defined in equations (3.56) and (3.57).

3.4.2 No-washout solution

The no-washout steady-state solutions of the bioreactor are given by

$$S_{\mathrm{nw}}^* = \frac{(DV^* + \gamma_{\mathrm{b}}^*\tau^*)[1 - R^* + k_d^*\tau^*] + D\gamma_{\mathrm{b}}^*\tau^*}{(DV^* + \gamma_{\mathrm{b}}^*\tau^*)[R^* - 1 + (1 - k_d^*)\tau^*] - D\gamma_{\mathrm{b}}^*\tau^*}, \tag{3.62}$$

$$X_{\mathrm{b,nw}}^* = \frac{-U}{N}, \tag{3.63}$$

$$X_{\mathrm{i,nw}}^* = \frac{G}{F}X_{\mathrm{i,0}}^* + \frac{K}{FP}X_{\mathrm{b,nw}}^*, \tag{3.64}$$

$$X_{\mathrm{s,nw}}^* = \frac{H}{C}X_{\mathrm{s,0}}^* + \frac{J}{CP}X_{\mathrm{b,nw}}^*, \tag{3.65}$$

$$\mathrm{COD}_{\mathrm{nw}}^* = \frac{(1 - R^* + k_d^*\tau^*)P + D\gamma_{\mathrm{b}}^*\tau^*}{[R^* - 1 + (1 - k_d^*)\tau^*]P - D\gamma_{\mathrm{b}}^*\tau^*} + \alpha_{\mathrm{g,h}}\frac{H}{C}X_{\mathrm{s,0}}^* + \frac{J}{CP}X_{\mathrm{b,nw}}^*, \tag{3.66}$$

$$\mathrm{VSS}_{\mathrm{nw}}^* = \left(1 + \frac{K}{FP} + \frac{J}{CP}\right)X_{\mathrm{b,nw}}^* + \frac{G}{F}X_{\mathrm{i,0}}^* + \frac{H}{C}X_{\mathrm{s,0}}^*, \tag{3.67}$$

where

$$B = P(1 - R^* + k_d^*\tau^*) + D\gamma_{\mathrm{b}}^*\tau^* > 0,$$

$$E = P(R^* - 1 - (k_d^* - 1)\tau^*) - D\gamma_{\mathrm{b}}^*\tau^* > 0 \quad \text{provided} \quad \tau^* > \frac{P(1 - R^*)}{(1 - k_d^*)P - D\gamma_{\mathrm{b}}^*},$$

if $(1 - k_d^*)P - D\gamma_{\mathrm{b}}^* > 0 \Rightarrow \tau^* > 0$, if $(1 - k_d^*)P - D\gamma_{\mathrm{b}}^* < 0 \Rightarrow \tau^* < 0$.

$$J = (1 - \alpha - f_{\mathrm{p,s}})D^2V^*\gamma_{\mathrm{b}}^*\tau^* > 0 \quad \text{from (3.2)}, \tag{3.68}$$

$$K = \{DV^*[f_{\mathrm{i}}k_d^*(\gamma_{\mathrm{b}}^*\tau^* + G) + Df_{\mathrm{p,s}}\gamma_{\mathrm{b}}^*] + f_{\mathrm{i}}k_d^*\gamma_{\mathrm{b}}^*\gamma_{\mathrm{i}}^*\beta_{\mathrm{i}}\tau^{*2}\}\tau^* > 0, \tag{3.69}$$

$$L = (1 - \alpha - f_{\mathrm{p,s}})\alpha_{\mathrm{g,h}}\gamma_{\mathrm{s}}^*\tau^* > 0,$$

$$M = \alpha_{\mathrm{g,SDU}}\gamma_{\mathrm{i}}^*\beta_{\mathrm{i}}f_{\mathrm{p,s}}\tau^* > 0,$$

$$N = \frac{1}{CP}\left\{\frac{N1}{FGH} + \frac{N2}{\tau^*}\right\},$$

$$N1 = D\alpha\{[C\gamma_{\mathrm{b}}^*(H(G\alpha_{\mathrm{g,s}} + M) + GL) + GJ\alpha_{\mathrm{g,h}}\gamma_{\mathrm{s}}^*]F + CHK\alpha_{\mathrm{g,SDU}}\gamma_{\mathrm{i}}^*\beta_{\mathrm{i}}\},$$

$$N2 = \tau^*[J\alpha_{\mathrm{g,h}}k_{\mathrm{h}}^* + CPf_{\mathrm{s}}\alpha_{\mathrm{g,s}}k_{\mathrm{d}}^*] - BC,$$

$$U = U1 + U2 + U3,$$

$$U1 = \frac{S_0^*E - B}{E\tau^*},$$

$$U2 = D\alpha\left(\frac{\alpha_{\mathrm{g,h}}\gamma_{\mathrm{s}}^*X_{\mathrm{s,0}}^*}{C} + \frac{\alpha_{\mathrm{g,SDU}}\gamma_{\mathrm{i}}^*\beta_{\mathrm{i}}X_{\mathrm{i,0}}^*}{F}\right),$$

$$U3 = \frac{H\alpha_{\mathrm{g,h}}k_{\mathrm{h}}^*X_{\mathrm{s,0}}^*}{C}.$$

The steady state value for the soluble substrate along the no-washout branch (S_{nw}^*) depends on the disintegration rate for the biomass (γ_{b}^*), but not the disintegration rate for the inert material (γ_{i}^*) and the disintegration rate for the soluble substrate (γ_{s}^*), which is interesting. The coefficients A, C, F, G, H, J, K and P are defined in equations (3.55), (3.56), (3.57), (3.42), (3.43), (3.68), (3.69), and (3.44).

The expressions $A, B, C, F, G, H, J, K, L, M, N1, P, U2, U3$ are all positive. The expression E is always negative if $(1 - k_d^*)P - D\gamma_{\mathrm{b}}^* < 0$. The coefficients $N2$ and $U1$ may change sign.

Substituting (3.62)-(3.65) into (3.38)-(3.41) we obtain the steady-state solutions along the no-washout branch inside the sludge disintegration unit

$$S^*_{\mathrm{s,nw}} = \frac{[1-R^*+k_d^*\tau^*]P + D\gamma_{\mathrm{b}}^*\tau^*}{[R^*-1+(1-k_d^*)\tau^*]P - D\gamma_{\mathrm{b}}^*\tau^*} + \left\{\frac{\alpha_{\mathrm{g,h}}\gamma_{\mathrm{s}}^* X_{\mathrm{s,0}}^*}{C} + \frac{\beta_{\mathrm{i}}\alpha_{\mathrm{g,SDU}}\gamma_{\mathrm{i}}^* X_{\mathrm{i,0}}^*}{F} - \frac{U}{PN}\left[\alpha_{\mathrm{g,s}}\gamma_{\mathrm{b}}^* + \frac{\alpha_{\mathrm{g,h}}\gamma_{\mathrm{s}}^*}{H}\left((1-\alpha-f_{\mathrm{p,s}})\gamma_{\mathrm{b}}^*\tau^* + \frac{J}{C}\right) + \frac{\beta_{\mathrm{i}}\alpha_{\mathrm{g,SDU}}\gamma_{\mathrm{i}}^*}{G}\left(\gamma_{\mathrm{b}}^* f_{\mathrm{p,s}}\tau^* + \frac{K}{F}\right)\right]\right\}\alpha\tau^*, \tag{3.70}$$

$$X^*_{\mathrm{b,snw}} = \frac{-UDV^*}{PN}, \tag{3.71}$$

$$X^*_{\mathrm{i,snw}} = DV^*\left[\frac{X_{\mathrm{i,0}}^*}{F} - \frac{U}{PGN}\left(\gamma_{\mathrm{b}}^* f_{\mathrm{p,s}}\tau^* + \frac{K}{F}\right)\right], \tag{3.72}$$

$$X^*_{\mathrm{s,snw}} = DV^*\left[\frac{X_{\mathrm{s,0}}^*}{C} - \frac{U}{HPN}\left((1-\alpha-f_{\mathrm{p,s}})\gamma_{\mathrm{b}}^*\tau^* + \frac{J}{C}\right)\right]. \tag{3.73}$$

3.4.2.1 The special case R^*=1

For a flow reactor with idealized recycle or an idealized membrane reactor ($R^* = 1$), the substrate concentration when $\gamma_{\mathrm{b}}^* = 0$ is the same as in the previous model its value independent of the residence time and is given by

$$S^*_{\mathrm{nw}}(R^* = 1) = \frac{k_{\mathrm{d}}^*}{1-k_{\mathrm{d}}^*}.$$

This shows that when ($\gamma_{\mathrm{b}}^* = 0$) the substrate concentration is constant, it does not depend upon the residence time. This is not true when (γ_{b}^*>0) as the substrate concentration is a function of the residence time.

$$S^*_{\mathrm{nw}}(R^* = 1) = \frac{(DV^* + \gamma_{\mathrm{b}}^*\tau^*)k_{\mathrm{d}}^*\tau^* + D\gamma_{\mathrm{b}}^*\tau^*}{(DV^* + \gamma_{\mathrm{b}}^*\tau^*)[1-k_{\mathrm{d}}^*]\tau^* - D\gamma_{\mathrm{b}}^*\tau^*}. \tag{3.74}$$

Differentiating equation (3.74) with respect to the sludge disintegration factor we have

$$\frac{dS^*_{\mathrm{nw}}}{dD}(R^* = 1) = \frac{\gamma_{\mathrm{b}}^{*2}\tau^*}{\{(1-k_{\mathrm{d}}^*)\gamma_{\mathrm{b}}^* + [(1-k_{\mathrm{d}}^*)DV^* - D\gamma_{\mathrm{b}}^*]\}^2} > 0.$$

The substrate concentration is an increasing function of the sludge disintegration factor.

When the sludge disintegration factor goes toward infinity we have

$$\lim_{D\to\infty} S^*_{\mathrm{nw}}(R^*=1) = \frac{V^*k^*_{\mathrm{d}}\tau^* + \gamma^*_{\mathrm{b}}\tau^*}{(1-k^*_{\mathrm{d}})V^*\tau^* - \gamma^*_{\mathrm{b}}\tau^*}.$$

Differentiating equation (3.74) with respect to the disintegration rate we have

$$\frac{dS^*_{\mathrm{nw}}}{d\gamma^*_{\mathrm{b}}}(R^*=1) = \frac{V^*D^2}{\{(1-k^*_{\mathrm{d}})\gamma^*_{\mathrm{b}} + [(1-k^*_{\mathrm{d}})DV^* - D\gamma^*_{\mathrm{b}}]\}^2} > 0.$$

The substrate concentration is an increasing function of the disintegration rate.

When the disintegration rate goes toward infinity we have

$$\lim_{\gamma^*_{\mathrm{b}}\to\infty} S^*_{\mathrm{nw}}(R^*=1) = \frac{k^*_{\mathrm{d}}\tau^* + D}{(1-k^*_{\mathrm{d}})\tau^* - D}.$$

Differentiating equation (3.74) with respect to the residence time we have

$$\frac{dS^*_{\mathrm{nw}}}{d\tau^*}(R^*=1) = \frac{-D\gamma^{*2}_{\mathrm{b}}}{\{(1-k^*_{\mathrm{d}})\gamma^*_{\mathrm{b}} + [(1-k^*_{\mathrm{d}})DV^* - D\gamma^*_{\mathrm{b}}]\}^2} < 0.$$

The substrate concentration is a decreasing function of the residence time.

When the residence time goes toward infinity we have

$$\lim_{\tau^*\to\infty} S^*_{\mathrm{nw}}(R^*=1) = \frac{k^*_{\mathrm{d}}}{1-k^*_{\mathrm{d}}}. \tag{3.75}$$

Equation (3.75) is same as equation (2.65).

When the sludge disintegration factor is equal to zero we have same result in chapter 2.

3.4.2.2 The general case $R^* \neq 1$

In the previous section we considered the special case when $R^* = 1$. Now we consider the general case when $0 \leq R^* < 1$.

Differentiating equation (3.62) with respect to the recycle parameter we obtain

$$\frac{dS^*_{\mathrm{nw}}}{dR^*} = -\frac{(DV^* + \gamma^*_{\mathrm{b}}\tau^*)^2\tau^*}{\{(1-k^*_{\mathrm{d}})\gamma^*_{\mathrm{b}}\tau^{*2} + [(1-k^*_{\mathrm{d}})DV^* - (1-R^*+D)\gamma^*_{\mathrm{b}}]\tau^* - (1-R^*)DV^*\}^2} < 0.$$

Hence the substrate concentration is a decreasing function of the effective recycle parameter (R^*). This makes sense because when the effective recycle parameter increases more biomass stay in the bioreactor which reduces the amount of the soluble substrate.

Differentiating equation (3.62) with respect to the residence time we obtain.

$$\frac{dS^*_{\mathrm{nw}}}{d\tau^*} = \frac{(R^*-1-D)\gamma^{*2}_{\mathrm{b}}\tau^{*2} + 2(R^*-1)DV^*\gamma^*_{\mathrm{b}}\tau^* + (R^*-1)D^2V^{*2}}{\{(1-k^*_{\mathrm{d}})\gamma^*_{\mathrm{b}}\tau^{*2} + [(1-k^*_{\mathrm{d}})DV^* - (1-R^*+D)\gamma^*_{\mathrm{b}}]\tau^* - (1-R^*)DV^*\}^2} < 0.$$

The substrate concentration along the no-washout branch is a strictly monotonically decreasing function of the residence time, i.e. the lowest effluent concentration is obtained at an infinite residence time. This makes sense on physical grounds.

When the residence time goes toward infinity in equation (3.62) we have

$$\lim_{\tau^* \to \infty} S^*_{\mathrm{nw}} = \frac{k^*_{\mathrm{d}}}{1-k^*_{\mathrm{d}}}.$$

Differentiating equation (3.62) with respect to the sludge disintegration factor we obtain

$$\frac{dS^*_{\mathrm{nw}}}{dD} = \frac{\gamma^{*2}_{\mathrm{b}}\tau^{*3}}{\{(1-k^*_{\mathrm{d}})\gamma^*_{\mathrm{b}}\tau^{*2} + [(1-k^*_{\mathrm{d}})DV^* - (1-R^*+D)\gamma^*_{\mathrm{b}}]\tau^* - (1-R^*)DV^*\}^2} > 0.$$

Hence the substrate concentration is an increasing function of the sludge disintegration factor (D). This makes sense because inside the sludge disintegration unit

killing biomass increases the amount of the soluble substrate.

When the sludge disintegration factor goes toward infinity in equation (3.62) we have

$$\lim_{D\to\infty} S^*_{\rm nw} = \frac{(1-R^*+k^*_{\rm d}\tau^*)V^*+\gamma^*_{\rm b}\tau^*}{[R^*-1+(1-k^*_{\rm d})\tau^*]V^*-\gamma^*_{\rm b}\tau^*}.$$

Differentiating equation (3.62) with respect to the disintegration rate we obtain.

$$\frac{dS^*_{\rm nw}}{d\gamma^*_{\rm b}} = \frac{V^*D^2\tau^{*2}}{\{(1-k^*_{\rm d})\gamma^*_{\rm b}\tau^{*2}+[(1-k^*_{\rm d})DV^*-(1-R^*+D)\gamma^*_{\rm b}]\tau^*-(1-R^*)DV^*\}^2}>0.$$

Hence the substrate concentration is an increasing function of the disintegration rate ($\gamma^*_{\rm b}$). This makes sense because when the disintegration unit of the biomass increases we have more biomass disintegrated.

When the disintegration rate goes toward infinity in equation (3.62) we have

$$\lim_{\gamma^*_{\rm b}\to\infty} S^*_{\rm nw} = \frac{1-R^*+k^*_{\rm d}\tau^*+D}{R^*-1+(1-k^*_{\rm d})\tau^*-D}.$$

3.4.3 Stability of the steady-state solutions

The Jacobian matrix for reduced model (3.45)-((3.48) is given by

$$J(S^*,X^*_{\rm b},X^*_i,X^*_{\rm s}) = \begin{pmatrix} a_1 & a_2 & a_3 & a_4 \\ b_1 & b_2 & 0 & 0 \\ 0 & c_2 & c_3 & 0 \\ 0 & d_2 & 0 & d_4 \end{pmatrix},$$

where

$$
\begin{aligned}
a_1 &= -\frac{X_{\mathrm{b}}^*}{(1+S^*)^2} - \frac{1}{\tau^*},\\
a_2 &= \frac{D\alpha\gamma_{\mathrm{b}}}{P}\left[\alpha_{\mathrm{g,s}} + \frac{\alpha_{\mathrm{g,h}}\gamma_{\mathrm{s}}(1-\alpha-f_{\mathrm{p,s}})\tau^*}{H} + \frac{\alpha_{\mathrm{g,SDU}}\beta_{\mathrm{i}}\gamma_{\mathrm{i}}f_{\mathrm{p,s}}\tau^*}{G}\right] + f_{\mathrm{s}}\alpha_{\mathrm{g,s}}k_{\mathrm{d}}^* - \frac{S^*}{1+S^*},\\
a_3 &= \frac{D\alpha\alpha_{\mathrm{g,SDU}}\beta_{\mathrm{i}}\gamma_{\mathrm{i}}}{G},\\
a_4 &= \frac{D\alpha\alpha_{\mathrm{g,h}}\gamma_{\mathrm{s}}}{H} + \alpha_{\mathrm{g,h}}k_{\mathrm{h}}^*,\\
b_1 &= \frac{X_{\mathrm{b}}^*}{(1+S^*)^2},\\
b_2 &= \frac{R^*-1}{\tau^*} - \frac{D\gamma_{\mathrm{b}}}{P} + \frac{S^*}{1+S^*} - k_{\mathrm{d}}^*,\\
c_2 &= f_{\mathrm{i}}k_{\mathrm{d}}^* + \frac{D^2V^*f_{\mathrm{p,s}}\gamma_{\mathrm{b}}}{GP},\\
c_3 &= \frac{1-R^*}{\tau^*} + \frac{D\beta_{\mathrm{i}}\gamma_{\mathrm{i}}}{G},\\
d_2 &= \frac{D^2V^*\gamma_{\mathrm{b}}(1-\alpha-f_{\mathrm{p,s}})}{HP},\\
d_4 &= \frac{1-R^*}{\tau^*} + k_{\mathrm{h}}^* + \frac{D\alpha\gamma_{\mathrm{s}}}{H}.
\end{aligned}
$$

The coefficients G, H and P are defined in equations (3.42), (3.43) and (3.44).

The expressions a_3, a_4, c_2, c_3, d_2 and d_4 are strictly positive.

3.4.3.1 Stability of the washout solution

The Jacobian matrix evaluated at the washout steady state solution is given by

$$
J(S_w^*, 0, X_{\mathrm{iw}}^*, X_{\mathrm{sw}}^*) = \begin{pmatrix} a_{1w} & a_{2w} & a_3 & a_4 \\ 0 & b_{2w} & 0 & 0 \\ 0 & c_2 & -c_3 & 0 \\ 0 & d_2 & 0 & -d_4 \end{pmatrix},
$$

where

$$
\begin{aligned}
a_{1w} &= -\frac{1}{\tau^*}, \\
a_{2w} &= \frac{D\alpha\gamma_{\mathrm{b}}}{P}\left[\alpha_{\mathrm{g,s}} + \frac{\alpha_{\mathrm{g,h}}\gamma_{\mathrm{s}}(1-\alpha-f_{\mathrm{p,s}})\tau^*}{H} + \frac{\alpha_{\mathrm{g,SDU}}\beta_{\mathrm{i}}\gamma_{\mathrm{i}}f_{\mathrm{p,s}}\tau^*}{G}\right] + f_{\mathrm{s}}\alpha_{\mathrm{g,s}}k_{\mathrm{d}}^* - \frac{S_w^*}{1+S_w^*}, \\
b_{2w} &= \frac{R^*-1}{\tau^*} - \frac{D\gamma_{\mathrm{b}}}{P} + \frac{S_w^*}{1+S_w^*} - k_{\mathrm{d}}^*.
\end{aligned}
$$

The eigenvalues of the matrix $J(S_w^*, 0, X_{\mathrm{iw}}^*, X_{\mathrm{sw}}^*)$ are

$$
\begin{aligned}
\lambda_{1w} &= a_{1w} = -\frac{1}{\tau^*} < 0, \\
\lambda_{2w} &= b_{2w} = \frac{R^*-1}{\tau^*} - \frac{D\gamma_{\mathrm{b}}}{P} + \frac{S_w^*}{1+S_w^*} - k_{\mathrm{d}}^*, \\
\lambda_3 &= -c_3 = -\frac{1-R^*}{\tau^*} - \frac{D\beta_{\mathrm{i}}\gamma_{\mathrm{i}}}{G} < 0, \\
\lambda_4 &= -d_4 = -\frac{1-R^*}{\tau^*} - k_{\mathrm{h}}^* - \frac{D\alpha\gamma_{\mathrm{s}}}{H} < 0,
\end{aligned}
$$

where G, H and P are positive (equations (3.42), (3.43) and (3.44)).

Recall that $0 \leq R^* \leq 1$. The stability of the washout branch depends upon the sign of λ_2.

Note that, the washout steady-state is always stable when

$$
\lambda_{2w} = b_{2w} = \frac{R^*-1}{\tau^*} - \frac{D\gamma_{\mathrm{b}}}{P} + \frac{S_w^*}{1+S_w^*} - k_{\mathrm{d}}^* < 0. \tag{3.76}
$$

This is always true when

$$
\begin{aligned}
& k_{\mathrm{d}}^* \geq 1, \\
\Rightarrow\ & \frac{k_{\mathrm{d}}}{\mu_{\mathrm{m}}} \geq 1, \\
\Rightarrow\ & k_{\mathrm{d}} \geq \mu_{\mathrm{m}}.
\end{aligned}
$$

This makes sense because it says that the washout steady state will always be stable if the death rate is greater than, or equal to, the maximum growth rate.

From equation (3.76) the eigenvalue λ_{2w} is negative when

$$\frac{R^*-1}{\tau^*}-\frac{D\gamma_{\mathrm{b}}}{P}+\frac{S_w^*}{1+S_w^*}-k_{\mathrm{d}}^*<0.$$

Substituting for the coefficient P which is defined in equation (3.44) and for S_w^* (3.49) gives the inequality

$$a_{\lambda_{2w}}\tau^{*5}+b_{\lambda_{2w}}\tau^{*4}+c_{\lambda_{2w}}\tau^{*3}+d_{\lambda_{2w}}\tau^{*3}+e_{\lambda_{2w}}\tau^{*2}+f_{\lambda_{2w}}\tau^*+g_{\lambda_{2w}}>0. \tag{3.77}$$

The coefficients are very large so they are not included. It is straightforward to solve this equation (numerically) using maple.

When we have $\gamma_b^*=\gamma_i^*=\gamma_s^*=\gamma$ the highest power of γ that appears in equation (3.77) is 3. Equation (3.77) can therefore be written in the form

$$\sum_{j=0}^{q=3}\sum_{i=0}^{p=5}a_{ij}\gamma^j\tau^{*i}=0. \tag{3.78}$$

We divide by γ^q to obtain $\sum_{j=0}^{q=3}\sum_{i=0}^{p=5}a_{ij}\gamma^{j-q}\tau^{*i}=0$.

To find the asymptote for the limit $\gamma\to\infty$ we take the leading order term to find the approximation equation $\sum_{i=0}^{p=5}a_{i3}\tau^{*i}=0$.

For the default values this is given by

$$(2.594613418\tau^{*2}-3.235519882\tau^*-0.2500527880)\tau^{*3}=0,$$

The solutions of this equation are

$$\tau^*=1.320023410,-0.07300916946,0.$$

This gives the asymptotic value for the residence time stated earlier ($\tau^*=1.201759685$). The negative value and the zero solution can be discarded as they are not physically meaningful.

For the default values we plot the curve $\lambda_{2w} = 0$ using equation (3.76) in figure 3.2 which shows how the value of the critical residence time varies as a function of the disintegration rate. For a fixed value of the disintegration rate, if the residence time is higher than the critical value $\tau^*(\gamma = \infty) = 1.3200$ then the washout solution is not stable. On the other hand if the residence time is smaller than the critical value then the washout solution is stable.

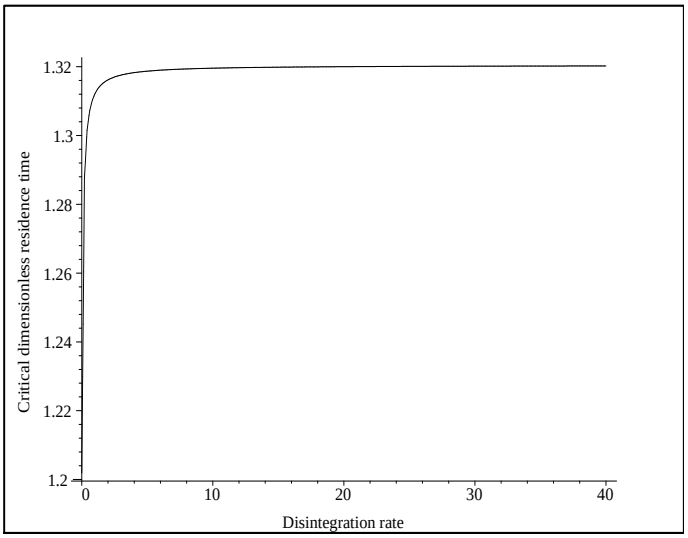

Figure 3.2: The residence time as a function of the disintegration rate γ. Parameter values: D=0.1, V^*=1 and R^*=0.

3.4.3.2 Stability of the no-washout solution

The Jacobian matrix for the no-washout branch is given by

$$J(S^*_{\rm nw}, X^*_{\rm b,nw}, X^*_{\rm i,nw}, X^*_{\rm s,nw}) = \begin{pmatrix} a_{1,\rm nw} & a_{2,\rm nw} & a_3 & a_4 \\ b_{1,\rm nw} & b_{2,\rm nw} & 0 & 0 \\ 0 & c_2 & -c_3 & 0 \\ 0 & d_2 & 0 & -d_4 \end{pmatrix},$$

where

$$a_{1,\mathrm{nw}} = -\frac{X^*_{\mathrm{b,nw}}}{(1+S^*_{\mathrm{nw}})^2} - \frac{1}{\tau^*},$$
$$a_{2,\mathrm{nw}} = \frac{D\alpha\gamma_{\mathrm{b}}}{P}\left[\alpha_{\mathrm{g,s}} + \frac{\alpha_{\mathrm{g,h}}\gamma_{\mathrm{s}}(1-\alpha-f_{\mathrm{p,s}})\tau^*}{H} + \frac{\alpha_{\mathrm{g,SDU}}\beta_{\mathrm{i}}\gamma_{\mathrm{i}}f_{\mathrm{p,s}}\tau^*}{G}\right] + f_{\mathrm{s}}\alpha_{\mathrm{g,s}}k^*_{\mathrm{d}} - \frac{S^*_{\mathrm{nw}}}{1+S^*_{\mathrm{nw}}},$$
$$b_{1,\mathrm{nw}} = \frac{X^*_{\mathrm{b,nw}}}{(1+S^*_{\mathrm{nw}})^2},$$
$$b_{2,\mathrm{nw}} = \frac{R^*-1}{\tau^*} - \frac{D\gamma_{\mathrm{b}}}{P} + \frac{S^*_{\mathrm{nw}}}{1+S^*_{\mathrm{nw}}} - k^*_{\mathrm{d}}.$$

The characteristic polynomial of the Jacobian matrix for the no-washout branch is given by

$$C(P) = \lambda^4_{\mathrm{nw}} + a_{1c}\lambda^3_{\mathrm{nw}} + a_{2c}\lambda^2_{\mathrm{nw}} + a_{3c}\lambda_{\mathrm{nw}} + a_{4c},$$

where

$$\begin{aligned}
a_{1c} &= d_4 + c_3 - b_{2,\mathrm{nw}} - a_{1,\mathrm{nw}},\\
a_{2c} &= -b_{1,\mathrm{nw}}a_{2,\mathrm{nw}} + b_{2,\mathrm{nw}}a_{1,\mathrm{nw}} - (a_{1,\mathrm{nw}} + b_{2,\mathrm{nw}})c_3 - (-c_3 + b_{2,\mathrm{nw}} + a_{1,\mathrm{nw}})d_4,\\
a_{3c} &= -d_2b_{1,\mathrm{nw}}a_4 + c_3b_{2,\mathrm{nw}}a_{1,\mathrm{nw}} - [-b_{2,\mathrm{nw}}a_{1,\mathrm{nw}} + (a_{1,\mathrm{nw}} + b_{2,\mathrm{nw}})c_3]d_4 - c_3b_{1,\mathrm{nw}}a_{2,\mathrm{nw}}\\
&\quad - d_4b_{1,\mathrm{nw}}a_{2,\mathrm{nw}} - c_2b_{1,\mathrm{nw}}a_3,\\
a_{4c} &= -d_2b_{1,\mathrm{nw}}a_4c_3 - d_4c_2b_{1,\mathrm{nw}}a_3 - d_4c_3b_{1,\mathrm{nw}}a_{2,\mathrm{nw}} + d_4c_3b_{2,\mathrm{nw}}a_{1,\mathrm{nw}}.
\end{aligned} \tag{3.79}$$

The no-washout steady state is stable when a_{1c}, a_{3c}, and a_{4c} are positive and $a_{1c}a_{2c}a_{3c}$ $>a^2_{3c} + a^2_{1c}a_{4c}$ [59]. No progress can be made analytically.

From equation (3.79) we have

$$a_{4c1}\tau^{*8} + b_{4c1}\tau^{*7} + c_{4c1}\tau^{*6} + d_{4c1}\tau^{*5} + e_{4c1}\tau^{*4} + f_{4c1}\tau^{*3} + g_{4c1}\tau^{*3} + h_{4c1}\tau^{*2} + i_{4c1}\tau^* + j_{4c1} > 0, \tag{3.80}$$

where

$$j_{4c1} = D^5 V^{*5} (R^* - 1)^5 (1 + S_0^*).$$

The other coefficients are very large so they are not included because there are many terms in the expansions. It is straightforward to solve this equation (numerically) using maple.

When we have $\gamma_b^* = \gamma_i^* = \gamma_s^* = \gamma$ the highest power of γ that appears in equation (3.80) is 5. Equation (3.80) can therefore be written in the form

$$\sum_{j=0}^{q=5} \sum_{i=0}^{p=8} a_{ij} \gamma^j \tau^{*i} = 0. \tag{3.81}$$

We divide by γ^q to obtain $\sum_{j=0}^{q=5} \sum_{i=0}^{p=8} a_{ij} \gamma^{j-q} \tau^{*i} = 0$.

To find the asymptote for the limit $\gamma \to \infty$ we take the leading order term to find the approximation equation $\sum_{i=0}^{p=8} a_{i5} \tau^{*i} = 0$.

For the default values this is given by

$$(-0.5708149520\tau^{*3} + 0.5862350846\tau^{*2} + 0.2116107757\tau^* + 0.1210255494)\tau^{*5} = 0,$$

The solutions of this equation are

$$\tau^* = 1.320023410, -0.07300916944, -0.2200000001, 0.$$

This gives the asymptotic value for the residence time stated earlier ($\tau^* = 1.201759685$). The two negative values and the zero solution can be discarded as they are not physically meaningful. For the default values we plot the curve $a_{4c} = 0$ using equation (3.79) in figure 3.3 which shows how the value of the critical residence time varies as a function of the disintegration rate. For a fixed value of the disintegration rate, if the residence time is higher than the critical value $\tau^*(\gamma = \infty) = 1.3200$ then the

no-washout solution is stable. On the other hand if the residence time is smaller than the critical value then the no-washout solution is unstable.

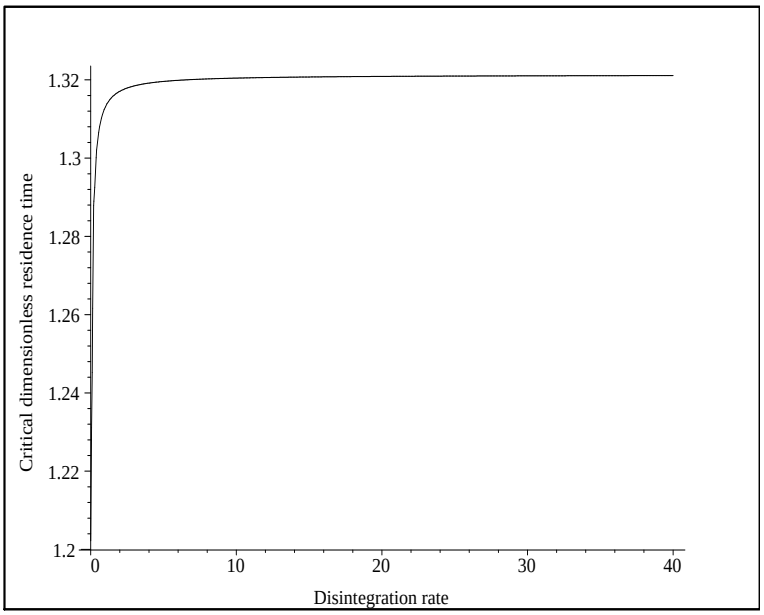

Figure 3.3: The residence time as a function of the disintegration rate γ. Parameter values: D=0.1, V^*=1 and R^*=0.

Figures 3.2 and 3.3 are identical. They *should* be the same because we expect that there is a trans-critical bifurcation at which the stability of the washout and the no-washout branches swap.

3.4.4 Large residence time approximations

In this section we obtained asymptotic solutions for large the no-washout branch residence times. We have

$$S^*_{\mathrm{nw}} \approx \frac{k^*_{\mathrm{d}}}{1-k^*_{\mathrm{d}}} + \frac{(1-R^*+D)}{(k^*_{\mathrm{d}}-1)^2}\cdot\frac{1}{\tau^*} + O\left(\frac{1}{\tau^{*2}}\right), \tag{3.82}$$

$$X^*_{\mathrm{b,nw}} \approx a_0\cdot\frac{1}{\tau^*} + O\left(\frac{1}{\tau^{*2}}\right), \tag{3.83}$$

$$X^*_{\mathrm{i,nw}} \approx \frac{X^*_{\mathrm{i},0}}{1-R^*+D} + \frac{f_{\mathrm{i}}k^*_{\mathrm{d}}}{1-R^*+D}a_0 + \frac{a_1}{\tau^*} + O\left(\frac{1}{\tau^{*2}}\right), \tag{3.84}$$

$$X^*_{\mathrm{s,nw}} \approx \frac{X^*_{\mathrm{s},0}}{k^*_{\mathrm{h}}}\cdot\frac{1}{\tau^*} + O\left(\frac{1}{\tau^{*2}}\right), \tag{3.85}$$

$$\mathrm{COD}^*_{\mathrm{nw}} \approx \frac{k^*_{\mathrm{d}}}{1-k^*_{\mathrm{d}}} + \left[\frac{(1-R^*+D)}{(k^*_{\mathrm{d}}-1)^2} + \frac{\alpha_{\mathrm{g,h}}X^*_{\mathrm{s},0}}{k^*_{\mathrm{h}}}\right]\cdot\frac{1}{\tau^*} + O\left(\frac{1}{\tau^{*2}}\right), \tag{3.86}$$

$$\mathrm{VSS}^*_{\mathrm{nw}} \approx \frac{X^*_{\mathrm{i},0}}{1-R^*+D} + \frac{f_{\mathrm{i}}k^*_{\mathrm{d}}}{1-R^*+D}a_0 + \left(a_0+a_1+\frac{X^*_{\mathrm{s},0}}{k^*_{\mathrm{h}}}\right)\cdot\frac{1}{\tau^*} + O\left(\frac{1}{\tau^{*2}}\right), \tag{3.87}$$

where

$$a_0 = \frac{(1-k^*_{\mathrm{d}})[(1-R^*+D)(\alpha_{\mathrm{g,h}}X^*_{\mathrm{s},0}+S^*_0) + D\alpha\alpha_{\mathrm{g,SDU}}X^*_{\mathrm{i},0}] - k^*_{\mathrm{d}}(1-R^*+D)}{k^*_{\mathrm{d}}(1-k^*_{\mathrm{d}})[(1-R^*+D)(1-f_{\mathrm{s}}\alpha_{\mathrm{g,s}}) - D\alpha\alpha_{\mathrm{g,SDU}}f_{\mathrm{i}}]}, \tag{3.88}$$

$$a_1 = \frac{A_{a1}+B_{a1}}{C_{a1}}, \tag{3.89}$$

where

$$A_{a1} = A_{\rm as}B_{\rm as}[C_{\rm as}(D_{\rm as} + E_{\rm as}F_{\rm as}) - G_{\rm as}(H_{\rm as} + I_{\rm as} + J_{\rm as}) - K_{\rm as}L_{\rm as}],$$

$$B_{a1} = M_{\rm as}\{N_{\rm as} + O_{\rm as} + P_{\rm as} + Q_{\rm as} + [R_{\rm as} + S_{\rm as}\gamma_{\rm b}^* + T_{\rm as}\alpha\gamma_{\rm b}^*\gamma_{\rm s}^* + (U_{\rm as} + V_{\rm as} + W_{\rm as})$$
$$B_{\rm as}]F_{\rm as}\},$$

$$C_{a1} = A_{\rm as}B_{\rm as}(D_{\rm as} + E_{\rm as}F_{\rm as}),$$

$$A_{\rm as} = (1 - k_{\rm d}^*)(1 - R^* + d)[D\alpha\alpha_{\rm g,SDU}f_{\rm i} + (f_{\rm s}\alpha_{\rm g,s} - 1)(1 - R^* + d)],$$

$$B_{\rm as} = \alpha\beta_{\rm i}\gamma_{\rm i}\gamma_{\rm b}\gamma_{\rm s},$$

$$C_{\rm as} = \frac{D^2V^*X_{\rm i,0}^*}{F_{\rm as}(1 - R^* + D)},$$

$$D_{\rm as} = D\alpha\alpha_{\rm g,SDU}f_{\rm i}, \beta_{\rm i}\gamma_{\rm i}k_{\rm d}^*,$$

$$E_{\rm as} = k_{\rm d}^*(f_{\rm s}\alpha_{\rm g,s} - 1),$$

$$F_{\rm as} = (1 - R^* + D)\beta_{\rm i}\gamma_{\rm i},$$

$$G_{\rm as} = f_{\rm i}k_{\rm d}^*\beta_{\rm i}\gamma_{\rm i},$$

$$H_{\rm as} = \frac{-(1 - R^* + D)}{(k_{\rm d}^* - 1)^2},$$

$$I_{\rm as} = D\alpha\left(\frac{\alpha_{\rm g,h}X_{\rm s,0}^*}{\alpha k_{\rm h}^*} - \frac{(1 - R^*)DV^*\alpha_{\rm g,SDU}X_{\rm i,0}^*}{F_{\rm as}(1 - R^* + D)}\right),$$

$$J_{\rm as} = -\frac{(1 - R^* + D)\alpha_{\rm g,h}X_{\rm s,0}^*}{k_{\rm h}^*},$$

$$K_{\rm as} = \frac{D^2V^*f_{\rm i}k_{\rm d}^*}{1 - R^* + D},$$

$$L_{\rm as} = \frac{S_0^*(1 - k_{\rm d}^*) - k_{\rm d}^*}{1 - k_{\rm d}^*} + \frac{D\alpha\alpha_{\rm g,SDU}X_{\rm i,0}^*}{1 - R^* + D} + \alpha_{\rm g,h}X_{\rm s,0}^*,$$

$$M_{\rm as} = f_{\rm i}\{(-1 + R^* - D)[(k_{\rm d}^* - 1)(S_0^* + \alpha_{\rm g,h}X_{\rm s,0}^*) + k_{\rm d}^*] + D\alpha\alpha_{\rm g,SDU}X_{\rm i,0}^*(1 - k_{\rm d}^*)\},$$

$$N_{\rm as} = \{D\beta_{\rm i}\gamma_{\rm i}\gamma_{\rm b}[k_{\rm h}^*\alpha F_{\rm as}[\alpha\gamma_{\rm s}(\alpha_{\rm g,s} + \alpha_{\rm g,SDU}f_{\rm p,s}) + \alpha_{\rm g,h}\gamma_{\rm s}(1 - \alpha - f_{\rm p,s})] +$$
$$\beta_{\rm i}\gamma_{\rm i}\alpha\alpha_{\rm g,SDU}f_{\rm i}k_{\rm d}^*[DV^*k_{\rm h}^* + \alpha\gamma_{\rm s}(1 - R^* + D)]]\}/k_{\rm h}^*,$$

$$O_{\rm as} = D^2V^*\alpha\beta_{\rm i}\gamma_{\rm i}f_{\rm i}k_{\rm d}^*\alpha_{\rm g,SDU}[\beta_{\rm i}\gamma_{\rm i}(\gamma_{\rm b} + \gamma_{\rm s}\alpha) + \gamma_{\rm b}\gamma_{\rm s}\alpha],$$

$$P_{\rm as} = -\frac{D\alpha\gamma_{\rm b}\beta_{\rm i}^2\gamma_{\rm i}^2f_{\rm i}k_{\rm d}^*\alpha_{\rm g,SDU}[DV^*k_{\rm h}^* + \alpha\gamma_{\rm s}(1 - R^* + D)]}{k_{\rm h}^*},$$

$$Q_{\rm as} = T_{\rm as}\alpha\beta_{\rm i}\gamma_{\rm i}\gamma_{\rm b}\gamma_{\rm s}(1 - R^*),$$

$$R_{\rm as} = T_{\rm as}\alpha\beta_{\rm i}\gamma_{\rm i}\gamma_{\rm s},$$

$$S_{\rm as} = T_{\rm as}\beta_{\rm i}\gamma_{\rm i},$$

$$T_{\rm as} = \frac{D^2V^*\alpha\alpha_{\rm g,SDU}f_{\rm i}k^*_{\rm d}}{1-R^*+D},$$

$$U_{\rm as} = \frac{k^*_{\rm d}\{\gamma_{\rm b}(f_{\rm s}\alpha_{\rm g,s}-1)[k^*_{\rm h}DV^*+(1-R^*+d)\alpha\gamma_{\rm s}]+DV^*k^*_{\rm h}\alpha\gamma_{\rm s}f_{\rm s}\alpha_{\rm g,s}\}}{k^*_{\rm h}\alpha\gamma_{\rm b}\gamma_{\rm s}},$$

$$V_{\rm as} = \frac{-[k^*_{\rm d}DV^*+(1-R^*+d)\gamma_{\rm b}]k^*_{\rm h}\alpha\gamma_{\rm s}-k^*_{\rm d}\gamma_{\rm b}(f_{\rm s}\alpha_{\rm g,s}-1)[k^*_{\rm h}DV^*+(1-R^*+d)\alpha\gamma_{\rm s}]}{k^*_{\rm h}\alpha\gamma_{\rm b}\gamma_{\rm s}},$$

$$W_{\rm as} = -\frac{DV^*k^*_{\rm d}(f_{\rm s}\alpha_{\rm g,s}-1)}{\gamma_{\rm b}}.$$

When the rate constants of the three sludge disintegration processes are equal $\gamma_{\rm b}=\gamma_{\rm i}=\gamma_{\rm s}=\gamma$ the expressions do not have any significant simplification.

To order $\frac{1}{\tau^*}$ at large residence time the value of the chemical oxygen demand only depends upon one parameter associated withe the operation of the sludge disintegration unit, i.e. the sludge disintegration factor (D).

Differentiating equation (3.86) with respect to the disintegration rate we have

$$\frac{d{\rm COD}^*_{\rm nw}}{dD} = \frac{1}{(1-k^*_{\rm d})^2}\cdot\frac{1}{\tau^*}>0.$$

The value of the chemical oxygen demand is an increasing function of the sludge disintegration factor D.

Differentiating equation (3.87) with respect to the disintegration rate we have

$$\frac{d{\rm VSS}^*_{\rm nw}}{dD} = \frac{\{(k^*_d-1)[f_i(\alpha_{\rm g,h}X^*_{\rm s,0}+S^*_0)+X^*_{\rm i,0}(1-f_s\alpha_{\rm g,s})]+f_ik^*_d\}(1-f_s\alpha_{\rm g,s}-\alpha\alpha_{\rm g,SDU}f_i)}{(1-k^*_{\rm d})[(1+D-R^*)(f_s\alpha_{\rm g,s}-1)+D\alpha\alpha_{\rm g,SDU}f_i]^2}<0.$$

Numerical experiment shows that the value of the volatile suspended solids is a decreasing function of the sludge disintegration factor D.

We could anticipate that the sludge disintegration unit increases the effluent concentration for two reasons: firstly it kills the biomass and secondly in so doing it

converts the biomass into inert material and soluble substrate.

When the residence time goes toward infinity the volatile suspended solids only depends upon three parameters associated with the operation of the sludge disintegration unit D, and the parameter group $\alpha\alpha_{\mathrm{g,SDU}}$.

3.5 Results (when $\gamma_{\mathrm{b}}^* = \gamma_i^* = \gamma_{\mathrm{s}}^* = \gamma$)

In this section we consider the special case when the values of the three disintegration rates are equal, that to say when $\gamma_{\mathrm{b}}^* = \gamma_i^* = \gamma_{\mathrm{s}}^* = \gamma$. In particular we study the limit when $\gamma \to \infty$.

3.5.1 Steady-state solution branches

From equations (3.34)-(3.37) we have inside the sludge disintegration unit when $\gamma_{\mathrm{b}}^* = \gamma_i^* = \gamma_{\mathrm{s}}^* = \gamma$ that

$$\frac{dS_{\mathrm{s}}^*}{dt^*} = \frac{DV^*}{\tau^*}(S^* - S_{\mathrm{s}}^*) + \gamma[\alpha\alpha_{\mathrm{g,s}}X_{\mathrm{b,s}}^* + \alpha\alpha_{\mathrm{g,h}}X_{\mathrm{s,s}}^* + \beta_{\mathrm{i}}\alpha\alpha_{\mathrm{g,SDU}}X_{\mathrm{i,s}}^*], \tag{3.90}$$

$$\frac{dX_{\mathrm{b,s}}^*}{dt^*} = \frac{DV^*}{\tau^*}(X_{\mathrm{b}}^* - X_{\mathrm{b,s}}^*) - \gamma X_{\mathrm{b,s}}^*, \tag{3.91}$$

$$\frac{dX_{\mathrm{i,s}}^*}{dt^*} = \frac{DV^*}{\tau^*}(X_i^* - X_{\mathrm{i,s}}^*) + \gamma[f_{\mathrm{p,s}}X_{\mathrm{b,s}}^* - \beta_{\mathrm{i}}X_{\mathrm{i,s}}^*], \tag{3.92}$$

$$\frac{dX_{\mathrm{s,s}}^*}{dt^*} = \frac{DV^*}{\tau^*}(X_{\mathrm{s}}^* - X_{\mathrm{s,s}}^*) + \gamma[(1-\alpha-f_{\mathrm{p,s}})X_{\mathrm{b,s}}^* - \alpha X_{\mathrm{s,s}}^*]. \tag{3.93}$$

The steady-state solutions in the sludge disintegration unit are given by

$$\begin{aligned} S_s^* &= S^* + \left[\frac{\alpha_{g,s}\gamma X_{b,s}^* + \alpha_{g,h}\gamma X_{s,s}^* + \beta_i\alpha_{\mathrm{g,SDU}}\gamma X_{i,s}^*}{DV^*}\right]\alpha\tau^*, \\ &= S^* + \left[\frac{\gamma}{P}\left(\alpha_{g,s} + \frac{\alpha_{g,h}\gamma(1-\alpha-f_{p,s})\tau^*}{H} + \frac{\beta_i\alpha_{\mathrm{g,SDU}}\gamma f_{p,s}\tau^*}{G}\right)X_b^* \right. \\ &\quad \left. + \left(\frac{\alpha_{g,h}\gamma X_s^*}{H} + \frac{\beta_i\alpha_{\mathrm{g,SDU}}\gamma X_i^*}{G}\right)\right]\alpha\tau^*, \end{aligned} \tag{3.94}$$

$$X_{b,s}^* = \frac{DV^*}{P} X_b^*, \tag{3.95}$$

$$\begin{aligned} X_{i,s}^* &= \frac{1}{G}(DV^* X_i^* + f_{p,s}\gamma X_{b,s}^* \tau^*), \\ &= \frac{DV^*}{GP}\left(PX_i^* + f_{p,s}\gamma X_b^* \tau^*\right), \end{aligned} \tag{3.96}$$

$$\begin{aligned} X_{s,s}^* &= \frac{1}{H}\left[DV^* X_s^* + (1-\alpha-f_{p,s})\gamma X_{b,s}^* \tau^*\right], \\ &= \frac{DV^*}{PH}\left[PX_s^* + (1-\alpha-f_{p,s})\gamma X_b^* \tau^*\right], \end{aligned} \tag{3.97}$$

where G, H and B are defined in equations (3.42), (3.43) and (3.44).

Substituting expressions (3.94)-(3.97) into (3.21)-(3.24) we obtain the reduced model for the bioreactor

$$\begin{aligned} \frac{dS^*}{dt^*} = \frac{S_0^* - S^*}{\tau^*} + \Bigg\{ \frac{D\alpha\gamma}{P_\gamma}\left[\alpha_{\mathrm{g,s}} + \frac{\alpha_{\mathrm{g,h}}\gamma(1-\alpha-f_{\mathrm{p,s}})\tau^*}{H_\gamma} + \frac{\beta_{\mathrm{i}}\alpha_{\mathrm{g,SDU}}\gamma f_{\mathrm{p,s}}\tau^*}{G_\gamma}\right] \\ + f_{\mathrm{s}}\alpha_{\mathrm{g,s}} k_d^* \tau^* - \frac{S^*}{1+S^*}\Bigg\} X_{\mathrm{b}}^* + D\alpha\gamma\left[\frac{\alpha_{\mathrm{g,h}} X_{\mathrm{s}}^*}{H_\gamma} + \frac{\beta_{\mathrm{i}}\alpha_{\mathrm{g,SDU}} X_{\mathrm{i}}^*}{G_\gamma}\right] + \alpha_{\mathrm{g,h}} k_h^* X_{\mathrm{s}}^*, \end{aligned} \tag{3.98}$$

$$\frac{dX_{\mathrm{b}}^*}{dt^*} = \left[\frac{R^*-1}{\tau^*} - \frac{D\gamma}{P_\gamma} + \frac{S^*}{1+S^*} - k_d^*\right] X_{\mathrm{b}}^*, \tag{3.99}$$

$$\frac{dX_i^*}{dt^*} = \frac{X_{\mathrm{i,0}}^*}{\tau^*} + \left[R^* - 1 - \frac{D\beta_{\mathrm{i}}\gamma\tau^*}{G_\gamma}\right]\frac{X_i^*}{\tau^*} + \left[\frac{D^2 V^* f_{\mathrm{p,s}}\gamma}{P_\gamma G_\gamma} + f_{\mathrm{i}} k_d^*\right] X_{\mathrm{b}}^*, \tag{3.100}$$

$$\frac{dX_{\mathrm{s}}^*}{dt^*} = \frac{X_{\mathrm{s,0}}^*}{\tau^*} + \left[R^* - 1 - k_h^*\tau^* - \frac{D\alpha\gamma\tau^*}{H_\gamma}\right]\frac{X_{\mathrm{s}}^*}{\tau^*} + \left[\frac{D^2 V^*(1-\alpha-f_{\mathrm{p,s}})\gamma}{P_\gamma H_\gamma}\right] X_{\mathrm{b}}^*. \tag{3.101}$$

The washout steady-state solutions inside the bioreactor are given by

$$S_w^* = S_0^* + \frac{(D\alpha\alpha_{\mathrm{g,h}}\gamma + A_\gamma)X_{\mathrm{s,0}}^*\tau^*}{C_\gamma} + \frac{D\alpha\alpha_{\mathrm{g,SDU}}\gamma\beta_{\mathrm{i}} X_{\mathrm{i,0}}^*\tau^*}{F_\gamma} > 0, \tag{3.102}$$

$$X_{\mathrm{bw}}^* = 0, \tag{3.103}$$

$$X_{\mathrm{iw}}^* = \frac{G_\gamma}{F_\gamma} X_{\mathrm{i,0}}^* > 0, \tag{3.104}$$

$$X_{\mathrm{sw}}^* = \frac{H_\gamma}{C_\gamma} X_{\mathrm{s,0}}^* > 0. \tag{3.105}$$

The washout steady-state solutions in the sludge disintegration unit are given by

$$S_{\mathrm{sw}}^* = S_0^* + \frac{(D\alpha\alpha_{\mathrm{g,h}}\gamma + A_\gamma)X_{\mathrm{s,0}}^*\tau^*}{C_\gamma} + \frac{D\alpha\alpha_{\mathrm{g,SDU}}\gamma\beta_{\mathrm{i}}X_{\mathrm{i,0}}^*\tau^*}{F_\gamma} + \left(\frac{\alpha_{\mathrm{g,h}}\gamma X_{\mathrm{s,0}}^*}{C_\gamma} + \frac{\beta_{\mathrm{i}}\alpha_{\mathrm{g,SDU}}\gamma X_{\mathrm{i,0}}^*}{F_\gamma}\right)\alpha\tau^*, \tag{3.106}$$

$$X_{\mathrm{b,sw}}^* = 0, \tag{3.107}$$

$$X_{\mathrm{i,sw}}^* = \frac{DV^*}{F_\gamma}X_{\mathrm{i,0}}^*, \tag{3.108}$$

$$X_{\mathrm{s,sw}}^* = \frac{DV^*}{C_\gamma}X_{\mathrm{s,0}}^*. \tag{3.109}$$

The no-washout steady-state solutions inside the bioreactor are given by

$$S_{\mathrm{nw}}^* = \frac{(DV^* + \gamma\tau^*)[1 - R^* + k_d^*\tau^*] + D\gamma\tau^*}{(DV^* + \gamma\tau^*)[R^* - 1 + (1 - k_d^*)\tau^*] - D\gamma\tau^*}, \tag{3.110}$$

$$X_{\mathrm{b,nw}}^* = \frac{-U_\gamma}{N_\gamma}, \tag{3.111}$$

$$X_{\mathrm{i,nw}}^* = \frac{G_\gamma}{F_\gamma}X_{\mathrm{i,0}}^* + \frac{K_\gamma}{F_\gamma P_\gamma}X_{\mathrm{b,nw}}^*, \tag{3.112}$$

$$X_{\mathrm{s,nw}}^* = \frac{H_\gamma}{C_\gamma}X_{\mathrm{s,0}}^* + \frac{J_\gamma}{C_\gamma P_\gamma}X_{\mathrm{b,nw}}^*. \tag{3.113}$$

The no-washout steady-state solutions in the sludge disintegration unit are given by

$$S_{\mathrm{s,nw}}^* = \frac{[1 - R^* + k_d^*\tau^*]P_\gamma + D\gamma\tau^*}{[R^* - 1 + (1 - k_d^*)\tau^*]P_\gamma - D\gamma\tau^*} + \left\{\frac{\alpha_{\mathrm{g,h}}\gamma X_{\mathrm{s,0}}^*}{C_\gamma} + \frac{\beta_{\mathrm{i}}\alpha_{\mathrm{g,SDU}}\gamma X_{\mathrm{i,0}}^*}{F_\gamma} - \frac{U_\gamma}{P_\gamma N_\gamma}\left[\alpha_{\mathrm{g,s}}\gamma + \frac{\alpha_{\mathrm{g,h}}\gamma}{H_\gamma}\left((1 - \alpha - f_{\mathrm{p,s}})\gamma\tau^* + \frac{J_\gamma}{C_\gamma}\right) + \frac{\beta_{\mathrm{i}}\alpha_{\mathrm{g,SDU}}\gamma}{G_\gamma}\left(\gamma f_{\mathrm{p,s}}\tau^* + \frac{K_\gamma}{F_\gamma}\right)\right]\right\} \alpha\tau^*, \tag{3.114}$$

$$X_{\mathrm{b,snw}}^* = \frac{-U_\gamma DV^*}{P_\gamma N_\gamma}, \tag{3.115}$$

$$X_{\mathrm{i,snw}}^* = DV^*\left[\frac{X_{\mathrm{i,0}}^*}{F_\gamma} - \frac{U}{P_\gamma G_\gamma N_\gamma}\left(\gamma f_{\mathrm{p,s}}\tau^* + \frac{K_\gamma}{F_\gamma}\right)\right], \tag{3.116}$$

$$X_{\mathrm{s,snw}}^* = DV^*\left[\frac{X_{\mathrm{s,0}}^*}{C_\gamma} - \frac{U_\gamma}{H_\gamma P_\gamma N_\gamma}\left((1 - \alpha - f_{\mathrm{p,s}})\gamma\tau^* + \frac{J_\gamma}{C_\gamma}\right)\right], \tag{3.117}$$

where

$$A_\gamma = H_\gamma \alpha_{\mathrm{g,h}} k_h^* > 0,$$

$$B_\gamma = P_\gamma(1 - R^* + k_d^* \tau^*) + D\gamma\tau^* > 0,$$

$$C_\gamma = H_\gamma(1 - R^* + k_h^* \tau^*) + D\alpha\gamma\tau^* > 0,$$

$$E_\gamma = P_\gamma(R^* - 1 - (k_d^* - 1)\tau^*) - D\gamma\tau^* > 0 \quad \text{provided} \quad \tau^* > \frac{P_\gamma(1 - R^*)}{(1 - k_d^*)P_\gamma - D\gamma},$$

if $(1 - k_d^*)P_\gamma - D\gamma > 0 \Rightarrow \tau^* > 0$, if $(1 - k_d^*)P_\gamma - D\gamma < 0 \Rightarrow \tau^* < 0$.

$$F_\gamma = G_\gamma(1 - R^*) + D\gamma\beta_{\mathrm{i}}\tau^* > 0,$$

$$G_\gamma = DV^* + \beta_{\mathrm{i}}\gamma\tau^* > 0,$$

$$H_\gamma = DV^* + \alpha\gamma\tau^* > 0,$$

$$J_\gamma = (1 - \alpha - f_{\mathrm{p,s}})D^2 V^* \gamma\tau^* > 0 \quad \text{from (3.2)},$$

$$K_\gamma = \{DV^*[f_{\mathrm{i}} k_d^*(\gamma\tau^* + G_\gamma) + D f_{\mathrm{p,s}}\gamma] + f_{\mathrm{i}} k_d^* \gamma^2 \beta_{\mathrm{i}} \tau^{*2}\}\tau^* > 0,$$

$$L_\gamma = (1 - \alpha - f_{\mathrm{p,s}})\alpha_{\mathrm{g,h}}\gamma\tau^* > 0,$$

$$M_\gamma = \alpha_{\mathrm{g,SDU}}\gamma\beta_{\mathrm{i}} f_{\mathrm{p,s}}\tau^* > 0,$$

$$N_\gamma = \frac{1}{C_\gamma P_\gamma}\left(\frac{N1_\gamma}{F_\gamma G_\gamma H_\gamma} + \frac{N2_\gamma}{\tau^*}\right),$$

$$N1_\gamma = D\alpha\{[C_\gamma\gamma(H_\gamma(G_\gamma\alpha_{\mathrm{g,s}} + M_\gamma) + G_\gamma L_\gamma) + G_\gamma J_\gamma \alpha_{\mathrm{g,h}}\gamma]F_\gamma + C_\gamma H_\gamma K_\gamma \alpha_{\mathrm{g,SDU}}\gamma\beta_{\mathrm{i}}\},$$

$$N2_\gamma = \tau^*[J\alpha_{\mathrm{g,h}} k_{\mathrm{h}}^* + CP f_{\mathrm{s}} \alpha_{\mathrm{g,s}} k_{\mathrm{d}}^*] - B_\gamma C_\gamma,$$

$$P_\gamma = DV^* + \gamma\tau^* > 0,$$

$$U_\gamma = U1_\gamma + U2_\gamma + U3_\gamma,$$

$$U1_\gamma = \frac{S_0^* E_\gamma - B_\gamma}{E_\gamma \tau^*},$$

$$U2_\gamma = D\alpha\left(\frac{\alpha_{\mathrm{g,h}}\gamma X_{\mathrm{s,0}}^*}{C_\gamma} + \frac{\alpha_{\mathrm{g,SDU}}\gamma\beta_{\mathrm{i}} X_{\mathrm{i,0}}^*}{F_\gamma}\right),$$

$$U3_\gamma = \frac{H_\gamma \alpha_{\mathrm{g,h}} k_{\mathrm{h}}^* X_{\mathrm{s,0}}^*}{C_\gamma}.$$

In the limit that $\gamma \to \infty$ from (3.102)-(3.105) we have

Washout solution in the bioreactor

$$S_w^* = S_0^* + \frac{(D + k_h^*)K_{\gamma\to\infty}}{A_{\gamma\to\infty} + k_{\mathrm{h}}^*\tau^*} + \frac{D\alpha_{\mathrm{g,SDU}}X_{\mathrm{i,0}}^*}{A_{\gamma\to\infty}} + \frac{A_*}{\gamma} + O\left(\frac{1}{\gamma^2}\right), \tag{3.118}$$

$$X_{\mathrm{bw}}^* = 0, \tag{3.119}$$

$$X_{\mathrm{iw}}^* = \frac{X_{\mathrm{i,0}}^*}{A_{\gamma\to\infty}} + \frac{D^2V^*X_{\mathrm{i,0}}^*}{A_{\gamma\to\infty}^2\beta_{\mathrm{i}}\tau^*} \cdot \frac{1}{\gamma} + O\left(\frac{1}{\gamma^2}\right), \tag{3.120}$$

$$X_{\mathrm{sw}}^* = \frac{X_{\mathrm{s,0}}^*}{A_{\gamma\to\infty} + k_{\mathrm{h}}^*\tau^*} + \left(1 + \frac{D^2V^*}{(A_{\gamma\to\infty} + k_{\mathrm{h}}^*\tau^*)\alpha\tau^*} \cdot \frac{1}{\gamma}\right) + O\left(\frac{1}{\gamma^2}\right). \tag{3.121}$$

From (3.106)-(3.109) we have

Washout solution inside the sludge disintegration unit

$$S_{\mathrm{sw}}^* = S_0^* + \frac{(1 + D + k_h^*\tau^*)K_{\gamma\to\infty}}{A_{\gamma\to\infty} + k_{\mathrm{h}}^*\tau^*} + \frac{\alpha\alpha_{\mathrm{g,SDU}}X_{\mathrm{i,0}}^*(1+D)}{A_{\gamma\to\infty}} + \frac{B_*}{\gamma} + O\left(\frac{1}{\gamma^2}\right), \tag{3.122}$$

$$X_{\mathrm{b,sw}}^* = 0, \tag{3.123}$$

$$X_{\mathrm{i,sw}}^* = \frac{DV^*X_{\mathrm{i,0}}^*}{A_{\gamma\to\infty}\beta_{\mathrm{i}}\tau^*} \cdot \frac{1}{\gamma} + O\left(\frac{1}{\gamma^2}\right), \tag{3.124}$$

$$X_{\mathrm{s,sw}}^* = \frac{DV^*X_{\mathrm{s,0}}^*}{(A_{\gamma\to\infty} + k_{\mathrm{h}}^*)\alpha\tau^*} \cdot \frac{1}{\gamma} + O\left(\frac{1}{\gamma^2}\right). \tag{3.125}$$

From (3.110)-(3.113) we have

No-washout solution in the bioreactor

$$S_{\mathrm{nw}}^* = -\frac{O_{\gamma\to\infty}}{R_{\gamma\to\infty}} + \frac{O_{\gamma\to\infty}}{R_{\gamma\to\infty}} \cdot \frac{1}{\gamma} + O\left(\frac{1}{\gamma^2}\right), \tag{3.126}$$

$$X_{\mathrm{b,nw}}^* = \frac{C_{\gamma\to\infty} - D_{\gamma\to\infty}}{E_{\gamma\to\infty}} + \frac{C_*}{\gamma} + O\left(\frac{1}{\gamma^2}\right), \tag{3.127}$$

$$X_{\mathrm{i,nw}}^* = \frac{X_{\mathrm{i,0}}^*}{A_{\gamma\to\infty}} - \frac{X_{\gamma\to\infty}}{Y_{\gamma\to\infty}} + \frac{D_*}{\gamma} + O\left(\frac{1}{\gamma^2}\right), \tag{3.128}$$

$$X_{\mathrm{s,nw}}^* = \frac{X_{\mathrm{s,0}}^*\tau^*}{U_{\gamma\to\infty}} + \frac{E_*}{\gamma} + O\left(\frac{1}{\gamma^2}\right). \tag{3.129}$$

From (3.114)-(3.117) we have

No-washout solution inside the sludge disintegration unit

$$S_{\mathrm{s,nw}}^* = \frac{A_{\gamma\to\infty} + k_d^*\tau^*}{-A_{\gamma\to\infty} + (1-k_d^*)\tau^*} - \frac{(G_{\gamma\to\infty} + I_{\gamma\to\infty} + L_{\gamma\to\infty})(\alpha\alpha_{\mathrm{g,s}} + B_{\gamma\to\infty})}{M_{\gamma\to\infty} + F_{\gamma\to\infty}\tau^*} + \frac{\alpha_{\mathrm{g,h}} X_{\mathrm{s,0}}^*}{A_{\gamma\to\infty} + k_{\mathrm{h}}^*\tau^*} + \frac{J_{\gamma\to\infty} X_{\mathrm{i,0}}^*}{A_{\gamma\to\infty}\beta_{\mathrm{i}}} - \frac{(G_{\gamma\to\infty} + I_{\gamma\to\infty} + L_{\gamma\to\infty}) J_{\gamma\to\infty} f_{\mathrm{i}} k_d^*\tau^*}{(M_{\gamma\to\infty} + F_{\gamma\to\infty}\tau^*) A_{\gamma\to\infty}\beta_{\mathrm{i}}} + \frac{F_*}{\gamma} + O\left(\frac{1}{\gamma^2}\right), \tag{3.130}$$

$$X_{\mathrm{b,snw}}^* = \frac{G_*}{\gamma} + O\left(\frac{1}{\gamma^2}\right), \tag{3.131}$$

$$X_{\mathrm{i,snw}}^* = \frac{H_*}{\gamma} + O\left(\frac{1}{\gamma^2}\right), \tag{3.132}$$

$$X_{\mathrm{s,snw}}^* = \frac{I_*}{\gamma} + O\left(\frac{1}{\gamma^2}\right), \tag{3.133}$$

where

$$A_{\gamma\to\infty} = 1 - R^* + D,$$

$$B_{\gamma\to\infty} = \alpha\alpha_{\mathrm{g,SDU}} f_{\mathrm{p,s}} + \alpha_{\mathrm{g,h}}(1 - \alpha - f_{\mathrm{p,s}}),$$

$$C_{\gamma\to\infty} = V_{\gamma\to\infty}[U_{\gamma\to\infty}(O_{\gamma\to\infty} - R_{\gamma\to\infty} S_0^*) - (D + k_h^*\tau^*) R_{\gamma\to\infty} K_{\gamma\to\infty}\tau^*],$$

$$D_{\gamma\to\infty} = D R_{\gamma\to\infty} U_{\gamma\to\infty} W_{\gamma\to\infty}\alpha\tau^*,$$

$$E_{\gamma\to\infty} = U_{\gamma\to\infty} R_{\gamma\to\infty}\{V_{\gamma\to\infty}[S_{\gamma\to\infty} - O_{\gamma\to\infty} + D(H_{\gamma\to\infty} B_{\gamma\to\infty})]\},$$

$$F_{\gamma\to\infty} = \frac{[D J_{\gamma\to\infty} f_{\mathrm{i}} + A_{\gamma\to\infty}\beta_{\mathrm{i}}(f_{\mathrm{s}}\alpha_{\mathrm{g,s}} - 1)]k_{\mathrm{d}}^*}{A_{\gamma\to\infty}\beta_{\mathrm{i}}},$$

$$G_{\gamma\to\infty} = \frac{N_{\gamma\to\infty}}{A_{\gamma\to\infty}\beta_{\mathrm{i}}},$$

$$H_{\gamma\to\infty} = \alpha\alpha_{\mathrm{g,s}},$$

$$I_{\gamma\to\infty} = \frac{K_{\gamma\to\infty}(D + k_{\mathrm{h}}^*\tau^*)}{A_{\gamma\to\infty} + k_{\mathrm{h}}^*\tau^*},$$

$$J_{\gamma\to\infty} = \alpha\beta_{\mathrm{i}}\alpha_{\mathrm{g,SDU}},$$

$$K_{\gamma\to\infty} = \alpha_{\mathrm{g,h}} X_{\mathrm{s,0}}^*,$$

$$L_{\gamma\to\infty} = \frac{A_{\gamma\to\infty} + k_{\mathrm{d}}^*\tau^*}{A_{\gamma\to\infty} + (k_{\mathrm{d}}^* - 1)\tau^*},$$

$$
\begin{aligned}
M_{\gamma\to\infty} &= (\alpha\alpha_{\mathrm{g,s}} + B_{\gamma\to\infty})D - A_{\gamma\to\infty},\\
N_{\gamma\to\infty} &= A_{\gamma\to\infty}\beta_{\mathrm{i}}S_0^* + DJ_{\gamma\to\infty}X_{\mathrm{i},0}^*,\\
O_{\gamma\to\infty} &= 1 - R^* + D + k_{\mathrm{d}}^*\tau^*,\\
P_{\gamma\to\infty} &= \alpha\alpha_{\mathrm{g,SDU}}f_{\mathrm{i}}k_{\mathrm{d}}^*\tau^*,\\
Q_{\gamma\to\infty} &= f_{\mathrm{s}}\alpha_{\mathrm{g,s}}k_{\mathrm{d}}^*\tau^*,\\
R_{\gamma\to\infty} &= R^* - 1 - D - (k_{\mathrm{d}}^* - 1)\tau^*,\\
T_{\gamma\to\infty} &= f_{\mathrm{i}}k_{\mathrm{d}}^*\tau^{*2},\\
U_{\gamma\to\infty} &= (1 - R^* + D + k_{\mathrm{h}}^*\tau^*)\tau^*,\\
V_{\gamma\to\infty} &= (1 - R^* + D)\beta_{\mathrm{i}}\tau^*,\\
W_{\gamma\to\infty} &= \beta_{\mathrm{i}}\alpha_{\mathrm{g,SDU}}X_{\mathrm{s},0}^*,\\
X_{\gamma\to\infty} &= \{R_{\gamma\to\infty}[A_{\gamma\to\infty}\beta_{\mathrm{i}}(U_{\gamma\to\infty}S_0^* + (D + k_{\mathrm{h}}^*)K_{\gamma\to\infty}\tau^*) + \alpha DU_{\gamma\to\infty}W_{\gamma\to\infty}\\
&\qquad - \beta_{\mathrm{i}}A_{\gamma\to\infty}O_{\gamma\to\infty}U_{\gamma\to\infty}]\}T_{\gamma\to\infty},\\
Y_{\gamma\to\infty} &= \{D[A_{\gamma\to\infty}(H_{\gamma\to\infty} + B_{\gamma\to\infty}) + P_{\gamma\to\infty}] + A_{\gamma\to\infty}(Q_{\gamma\to\infty} - O_{\gamma\to\infty})\}\\
&\qquad \beta_{\mathrm{i}}A_{\gamma\to\infty}R_{\gamma\to\infty}U_{\gamma\to\infty}\tau^*.
\end{aligned}
$$

The coefficients $A_*, B_*, C_*, D_*, E_*, F_*, G_*, H_*$ and I_* are too long to include here. Although we analytic solution for the steady state solution when the disintegration rate goes toward infinity, the calculation to determine the stability is too difficult to do analytically.

3.6 Discussion

When there is no sludge disintegration unit, the model reduces to that investigated in chapter 2. In section 3.6.1 and 3.6.2 we briefly recap the discussion from chapter 2. In section 3.6.3 we use the result from the previous section to investigate the change in the behavior when a sludge disintegration unit is attached.

3.6.1 The chemical oxygen demand with no sludge disintegration unit ($D = 0$)

Figure 3.4 shows the chemical oxygen demand as a function of the residence time. When ($D = 0$) the chemical oxygen demand is constant along the washout branch ($\tau^* < \tau^*_{\mathrm{cr}} = 1.2018$).

$$\mathrm{COD}^*_w = S^*_0 + \alpha_{\mathrm{g,h}} X^*_{\mathrm{s},0} = 10.1788.$$

Along the no-washout branch the chemical oxygen demand is a decreasing function. From equation (3.86) it has limiting value when the residence time approaches infinity ($\tau^* \to \infty$) given by

$$\lim_{\tau^* \to \infty} \mathrm{COD}^*_{\mathrm{nw}} = \frac{k^*_{\mathrm{d}}}{1 - k^*_{\mathrm{d}}} = 0.0730. \tag{3.134}$$

(This value applies whether or not a sludge disintegration unit is used (2.90).)

The efficiency at which the chemical oxygen demand is removed can be defined by

$$E_{\mathrm{COD}^*} = \frac{\mathrm{COD}^*_{\mathrm{in}} - \mathrm{COD}^*_{\mathrm{out}}}{\mathrm{COD}^*_{\mathrm{in}}}.$$

From equation (3.134) the efficiency can not be increased over the limiting value $E_{\mathrm{COD}^*_{\mathrm{nw}}}(\tau^* = \infty) = 0.9928$. This means that it is impossible to remove more that 99.28 % of the chemical oxygen demand flowing into the reactor.

When $E_{\mathrm{COD}^*} = 0.90$, the chemical oxygen demand in the effluent has been reduced to 90 % of the value in the influent. The required value of the residence time is $\tau^* = 3.4131$. On figure 3.4 the target value $E_{\mathrm{COD}^*} = 0.9$ is indicated by the horizontal line.

In order to reduce the chemical oxygen demand in the effluent to 1 % of the value in the influent ($E_{\mathrm{COD}^*} = 0.99$) the required value of the residence time is $\tau^* = 97.0394$.

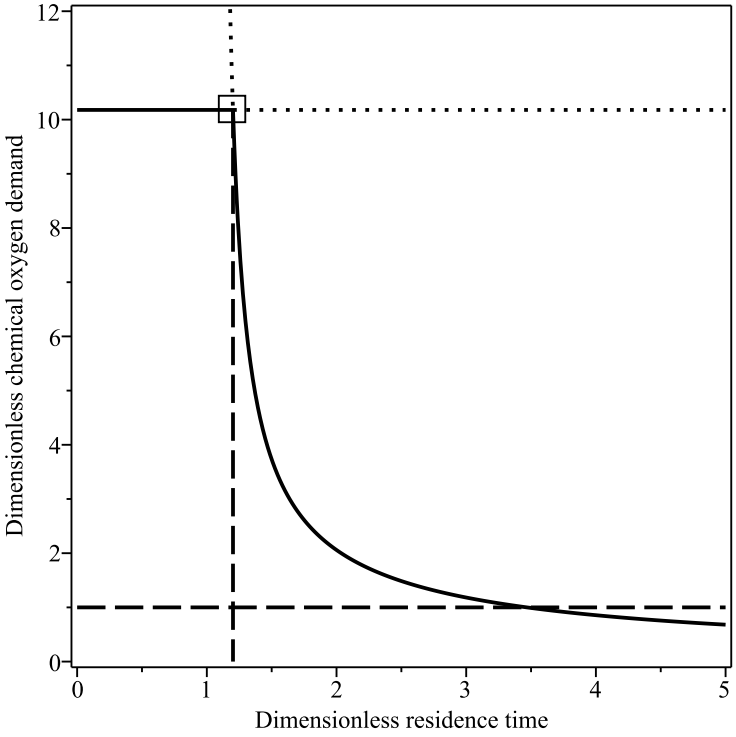

Figure 3.4: Steady state diagram for the chemical oxygen demand. Parameter values $R^* = 0$ and $D = 0$. The horizontal line correspond to a chemical oxygen demand removal efficiency of 90%.

3.6.2 The volatile suspended solids ($D = 0$)

When there is no sludge disintegration unit, the model reduces to that investigated in chapter 2. We briefly recap the discussion from chapter 2.

3.6.3 Discussion ($\gamma_b^* = \gamma_i^* = \gamma_s^* = \gamma$)

In this section we investigate how the chemical oxygen demand in the effluent streams depends upon the operation of the sludge disintegration unit. We take $\gamma_b^* = \gamma_i^* = \gamma_s^* = \gamma$.

3.6.3.1 The chemical oxygen demand

Figure 3.5(a) shows the value of the residence time required to achieve a chemical oxygen demand efficiency of 10% ($E_{\text{COD}}^* = 0.90$) as a function of the sludge disintegration rate. The value of the residence time (τ^*) has rapid increasing by 6.08%

from 3.4131 ($\gamma = 0$) to 3.6205 ($\gamma = 10$). It approaches its asymptotic limit very quickly ($\tau^*(\gamma = \infty) \cong 3.6156$).

Figure 3.5(b) shows the value of the residence time required to achieve the chemical oxygen demand efficiency of 1% ($E^*_{\mathrm{COD}} = 0.99$) as a function of the sludge disintegration rate. The value of the residence time (τ^*) has rapid increasing by 4.18% from 97.0394 ($\gamma = 0$) to 101.0986 ($\gamma = 10$). It approaches its asymptotic limit very quickly ($\tau^*(\gamma = \infty) \cong 100.4911$).

We expected that the residence time required to achieve a specific chemical oxygen demand efficiency increases because the sludge disintegration unit increases the effluent concentration for two reasons: firstly it kills the biomass and secondly, in so doing, it converts biomass into inert material and soluble substrate.

To calculate the residence time we solve the equation

$$\mathrm{COD}^*_{nw} = 0.1 \cdot \mathrm{COD}^*_{w}. \tag{3.135}$$

Using maple we find that this equation can be written in the form

$$\sum_{j=0}^{q=8} \sum_{i=0}^{p=12} a_{ij} \gamma^j \tau^{*i} = 0. \tag{3.136}$$

We divide by γ^q to obtain $\sum_{j=0}^{q=8} \sum_{i=0}^{p=12} a_{ij} \gamma^{j-q} \tau^{*i} = 0$, and take the leading term.

To find the asymptote for the limit $\gamma \to \infty$ we find the approximation equation $\sum_{i=0}^{p=12} a_{i8} \tau^{*i} = 0$.

For the default values this gives

$$(0.001194702079 + 0.002265670014\,\tau^* - 0.01377577233\,\tau^{*2} + 0.002819357180\,\tau^{*3} + 0.0002190849770\,\tau^{*4})\,\tau^{*8} = 0.$$

The solutions of this equations are

$$\tau^* = 3.6156, 0.4111, -0.2200, -16.6755, 0.$$

This gives the asymptotic value for the residence time stated earlier ($\tau^* = 3.6156$). The value $\tau^* = 0.4111$ is also not physically meaningful because it is below the limiting value of the washout value indicated in figure 3.2. The two negative values and the zero solution can be discarded as they are not physically meaningful.
From the equation $\mathrm{COD}^*_{nw} = 0.01 \cdot \mathrm{COD}^*_w$ we have the leading order approximation in the limit that the disintegration rate goes toward infinity.

$$(0.001397004519 + 0.003945509461\,\tau^* - 0.01105419085\,\tau^{*2} - 0.0005648645907\,\tau^{*3} + 0.00000671177936\,\tau^{*4})\,\tau^{*8} = 0,$$

The solutions of this equations are

$$\tau^* = 100.4911, 0.565, -0.2200, -16.6755, 0.$$

This gives the asymptotic value for the residence time stated earlier ($\tau^* = 100.4911$), The value $\tau^* = 0.565$ is also not physically meaningful because it is below the limiting value of the washout value indicated in figure 3.2.
The two negative values and the zero solution can be discarded as they are not physically meaningful.

3.6.3.2 Sludge content

3.6.3.3 What happens as the disintegration rate increases?

Figure 3.6 shows the steady state sludge content as a function of the residence time when there is no recycle (R^*=0) and when the values of the disintegration rate (γ) are 0, 0.1 and 10. This figure corresponds to case two in the absence of the sludge

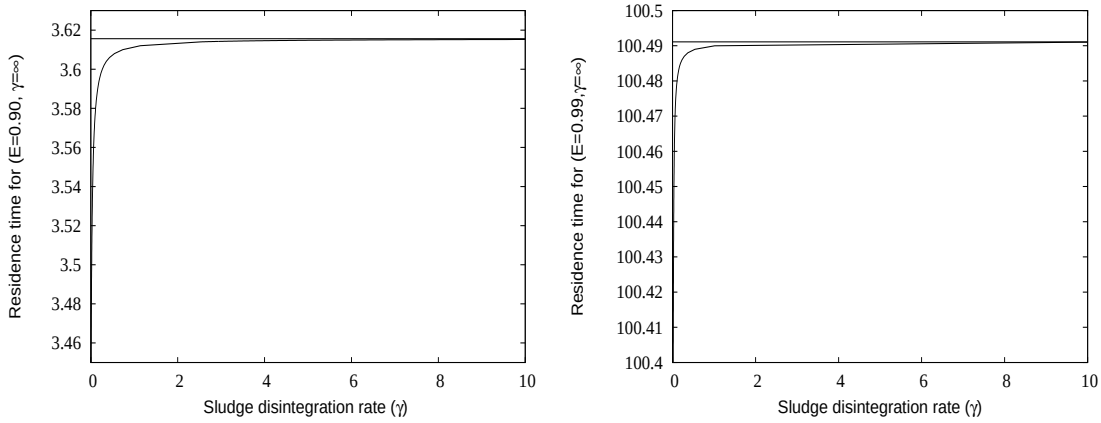

(a) E = 0.9 (b) E = 0.99

Figure 3.5: The residence time required to achieve the chemical oxygen demand efficiency E = 0.9 and E = 0.99 as a function of the sludge disintegration rate (γ), D=0.1, V^*=1.

disintegration unit. It shows how the volatile suspended solids content changes as the value of the disintegration rate is increased: when the disintegration rate increases the sludge content decreases. Although it is not very clear, due to the scale of the figure, the intersection point along the no-washout branch decreases as the disintegration rate increases.

Figure 3.7 shows the residence time where the volatile suspended solids content along the washout branch is equal to the target value as a function of the disintegration rate γ when R^*=0. The residence time decreases as the disintegration rate increases.

Figure 3.8 shows the steady state sludge content as a function of the residence time when the effective recycle parameter is R^*=0.48 and when the values of the disintegration rate (γ) is 0, 0.1,1 and 10. This figure corresponds to case three in the absence of the sludge disintegration unit. This figure show how the volatile suspended solids content changes as we change the value of the disintegration rate: when the disintegration increases the sludge content decreases. An important feature of this figure is that in the parameter range ($0<\gamma<0.1$) the behavior changes from case three to case two.

Figure 3.9 shows the residence time where the volatile suspended solids along either

the washout or the no-washout branch is equal to the target value. The limit point bifurcation at τ^*=0.7521 and $\gamma = 0.0537$ demarcates the transition point between case three and case two.

Figure 3.10 shows the steady state sludge content as a function of the residence time when the effective recycle parameter is R^*=0.55 and when the values of the disintegration rate (γ) is 0, 0.1,1 and 10. This figure show how the volatile suspended solids content changes as we change the value of the disintegration rate: when the disintegration rate increases the sludge content decreases. This figure corresponds to case two ($\gamma = 0$), three ($\gamma = 0.1$) and four ($\gamma = 1, 10$). As the value of the disintegration rate is increased over the range $0.1<\gamma<1$ the behavior changes from case four to case three to case two.

Figure 3.11 shows the residence time where the volatile suspended solids content along the washout and the no-washout branches is equal to the target value. The figure has two limit points at (τ^*=0.7509, $\gamma = 3.4665$) and (τ^*=0.6282, $\gamma = 0.4486$). The former is the transition from case four to case three and the latter is the transition from case three to case two. In this figure we have three branches, the residence time in the top branch and the bottom branch decreases as the disintegration rate increases but in the middle branch it increased as the disintegration rate increases.

Figure 3.12 shows the steady state sludge content as a function of the residence time when the effective recycle parameter is R^*=0.65 and when the values of the disintegration rate (γ) is 0, 0.1,1 and 10. This figure corresponds to case four in the absence of the sludge disintegration unit. This figure show how the volatile suspended solids content changes as we change the value of the disintegration rate: when the disintegration rate increases the sludge content decreases. When the disintegration rate in the range ($0<\gamma<10$) the behavior is always case four. No matter how high the value for the disintegration rate, the steady-state diagram is always case four. The tatal volatile suspended solids in the limit when the disintegration rate is equal to infinity is given by equations (3.127), (3.128) and (3.129). This curve is visually identical

to the curve when the disintegration rate is equal to ten. Therefore although the sludge content decreases the response diagram always remains case four.

Figure 3.13 shows the residence time where the volatile suspended solids content along the no-washout branch is equal to the target value as a function of the disintegration rate when the effective recycle parameter is R^*=0.65. The residence time decreases as the disintegration rate increases.

Up to now we have investigated what happens when the steady-state diagram in the absence of the sludge disintegration unit ranges from cases two to case four. We have shown that the operation of a sludge disintegration unit reduces the sludge content. We showed that some times the use of a sludge disintegration unit results in changes in the type of response curve. From a practical perspective the most important transition is that which we investigate now, namely the transition from case five to case four.

Figure 3.14 shows the steady state sludge content as a function of the residence time when the effective recycle parameter is R^*=0.7386 and when the values of the disintegration rate (γ) is 0, 0.1,1 and 10. This figure corresponds to case four in the absence of the sludge disintegration unit. This figure show how the volatile suspended solids content changes as we change the value of the disintegration rate: when the disintegration rate increases the sludge content decreases. When the disintegration rate is in the range $0<\gamma<0.1$ the behavior changes from case five to case four. The transition happens when the asymptotic value of the volatile suspended solids along the no-washout branch equals the target value.

Figure 3.15 shows the steady state sludge content as a function of the residence time for R^*=0.9 and when the values of the disintegration rate (γ) are 0, 0.1,1 and 10. This figure corresponds to case five in the absence of the sludge disintegration unit. In this case although as the disintegration rate increases the sludge content decreases the behavior is always case five, similar to figure 3.12 where it is always case four.

Figure 3.16 shows the steady state sludge content as a function of the residence time for a higher value of the effective recycle parameter, R^*=0.9, and when the values of the disintegration rate (γ) is 0, 0.1,1 and 10. The dotted line is the volatile suspended solids concentration at infinite residence time in the limit when the disintegration rate goes towards infinity. It is indistinguishable from the case when the disintegration rate is equal to ten. This shown that when R^*=0.9 we always have case five.

In chapter 2 we found the effective recycle parameter values (R^*) for the transitions from case two to case three, case three to case four and case four to case five. All these transitions are well defined mathematically when there is no sludge disintegration (D=0). The definitions of the transitions are same when there is a sludge disintegration unit ($D \neq 0$). This means that if we fix the disintegration rate then we can apply the method from chapter 2 to find the critical value of the effective recycle parameter or if we fix the value of the effective recycle parameter we can find the critical value of the disintegration rate.

Figure 3.17 shows the value of the disintegration rate (γ) as a function of the effective recycle ratio (R^*) at which a transition occurs in the steady state digram. There are two transition curves from case four to three and from case three to two and one transition point from case five. It can be seen that the transition values for case two to case three and case three to four are rapidly approaching vertical asymptote.

The transition from case two to three occurs when the maximum value of the volatile suspended solids along the no-washout branch is equal to the target value ($\mathrm{VSS}^*(\tau^*, R^*, \gamma) = \mathrm{VSS}_t^*$). The transition from case three to four occurs when the concentration of volatile suspended solids at the washout point (τ_{cr}^*) is equal to the target value. The transition from case four to five occurs when the concentration of volatile suspended solids along the no-washout branch at infinite residence time is equal to the target value. In figure 3.17 the transition from case five to case four

is a vertical line, i.e. it is independent of the value of the disintegration rate. This is explained in section 3.6.3.2. It is essentially due to the fact that the transition occurs at an infinite residence time. Therefore the infinite amount of time spend in the reactor is more important than the finite value of the disintegration rate.

Note that the critical value of the effective recycle parameter when the disintegration rate is equal to zero is not equal to the critical value of the effective recycle parameter when the disintegration rate approaches zero.

The transition from case four to case five is investigated analytically in the next section.

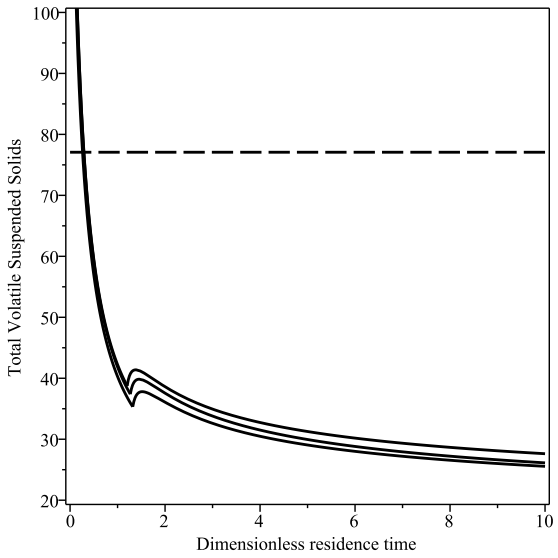

Figure 3.6: The volatile suspended solids concentration as a function of the residence time is case two. Parameter values: R^*=0, D=0.1, V^*=1 and γ=0 (top line) and 10 (bottom line).

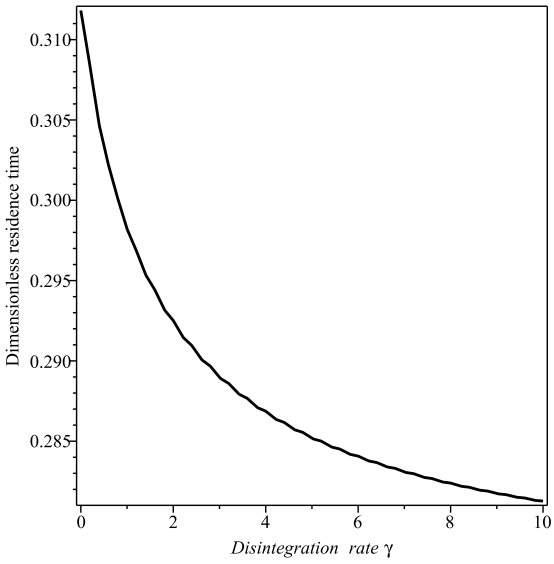

Figure 3.7: The residence time when $\mathrm{VSS}_w^* = \mathrm{VSS}_t^*$ as a function of the disintegration rate γ. When $\gamma = 0$ the volatile suspended solids steady-state diagram is case two. Parameter values: D=0.1, V^*=1 and R^*=0.

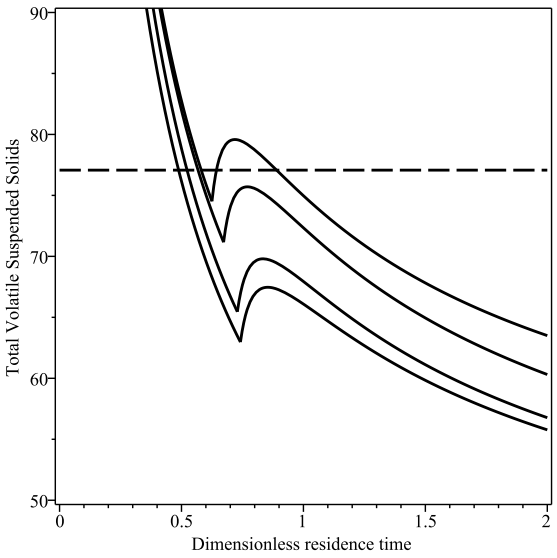

Figure 3.8: The volatile suspended solids concentration as a function of the residence time is case three to two. Parameter values: R^*=0.48, D=0.1, V^*=1 and γ=0 (top line), 0.1,1 and 10 (bottom line).

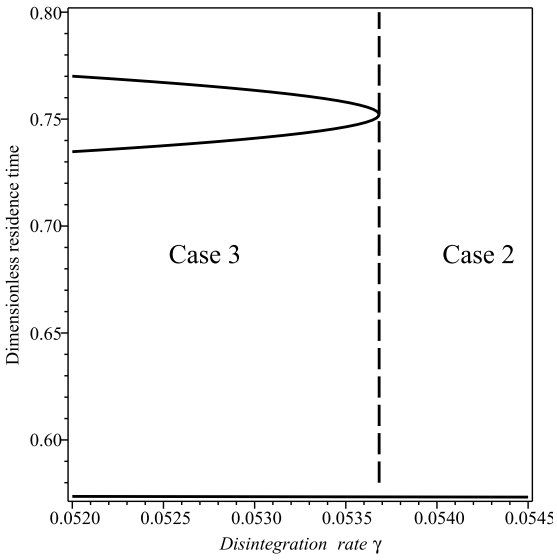

Figure 3.9: The residence time as a function of the disintegration rate γ. When $\gamma = 0$ the volatile suspended solids steady-state diagram is case three to two. Parameter values: D=0.1, V^*=1 and R^*=0.48.

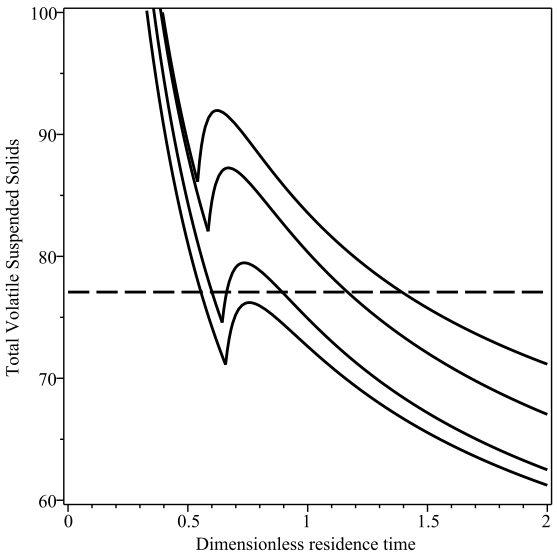

Figure 3.10: The volatile suspended solids concentration as a function of the residence time is case four to three to two. Parameter values: R^*=0.55, D=0.1, V^*=1 and γ=0 (top line), 0.1,1 and 10 (bottom line).

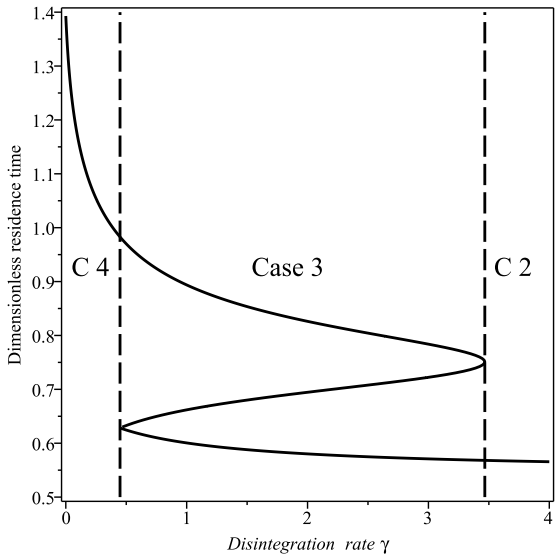

Figure 3.11: The residence time as a function of the disintegration rate γ. When $\gamma = 0$ the volatile suspended solids steady-state diagram is case three to two. Parameter values: D=0.1, V^*=1 and R^*=0.55.

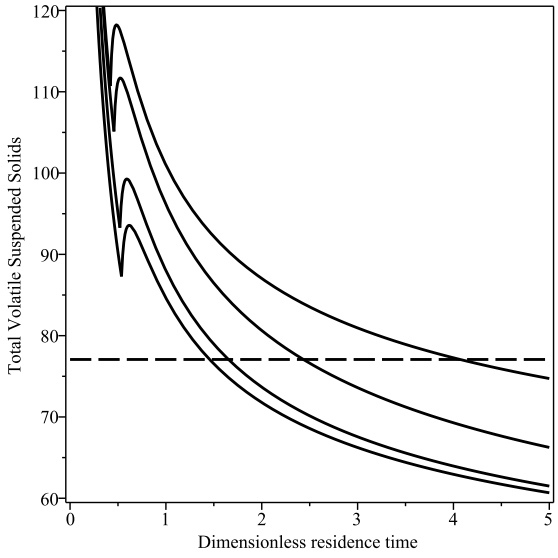

Figure 3.12: The volatile suspended solids concentration as a function of the residence time is case four. Parameter values: R^*=0.65, D=0.1, V^*=1 and γ=0 (top line), 0.1,1 and 10 (bottom line).

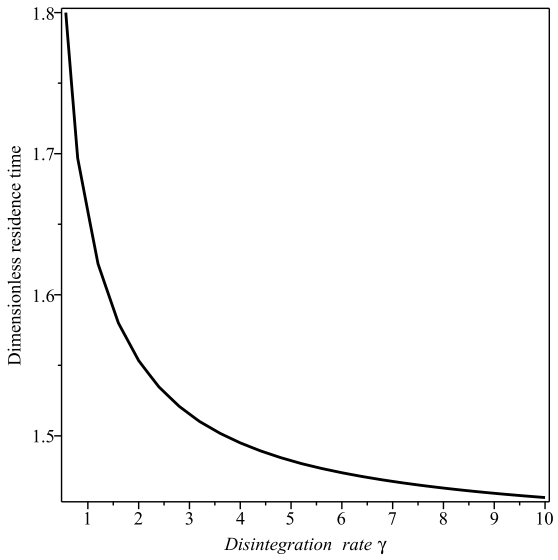

Figure 3.13: The residence time as a function of the disintegration rate γ. When $\gamma = 0$ the volatile suspended solids steady-state diagram is case four. Parameter values: D=0.1, V^*=1 and R^*=0.65.

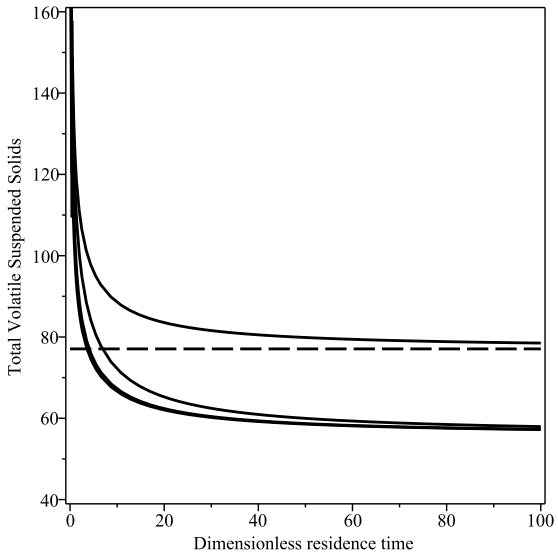

Figure 3.14: The residence time as a function of the disintegration rate γ. When $\gamma = 0$ the volatile suspended solids steady-state diagram is case four. Parameter values: D=0.1, V^*=1 and R^*=0.7386.

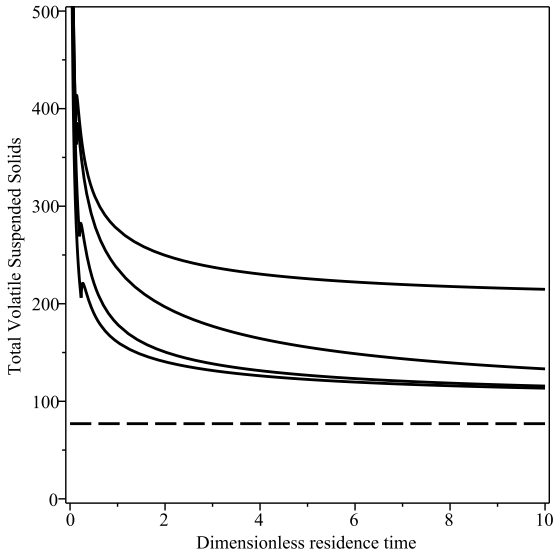

Figure 3.15: The volatile suspended solids as a function of the residence time is always case five. Parameter values: R^*=0.9, D=0.1, V^*=1 and γ=0 (top line), 0.1,1 and 10 (bottom line).

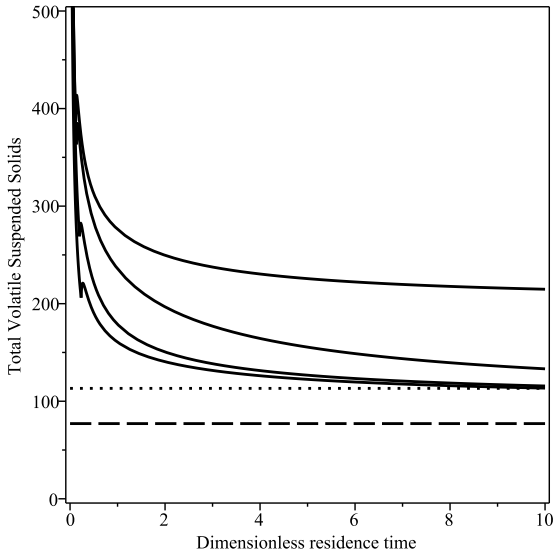

Figure 3.16: The volatile suspended solids as a function of the residence time is always case five. Parameter values: R^*=0.9, D=0.1, V^*=1 and γ=0 (top line), 0.1,1 and 10 (bottom line). The dotted horizontal line is the limiting value $\mathrm{VSS}^*(\tau^* = \infty, \gamma = \infty)$.

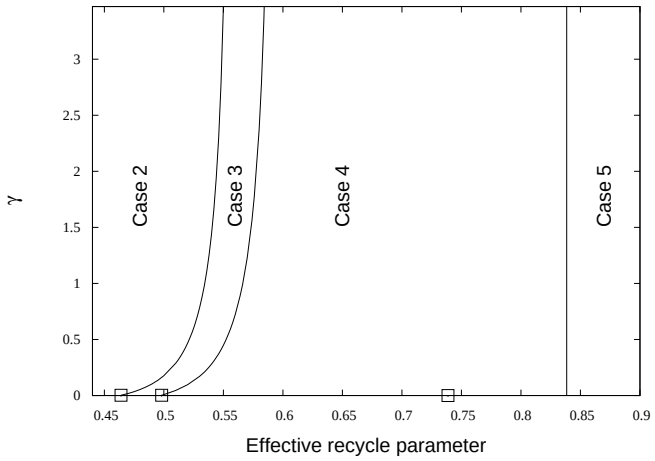

Figure 3.17: Classification figure showing how the volatile suspended solids steady-state diagram depends upon the values of the disintegration rate and the effective recycle ratio. The transition for volatile suspended solids concentration from case five to four, four to three and three to two. Parameter values: D=0.1 and V^*=1

3.6.3.4 The transition from case four to case five

In the limit of infinite residence time equation (3.87) becomes

$$\mathrm{VSS}^*_{\mathrm{nw}} \approx \frac{X^*_{i,0}}{1 - R^* + D} + \frac{f_i k^*_d}{1 - R^* + D} a_0,$$

where a_0 is defined by equation (3.88).

This shows that the performance of the sludge disintegration unit does not depend upon the values $\gamma_b, \gamma_i, \gamma_s$ and β_i, but that it does depend upon the values of the sludge disintegration factor, D, the solubilization efficiency of the sludge disintegration unit, α, and the coefficient $\alpha_{\mathrm{g,SDU}}$. That is to say, the controlling factor is the rate at which sludge is moved into the sludge disintegration unit not the particular sludge disintegration rates within the sludge disintegration unit ($\gamma_b, \gamma_i, \gamma_s$).

Using the asymptotic limit for the volatile suspended solids ($\tau^* \to \infty$) and setting this equal to the target value we find, after some algebra, that the asymptotic limit

is equal to the target value when

$$Q(D) = a_D D^2 + b_D D + c_D = 0, \tag{3.137}$$

where the coefficients are

$$\begin{aligned}
a_D &= -\mathrm{VSS}_t^*(1-k_d^*)[1-\alpha\alpha_{\mathrm{g,SDU}} f_i - f_s\alpha_{g,s}]<0,\\
b_D &= (1-k_d^*)\{(1-f_s\alpha_{g,s})X_{i,0}^* + (\alpha_{g,h}X_{s,0}^* + S_0^*)f_i - \mathrm{VSS}_t^*(1-R^*)[2(1-f_s\alpha_{g,s})\\
&\quad - \alpha\alpha_{\mathrm{g,SDU}} f_i]\} - f_i k_d^*,\\
c_D &= (1-R^*)\{(1-k_d^*)[(1-f_s\alpha_{g,s})(X_{i,0}^* - \mathrm{VSS}_t^*(1-R^*)) + (\alpha_{g,h}X_{s,0}^* + S_0^*)f_i]\\
&\quad - f_i k_d^*\}.
\end{aligned}$$

It is interesting to note that the quadratic equation (3.137) does not depend on the volume of the bioreactor (V^*). The sludge disintegration factor D>0 must be positive. As a_D>0 we have

$$D_{\mathrm{cr}} = \frac{-b_D - \sqrt{b_D^2 - 4a_D c_D}}{2a_D}. \tag{3.138}$$

We first consider the limiting cases $D = 0$, i.e. the asymptotic limit without a sludge disintegration unit, and $R^* = 1$ corresponding to perfect recycle. The former case gives

$$Q(D = 0) = c_D,$$

which give two solutions

$$R_1^* = 1 \quad \text{and} \tag{3.139}$$

$$R_2^* = \frac{(1-k_d^*)[(1-f_s\alpha_{g,s})(\mathrm{VSS}_t^* - X_{i,0}^*) - (\alpha_{g,h}X_{s,0}^* + S_0^*)f_i] + f_i k_d^*}{(1-k_d^*)[1-f_s\alpha_{g,s}]\mathrm{VSS}_t^*}, \tag{3.140}$$

In chapter 2 we have same expressions for equations (3.139) (3.140) c.f. (2.99) and (2.100). (This is expected !)

Using the default parameter values we find that $R_2^* = 0.7387$.

Thus when D=0 the transition from case four to case five happens when R_2^*=0.7387.

When $R^* = 1$ i.e. when we have perfect recycle, then from equation (3.137) we have

$$Q(D) = D(a_D D + b_D) = 0,$$

which has two solutions

$$\begin{aligned} D_1 &= 0 \quad \text{and} \\ D_2 &= -\frac{b_D}{a_D}, \\ &= \frac{b_{DA} - f_i k_d^*}{\text{VSS}_t^*(1-k_d^*)[1 - \alpha\alpha_{\text{g,SDU}} f_i - f_s\alpha_{g,s}]}, \end{aligned}$$

where

$$b_{DA} = (1-k_d^*)\{(1-f_s\alpha_{g,s})X_{i,0}^* + (\alpha_{g,h}X_{s,0}^* + S_0^*)f_i\}.$$

Using the default parameter values we find that

$$D_2 = 0.2619.$$

Thus when R^*=1 the transition from case four to case five happens when D_2=0.2619.

Figure 3.18 plots the function defined by equation (3.137). To the left hand side of this curve the volatile suspended solids at an infinite residence time is smaller than the target value ($\text{VSS}^*(t^* = \infty) < \text{VSS}_t^*$). In this region the steady state digram can be case two, three or four. To the right hand side of the curve the volatile suspended solids at an infinite residence time is larger than the target value ($\text{VSS}^*(t^* = \infty) > \text{VSS}_t^*$). In this region the steady state digram must be case five.

The importance of figure 3.18 is that the left hand side is 'good' but the right hand side is 'bad'. Note if the recycle ratio R^* is less than 0.7387 then we do not need the sludge integration unit, if the value of the sludge disintegration factor is larger than the minimum value then there is always a critical value of the residence time above which the sludge content is below the target value. If the recycle ratio R^* is greater than 0.7387 then there is a minimum value of D that is required, we want D to be greater than the minimum value.

It is surprising that the curve defined by equation (3.137), a quadratic equation, appears to be a straight line. Examination of the discriminant of the quadratic equation (3.137) reveals that it is essentially independent of the value of the effective recycle parameter over the range $0 \leq R^* \leq 1$. From this it then follows that there is a linear relationship between the sludge disintegration factor (D) and the effective recycle parameter (R^*).

We now show that the discriminant of (3.138) is near enough independent of the effective recycle parameter over the range $0 \leq R^* \leq 1$. Using the default parameter values we have

$$\begin{aligned} a_D &= -69.2295, \\ b_D &= -120.4812 + 138.6119R, \\ c_D &= (1-R)(-51.2517 + 69.3825R). \end{aligned}$$

The discriminant function of (3.138) is given by

$$\begin{aligned} \Delta(R^*) &= \sqrt{b_D^2 - 4a_D c_D}, \\ \Delta(R^*) &= \sqrt{0.0234(R^* + 120.7325)(R^* + 114.4405)}. \end{aligned} \tag{3.141}$$

The discriminant function (3.141) has a global minimum when $R^* = -117.5968$. Consequently, over the parameter region ($0 \leq R^* \leq 1$) the discriminant function is an increasing function of R^* which is minimized when $R^* = 0$ and maximized when

($R^* = 1$).

The minimum value of expression (3.141) is 17.9778 ($R^* = 0$) and the maximum value is 18.1308 ($R^* = 1$). Thus there is little change in its value over the range $0 \leq R^* \leq 1$. Replacing the discriminant function by the average value (18.0543) we find

$$D \approx \frac{-b_D - 18.0543}{2a_D} = -0.7398 + 1.0011R^*. \tag{3.142}$$

This shows that the value for the sludge disintegration factor (D) when the volatile suspended solids at infinity is equal to the target value is effectively a linear function of the effected recycle ratio R^*, as shown in figure 3.18.

If we plot function (3.142) in figure 3.18 we found that it is indistinguishable from the exact curve fond from the discriminant function (3.138).

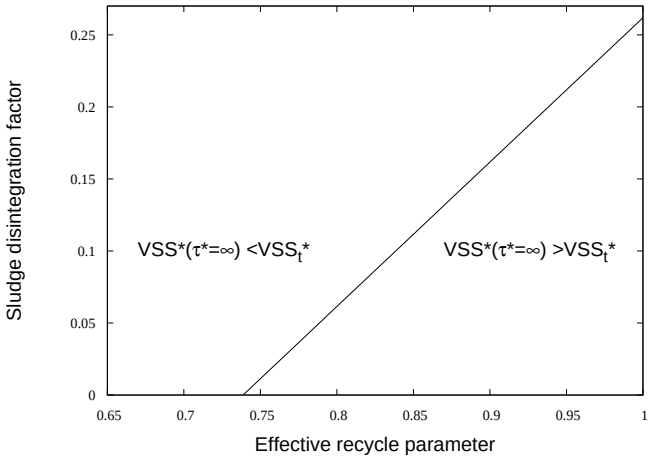

Figure 3.18: The transition between the behavior shown in figure 3.12and figure 3.15 as a function of the effective recycle parameter (R^*) and the sludge disintegration factor D. Parameter value: V^*=1.

3.7 Conclusion

We have extended our model for sludge formation in the activated sludge process, that was analyzed in chapter 2, to include a sludge disintegration unit. There are three disintegration processes occurring inside the sludge disintegration unit.

Biomass is disintegrated into non-biodegradable particulate, biodegradable particulate substrate and soluble substrate. Biodegradable particulate substrate is disintegrated to biodegradable particulate substrate and soluble substrate. Non-biodegradable particulate is disintegrated to non-biodegradable particulate substrate and soluble substrate.

We assumed that the disintegration processes are much quicker than the standard biochemical processes, so that the latter can be ignored. We found analytic expressions for the washout and the no-washout steady-state solutions in both the bioreactor and the sludge disintegration unit. However, stability has to be determined numerically. We simplified the steady-state expressions by assuming that the three disintegration rates are equal ($\gamma_b^* = \gamma_i^* = \gamma_s^* = \gamma$).

We investigated how the chemical oxygen demand and the volatile suspended solids vary as the disintegration rate increases toward infinity. The chemical oxygen demand increases when the disintegration rate (γ) increases, this what we expect to happen because the sludge disintegration unit kills the biomass and in so doing it converts the biomass into inert material and soluble substrate.

We are particularly interested in how the response digram of the volatile suspended solids changes as the disintegration rate is increased. We showed that as the value of the disintegration rate increases the amount of sludge in the bioreactor decreases, which is expected. We also showed that sometimes we can get transitions from case four to three or from case three to case two.

The most important feature of interest is whether it is possible to have a transition from case five to case four. When we investigated this transition we found two forms of behavior as the disintegration rate is increased. One is when we have the transition from case five to four, which is desirable, and the other is when we always remain in case five, although the sludge content is reduced. The transition between the two types is governed by the volatile suspended solids value when the residence time is infinity.

We used our steady state solutions when the residence time goes toward infinity to find a formula for the critical value of the sludge disintegration factor from the transition from case four to case five. If the value of the sludge disintegration factor (D) is sufficiently high then the sludge content is is guaranteed to be below the target value if the residence time is larger than some critical value. If the value of the disintegration factor is below the critical value, then the sludge content is always above the target value for any value of the residence time and we always have case five. The critical value does not depend on the the volume of the bioreactor (V^*) or the disintegration rate (γ).

Some of the results from this chapter have been published [7].

Chapter 4

Simple extension of the standard model (model two)

4.1 Introduction

In chapter 2 we analysed a model due to Chung and Neethling [23]. This extends the basic model in two ways. Firstly, it includes a slowly biodegradable substrate component which is hydrolysed to produce small soluble organic materials. (These are the limiting substrate of the basic model). Secondly, a fraction of the dead biomass is recycled back into the soluble substrate pool.

In particular we studied how the 'sludge response diagram', which shows the steady-state sludge content as a function of the residence time, changes as the effective recycle parameter, which characterizes the operation of the recycle unit, is varied.

Here we change one of the assumptions in the Chung and Neethling model. Namely, instead of a fraction of the dead biomass being recycled into the pool of soluble substrate it is assumed that it is instead recycled into the pool of insoluble substrate. Where appropriate we discuss where the results of these models agree and differ.

We find the steady-state solutions and determine their stability as a function of process parameters. These are used to calculate the steady-state chemical oxygen

demand and the steady-state volatile suspended solids as a function of the residence time. We use the steady-state results to investigate the circumstances under which it is possible to operate the reactor at, or below, a target value for the volatile suspended solids. We formulate all components of the model in terms of chemical oxygen demand.

We have made a seemingly *minor* change to the second assumption of the biochemistry in the Chung and Neethling model. How is this modification reflected in the model production? Does our minor change lead to minor differences?

Some of the results from this chapter have been published in a refereed conference proceeding [6].

There were five hundred papers presented at this conference. We were one of a handful of presenters invited to submit a paper to a special issue of a journal [5].

4.2 Biochemistry

4.2.1 Microbial reactions

In this section we discuss the biochemistry of the model. The three biological processes occurring in the model are shown schematically in figure 4.1. In figure 4.1 (X_b) is the concentration of biomass, (X_p) is the concentration of non-biodegradable particulate material, (X_s) is the concentration of slowly biodegradable particulate substrate, (S) is the concentration of soluble substrate, $\mu(s)$ is the specific growth rate, (k_d) is the death coefficient, and (k_h) is the hydrolysis rate of insoluble organic compound (X_s). These processes are described below.

1. Biodegradable particulate substrate (X_s) is hydrolysed to give soluble substrate (S).

$$X_s \xrightarrow{k_h} S. \tag{4.1}$$

2. Soluble organic materials (S) are used as substrates for energy and growth by the biomass (X_b).

$$S \xrightarrow{\mu(s)} \alpha_g X_b, \tag{4.2}$$

where α_g ($0<\alpha_g \leq 1$) is the yield factor for growth of biomass.

3. The death of biomass adds to the pool of soluble substrate (S) in addition to producing non-biodegradable particulates (X_p).

$$X_b \xrightarrow{k_d} f_p X_p + (1 - f_p) X_s, \tag{4.3}$$

where f_p is the fraction of dead biomass converted to to non-biodegradable particulate ($0 \leq f_p \leq 1$).

The sequence of biological reactions (4.1) – (4.3) converts slowly biodegradable substrate through biomass back to slowly biodegradable particulate substrate. In addition to the variables identified above (S, X_b, X_p and X_S) we also allow for the possibility that the feed contains particulate inert material (X_i).

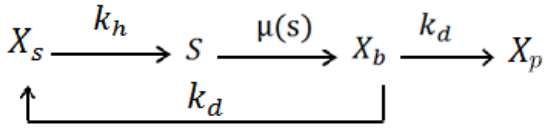

Figure 4.1: Overview of biochemical processes in model two.

4.3 Equations

In this section we write down the model equations for the concentration of microorganisms, non-biodegradable particulates, slowly biodegradable particulates, particulate inert material, and soluble substrate within a well-stirred, well-aerated, bioreactor.

4.3.1 The dimensional model

In chapter 2 the system of four equations reduces to a planer system. However in the new model the system does not reduce to a planer system. In the old model when the biomass dies it gives soluble substrate whereas in the new model the biomass becomes insoluble substrate, we can not eliminate the insoluble substrate equation from the model.

The model equations in the bioreactor are given by

The rate of change of soluble substrate

$$V\frac{dS}{dt} = F(S_0 - S) + Vk_hX_s - \frac{VX_b\mu(S)}{\alpha_g}. \tag{4.4}$$

The rate of change of biomass

$$V\frac{dX_b}{dt} = F(X_{b,0} - X_b) + RF(C-1)X_b + VX_b\mu(S) - Vk_dX_b. \tag{4.5}$$

The rate of change of slowly biodegradable particulates.

$$V\frac{dX_s}{dt} = F(X_{s,0} - X_s) + RF(C-1)X_s + V(1-f_p)k_dX_b - Vk_hX_s. \tag{4.6}$$

The rate of change of non-biodegradable particulates

$$V\frac{dX_p}{dt} = F(X_{p,0} - X_p) + RF(C-1)X_p + Vf_pk_dX_b. \tag{4.7}$$

The rate of change of particulate inert material

$$V\frac{dX_i}{dt} = F(X_{i,0} - X_i) + RF(C-1)X_i. \tag{4.8}$$

The specific growth rate is given by

$$\mu(S) = \frac{\mu_m S}{K_s + S}. \tag{4.9}$$

The residence time is defined by

$$\tau = \frac{V}{F}. \tag{4.10}$$

The chemical demand oxygen is defined by

$$\text{COD} = S + X_s. \tag{4.11}$$

The total Volatile Suspended Solids (VSS) are defined by

$$X_t = X_b + X_s + X_p + X_i. \tag{4.12}$$

Note that we can assume that C $\geq$ 1, as otherwise recycle leads to a decrease in performance of the bioreactor.

For a specific wastewater, a given biological community, and a particular set of environmental conditions, the parameters K_s, k_d,k_h, α_g and μ_m are fixed. The parameters that can be varied are the feed concentrations S_0, $X_{j,0}(j = b, p, i, s)$, and the residence tine τ . All parameters in the model are defined in table 4.1. In particular note that we take $|S|$ = g COD dm^{-3}.

4.3.2 The dimensionless model

By introducing dimensionless variables for the concentration of the substrate [S^* =S/K_s], the dimensionless substrate concentration in the feed [$S_0^* = S_0/K_s$], the concentration of the microorganism and particulates [X_j^* =$X_j/(\alpha_g K_s)$, $(j = b, s, p, i)$], the dimensionless decay rate [k_d^*= k_d/μ_m], the dimensionless hydrolysis rate of in-

soluble organic compounds [k_h^*= k_h/μ_m] and time [t^*=$\mu_m t$] the dimensional model, equations (4.4)-(4.8), can be written in the dimensionless form.

Equations in the bioreactor

$$\frac{dS^*}{dt^*} = \frac{1}{\tau^*}(S_0^* - S^*) + \alpha_g k_h^* X_s^* - \frac{S^* X_b^*}{1+S^*}, \tag{4.13}$$

$$\frac{dX_b^*}{dt^*} = \frac{1}{\tau^*}(X_{b,0}^* - X_b^*) + \frac{R^*}{\tau^*}X_b^* + \frac{X_b^* S^*}{1+S^*} - k_d^* X_b^*, \tag{4.14}$$

$$\frac{dX_s^*}{dt^*} = \frac{1}{\tau^*}(X_{s,0}^* - X_s^*) + \frac{R^*}{\tau^*}X_s^* + (1-f_p)k_d^* X_b^* - k_h^* X_s^*, \tag{4.15}$$

$$\frac{dX_p^*}{dt^*} = \frac{1}{\tau^*}(X_{p,0}^* - X_p^*) + \frac{R^*}{\tau^*}X_p^* + f_p k_d^* X_b^*, \tag{4.16}$$

$$\frac{dX_i^*}{dt^*} = \frac{1}{\tau^*}(X_{i,0}^* - X_i^*) + \frac{R^*}{\tau^*}X_i^*. \tag{4.17}$$

The dimensionless chemical oxygen demand COD* inside the bioreactor

$$\mathrm{COD}^* = S^* + \alpha_g X_s^*. \tag{4.18}$$

Dimensionless total Volatile Suspended Solids VSS* inside the bioreactor

$$X_t^* = X_b^* + X_s^* + X_p^* + X_i^*.$$

Dimensionless total Volatile Suspended Solids VSS* in the feed

$$\begin{aligned}\mathrm{VSS}_{\mathrm{in}}^* &= X_{b,0}^* + X_{s,0}^* + X_{p,0}^* + X_{i,0}^*, \\ &= X_{s,0}^* + X_{i,0}^*. \end{aligned} \tag{4.19}$$

The effective recycle parameter is defined by [$R^* = (C\text{-}1)R$].

The cases $R^* = 0$, $0<R^*<1$ and $R^* = 1$ represent a flow reactor without recycle, a flow reactor with non-idealized recycle, and a flow reactor with idealized recycle, respectively [70].

From now on we assume that the growth medium fed into the bioreactor is sterile,

i.e. there are no microorganisms in the influent ($X_{b,0} = X^*_{b,0} = 0$). We also assume that there are no non-biodegradable particulates in the feed ($X_{p,0} = X^*_{p,0} = 0$). It is important to note for what follow that the effective recycle parameter is bounded: $0 \leq R^* \leq 1$.

Note that the target value for volatile suspended solid becomes

$$\mathrm{VSS}^*_{\mathrm{t}} = \frac{\mathrm{VSS}_{\mathrm{t}}}{\alpha_g K_s} = \frac{12000}{\alpha_g K_s} = 3.4510. \tag{4.20}$$

4.3.3 Model simplification

4.3.3.1 The equation for the particulate inert material

Note that the differential equation for the particulate inert material equation (4.17) decouples from the model equations.

We write the initial condition for the variable X^*_i in the form

$$X^*_i(0) = X^*_{i,i}.$$

Solving equation (4.17), we have

$$X^*_i = \frac{B}{A} + \left(X^*_{i,i} - \frac{B}{A} \right) e^{-At^*},$$

where the coefficients are

$$A = \frac{1 - R^*}{\tau^*},$$

$$B = \frac{X^*_{i,0}}{\tau^*}.$$

In the limit of large time we have

$$X^*_{i,\infty} = \lim_{t^* \to \infty} X^*_i = \frac{B}{A} = \frac{X^*_{i,0}}{1 - R^*}.$$

4.3.3.2 The equation for the non-biodegradable particulate

Note that the differential equation for the non-biodegradable particulate material equation (4.16) decouples from the model equations.

We write the initial condition for the variable X^*_p in the form

$$X^*_p(0) = X^*_{p,i}.$$

The formal solution of equation (4.16) is given by

$$X^*_p = \frac{E}{D} + Fe^{-Dt^*} + Ge^{-Dt^*} \int e^{Dt^*} X^*_b(t)dt,$$

where the coefficients are

$$E = \frac{X^*_{p,0}}{\tau^*}, \quad D = \frac{1 - R^*}{\tau^*}, \quad G = f_p k^*_d, \quad \text{and } F \text{ is an integration constant.}$$

From equation (4.16). The steady state value for X^*_p is

$$X^*_{p,\infty} = \frac{X^*_{p,0}}{1 - R^*} + \frac{f_p k^*_d X^*_b \tau^*}{1 - R^*}.$$

4.3.3.3 The reduced system when

In the limit of large time the system (4.13) – (4.17) reduces to

$$\frac{dS^*}{dt^*} = \frac{1}{\tau^*}(S_0^* - S^*) + \alpha_g k_h^* X_s^* - \frac{S^* X_b^*}{1+S^*}, \tag{4.21}$$

$$\frac{dX_b^*}{dt^*} = \frac{1}{\tau^*}(X_{b,0}^* - X_b^*) + \frac{R^*}{\tau^*}X_b^* + \frac{X_b^* S^*}{1+S^*} - k_d^* X_b^*, \tag{4.22}$$

$$\frac{dX_s^*}{dt^*} = \frac{1}{\tau^*}(X_{s,0}^* - X_s^*) + \frac{R^*}{\tau^*}X_s^* + (1-f_p)k_d^* X_b^* - k_h^* X_s^*, \tag{4.23}$$

$$X_{p,\infty}^* = \frac{X_{p,0}^*}{1-R^*} + \frac{f_p k_d^* X_b^* \tau^*}{1-R^*}, \tag{4.24}$$

$$X_{i,\infty}^* = \frac{X_{i,0}^*}{1-R^*}. \tag{4.25}$$

4.4 Results

4.4.1 Steady-state solution branches

The steady-state solutions are found by putting the derivative equal to zero in equations (4.13)(4.17) and then solving the resulting system of equations.

The steady-state solutions are given by

Washout branch.

$$S^* = S_w^* = S_0^* + \frac{\alpha_g k_h^* X_{s,0}^* \tau^*}{1 - R^* + k_h^* \tau^*}, \tag{4.26}$$

$$X_b^* = 0, \tag{4.27}$$

$$X_s^* = X_{\mathrm{sw}}^* = \frac{X_{s,0}^*}{1 - R^* + k_h^* \tau^*}, \tag{4.28}$$

$$X_p^* = X_{\mathrm{pw}}^* = \frac{X_{p,0}^*}{1-R^*}, \tag{4.29}$$

$$X_i^* = \frac{X_{i,0}^*}{1-R^*}, \tag{4.30}$$

$$\mathrm{COD}_w^* = S_0^* + \frac{(1+k_h^*\tau^*)\alpha_g X_{s,0}^*}{1 - R^* + k_h^* \tau^*}, \tag{4.31}$$

$$\mathrm{VSS}_w^* = \frac{X_{s,0}^*}{1 - R^* + k_h^* \tau^*} + \frac{X_{p,0}^*}{1-R^*} + \frac{X_{i,0}^*}{1-R^*}. \tag{4.32}$$

The washout branch corresponds to process failure due to removal of all the biomass ($X_b^* = 0$). The steady-state expressions for the washout branch are identical to the equivalent expressions in our first model-see chapter 2. This is unsurprising as the biochemistry of the two models are identical when there is no biomass *present in the reactor* ($X_b^* = 0$).

Differentiating equation (4.26) with respect to the residence time we obtain an increasing function.

$$\frac{dS_w^*}{d\tau^*} = \frac{\alpha_g k_h^* X_{s,0}^* (1 - R^*)}{(1 - R^* + k_h^* \tau^*)^2} > 0.$$

The soluble substrate is an increasing function of the residence time along the washout branch, because the slowly biodegradable substrates are hydrolysed to give soluble substrate and there are no microorganism present to remove the soluble substrate.

No-washout branch.

$$S^* = S_{\text{nw}}^* = \frac{1 - R^* + k_d^* \tau^*}{R^* - 1 + (1 - k_d^*)\,\tau^*}, \tag{4.33}$$

$$X_{\text{b,nw}}^* = \frac{(aS_{\text{nw}}^{*2} + bS_{\text{nw}}^* + c)(R^* - 1 + (1 - k_d^*)\tau^*)}{(a_1\tau^{*2} + b_1\tau^* + c_1)\tau^*}, \tag{4.34}$$

$$X_s^* = X_{\text{s,nw}}^* = \frac{X_{s,0}^* + (1 - f_p)k_d^* X_{\text{b,nw}}\tau^*}{1 - R^* + k_h^*\tau^*}, \tag{4.35}$$

$$X_p^* = X_{\text{p,nw}}^* = \frac{X_{p,0}^* + f_p k_d X_{\text{b,nw}}\tau^*}{1 - R^*}, \tag{4.36}$$

$$X_i^* = \frac{X_{i,0}^*}{1 - R^*}, \tag{4.37}$$

$$\text{COD}_{\text{nw}}^* = \frac{1 - R^* + k_d^*\tau^*}{(1 - k_d^*)\tau^* - 1 + R^*} + \frac{\alpha_g X_{s,0}^* + (1 - f_p)\alpha_g k_d^* X_{\text{b,nw}}\tau^*}{1 - R^* + k_h^*\tau^*}, \tag{4.38}$$

$$\begin{aligned}\text{VSS}_{\text{nw}}^* = &\left(1 + \frac{f_p k_d^*\tau^*}{1 - R^*} + \frac{(1 - f_p)k_d^*\tau^*}{1 - R^* + k_h^*\tau^*}\right) X_{\text{b,nw}}^* + \frac{X_{s,0}^*}{1 - R^* + k_h^*\tau^*} \\ &+ \frac{X_{p,0}^*}{1 - R^*} + \frac{X_{i,0}^*}{1 - R^*}.\end{aligned} \tag{4.39}$$

The coefficients are

$$
\begin{aligned}
a &= 1 - R^* + k_h^*\tau^* > 0, \\
b &= (1 - R^*)(1 - S_0^*) + (1 - S_0^* - \alpha_g X_{s,0}^*)k_h^*\tau^*, \\
c &= (R^* - 1)S_0^* - (S_0^* + \alpha_g X_{s,0}^*)k_h^*\tau^*] < 0, \\
a_1 &= ((1 - f_p)\alpha_g - 1)\, k_h^* k_d^* < 0, \\
b_1 &= (R^* - 1)(k_h^* + k_d^*) < 0, \\
c_1 &= -(R^* - 1)^2 < 0.
\end{aligned}
$$

It is interesting to observe that, although the biochemical pathways differ, the expression for the substrate concentration is identical to that in our earlier model equations (2.49) and (2.56) in section 2.4.2. Indeed they are both identical to the expression in the basic model [71]. However, the expressions for all other equivalent state variables are not identical.

In appendix C.3.4 conditions are established for the no-washout branch to be physically meaningful these are giving by

$$
k_d^* < \frac{S_0^* + \alpha_g X_{s,0}^*}{S_0^* + \alpha_g X_{s,0}^* + 1} = \frac{\mathrm{COD}_{\mathrm{in}}^*}{1 + \mathrm{COD}_{\mathrm{in}}^*},
$$

and

$$
\tau^* > \tau_+^* = (1 - R^*) \left[\frac{b_2^* + \sqrt{b_2^{*2} + 4a_2 c_2^*}}{2a_2} \right] > 0,
$$

where

$$
\begin{aligned}
a_2 &= [(1 - k_d^*)(S_0^* + \alpha_g X_{s,0}^*) - k_d^*]k_h^*, \\
b_2^* &= (1 + S_0^*)(k_h^* + k_d^*) + k_h^* \alpha_g X_{s,0}^* - S_0^*, \\
c_2^* &= (1 + S_0^*).
\end{aligned}
$$

Differentiating equation (4.33) with respect to the recycle parameter we obtain

$$\frac{dS^*_{\text{nw}}}{dR^*} = \frac{-\tau^*}{[(1-k^*_d)\tau^* - 1 + R^*]^2} < 0. \tag{4.40}$$

Hence the soluble substrate concentration is a decreasing function of the effective recycle parameter (R^*). Thus the minimal substrate concentration is obtained for the case of perfect recycle ($R^* = 1$) which is

$$S^*_{\text{nw}}(R^* = 1, \tau^*) = \frac{k^*_d}{1-k^*_d}. \tag{4.41}$$

Note, for the case of perfect recycle the soluble substrate is independent of the residence time.

Differentiating equation (4.33) with respect to the residence time we obtain.

$$\frac{dS^*_{\text{nw}}}{d\tau^*} = \frac{R^* - 1}{[(1-k^*_d)\tau^* - 1 + R^*]^2} \leq 0. \tag{4.42}$$

This equation has a vertical asymptote when

$$\tau^* = \frac{1-R^*}{1-k^*_d} = \tau^*_{\text{pm},1}.$$

In appendix C.3 we show that $\tau^*_+ > \tau^*_{\text{pm},1}$.

Thus when the substrate concentration along the no-washout branch is physically meaningful it is a strictly monotonically decreasing function of the residence time, i.e. the lowest effluent concentration is obtained at an infinite residence time.

In the limit of infinite residence time, the soluble substrate is independent of the effective recycle parameter.

$$S^*_{\text{nw}} \lim_{\tau^* \to \infty} (\tau^*, R^*) = \frac{k^*_d}{1-k^*_d}. \tag{4.43}$$

These results (equations (4.40) (4.41) and (4.43)) for the soluble substrate are the same with the basic model and our model in section 2.4.2.

Notice that operating the activated sludge process with perfect recycle is equivalent to operating it with an infinite residence time.

4.4.2 Transcritical bifurcation

By comparing the identities (4.26) – (4.32) with the identities (4.33) – (4.39) we see that the washout branch and the no-washout branch are identical when

$$\begin{aligned} & S_w^* = S_{\mathrm{nw}}^*, \\ & \Rightarrow S_0^* + \frac{\alpha_g k_h^* X_{s,0}^* \tau^*}{1 - R^* + k_h^* \tau^*} = \frac{1 - R^* + k_d^* \tau^*}{(1 - k_d^*)\tau^* - 1 + R^*}. \end{aligned}$$

This intersection point corresponds to a trans-critical bifurcation.

After some algebra we find that this is true when the residence time satisfies the quadratic equation $Q(\tau^*) = 0$, where

$$Q(\tau^*) = a_2 \tau^{2*} + b_2 \tau^* + c_2, \quad \text{and the coefficients are} \tag{4.44}$$

$$a_2 = [(1 - k_d^*)(S_0^* + \alpha_g X_{s,0}^*) - k_d^*] k_h^*,$$

$$b_2 = -(1 - R^*)[(1 + S_0^*)(k_h^* + k_d^*) + k_h^* \alpha_g X_{s,0}^* - S_0^*], \tag{4.45}$$

$$c_2 = -(1 - R^*)^2 (1 + S_0^*) < 0. \tag{4.46}$$

Equations (4.44)-(4.46) are identical to the equations in chapter 2.4.1.2.

It follows from the analysis in appendix C.3.4 that trans-critical bifurcation point is physically meaningful only when $a_2 > 0$ and is given by

$$\tau_+^* = (1 - R^*)\tau_{\mathrm{cr}}^* (R^* = 0), \tag{4.47}$$

where

$$\tau^*_{\mathrm{cr}}(R^*=0)=\frac{b^*_2+\sqrt{b^{*2}_2+4a_2c^*_2}}{2a_2}, \tag{4.48}$$

$$b^*_2=(1+S^*_0)(k^*_h+k^*_d)+k^*_h\alpha_g X^*_{s,0}-S^*_0, \tag{4.49}$$

$$c^*_2=(1+S^*_0). \tag{4.50}$$

The condition $a_2>0$ is

$$k^*_d<\frac{S^*_0+\alpha_g X^*_{s,0}}{1+S^*_0+\alpha_g X^*_{s,0}}=\frac{\mathrm{COD}^*_{\mathrm{in}}}{1+\mathrm{COD}^*_{\mathrm{in}}}. \tag{4.51}$$

The expression for the critical value of the decay rate, equation (4.51) only depends upon the value of the chemical oxygen demand flow in the feed. However, the expression for the critical value of the residence time depends upon how the chemical oxygen demand is partitioned into its components, as shown in the expressions for the coefficients of b^*_2 and c^*_2. These expressions are identical to those in our earlier model in chapter 2.

When the no-washout branch is not physically meaningful then the only stable steady state is the washout solution. In this circumstances process failure must occur. This case can therefore be ignored.

4.4.3 Stability of the steady-state solutions

The Jacobian matrix is given by

$$J(S^*,X^*_b,X^*_s)=\begin{pmatrix} -\frac{1}{\tau^*}-\frac{X^*_b}{(1+S^*)^2} & -\frac{S^*}{1+S^*} & \alpha_g k^*_h \\ \frac{X^*_b}{(1+S^*)^2} & \frac{R^*-1}{\tau^*}+\frac{S^*}{1+S^*}-k^*_d & 0 \\ 0 & (1-f_p)k^*_d & \frac{R^*-1}{\tau^*}-k^*_h \end{pmatrix}. \tag{4.52}$$

4.4.3.1 Stability of the washout branch

The Jacobian matrix 4.52 evaluated at the washout steady-state solution is given by

$$J(S_w^*, 0, X_{\text{sw}}^*) = \begin{pmatrix} -\frac{1}{\tau^*} & -\frac{S_w^*}{1+S_w^*} & \alpha_g k_h^* \\ 0 & \frac{R^*-1}{\tau^*} + \frac{S_w^*}{1+S_w^*} - k_d^* & 0 \\ 0 & (1-f_p)k_d^* & \frac{R^*-1}{\tau^*} - k_h^* \end{pmatrix}.$$

The eigenvalues of this matrix are

$$\begin{aligned} \lambda_1 &= -\frac{1}{\tau^*} < 0, \\ \lambda_2 &= \frac{R^*-1}{\tau^*} - k_h^* < 0. \end{aligned}$$

Recall that $0 \leq R^* \leq 1$) and

$$\lambda_3 = \frac{R^*-1}{\tau^*} + \frac{S_w^*}{1+S_w^*} - k_d^*.$$

The stability of the washout branch depends upon the sign of λ_3.

Note that, the washout steady-state is always stable when

$$\begin{aligned} & k_d^* \geq 1, \\ \Rightarrow & \frac{k_d}{\mu_m} \geq 1, \\ \Rightarrow & k_d \geq \mu_m. \end{aligned}$$

This makes sense because it says that the washout steady state will always be stable if the death rate is greater than, or equal to, the maximum growth rate.

We now show that there is a critical value ($k_{\text{d,cr},\infty}^*$) such that the washout branch is

always stable when $k^*_{\mathrm{d,cr},\infty}<k^*_d \leq 1$. The eigenvalue λ_3 will be negative when

$$k^*_d>k^*_{\mathrm{d,cr}} = \frac{S^*_w}{1+S^*_w} = \frac{S^*_0(1-R^*)+(S^*_0+\alpha_g X^*_{s,0})k^*_h\tau^*}{(1+S^*_0)(1-R^*)+(1+S^*_0+\alpha_g X^*_{s,0})k^*_h\tau^*}.$$

Note that

$$\frac{dk^*_{\mathrm{d,cr}}}{d\tau^*} = \frac{\alpha_g X^*_{s,0}k^*_h(1-R^*)}{[(1+S^*_0)(1-R^*)+(1+S^*_0+\alpha_g X^*_{s,0})k^*_h\tau^*]^2}>0.$$

Thus $k^*_{\mathrm{d,cr}}$ has a minimum value $S^*_0/(1+S^*_0)$ when $(\tau^*=0)$ and a maximum value $(k^*_{\mathrm{d,cr},\infty})$ when

$$\begin{aligned} k^*_{\mathrm{d,cr},\infty} = \lim_{\tau^*\to\infty} k^*_{\mathrm{d,cr}} &= \frac{S^*_0(1-R^*)+(S^*_0+\alpha_g X^*_{s,0})k^*_h\tau^*}{(1+S^*_0)(1-R^*)+(1+S^*_0+\alpha_g X^*_{s,0})k^*_h\tau^*}, \\ &= \frac{S^*_0+\alpha_g X^*_{s,0}}{1+S^*_0+\alpha_g X^*_{s,0}}. \\ &= \frac{\mathrm{COD}^*_{\mathrm{in}}}{1+\mathrm{COD}^*_{\mathrm{in}}}. \end{aligned} \tag{4.53}$$

Thus if $k^*_d>k^*_{\mathrm{d,cr},\infty}$ then the washout branch is always stable.

We now consider the case $k^*_d<k^*_{\mathrm{d,cr},\infty}$ and show that there is a critical value of the residence time, τ^*_{cr}, such that if $\tau^*<\tau^*_{\mathrm{cr}}$ then the washout solution is locally stable. After some algebra we find that

$$\begin{aligned} \lambda_3 &= \frac{R^*-1}{\tau^*} + \frac{S^*_w}{1+S^*_w} - k^*_d, \\ &= \frac{-Q(\tau^*)}{B}, \end{aligned}$$

where $Q(\tau^*)$ is defined by equation (4.44) and the coefficient B is given by

$$B = (R^*-1)(1+S^*_0)\tau^* - (1+S^*_0+\alpha_g X^*_{s,0})k^*_h\tau^{*2}<0.$$

(Recall that $0 \leq R^* \leq 1$).

The denominator B is always negative. Hence the problem of establishing $\lambda_2<0$

reduces to determining when $-Q(\tau^*)$ is positive, i.e. when the quadratic $Q(\tau^*)$ is negative.

We only need to consider the case

$$k_d^* < \frac{S_0^* + \alpha_g X_{s,0}^*}{1 + S_0^* + \alpha_g X_{s,0}^*} = k_{\mathrm{d,cr},\infty}^*.$$

This condition implies that the coefficient a is positive ($a>0$). Then the graph of the quadratic function $Q(\tau^*)$ is shown in appendix C.3.4 in figure C.1. Therefore the inequality $Q(\tau^*)>0$ is only true if $0<\tau^*<\tau_+^*$. Thus, the washout solution is stable when the no-washout solution is not physically meaningful.

4.4.3.2 Stability of the no-washout branch

The Jacobian matrix for the no-washout branch is given by

$$J(S_{\mathrm{nw}}^*, X_{\mathrm{b,nw}}^*, X_{\mathrm{s,nw}}^*) = \begin{pmatrix} f_1 & f_2 & f_3 \\ g_1 & 0 & 0 \\ 0 & h_2 & h_3 \end{pmatrix}. \tag{4.54}$$

Note that J(2,2)=0 because along the no-washout branch we have $X_{\mathrm{b,nw}}^* \neq 0$.

The coefficients in the Jacobian matrix are

$$\begin{aligned} f_1 &= -\frac{1}{\tau^*} - \frac{X_{\mathrm{b,nw}}^*}{(1 + S_{\mathrm{nw}}^*)^2} < 0, \\ f_2 &= -\frac{S_{\mathrm{nw}}^*}{1 + S_{\mathrm{nw}}^*} < 0, \\ f_3 &= \alpha_g k_h^* > 0, \\ g_1 &= \frac{X_{\mathrm{b,nw}}^*}{(1 + S_{\mathrm{nw}}^*)^2} > 0, \\ h_2 &= (1 - f_p) k_d^* > 0, \end{aligned}$$

$$h_3 = \frac{R^* - 1}{\tau^*} - k_h^* < 0,$$

where we have assumed that the no-washout solution branch is physically meaningful. The characteristic polynomial of the Jacobian matrix (4.54) is given by

$$\lambda^3 + d_1\lambda^2 + d_2\lambda + d_3 = 0, \tag{4.55}$$

where the coefficients are given by

$$\begin{aligned} d_1 &= -(h_3 + f_1) > 0, \\ d_2 &= -(g_1 f_2 - h_3 f_1) > 0, \\ d_3 &= g_1(f_2 h_3 - h_2 f_3). \end{aligned}$$

By the Routh-Hurwitz criteria [58] the polynomial (4.55) has negative real roots when $d_1 > 0$, $d_3 > 0$ and $d_1 d_2 - d_3 > 0$. Consider the first condition $d_1 > 0$. We have

$$\begin{aligned} d_1 &= -(h_3 + f_1), \\ &= -\left(\frac{R^* - 1}{\tau^*} - k_h^* - \frac{1}{\tau^*} - \frac{X_{\mathrm{b,nw}}^*}{(1 + S_{\mathrm{nw}}^*)^2}\right) > 0. \end{aligned}$$

This is always true when the no-washout solution branch is physically meaningful. Consider the second condition $d_3 > 0$.

$$d_3 = g_1(f_2 h_3 - h_2 f_3).$$

Note that

$$g_1 = \frac{X_{\mathrm{b,nw}}^*}{(1 + S_{\mathrm{nw}}^*)^2} > 0,$$

when the no-washout solution branch is physically meaningful. So the condition $d_3>0$ becomes

$$f_2h_3 - h_2f_3>0 \Rightarrow -\frac{S^*_{\rm nw}}{1+S^*_{\rm nw}}\left(\frac{R^*-1}{\tau^*} - k^*_h\right) - (1-f_p)k^*_d\alpha_g k^*_h>0.$$

After some work we have

$$f_2h_3 - h_2f_3>0 \Rightarrow \frac{-B(\tau^*)}{\tau^{*2}}>0,$$

where

$$\begin{aligned} B(\tau^*) &= a_1\tau^{*2} + b_1\tau^* + c_1, \\ a_1 &= \left((1-f_p)\alpha_g - 1\right)k^*_h k^*_d<0, \\ b_1 &= (R^*-1)(k^*_h + k^*_d)<0, \\ c_1 &= -(1-R^*)^2<0. \end{aligned}$$

Note that the coefficient a_1 is negative because $(1-f_p)\alpha_g \leq 1$. The condition $d_3>0$ reduces to showing when

$$B(\tau^*) = a_1\tau^{*2} + b_1\tau^* + c_1<0.$$

As $\tau^*>0$ and the coefficients a_1, b_1 and c_1 are negative then $B(\tau^*)$ must be negative. Now we consider the final condition $d_1d_2 - d_3>0$. We have

$$\begin{aligned} d_1d_2 - d_3 &= (h_3+f_1)(g_1f_2 - h_3f_1) + g_1(h_2f_3 - f_2h_3), \\ &= g_1(f_1f_2 + h_2f_3) - f_1h_3(f_1+h_3), \\ &= \frac{(1-f_p)k^*_d\alpha_g k^*_h X^*_{\rm b,nw}}{(1+S^*_{\rm nw})^2} + \left(\frac{1}{\tau^*} + \frac{X^*_{\rm b,nw}}{(1+S^*_{\rm nw})^2}\right)\times \\ &\quad \left[\left(\frac{R^*-2}{\tau^*} - \frac{X^*_{\rm b,nw}}{(1+S^*_{\rm nw})^2} - k^*_h\right)\left(\frac{R^*-1}{\tau^*} - k^*_h\right) + \frac{S^*_{\rm nw}X^*_{\rm b,nw}}{(1+S^*_{\rm nw})^3}\right]>0, \end{aligned}$$

for a physically meaningful solution ($X^*_{\mathrm{b,nw}}>0, S^*_{\mathrm{nw}}>0$) (Recall that $0 \leq R^* \leq 1$). Hence, the no-washout solution branch is always stable when it is physically meaningful.

4.4.4 Asymptotic solutions

In this section we obtained asymptotic solutions for large residence times.

4.4.4.1 Large residence time approximations

At large residence times, we have

$$S^*_{\mathrm{nw}} \approx \frac{k^*_d}{1-k^*_d} + \frac{(1-R^*)}{(1-k^*_d)^2} \cdot \frac{1}{\tau^*} + O\left(\frac{1}{\tau^{*2}}\right), \tag{4.56}$$

$$X^*_{\mathrm{b,nw}} \approx a_0 \cdot \frac{1}{\tau^*} + O\left(\frac{1}{\tau^{*2}}\right), \tag{4.57}$$

$$X^*_{\mathrm{s,nw}} \approx \frac{X^*_{s,0} + (1-f_p)k^*_d a_0}{k^*_h} \cdot \frac{1}{\tau^*} + O\left(\frac{1}{\tau^{*2}}\right), \tag{4.58}$$

$$X^*_{\mathrm{p,nw}} \approx \frac{X^*_{p,0} + f_p k^*_d a_0}{1-R^*} + (b_0 + a_0 c_0) \cdot \frac{1}{\tau^*} + O\left(\frac{1}{\tau^{*2}}\right), \tag{4.59}$$

$$X^*_i \approx \frac{X^*_{i,0}}{1-R^*}, \tag{4.60}$$

$$\mathrm{COD}^*_{\mathrm{nw}} \approx \frac{k^*_d}{1-k^*_d} + \left[\frac{(1-R^*)}{(1-k^*_d)^2} + \frac{[X^*_{s,0} + (1-f_p)k^*_d a_0]\alpha_g}{k^*_h}\right] \cdot \frac{1}{\tau^*} + O\left(\frac{1}{\tau^{*2}}\right), \tag{4.61}$$

$$\mathrm{VSS}^*_{\mathrm{nw}} \approx \frac{X^*_{i,0}}{1-R^*} + \frac{X^*_{p,0} + f_p k^*_d}{1-R^*} a_0 + \left\{b_0 + a_0\left[1 + c_0 + \frac{X^*_{s,0} + (1-f_p)k^*_d}{k^*_h}\right]\right\} \cdot \frac{1}{\tau^*} + O\left(\frac{1}{\tau^{*2}}\right), \tag{4.62}$$

where

$$a_0 = \frac{S^*_0(1-k^*_d) - k^*_d + \alpha_g X^*_{s,0}(1-k^*_d)}{k^*_d(1-k^*_d)[1-(1-f_p)\alpha_g]}, \tag{4.63}$$

$$b_0 = \frac{f_p[S_0^*(1-k_d^*)^2 + k_d^*(k_d^*-1) - k_h^*]}{(1-k_d^*)^2[1-(1-f_p)\alpha_g]k_h^*}, \tag{4.64}$$

$$c_0 = \frac{f_p(k_d^* + k_h^*)}{[(1-f_p)\alpha_g - 1]k_h^*}. \tag{4.65}$$

It is useful to note that coefficient a_0 can be written as

$$a_0 = \frac{\mathrm{COD}_{\mathrm{in}}^*(1-k_d^*) - k_d^*}{k_d^*(1-k_d^*)(1-(1-f_p)\alpha_g)}, \tag{4.66}$$

where

$$\mathrm{COD}_{\mathrm{in}}^* = S_0^* + \alpha_g X_{s,0}^*.$$

For the default parameter values in appendix C.4 we have $a_0 = 386.2856$. We have $1-(1-f_p)\alpha_g > 0$ from (4.3) and $S_0^*(1-k_d^*) - k_d^* > 0$ from the condition for the no-washout branch to be physical meaningful. At large value of residence time the biomass concentration is independent of the value of the effective recycle factor (R^*). The case $k_d^* = 1$ is not allowed in the asymptotic formula, because when this is true then the no-washout branch is not physically meaningful.

The leading order term for the chemical oxygen demand is identical to both that in our earlier model in equation (2.80) and in the basic model [71]. The leading order term for the volatile suspended solids is also identical provided that there are no non-biodegradable particulates in the feed, i.e. $X_{p,0}^* = 0$.

It is important to note that the effluent concentration can not be reduced below the limiting value

$$\lim_{t^*\to\infty} S_{\mathrm{nw}}^* = \frac{k_d^*}{1-k_d^*} > 0.$$

This is identical to our model in chapter 2.

4.4.5 Steady-state diagram

Figures 4.2 shows the steady state diagrams for the five state variables in the model. In figure 4.2(a), as explained in section 4.4.1 the soluble substrate increases along the washout branch as additional soluble substrate is produced by the hydrolysis of the insoluble substrate and there is no biomass to consume it. After the transcritical bifurcation the soluble substrate is a decreasing function of the residence time, as shown by equation (4.42). From equation (4.56) we know that in the limit when the residence time approaches infinity the soluble substrate concentration approaches the limiting value $S^* = k_d^*/(1 - k_d^*)$. Figure 4.2(b) shows that the biomass concentration is zero along the washout branch (as shown by equation (4.27)). After the trans-critical bifurcation it increases sharply to a maximum value, $X^*_{\text{b,max}} = 8.3789$ when $\tau^*_{\text{max}} = 4.0546$; thereafter it gradual decreases along the no-washout branch. From equation (4.57) we know that in the limit when the residence time approaches infinity the biomass concentration approaches the limiting value $X_b^* = 0$. Figure 4.2(c) shows that the insoluble substrate concentration decreases with the residence time towards the limiting value, zero, given by equation (4.58).

Figure 4.2(d) shows that along the washout branch the non-biodegradable particulates is equal to the influent value, in this case zero, and after the trans-critical bifurcation it increases. Along the no-washout branch the steady-state biomass concentration is non-zero as there is a contribution to the pool of non-biodegradable particulates through the decay of biomass. From equation (4.59) we know that in the limit when the residence time approaches infinity the non-biodegradable particulates concentration approaches the limiting value $(X^*_{p,0} + f_p k_d^* a_0)/(1 - R^*)$. For the default parameter values the limit value is 2.1076. This has two components, the first component is due the the concentration of non-biodegradable particulates in the inflow and the second component is due to the death of biomass. Figure 4.2(e) shows the particulate inert material concentration (X_i^*) as a function of the residence time. Not very interesting!

4.4.6 The chemical oxygen demand

Figure 4.3 shows the chemical oxygen demand as a function of the residence time when there is no recycle.

When there is no recycle ($R^* = 0$) the chemical oxygen demand is constant along the washout branch ($\tau^* < \tau^*_{\text{cr}} = 1.2020$).

$$\text{COD}^*_w = S^*_0 + \frac{(1 + k^*_h \tau^*)\alpha_g X^*_{s,0}}{1 - R^* + k^*_h \tau^*},$$

$$\text{COD}^*_w(R^* = 0) = S^*_0 + \alpha_g X^*_{s,0} = \text{COD}^*_{\text{in}} = 10.1790.$$

Along the no-washout branch the chemical oxygen demand is a decreasing function of the residence time. From equation (4.61) it has limiting value when the residence time approaches infinity ($\tau^* \to \infty$) given by

$$\lim_{\tau^* \to \infty} \text{COD}^*_{\text{nw}} = \frac{k^*_d}{1 - k^*_d} = 0.0732. \tag{4.67}$$

This is identical to our model in chapter 2.

The efficiency at which the chemical oxygen demand is removed can be defined by

$$E_{\text{COD}^*} = \frac{\text{COD}^*_{\text{in}} - \text{COD}^*_{\text{out}}}{\text{COD}^*_{\text{in}}}.$$

From equation (2.90) the efficiency can not be increased over the limiting value

$$E_{\text{COD}^*_{\text{nw}}}(\tau^* = \infty) = 0.9928.$$

This means that it is impossible to remove more that 99.28% of the chemical oxygen demand flowing into the reactor.

When $E_{\text{COD}^*} = 0.90$, the chemical oxygen demand in the effluent has been reduced to 90% of the value in the influent. The required value of the residence time is τ^*=3.6291 (16.5 days). On figure 4.3 the residence time requested to obtain the

target value $E_{\mathrm{COD}^*} = 0.9$ is indicated by the horizontal line.

In order to reduce the chemical oxygen demand in the effluent to 1% of the value in the influent ($E_{\mathrm{COD}^*} = 0.99$) the required value of the residence time is τ^*=192.0100 (872.8 days).

Thus in practice an efficiency (E_{COD^*}=0.99) can not be achieved.

When the effective recycle parameter takes its theoretical maximum (R^*=1) then the residence time to achieve an efficiency E_{COD^*}=0.99 is reduced to τ^*=170.2187 (773.7 days). This is still too large for practical purposes.

4.4.7 The volatile suspended solids

In section 4.4.7.1 we consider the case when there is no recycle ($R^* = 0$). In section 4.4.7.2 we investigate what happens when we increase the value of the effective recycle parameter to the maximum value ($R^* = 1$).

4.4.7.1 The case $R^* = 0$

Figure 4.4 shows a steady state diagram for the volatile suspended solids as a function of the residence time when there is no recycle. Along the washout branch ($0<\tau^*<\tau^*_{\mathrm{cr}}$) we have

$$\begin{aligned} \mathrm{VSS}^*_w &= \frac{X^*_{p,0} + X^*_{i,0}}{1 - R^*} + \frac{X^*_{s,0}}{1 - R^* + k^*_h \tau^*}, \\ \mathrm{VSS}^*_w(R^* = 0) &= X^*_{p,0} + X^*_{i,0} + \frac{X^*_{s,0}}{1 + k^*_h \tau^*}. \end{aligned} \tag{4.68}$$

which is a decreasing function of the residence time. The volatile suspended solid is decreasing because insoluble substrate is converted to soluble substrate. It's maximum value is when the residence time is zero. For the case of no recycle ($R^* = 0$) we have.

$$\mathrm{VSS}^*_{w,\max} = X^*_{p,0} + X^*_{i,0} + X^*_{s,0} = 12.2142.$$

When there is no settling unit ($R^* = 0$) the volatile suspended solids at the trans-critical bifurcation (4.47), $\tau^*_{\text{cr}} = 1.2020$, has decreased to the value $\text{VSS}^*_w(\tau^* = \tau^*_{\text{cr}})$=1.7432.

After the trans-critical bifurcation the volatile suspended solids is given by

$$\begin{aligned}\text{VSS}^*_{\text{nw}} &= \left(1 + \frac{f_p k_d^* \tau^*}{1 - R^*} + \frac{(1 - f_p) k_d^* \tau^*}{1 - R^* + k_h^* \tau^*}\right) X^*_{\text{b,nw}} + \frac{X^*_{s,0}}{1 - R^* + k_h^* \tau^*} \\ &\quad + \frac{X^*_{p,0}}{1 - R^*} + \frac{X^*_{i,0}}{1 - R^*}, \\ \text{VSS}^*_{\text{nw}}(R^* = 0) &= \left(1 + f_p k_d^* \tau^* + \frac{(1 - f_p) k_d^* \tau^*}{1 + k_h^* \tau^*}\right) X^*_{\text{b,nw}} + \frac{X^*_{s,0}}{1 + k_h^* \tau^*} + X^*_{p,0} \\ &\quad + X^*_{i,0}. \end{aligned} \tag{4.69}$$

where the value for $X^*_{\text{b,nw}}$ is given by equation (4.34).

The volatile suspended solids increases to a local maximum $\text{VSS}^*_{\text{nw,max}} = 9.2834$ when $\tau^* = 3.2167$. Thereafter it decreases toward its limiting value. From equation (4.62) the limiting value when the residence time is infinity is given by

$$\text{VSS}^* \approx \frac{X^*_{i,0}}{1 - R^*} + \frac{X^*_{p,0} + f_i k_d^*}{1 - R^*} a_0 = 2.1085.$$

From equation (4.20) the target value of the volatile suspended solids is

$$\text{VSS}^*_t = \frac{\text{VSS}_t}{\alpha_g K_s} = \frac{12000}{\alpha_g K_s} = 3.4510.$$

From figure 4.4 we can see that the intersection points where the volatile suspended solids is equal to the target value are on the washout and the no-washout branch. The value of the residence time at the intersection point along the washout branch

is found from equation (4.68). We have

$$\tau^*_{i,w} = \frac{(1-R^*)\left[X^*_{p,0} + X^*_{i,0} + X^*_{s,0} - \mathrm{VSS}^*_t\ (1-R^*)\right]}{\left[\mathrm{VSS}^*_t\ (1-R^*) - (X^*_{p,0} + X^*_{i,0})\right] k^*_h},$$
$$\tau^*_{i,w}(R^*=0) = \frac{X^*_{p,0} + X^*_{i,0} + X^*_{s,0} - \mathrm{VSS}^*_t}{\left[\mathrm{VSS}^*_t - (X^*_{p,0} + X^*_{i,0})\right] k^*_h} = 0.5080. \tag{4.70}$$

The values of the residence time at the intersection points along the no-washout branch are found from equation (4.69). We have $\tau^*_{\mathrm{i,nw1}}$=1.2336 and $\tau^*_{\mathrm{i,nw2}}$=193.6117. Consequently the asymptotic value is *below* the target value.

Figure 4.4 shows the steady state diagram for the volatile suspended solids as a function of the residence time. Note that there is no recycle. The target value is between the maximum value of the volatile suspended solids along the no-washout branch and the asymptotic value along the no-washout branch (when the residence time approaches infinity). The volatile suspended solids intersects the target value at three points: once along the washout branch, $\tau^* = 0.5080$ (2.3 days), and twice along the no-washout branch, τ^*=1.2336 (5.6 days) and τ^* =193.6117 (880 days). The latter is clearly too large to be practical. The volatile suspended solids is lower than the target value if the residence time is between the intersection point on the washout branch and the first intersection point on the no-washout branch or larger than the second intersection point on the washout branch. The latter is clearly too large to be practical. The values of the chemical oxygen demand at the first two intersection points are 10.1790 and 8.4075 corresponding to COD efficiencies of 0 and 0.1740. Therefore in practice the residence time would need to be larger than the second intersection point on the no-washout branch in order to achieve significant chemical oxygen demand removal. However, such values for the residence time lead to excessive sludge production. Using the nomenclature of our earlier chapter this response diagram is 'case three'. In practice, the response diagram shown in figure 4.4 is undesirable.

4.4.7.2 The case $R^*>0$

When investigating our earlier model we found that as the value of the effective recycle parameter was varied over the range $0 \leq R^*<1$ that there were five generic response diagrams showing how the volatile suspended solids varied as a function of the residence time-see chapter 2.5. The model considered in this chapter only exhibits three cases of response diagram for the default parameter values. We discuss these diagrams within the context of these found in our earlier model. We first describes two cases, which are not exhibited in the current model.

Case one corresponds to a response diagram in which the target value is larger than the maximum value along the washout branch. Thus the volatile suspended solids concentration in the effluent is always below the target value. From equation (4.68) this is when

$$\mathrm{VSS}_t^*>\frac{1}{1-R^*}(X_{i,0}^*+X_{p,0}^*+X_{s,0}^*).$$

In this case there are no intersection points as the volatile suspended solids are below the target value for all residence times. This is not realistic. In case two the target value is lower than the maximum value along the washout branch but above the maximum value along the no-washout branch. Thus there is only one intersection point, which is on the washout branch. This is a good case to have because the volatile suspended solids at any point on the no-washout branch is below the target value. Although cases one and two are very desirable they are not observed in practice.

In the nomenclature of our previous chapter, the response diagram shown in figure 4.4 is 'case three'. This occurs when the target value is between the maximum value of the volatile suspended solids along the no-washout branch and the minimum value along the no-washout branch. As noted in the discussion of these figures there is one intersection point on the washout branch and two intersection points

on the no-washout branch. The target value is larger than the steady-state volatile suspended solids value if the residence time is between the intersection point on the washout branch and the first intersection point on the no-washout branch or larger than the second intersection point on the washout branch. In practice a wastewater treatment plant would have to be operated with the residence time larger than the second intersection point on the washout branch.

In our original model as the recycle parameter is further increased 'case three' becomes 'case four', in which there is only one intersection point on the no-washout branch. In the new model this transition does not occur. Instead, what happens is that the asymptotic value for the volatile suspended solids at infinite residence time increases through the target value. However, the value for the volatile suspended solids at the transcritical bifurcation remains below the target value. This leads to a new case of response diagram, case six, in which there are two intersection points: one on each of the washout and no-washout branches. This response diagram is illustrated in figure 4.5. The intersection points are when ($\tau^* = 0.5981$) and when ($\tau^* = 0.6624$). Figure 4.5(a) shows that that volatile suspended solids at the transcritical bifurcation is below the target value. Figures 4.5(b) and 4.5(c) show that the asymptotic value is higher than the target value.

In case six diagrams the volatile suspended solids can only be maintained below the target value if the reactor is operated at residence times between the two intersection points. This is likely to be very undesirable in practice, due to the corresponding values of the chemical oxygen demand in the effluent. The values of the chemical oxygen demand at the intersection points are 11.2190 and 10.9734 corresponding to the chemical oxygen demand efficiencies of -0.1022 and -0.0780. Thus case six is highly undesirable for the default parameter values. The chemical oxygen demand in the effluent is higher than that in the influent!

In the original model the final transition, from case four to case five, corresponded to the asymptotic value of the volatile suspended solids at infinity increasing through

the target value. In the new model the final transition corresponds to the value of the volatile suspended solids at the trans-critical bifurcation increasing through the target value. This leads to the 'case five' response diagram shown in figure 4.6. There are now no intersection points. This is undesirable because the volatile suspended solids can never be reduced below the target value.

There are two non-generic cases. One of these happens when the target value of the volatile suspended solid is exactly equal to the maximum value along the washout branch: we then have two finite intersection points and one at infinity. (This is the transition from case three to case six). The second happens when the target value of the volatile suspended solid is exactly equal to equal to the value at the trans-critical bifurcation: we then have one intersection point. (This is the transition from case six to case five)

The location of the different regions as a function of the effective recycle parameter is shown in table 4.2. The calculation of the transition values is explained in section 4.5.2. Only case three leads to the possibility of desirable behavior, i.e. the value of the effective recycle parameter is limited to: $0 \leq R^* < 0.3890$. However, in practice even the case three response digram is undesirable for our default parameter values. Thus excessive sludge formation is inevitable without a mechanism to reduce the sludge content. (even when $R^* = 0$.)

Abbreviation	Explanation	Unit
C	The recycle concentration factor	(–)
F	Flow rate through bioreactor	(dm^3 hr^{-1})
K_s	Monod constant	($\|S\|$)
R	Recycle ratio based on volumetric flow rates	(–)
S	Substrate concentration within the bioreactor	($\|S\|$)
S_0	Concentration of substrate flowing into the reactor	($\|S\|$)
V	Volume of the bioreactor	(dm^3)
X_b	Concentration of biomass	($\|S\|$)
X_i	Concentration of of particulate inert material	($\|S\|$)
X_s	Concentration of slowly biodegradable particulate	($\|S\|$)
X_p	Concentration of non-biodegradable particulate	($\|S\|$)
$X_{j,0}(j = b, s, p, i)$	Concentration flowing into the reactor	($\|S\|$)
X_t	Total biomass	($\|S\|$)
k_h	Hydrolysis rate of insoluble organic compounds	(hr^{-1})
k_d	Death coefficient	(hr^{-1})
f_p	The fraction of dead biomass converted to non-biodegradable particulate	(–)
t	Time	(hr^{-1})
β_i	Conversion efficiency from non-biodegradable particulates to readily biodegradable (soluble) substrate,	(–)
α_g	Yield factor for growth of biomass	($\|S\|\|S\|^{-1}$)
$\mu(S)$	Specific growth rate model	(hr^{-1})
$\mu(S_s)$	Specific growth rate model in the sludge integration unit	(hr^{-1})
μ_m	Maximum specific growth rate	(hr^{-1})
τ	Residence time	(hr)
χ	Modelling parameter for the sludge integration unit	(–)

Table 4.1: The definitions of the parameters (model two). Note, all concentration are measured in units of $|S|$(COD).

R^*	Case	Figure
$0 < R^* < R^*_{3,6}$=0.3890	Case three	Figure 4.4
$R^*_{3,6} < R^* < R^*_{6,5}$=0.4949	Case six	Figure 4.5
$R^*_{6,5} < R^*$	Case five	Figure 4.6

Table 4.2: The generic behavior of the reactor as a function of the effective recycle parameter.

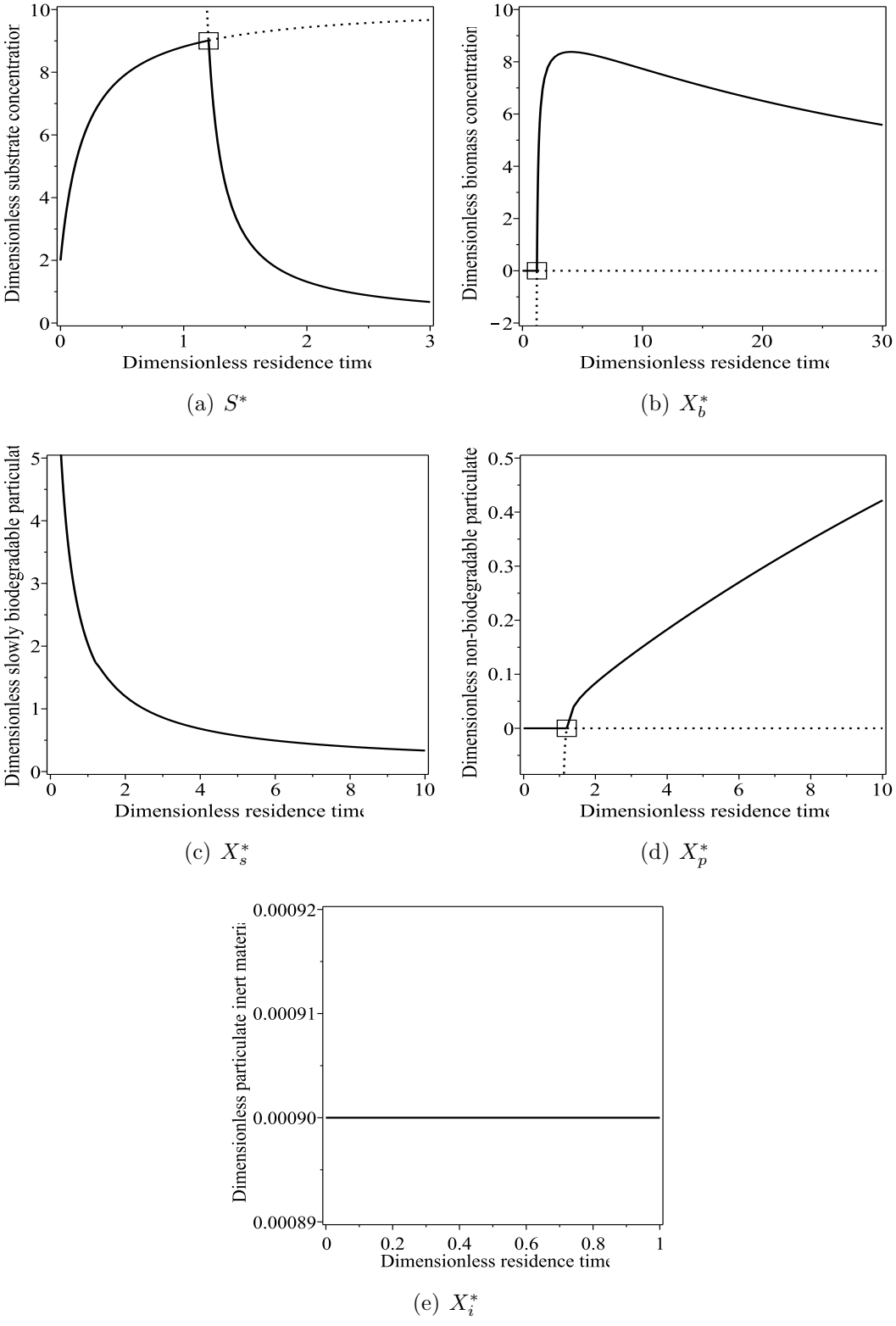

(a) S^* (b) X_b^*

(c) X_s^* (d) X_p^*

(e) X_i^*

Figure 4.2: Steady-state diagrams showing the variation of dimensionless substrate concentration (S^*), biomass concentration (X_b^*), slowly biodegradable particulates concentration (X_s^*), non-biodegradable particulates concentration (X_p^*) and particulate inert material concentration (X_i^*) as a function of the dimensionless residence time (τ^*). The box denotes the location of the trans-critical bifurcation. The solid and dotted lines represent stable and unstable solutions respectively. Parameter value $R^* = 0$.

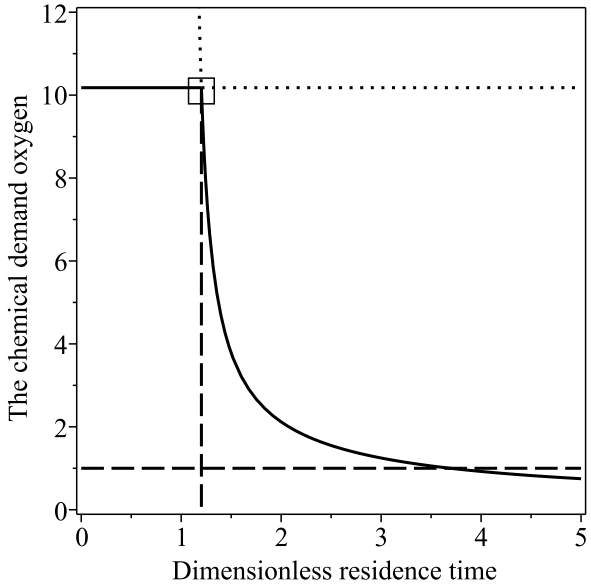

Figure 4.3: Steady state diagram for the chemical oxygen demand. Parameter value $R^* = 0$. The horizontal line correspond to a chemical oxygen demand removal efficiency of 90%. The solid and dotted lines represent stable and unstable solutions respectively. The square denotes the critical value for the residence time when the washout solution becomes unstable.

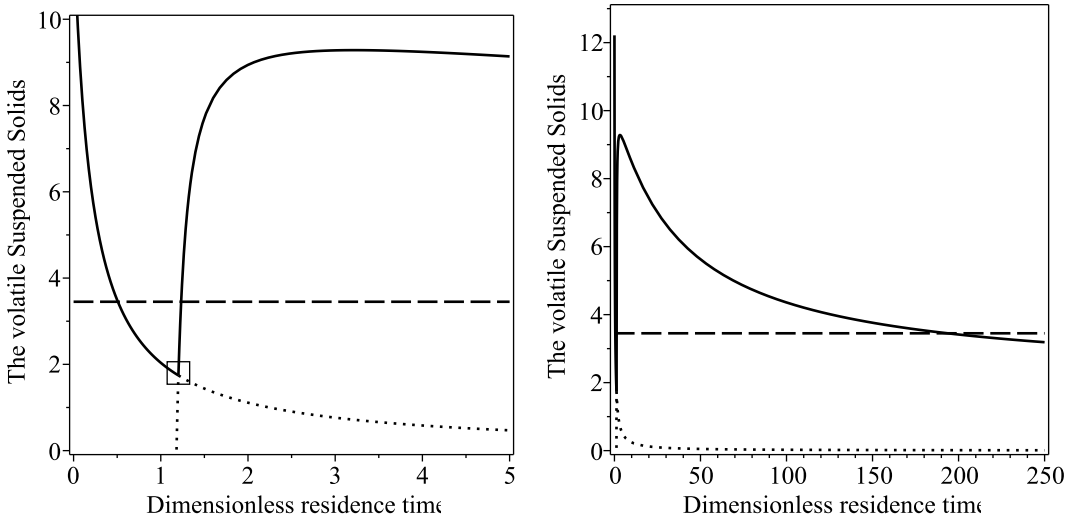

(a) $0 \leq \tau^* \leq 5$ (b) $0 \leq \tau^* \leq 250$

Figure 4.4: Steady state diagram for the volatile suspended solids (case three). Parameter values $R^* = 0, \tau^*_{\text{cr}} = 1.2020$. The horizontal line denotes the target value of the volatile suspended solids. The square denotes the critical value for the residence time when the washout solution becomes unstable. The solid and dotted lines represent stable and unstable solutions respectively. Case three response digram.

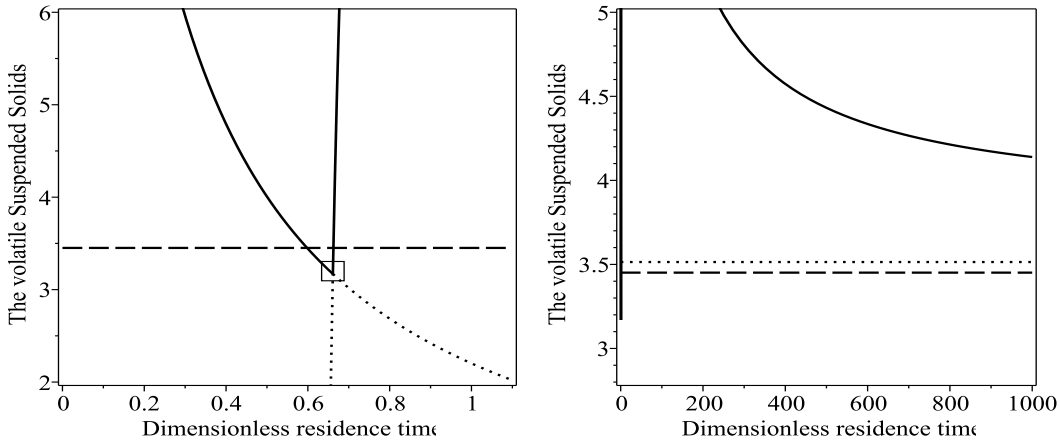

(a) $0 \leq \tau^* \leq 1$ (b) $0 \leq \tau^* \leq 1000$

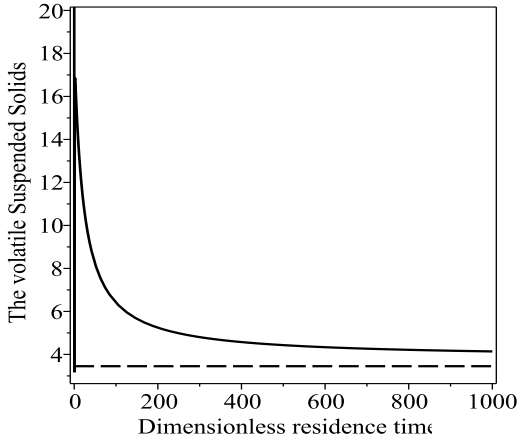

(c) $0 \leq \tau^* \leq 1000$

Figure 4.5: Steady state diagram for the volatile suspended solids (case six). Parameter value $R^* = 0.45, \tau^*_{\text{cr}} = 0.6611$. The horizontal line denotes the target value of the volatile suspended solids. The square denotes the critical value for the residence time when the washout solution becomes unstable. The solid and dotted lines represent stable and unstable solutions respectively. Case six response digram.

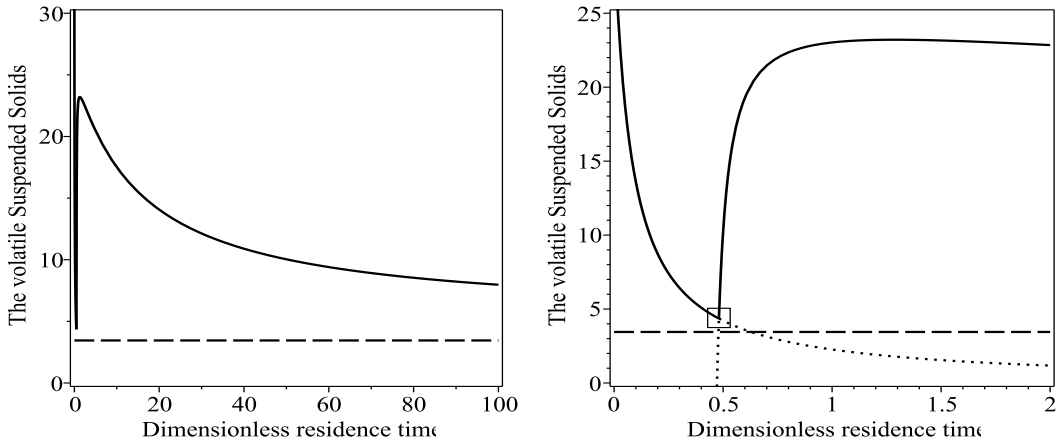

(a) $0 \leq \tau^* \leq 100$ (b) $0 \leq \tau^* \leq 5$

Figure 4.6: Steady state diagram for the volatile suspended solids (case five). Parameter value $R^* = 0.6, \tau^*_{\text{cr}} = 0.4808$. The horizontal line denotes the target value of the volatile suspended solids. The square denotes the critical value for the residence time when the washout solution becomes unstable. The solid and dotted lines represent stable and unstable solutions respectively. Case five response digram.

4.5 Discussion ($R^* \neq 0$)

In this section we investigate the effect of the effective recycle parameter upon the performance of the reactor.

4.5.1 The chemical oxygen demand

Figure 4.7(a) shows how the value of the residence time required to achieve a chemical oxygen demand efficiency of 10% ($E^*_{\text{COD}} = 0.90$) as a function of the value of the effective recycle parameter. The value of the residence time (τ^*) increases by 42.47 % from 3.6291, when there is no recycle ($R^* = 0$), to 5.1702, when the effective recycle parameter takes its maximum value ($R^* = 1$).

The figure shows that there is a critical value of the effective recycle ratio (R^*_{cr}). If the effective recycle ratio is smaller than the critical value ($R^* < R^*_{\text{cr}}$) then the value of the residence time is a decreasing function of the effective recycle ratio $\left(\frac{d\tau^*}{dR^*} < 0\right)$.

If the effective recycle ratio is larger than the critical value ($R^* > R^*_{\text{cr}}$) then the value of the residence time is an increasing function of the effective recycle ratio $\left(\frac{d\tau^*}{dR^*} > 0\right)$ which is unexpected behavior. Therefore increasing the effective recycle ratio is not always reduce the chemical oxygen demand.

Figure 4.7(b) shows how the value of the residence time required to achieve the chemical oxygen demand efficiency of 1% ($E^*_{\text{COD}} = 0.99$) as a function of the value of the effective recycle parameter. The value of the residence time(τ^*) decreases by 11.05 % from 192.0100, when there is no recycle ($R^* = 0$), to 170.7909, when the effective recycle parameter takes its maximum value ($R^* = 1$). Note the value of the residence time is always a decreasing function of the effective recycle ratio $\left(\frac{d\tau^*}{dR^*} < 0\right)$. In both cases the use of a settling unit has the potential to decrease the residence time.

Note that the limiting value $R^* = 1$ is not physically meaningful because the volatile suspended solids approaches infinity, equation (4.39), even though the chemical oxygen demand is finite.

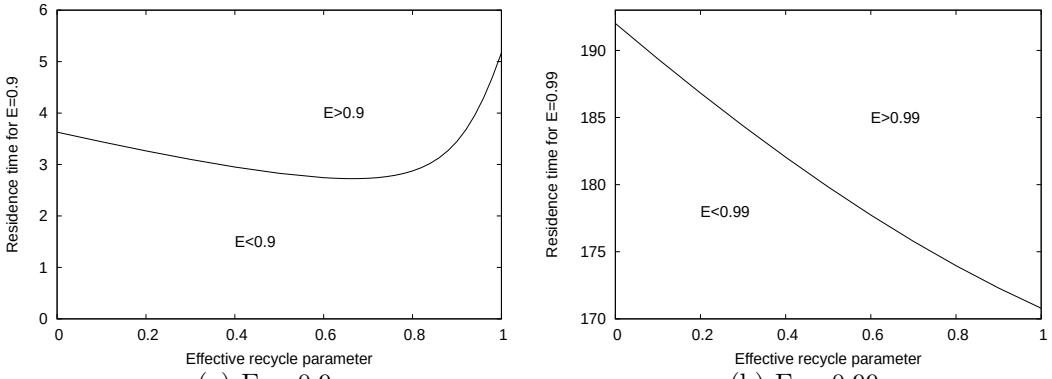

(a) E = 0.9 (b) E = 0.99

Figure 4.7: The residence time required to achieve the chemical oxygen demand efficiency $E = 0.9$ and $E = 0.99$ as a function of the effective recycle parameter (R^*).

4.5.2 The volatile suspended solids

In this section we explore in greater detail the effect of the effective recycle parameter (R^*) upon the value of the residence time at when the volatile suspended solids concentration is equal to the target value.

4.5.2.1 Intersection points on the washout branch

We start by noting that the value of the residence time when the target value is reached on the washout branch is given by equation (4.70). The value of the residence time given by this equation is physically meaningful if the target value is lower than the maximum value along the washout branch, which is found by substituting $\tau^* = 0$ into equation (4.68), and greater than the value at the washout branch, which is found by substituting $\tau^* = \tau^*_{\text{cr}}$ in equation (4.68). It is not physically meaningful when the intersection point is either negative or larger than the washout value.

4.5.2.2 Intersection point on the no-washout branch

We now investigate when there is an intersection point along the no-washout branch. This happens when

$$\begin{aligned}\text{VSS}^*_{\text{nw}} = &\left(1 + \frac{f_p k_d^* \tau^*}{1 - R^*} + \frac{(1 - f_p) k_d^* \tau^*}{1 - R^* + k_h^* \tau^*}\right) X^*_{\text{b,nw}} + \frac{X^*_{s,0}}{1 - R^* + k_h^* \tau^*} + \frac{X^*_{p,0}}{1 - R^*} \\ &+ \frac{X^*_{i,0}}{1 - R^*} = \text{VSS}^*_{\text{t}},\end{aligned} \tag{4.71}$$

Rearranging equation (4.71) and using equations (4.26) and (4.33) to substitute for the biomass concentration (X^*_b) the intersection point is found to solve a cubic equation of the residence time

$$a_{\text{VSS}} \tau^{*3} + b_{\text{VSS}} \tau^{*2} + c_{\text{VSS}} \tau^* + d_{\text{VSS}} = 0, \tag{4.72}$$

where the coefficients are

$$a_{\mathrm{VSS}} = k_h^* k_d^* \left\{ k_d^* f_p + (1 - k_d^*) \left(\left[X_{i,0}^* + X_{p,0}^* + \mathrm{VSS}_{\mathrm{t}}^* \left(-1 + R^* \right) \right] \left[(1 - f_p)\, \alpha_g - 1 \right] \right. \right.$$

$$\left. \left. - f_p, \left[S_0^* + \alpha_g X_{s,0}^* \right] \right) \right\},$$

$$b_{\mathrm{VSS}} = (1 - R^*) \left\{ \left[\mathrm{VSS}_{\mathrm{t}}^* \left(1 - R^* \right) - X_{i,0}^* - X_{p,0}^* \right] \left\{ \left[\left\{ (1 - f_p)\, \alpha_g - 2 \right\} k_d^* + 1 \right] k_h^* \right. \right.$$

$$\left. + (1 - k_d^*)\, k_d^* \right\} + \left\{ \left[1 + S_0^* + \alpha_g X_{s,0}^* \right] (1 + f_p)\, k_d^* - S_0^* - \alpha_g X_{s,0}^* \right\} k_h^*$$

$$\left. + \left\{ \left[S_0^* + X_{s,0}^* \right] \left(-1 + k_d^* \right) + k_d^* \right\} k_d^* \right\},$$

$$c_{\mathrm{VSS}} = (1 - R^*)^2 \left\{ \left[S_0^* + X_{i,0}^* + X_{p,0}^* - \mathrm{VSS}_{\mathrm{t}}^* \left(1 - R^* \right) \right] \left(-1 + k_h^* + 2 k_d^* \right) \right.$$

$$\left. + X_{s,0}^* \left(2 k_d^* + k_h^* \alpha_g - 1 \right) + k_h^* + 2 k_d^* \right\},$$

$$d_{\mathrm{VSS}} = (1 - R^*)^3 \left\{ 1 + S_0^* + X_{i,0}^* + X_{p,0}^* + X_{s,0}^* - \mathrm{VSS}_{\mathrm{t}}^* \left(1 - R^* \right) \right\}.$$

For a given value of the effective recycle parameter, R^*, equation (4.72) is readily solved to find the corresponding values for the intersection points. These values are only physically meaningful if they are larger than the value of the residence time at the trans-critical bifurcation point (τ_{cr}^*).

Information regarding the location of all intersection points is summarized in figure 4.8. In this figure the dotted line is the critical value for the residence time (τ_{cr}^*), it is a linearly decreasing function of the effective recycle parameter-as shown by equation (4.47). The dash line is the intersection point along the washout branch equation is given by (4.70). This is only physically meaningful when it is lower than the dotted line. The solid lines are the intersection points along the no-washout branch equation, found from equation (4.72). These are only physically meaningful when they are higher than dotted line.

For example, when R^*=0 there are three physically meaningful intersection points: one on the washout branch ($\tau_{i,w}^*$=0.5080) and two on the no-washout branch ($\tau_{\mathrm{i,nw1}}^*$= 1.2336) and ($\tau_{\mathrm{i,nw2}}^*$=193.6117). The corresponding steady-state digram is shown in

figure 4.4. When R^*=0.45 there are two physically meaningful intersection points, one along the washout branch and two intersection points: one along the washout branch ($\tau^*_{i,w}$=0.5981 and one along the no-washout branch $\tau^*_{\text{i,nw1}}$=0.6624). The corresponding steady-state digram is shown in figure 4.5. When R^*=0.6 there are no physically meaningful intersection points. The corresponding steady-state digram is shown in figure 4.6. Table 4.3 shows all the intersection points, including the physically non-meaningful points. Observe that in figure 4.8(b) a solution asymptotes to the value $\tau^*_{\text{i,nw}} = \infty$ as the effective recycle parameter approaches the value $R^*_{3,6}$=0.3890 from below. This corresponds to the transition from case three to case six. In figure 4.8(a) the value for the intersection point along the washout branch is equal to the value of the residence time at the washout point when the effective recycle parameter is 0.4949. This corresponds to the transition from case six to case five.

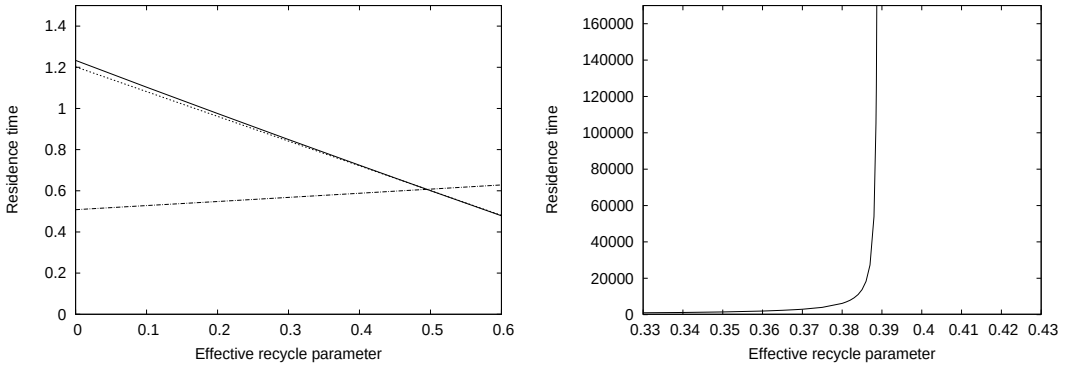

(a) $0 \leq R^* \leq 0.6$ (b) $0 \leq R^* \leq 0.4$

Figure 4.8: The values of the residence time where the the volatile suspended solids concentration is equal to the target value as a function of the effective recycle parameter. The dotted line is the critical value for the residence time, the dash line is the intersection point along the washout branch and the solid line is the intersection point along the no-washout branch equation.

4.5.2.3 The transition from case three to case six ($R^*_{3,6}$=0.3890).

As discussed in the previous section case three (figure 4.4) happens when there are three intersection points, one along the washout branch and two along the no-

R^*	τ^*_{cr}	$\tau^*_{i,w}$	$\tau^*_{\text{i,nw}}$
0	1.2020	0.5080	1.2336, 193.6117, -0.300
0.45	0.6611	0.5981	0.6624, -0.1559, -836.0853
0.60	0.4808	0.6283	0.4788, -0.1116, -186.7135

Table 4.3: Different values of the effective recycle parameter, value of the critical value of the residence time and the intersection points along the washout and the no-washout branch.

washout branch. Case six (figure 4.5) happens when there are two intersection points: one along the washout branch and one along the no-washout branch.

The transition from case three to case six occurs when the target value is equal to the asymptotic value of the volatile suspended solids in the limit as the residence time approaches infinity. In table 4.2 we stated that this transition occurred when $R^*_{3,6} = 0.3890$. This transition is shown graphically in figure 4.8(b) as the vertical asymptote.

Figure 4.8(a) also shows that when the effective recycle parameter is larger than the critical value $R^*_{3,6} = 0.3890$ and lower than the value $R^*_{6,5}$=04949, there are two physically meaningful intersection points: one on the washout branch and one on the no-washout branch.

Setting the leading term of the asymptotic solution for the volatile suspended solids at large residence time (4.62) equal to the target value we find that

$$R^*_{3,6} = \frac{\text{VSS}^*_{\text{t}} - X^*_{i,0} - f_p k^*_d a_0}{\text{VSS}^*_{\text{t}}} = 0.3890, \tag{4.73}$$

where the coefficient a_0 is given by equation (4.66).

When the effective recycle parameter is smaller than this value ($R^* < R^*_{3,6}$) then the asymptotic value of the volatile suspended solids is below the target value $\text{VSS}^*(\tau^* = \infty) < \text{VSS}^*_{\text{t}}$. In this case there are three intersection points: one along the washout branch and two along the no-washout branch.

When the effective recycle parameter is larger than the critical value ($R^* > R^*_{3,6}$) then the asymptotic value of the volatile suspended solids is larger than the target

value $\mathrm{VSS}^*(\tau^* = \infty) > \mathrm{VSS}^*_{\mathrm{t}}$. In this case there are two intersection points (provided that $R^*_{3,6} < R^* < R^*_{6,5}$): one along the washout branch and one along the no-washout branch.

For case six the volatile suspended solids is always larger than the target value when the value of the residence time is larger than the single intersection point on the no-washout branch.

4.5.2.4 The transition from case six to case five ($R^*_{6,5}$=0.4949).

Case six (figure 4.5) happens when there are two intersection points, one along the washout branch and one along the no-washout branch. Case five (figure 4.6) happens when there are no intersection points. The transition occurs when the value of the volatile suspended solids at the trans-critical bifurcation is equal to the target value ($\mathrm{VSS}^*(\tau^*_{\mathrm{cr}}) = \mathrm{VSS}^*_t$).

Note that from equation (4.47) the value of the residence time at the trans-critical bifurcation is a linearly decreasing function of the effective recycle parameter ($\frac{d\tau^*_+}{dR^*} < 0$). It has a minimum value 0 when $R^* = 1$.

Figure 4.8(a) shows the volatile suspended solids concentration at the trans-critical bifurcation as a function of of the effective recycle parameter. When the effective recycle ratio is sufficiently small (large) the value of the volatile suspended solids at the intersection point is below (above) the critical value. The intersection point at $R^* = R^*_{6,5} \approx 0.4949$ denotes the transition from case six to case five. This intersection point is shown in figure 4.9.

From (4.47) the value of the residence time at the trans-critical bifurcation is given by

$$\tau^*_+ = (1 - R^*)\tau^*_{\mathrm{cr}}(R^* = 0), \tag{4.74}$$

where

$$\tau^*_{\text{cr}}(R^* = 0) = \frac{b^* + \sqrt{b^{*2} + 4ac^*}}{2a},$$

$$a = [(S^*_0 + \alpha_g X^*_{s,0}) - (1 + S^*_0 + \alpha_g X^*_{s,0})k^*_d]k^*_h,$$
$$b^* = (1 + S^*_0)(k^*_h + k^*_d) + k^*_h \alpha_g X^*_{s,0} - S^*_0,$$
$$c^* = (1 + S^*_0).$$

To draw figure 4.9, we fixed the value for the effective recycle parameter and then calculated the value of the trans-critical bifurcation using equation (4.74). This value is then substituted into equation (4.68) to determine the corresponding value for the volatile suspended solids.

Equating equation (4.68) to the target value and using equation (4.74) we find that

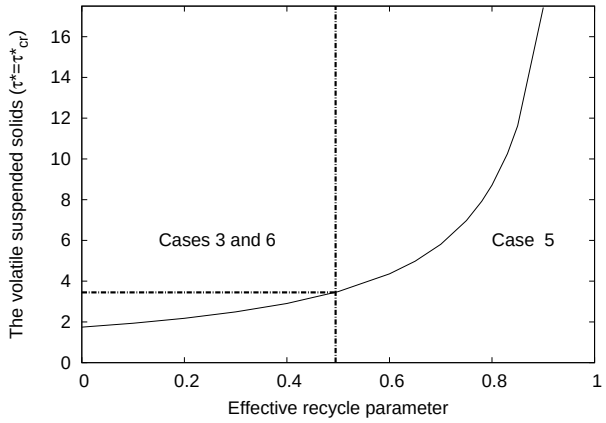

Figure 4.9: The volatile suspended solids concentration at the trans-critical bifurcation as a function of of the effective recycle parameter (R^*). When $R^* = R^*_{6,5} = 0..4949$, the volatile suspended solids is equal to the the target value ($\text{VSS}^*_t = 3.4510$).

the transition happens when

$$
\begin{aligned}
&(1 - R^*_{6,5}) \left\{ \mathrm{VSS}^*_t (1 - R^*_{6,5}) \left[1 + k^*_h \tau^*_{\mathrm{cr}} (R^* = 0) \right] - (X^*_{i,0} + X^*_{p,0})^2 \left[1 + k^*_h \tau^*_{\mathrm{cr}} (R^* = 0) \right] \right. \\
&\quad \left. + X^*_{s,0} \right\} = 0, \\
&\Rightarrow R^*_{6,5} = 1 \quad \text{or} \\
&\Rightarrow R^*_{6,5} = \frac{(\mathrm{VSS}^*_t - (X^*_{i,0} + X^*_{p,0})^2) \left[1 + k^*_h \tau^*_{\mathrm{cr}} (R^* = 0) \right] + X^*_{s,0}}{\mathrm{VSS}^*_t \left[1 + k^*_h \tau^*_{\mathrm{cr}} (R^* = 0) \right]} = 0.4949.
\end{aligned}
$$

Note that the solution $R^*_{6,5} = 1$ is invalid because equation (4.68) is not defined for this value.

If the effective recycle parameter is smaller than the critical value of the effective recycle parameter ($R^* < R^*_{6,5}$) then the volatile suspended solids at the trans-critical bifurcation is smaller than the target value. If $R^*_{3,6} < R^* < R^*_{6,5}$ there are two intersection points one on the washout branch and one on the no-washout branch. The volatile suspended solids steady-state diagram will be either case six or case three if $R^* < R^*_{3,6}$. If the effective recycle parameter is larger than the critical value ($R^* > R^*_{6,5}$) then the volatile suspended solids at the trans-critical bifurcation is larger than the target value. There are no intersection points.

4.5.2.5 Summary of transitions

Figure 4.8 shows graphically where the transitions from case three to case six and from case six to case five occur. Figure 4.8(b) shows the transition points from case three six when ($R^*_{3,6}$=0.3890). Figure 4.8(a) shows the transition from case six to case five when ($R^*_{6,5}$=0.4949).

4.5.2.6 The effect of partitioning the chemical oxygen demand

In section 4.5.2.4 we fond that if ($R^*_{3,6} < R^* < R^*_{6,5}$) then the volatile suspended solids at infinity is larger than the target value. Therefore there is one physically meaningful intersection point on the no-washout branch.

If ($R^*_{6,5}$<R^*) then the volatile suspended solids at infinity is larger than the target value. Therefore there is no physically meaningful intersection point on the no-washout branch. Case six is undesirable because for realistic value of the residence time the volatile suspended solids is larger than the target value.

Suppose that the chemical oxygen demand in the feed stream is fixed. Does the critical value of the effective recycle parameter for the transition from case three to case six $R^*_{3,6}$ depend upon how the chemical oxygen demand is partitioned into the components S^*_0 and $X^*_{s,0}$? Examining equation (4.66) and (4.73) we see that the critical value of the effective recycle parameter *only* depends upon the total chemical oxygen demand in the influent, not on the individual components (S^*_0 and $X^*_{s,0}$). This result make sense because at large residence time almost all of the insoluble substrate is converted to the soluble substrate, equation (4.35).

Substituting equation (4.66) for the coefficient a_0 into equation (4.73). We have

$$R^*_{3,6} = \frac{\mathrm{VSS}^*_{\mathrm{t}} - X^*_{i,0}}{\mathrm{VSS}^*_{\mathrm{t}}} - \frac{f_p k^*_d \mathrm{COD}^*_{\mathrm{in}}(1-k^*_d) - k^*_d}{\mathrm{VSS}^*_{\mathrm{t}} k^*_d (1-k^*_d)(1-(1-f_p)\alpha_g)} = 0.3890. \tag{4.75}$$

Clearly the transition value $R^*_{3,6}$ is a decreasing function of the chemical oxygen demand. We have $\mathrm{COD}^*_{\mathrm{in}}(R^*_{3,6}=0)$ =16.6164. Thus if the chemical oxygen demand in the feed is larger than 16.6164 then case three can never occur. We only get case six and case five which are undesirable. Figure 4.10 shows that the effective recycle parameter $R^*_{3,6}$ is a decreasing function of the chemical oxygen demand in the feed. Case three occurs when the chemical oxygen demand in the feed is lower than the line. Case five happens when the chemical oxygen demand in the feed is higher than the line.

If the wastewater is sufficiently polluted then it is impossible in practice to reduce the volatile suspended solids below the target value.

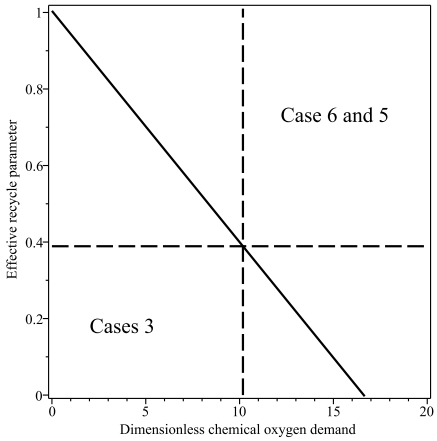

Figure 4.10: The effective recycle parameter $R^*_{3,6}$ as a function of the chemical oxygen demand $\mathrm{COD_{in}}$.

4.5.2.7 Model simplification

If we assume that there is no inert material flowing in ($X^*_{i,0} = 0$), which is a common assumption in mathematical modeling, then from equation (4.73) we have

$$R^*_{3,6} = \frac{\mathrm{VSS}^*_{\mathrm{t}} - f_p k^*_d a_0}{\mathrm{VSS}^*_{\mathrm{t}}} = 0.3893. \tag{4.76}$$

Even if no inert material flows into the reactor it is generated inside the reactor by the decay of biomass.

For the default parameter values the assumption that there is no inert material flowing in has negligible effect on the value of the effective recycle parameter in the transition from case six to three equation, if we compare equation(4.75) with equation (4.76) we can see that the difference is only in the fourth decimal place.

If there is no inert material in the feed then the value of the chemical oxygen demand in the feed at which the effective recycle parameter in the transition from case three to case six is zero is $\mathrm{COD}^*_{\mathrm{in}}(R^*_{3,6} = 0, X^*_{i,0} = 0)$ =16.6207.

The value for the default values was $\mathrm{COD}^*_{\mathrm{in}}(R^*_{3,6} = 0, X^*_{i,0} = 0.0009)$ =16.6164. The effect of the inert material in the feed is again negligible.

Note that in the basic model the degradation products from biomass decay are ignored. This corresponds to setting ($f_p = 0$). In this case ($R^*_{3,6} = 1$).

4.5.2.8 The effect of changing the chemical oxygen demand in the feed

In the previous two sections we investigate the effect of changing the effective recycle ratio (R^*) whilst the value for the chemical oxygen demand in the feed (COD^*_{in}) was fixed. In this section we change the value of the chemical oxygen demand in the feed (COD^*_{in}) to investigate how this effects the behavior. We write

$$S^*_0 = AS^*_{0,\text{old}},$$
$$X^*_{s,0} = AX^*_{\text{s,0,old}},$$

$$\text{COD}^*_{\text{in}} = A\text{COD}^*_{\text{in,old}}, \tag{4.77}$$

where $S^*_{0,\text{old}}$ and $X^*_{\text{s,0,old}}$ are the values for the soluble and insoluble substrate used in the previous section i.e. $S^*_{0,\text{old}}$=1.9961 and $X^*_{\text{s,0,old}}$=12.2133. The value of A is $0<A\leq 1$. We first note that as the chemical oxygen demand in the feed (COD^*_{in}) is decreased there is a critical value below which the washout branch is stable for all values of the residence time.

To find this critical value we substitute equation equation (4.77) into equation (4.51) and rearrange to obtain

$$A_{\text{cr}} = \frac{1}{\text{COD}^*_{\text{in,old}}}\left(\frac{k^*_d}{1-k^*_d}\right) = 0.0072.$$

This means that if $\text{COD}^*_{\text{in}} \leq A_{\text{cr}}\text{COD}^*_{\text{in,old}}$=0.0072(0.9105)=0.0066 then process failure occurs. We now investigate where the different volatile suspended solids steady-state solution digrams occur as a function as the effective recycle ratio (R^*) and the value of the chemical oxygen demand in the feed (though the parameter A).

The dotted vertical line in figure 4.11 represents the value A_{cr}, below which process failure automatically occurs. Line 1 in figure 4.11 shows where the volatile suspended solids on the washout branch at zero residence time is equal to the target

value of the volatile suspended solids ($\text{VSS}^*_{\text{w}}(\tau^* = 0) = \text{VSS}^*_{\text{t}}$). The line marks the transition from case one, where there are no intersection points and the volatile suspended solids is smaller than the target value as shown in figure 4.12(a), to case two, where there is one intersection point along the washout branch as shown in figure 4.12(b).

Using equation (4.32) when the residence time is zero we obtain the formula for the transition from case one to case two:

$$A_{12} = \frac{\text{VSS}^*_{\text{t}}(1 - R^*) - X^*_{i,0}}{X^*_{\text{s},0,\text{old}}}.$$

Line 2 in figure 4.11 shows the transition where the target value of the volatile suspended solids is equal to the maximum value of the volatile suspended solids along the no-washout branch ($\text{VSS}^*_{\text{nw}} = \text{VSS}^*_{\text{t}}$). The line marks the transition from case two, where there is one intersection point along the washout branch, as shown in figure 4.12(b), to case three, where there are three intersection points; one along the washout branch and two along the no-washout branch as shown in figure 4.12(c). To find this transition, A_{23}, we write $G = \text{VSS}^*_{\text{nw}} - \text{VSS}^*_{\text{t}}$ and solve the system of equation $G = 0$ and $\frac{dG}{d\tau^*}$=0.

Line 3 in figure 4.11 shows the transition where the volatile suspended solids along the no-washout branch at infinite residence time is equal to the target value of the volatile suspended solids ($\text{VSS}^*_{\text{nw}}(\tau^* = \infty) = \text{VSS}^*_{\text{t}}$). This line marks the transition from case three, where there are three intersection points (one along the washout and two along the no-washout branch) as shown in figure 4.12(c), to case six, where there are two intersection points one along the washout and one along the no-washout branch as shown in figure 4.12(d).

For the transition from case three to six we have

$$A_{36} = \frac{(1-k_d^*)[(1-R^*)\mathrm{VSS}_{\mathrm{t}}^* - X_{i,0}^*]\{1-\alpha_g(1-f_p)\} + f_p k_d^*}{f_p(1-k_d^*)[S_0^* + \alpha_g X_{s,0}^*]}.$$

Line 4 in figure 4.11 shows the transition where the volatile suspended solids along the no-washout branch at the critical value of the residence time is equal to the target value of the volatile suspended solids ($\mathrm{VSS}_{\mathrm{nw}}^*(\tau^* = \tau_{\mathrm{cr}}^*) = \mathrm{VSS}_{\mathrm{t}}^*$). The line marks the transition from case six, where there are two intersection points one along the washout and one along the no-washout branch as shown in figure 4.12(d), to case five, where there is no intersection point as shown in figure 4.12(e).

For the transition from case six to five we have

$$A_{65} = \frac{[\mathrm{VSS}_{\mathrm{t}}^* - X_{i,0}^*]\{1 + k_h^* \tau_{\mathrm{cr}}^*(R^* = 0)\}}{X_{s,0}^*},$$

where $\tau_{\mathrm{cr}}^*(R^* = 0)$ is defined in (4.48). For $R^* = 0$ we have A_{65}=1.8946.

In practice only regions one and two are acceptable.

In region three the volatile suspended solids along the no-washout branch is below the target value if the residence time is larger than the highest intersection point. In theory this looks desirable, but the value of the residence time at the intersection point is too high for it be practical.

In region the volatile suspended solids along the no-washout branch is below the target value when the residence time is larger than the trans-critical bifurcation and smaller than the highest intersection point. The value of the chemical oxygen demand in this region is very high, so this region is not of practical interest.

In region five the volatile suspended solids along the no-washout branch is above the target value. Therefore, the volatile suspended solids along the no-washout branch is always above the target value.

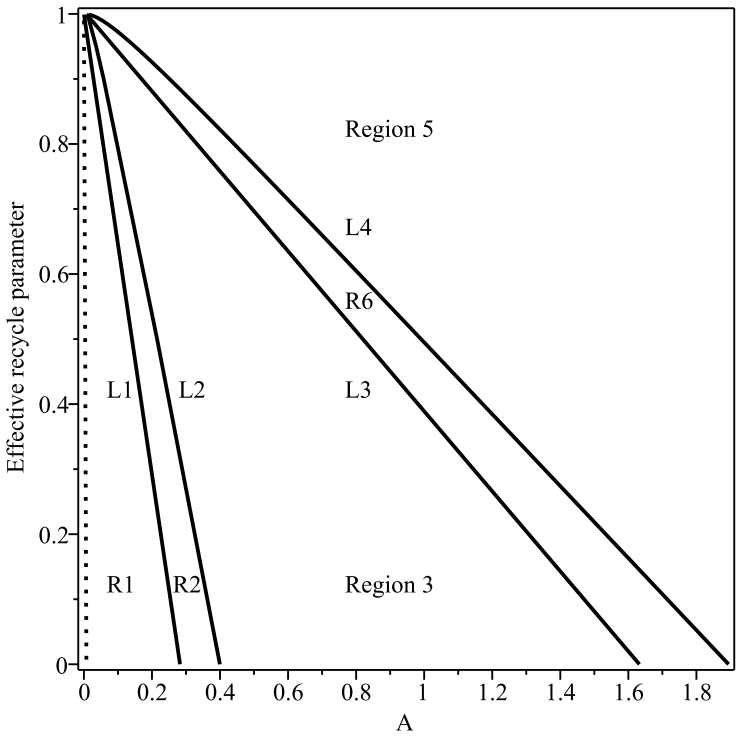

Figure 4.11: The location of the volatile suspended solids steady-state digrams in the effective recycle Parameter chemical oxygen demand parameter plane, where $\mathrm{COD}^*_{\mathrm{in}} = A\mathrm{COD}^*_{\mathrm{in,old}}$. The dotted line represent the minimum value A=0.0072.

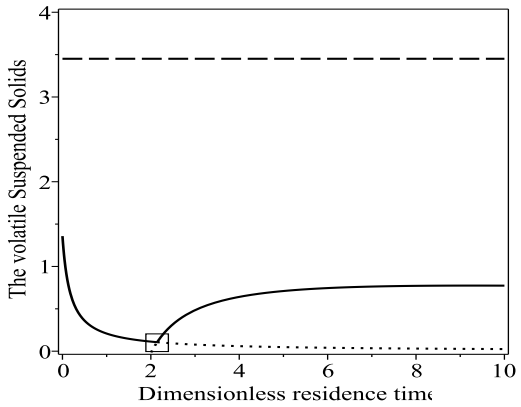

(a) Case one. Parameter values: R^*=0.1 and A=0.1.

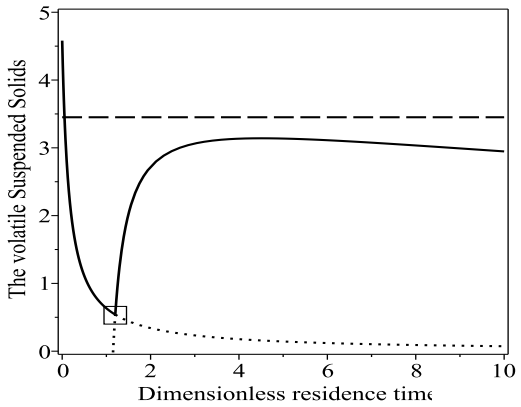

(b) Case two. Parameter values: R^*=0.2 and A=0.3.

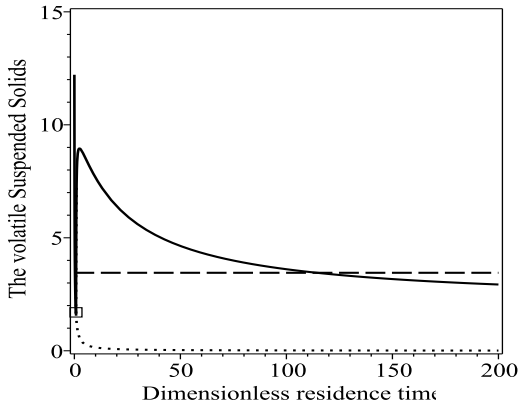

(c) Case three. Parameter values: R^*=0.4 and A=0.6.

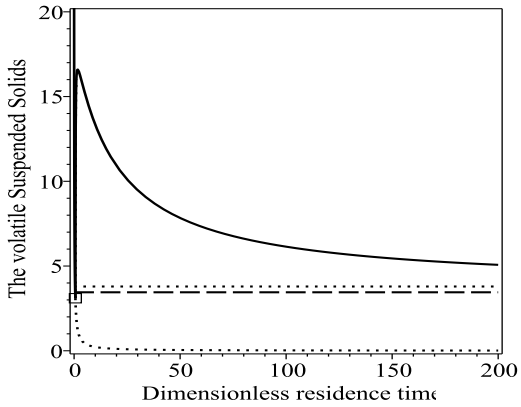

(d) Case four. Parameter values: R^*=0.5 and A=0.9.

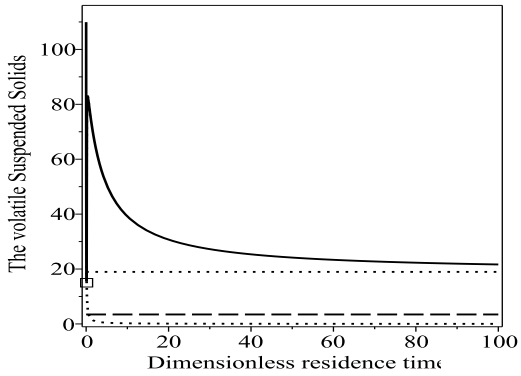

(e) Case five. Parameter values: R^*=0.9 and A=0.9.

Figure 4.12: Steady-state diagrams showing the volatile suspended solids as a function of the dimensionless residence time (τ^*). The box denotes the location of the trans-critical bifurcation. The solid and dotted lines represent stable and unstable solutions respectively.The horizontal dash line denotes the target value of the volatile suspended solids and the horizontal dotted line denotes the asymptotic value.

4.6 Conclusion

In this chapter we made a seemingly minor modification to the model investigated in chapter 2.

In this chapter when the biomass dies it gives non-biodegradable particulates and *slowly biodegradable* substrate, whereas in chapter 2 when the biomass dies it gives inert material and *soluble* substrate.

Initially we established some general mathematical results. Firstly, we reduced the model from four equations to three equations. Secondly, we showed that the solutions are always positive.

The washout branch corresponds to process failure and has to be avoided. We showed that if the decay rate is sufficiently high ($k_d^* \geq 1$), then the biomass must die out ($X_b^*(t^*) \to 0$), which means that the washout solution is globally asymptoticly stable.

We found two steady state solutions corresponding to washout and no-washout branches. We established conditions under which the solutions are positive.

For practical applications we can assume that (k_d^*<1). In appendix C.3.4 we proved that the no-washout branch is only physically meaningful when the decay coefficient is sufficiently small

$$k_d^* < k_{\mathrm{d,cr}}^* = \frac{S_0^* + \alpha_{g,h} X_{s,0}^*}{S_0^* + \alpha_{g,h} X_{s,0}^* + 1} = \frac{\mathrm{COD}_{\mathrm{in}}^*}{1 + \mathrm{COD}_{\mathrm{in}}^*} < 1,$$

and the residence time is sufficiently large

$$\tau^* > \tau_+^* = (1 - R^*) \left[\frac{b_2^* + \sqrt{b_2^{*2} + 4 a_2 c_2^*}}{2 a_2} \right] > 0.$$

When the no-washout branch is not physically meaningful, we showed the washout solution is locally stable. We showed that when the no-washout branch is physically meaningful then it is locally stable and the washout branch is not stable.

We found asymptotic solutions for large residence times. We showed that for high values of the residence time ($\tau^* \gg 1$), the steady state effluent concentration can not be reduced below a limiting value ($S^* = k_d^*/(1 + k_d^*)$). This is identical to the basic model and our model in chapter 2.

When we investigated the volatile suspended solids as a function of the residence time, for different values of the effective recycle ratio, we found that there are three generic cases. In case three it is possible to ensure that the suspended solids are below the target value by operating at sufficiently high residence times. However, the required minimum value of the residence time is too large; the activated sludge process in practice is operated at residence time for below these.

In case six it is only possible to ensure that the suspended solids are below the target value by operating the reactor in a very restrictive range of residence times. Over this range there is effectively no removal of chemical oxygen demand. Thus this scenario is not of practical interest.

In case five for any value of the residence time the volatile suspended solids are always above the target value.

In the biochemistry there is a *minor* change between this chapter and chapter 2. However, this simple change has significant practical consequences. In chapter 2 if the effective recycle parameter is smaller than the effective recycle parameter in the transition from case four to three then the response digram is desirable. In this chapter it does not matter what the value for the effective recycle parameter is: in *practice* the volatile suspended solids is always higher than the target value. This means that a sludge reduction mechanism, such as a disintegration unit, is essential to ensure desirable behavior.

Some of the results from this chapter have been published in a refereed conference proceeding [6]. There were five hundred papers presented at this conference. We were one of a handful of presenters invited to submit a paper to a special issue of a journal [5].

Chapter 5

Reducing sludge formation by increasing biomass biodegradability

5.1 The effect of changing the decay coefficient

In chapter 3 we investigated the model from chapter 2 with the addition of a sludge disintegration unit which kills the biomass. In this chapter we see what happens if we increase the biomass decay coefficient inside the main reactor, does this improve performance? Thus we investigate how changing the value of the biomass decay coefficient (k_d^*) effects both the chemical oxygen demand and the sludge formation within a bioreactor. We write

$$S_0^* = AS_{0,\text{old}}^*,$$
$$X_{s,0}^* = AX_{\text{s,0,old}}^*,$$

where $S_{0,\text{old}}^*$ and $X_{\text{s,0,old}}^*$ are the default values for the soluble and insoluble substrate. The value of A is $0<A \leq 1$.

5.2 Model one

For the model in chapter 2 we have $S^*_{0,\text{old}}$=1.9961 and $X^*_{\text{s},0,\text{old}}$=145.0857.

5.2.1 The chemical oxygen demand

From chapter equation (2.60) the chemical oxygen demand is given by

$$\text{COD}^*_{\text{nw}} = \frac{1 - R^* + k^*_d\tau^*}{(1 - k^*_d)\tau^* - 1 + R^*} + \frac{\alpha_{g,h}AX^*_{\text{s},0,\text{old}}}{1 - R^* + k^*_h\tau^*}. \tag{5.1}$$

We have

$$\frac{d\text{COD}^*_{\text{nw}}}{dk^*_d} = \frac{\tau^{*2}}{[(1 - k^*_d)\tau^* - 1 + R^*]^2} > 0.$$

Thus increasing the decay coefficient increases the chemical oxygen demand within the bioreactor.

Figure 5.1 shows the dimensionless chemical oxygen demand as a function of the residence time for three values of the decay coefficient. As the decay coefficient increases it becomes increasingly difficult to achieve 90% removal of the chemical oxygen demand. Note that the change in the value of the trans-critical bifurcation is relatively small compared to the change in the value of residence time to remove 90% of the chemical oxygen demand. For example: when k^*_d=0.005 the dimensionless residence time required to achieve a chemical oxygen demand efficiency of 90% is 3.0119 and the dimensionless residence time at the trans-critical bifurcation point is τ^*_{cr}=1.1181, when k^*_d=0.3 the dimensionless residence time required to achieve a chemical oxygen demand efficiency of 90% is 7.0444 and the value at the trans-critical bifurcation point is τ^*_{cr}=1.6587 and when k^*_d=0.5 the dimensionless residence time required to achieve a chemical oxygen demand efficiency of 90% is 316.5 and the value at the trans-critical bifurcation point τ^*_{cr}=2.4670. The corresponding dimensional values for the residence time at 90% of the chemical oxygen demand removed are

0.6626, 1.5 and 69.6 days for k_d^*=0.005, 0.3 and 0.5 respectively.

From equation (2.80) the minimum value for the chemical oxygen demand occurs at infinite residence time and it is given by

$$\mathrm{COD}^*(\tau^* = \infty) = \frac{k_d^*}{1 - k_d^*} \quad \text{as } (0 \leq k_d^* < 1),$$

which is an increasing function of k_d^*. We can not achieve 90% of the chemical oxygen demand removal if

$$\mathrm{COD}^*(\tau^* = \infty) > 0.1A\mathrm{COD}^*_{\mathrm{in,old}}.$$

This leads to a critical value for the decay rate.

$$k^*_{\mathrm{d,critical}} = \frac{0.1A\mathrm{COD}^*_{\mathrm{in,old}}}{1 + 0.1A\mathrm{COD}^*_{\mathrm{in,old}}} = 0.5044.$$

If $k_d^* > 0.5044$ then it is impossible to achieve a chemical oxygen demand efficiency of 90%.

In conclusion, when the decay coefficient increases the chemical oxygen demand inside the bioreactor increases. For sufficiently high values of the decay coefficient it is impossible to achieve 90% chemical oxygen demand removal.

5.2.2 The volatile suspended solids

From equation (2.61) the concentration of volatile suspended solids is given by

$$\mathrm{VSS}^*_{\mathrm{nw}} = \left(1 + \frac{f_i k_d^* \tau^*}{1 - R^*}\right) X^*_{\mathrm{b,nw}} + \frac{X^*_{i,0}}{1 - R^*} + \frac{AX^*_{\mathrm{s,0,old}}}{1 - R^* + k_h^* \tau^*}, \tag{5.2}$$

where $X^*_{\mathrm{b,nw}}$ is given by (2.57).

Figure 5.2 shows how the steady state diagram for the volatile suspended solids as a function of the residence time depends upon the value of the effective recycle

parameter and the decay rate.

Line 1 in figure 5.2 shows the transition where the target value of the volatile suspended solids is equal to the maximum value of the volatile suspended solids along the no-washout branch ($\text{VSS}^*_{\text{nw}} = \text{VSS}^*_{\text{t}}$). This line marks the transition from case two, where there is one intersection point along the washout branch, as shown in figure 5.3(a), to case three, where there are three intersection points; one along the washout branch and two along the no-washout branch as shown in figure 5.3(b). To find this transition, $k^*_{d,23}$, we write $G = \text{VSS}^*_{\text{nw}} - \text{VSS}^*_{\text{t}}$ (equation (2.61)) and solve the system $G = 0$ and $\frac{dG}{d\tau^*}$=0. As this system has no analytic solution, it is solved numerically.

Line 2 in figure 5.2 shows the transition where the volatile suspended solids along the no-washout branch at the critical value of the residence time is equal to the target value of the volatile suspended solids ($\text{VSS}^*_{\text{nw}}(\tau^* = \tau^*_{\text{cr}}) = \text{VSS}^*_{\text{t}}$). This line makes the transition from case three, where there are three intersection points (one along the washout and two along the no-washout branch) as shown in figure 5.3(b), to case four, where there is one intersection point along the no-washout branch, as shown in figure 5.3(c).

To find this transition we equate equation (2.53) to the target value and set the residence time equal to the critical value, equation (2.72). After some algebra the formula for the transition from case three to four is given by:

$$k^*_{\text{d,34}} = \frac{B_{\text{m1}} + C_{\text{m1}}}{D_{\text{m1}}},$$

where

$$\begin{aligned}
B_{\mathrm{m1}} =& -\mathrm{VSS}^*_{\mathrm{t}}\left(1-R^*\right)\left\{\alpha_{g,h}AX^*_{\mathrm{s,0,old}}+k^*_h+\left\{AS^*_{\mathrm{0,old}}+\left[AX^*_{\mathrm{s,0,old}}+2X^*_{i,0}\right.\right.\right.\\
&\left.\left.\left.-\left(1-R^*\right)\mathrm{VSS}^*_{\mathrm{t}}\right]\alpha_{g,h}\right\}\left(1+k^*_h\right)\right\},\\
C_{\mathrm{m1}} =& X^*_{i,0}\left\{\alpha_{g,h}AX^*_{\mathrm{s,0,old}}+k^*_h+\left(1+k^*_h\right)\left[X^*_{i,0}\alpha_{g,h}+A\mathrm{COD}^*_{\mathrm{in,old}}\right]\right\}\\
&+A^2X^*_{\mathrm{s,0,old}}\mathrm{COD}^*_{\mathrm{in,old}},\\
D_{\mathrm{m1}} =& \left[AX^*_{\mathrm{s,0,old}}+X^*_{i,0}-\left(1-R^*\right)\mathrm{VSS}^*_{\mathrm{t}}\right]\left\{A\mathrm{COD}^*_{\mathrm{in,old}}+1+\left[X^*_{i,0}-\left(1-R^*\right)\right.\right.\\
&\left.\left.\mathrm{VSS}^*_{\mathrm{t}}\right]\alpha_{g,h}\right\}.
\end{aligned}$$

In the limiting case of perfect recycle we have

$$k^*_{\mathrm{d,34}}(R^*=1)=\frac{C_{\mathrm{m1}}}{D^*_{\mathrm{m1}}},$$

where

$$D^*_{\mathrm{m1}}=\left[AX^*_{\mathrm{s,0,old}}+X^*_{i,0}\right]\left\{A\mathrm{COD}^*_{\mathrm{in,old}}+1+X^*_{i,0}\alpha_{g,h}\right\}.$$

Line 3 in figure 5.2 shows the transition where the volatile suspended solids along the no-washout branch at infinite residence time is equal to the target value of the volatile suspended solids ($\mathrm{VSS}^*_{\mathrm{nw}}(\tau^*=\infty)=\mathrm{VSS}^*_{\mathrm{t}}$). The line marks the transition from case four, where there is one intersection point along the no-washout branch, as shown in figure 5.3(c), to case five, where there are no intersection points, as shown in figure 5.3(d). To find this transition we set equation (2.81) equal to the target value. The transition from case four to five is given by:

$$k^*_{\mathrm{d,45}}=\frac{Af_i\mathrm{COD}^*_{\mathrm{in,old}}+[(1-R^*)\mathrm{VSS}^*_{\mathrm{t}}-X^*_{i,0}](f_s\alpha_{g,s}-1)}{Af_i\mathrm{COD}^*_{\mathrm{in,old}}+[(1-R^*)\mathrm{VSS}^*_{\mathrm{t}}-X^*_{i,0}](f_s\alpha_{g,s}-1)+f_i}. \tag{5.3}$$

Figure 5.4(a) shows a blow up of figure 5.2 showing that lines 2 and 3 intersect twice. The intersection points are where k^*_{d}=0.9105 and R^*=0.7658, for the first intersection

point, and where k_{d}^{*}=0.9193 and R^{*}=0.7691, for the second intersection point. This leads to the formation of a new steady-state digram (figure 5.5). However, this steady state digram is not of physical interest because the washout branch is always stable for the given values of the decay rate and the effective recycle parameter. From equation (2.47) when (A=1) there is a critical value of the decay coefficient (k_d^*) above which the biomass die out.

$$k_{\mathrm{d,cr2}}^{*} = \frac{A\mathrm{COD}_{\mathrm{in,old}}^{*}}{1 + A\mathrm{COD}_{\mathrm{in,old}}^{*}} = 0.9105 \leq k_d^{*} < k_{\mathrm{d,cr3}}^{*} = \frac{AS_{0,\mathrm{old}}^{*}}{(1 + AS_{0,\mathrm{old}}^{*}) f_s \alpha_{g,s}} = 19.5488.$$

When (A=0.5) we have

$$k_{\mathrm{d,cr2}}^{*} = \frac{A\mathrm{COD}_{\mathrm{in,old}}^{*}}{1 + A\mathrm{COD}_{\mathrm{in,old}}^{*}} = 0.8358 \leq k_d^{*} < k_{\mathrm{d,cr3}}^{*} = \frac{AS_{0,\mathrm{old}}^{*}}{(1 + AS_{0,\mathrm{old}}^{*}) f_s \alpha_{g,s}} = 14.6567.$$

When (A=0.1) we have

$$k_{\mathrm{d,cr2}}^{*} = \frac{A\mathrm{COD}_{\mathrm{in,old}}^{*}}{1 + A\mathrm{COD}_{\mathrm{in,old}}^{*}} = 0.5044 \leq k_d^{*} < k_{\mathrm{d,cr3}}^{*} = \frac{AS_{0,\mathrm{old}}^{*}}{(1 + AS_{0,\mathrm{old}}^{*}) f_s \alpha_{g,s}} = 4.8823.$$

Figure 5.4(b) shows the location of the critical value for the decay rate coincide with the first intersection point. The region of parameter space to the right of this line is not of interest.

Figure 5.6 revises figure 5.2 to include the critical value of the decay coefficient, if the decay coefficient is larger than the critical value then the washout solution is globally stable i.e. the biomass die out which leads to process failure.

In figure 5.6 case two is desirable because the volatile suspended solids is above the target value for all values of the residence time above the critical value, however this case does not occur in practice. In both cases three and four there exists a critical value of the residence time, if the residence time is above this critical value then the volatile suspended solids is below the target value. These cases are good because the critical value is small. However, once again these cases do not occur in practice.

In practice the transition from case four to five, $k^*_{\mathrm{d},45}$, is the transition of interest i.e. line 3.

Figure 5.7 shows the location of line 3 as a function of the value for A, the washout solution is globally stable if the decay rate is larger than the value at the circles. Rearranging equation (5.3) we have

$$R^*_{4,5} = \frac{\mathrm{VSS}^*_{\mathrm{t}} - X^*_{i,0} - f_i k^*_d a_{0,\mathrm{old}}}{\mathrm{VSS}^*_{\mathrm{t}}},$$

where

$$a_{0,\mathrm{old}} = \frac{AS^*_{0,\mathrm{old}}(1-k^*_d) - k^*_d + \alpha_{g,h} AX^*_{\mathrm{s},0,\mathrm{old}}(1-k^*_d)}{k^*_d(1-k^*_d)(1-f_s\alpha_{g,s})} > 0.$$

We have

$$\frac{dR^*_{4,5}}{dA} = \frac{-f_i \mathrm{COD}^*_{\mathrm{in,old}}}{\mathrm{VSS}^*_{\mathrm{t}}[1-f_s\alpha_{g,s}]} < 0,$$

and

$$\frac{dR^*_{4,5}}{dk^*_d} = \frac{f_i}{\mathrm{VSS}^*_{\mathrm{t}}[1-f_s\alpha_{g,s}](1-k^*_d)^2} > 0.$$

The former shows the more polluted the feed, the more likely we are to have case 5.

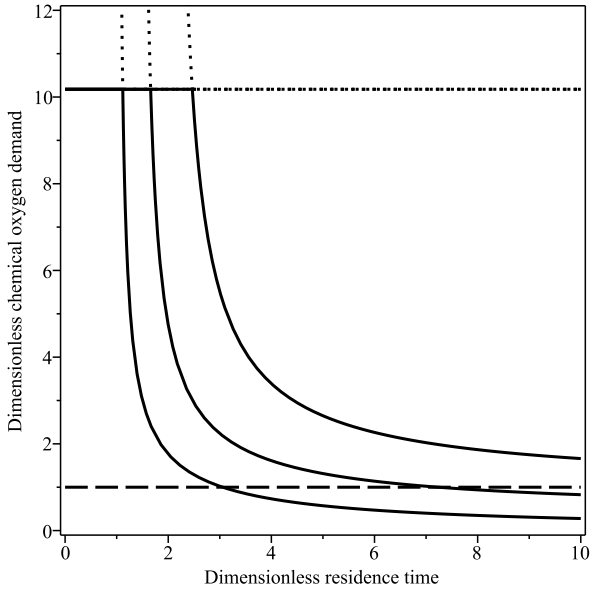

Figure 5.1: Steady state diagram for the dimensionless chemical oxygen demand. Parameter values $R^* = 0$, A=1 and k_{d}^*=0.005 (left), 0.3 and 0.5 (right) respectively. The dashed horizontal line correspond to a chemical oxygen demand removal efficiency of 90%. Model one from chapter 2.

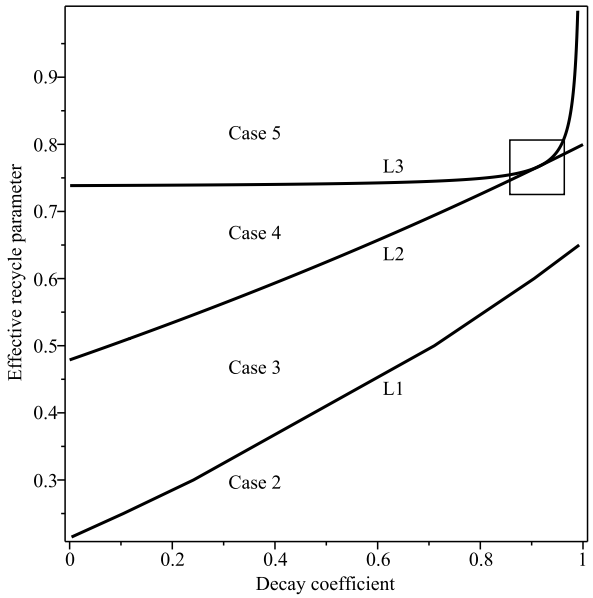

Figure 5.2: The location of the volatile suspended solids steady-state digrams in the effective recycle parameter (R^*) - decay coefficient (k_d^*) parameter plane, where A=1. The region inside the box is shown in figure 5.4.

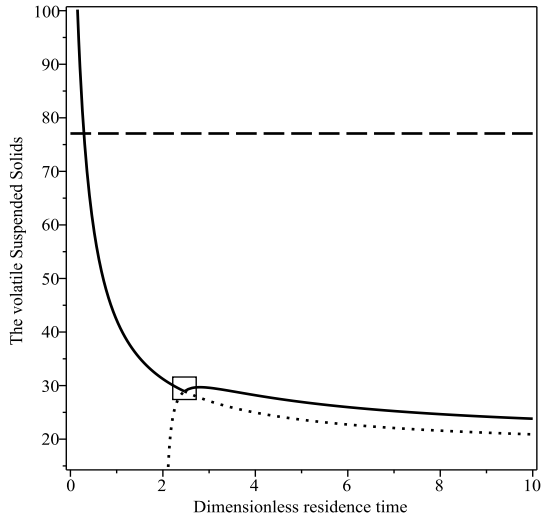

(a) Case two. Parameter values: R^*=0 and k_d^*=0.5.

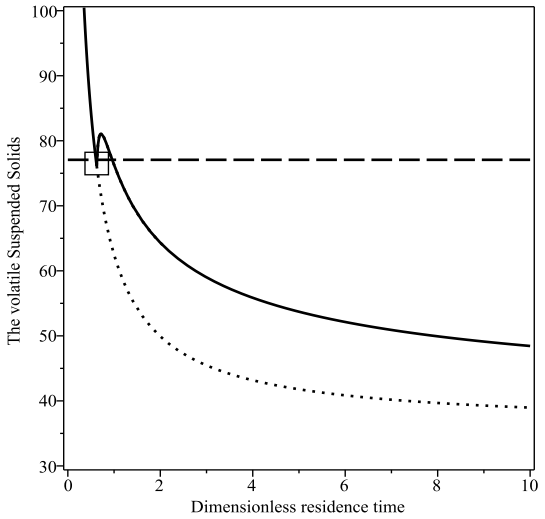

(b) Case three. Parameter values: R^*=0.5 and k_d^*=0.1.

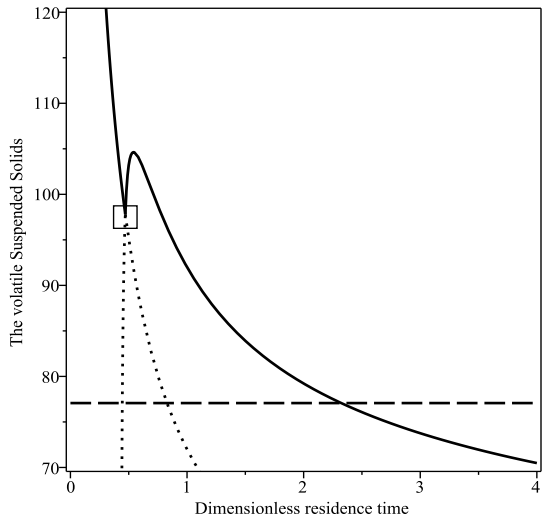

(c) Case four. Parameter values: R^*=0.6 and k_d^*=0.05.

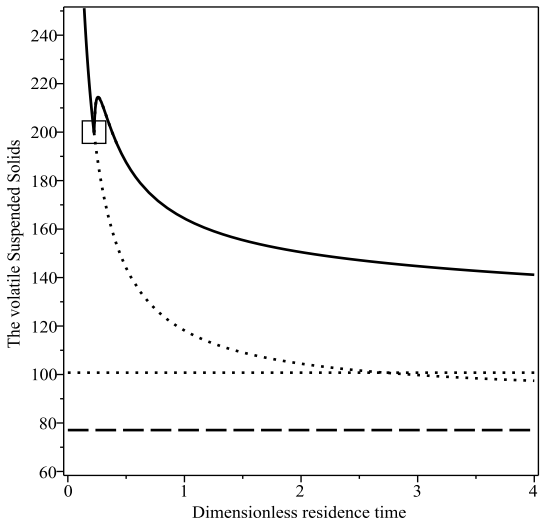

(d) Case five. Parameter values: R^*=0.8 and k_d^*=0.01.

Figure 5.3: Steady-state diagrams showing the volatile suspended solids as a function of the dimensionless residence time (τ^*). The box denotes the location of the trans-critical bifurcation. The solid and dotted lines represent stable and unstable solutions respectively.The horizontal dash line denotes the target value of the volatile suspended solids and the horizontal dotted line denotes the asymptotic value.

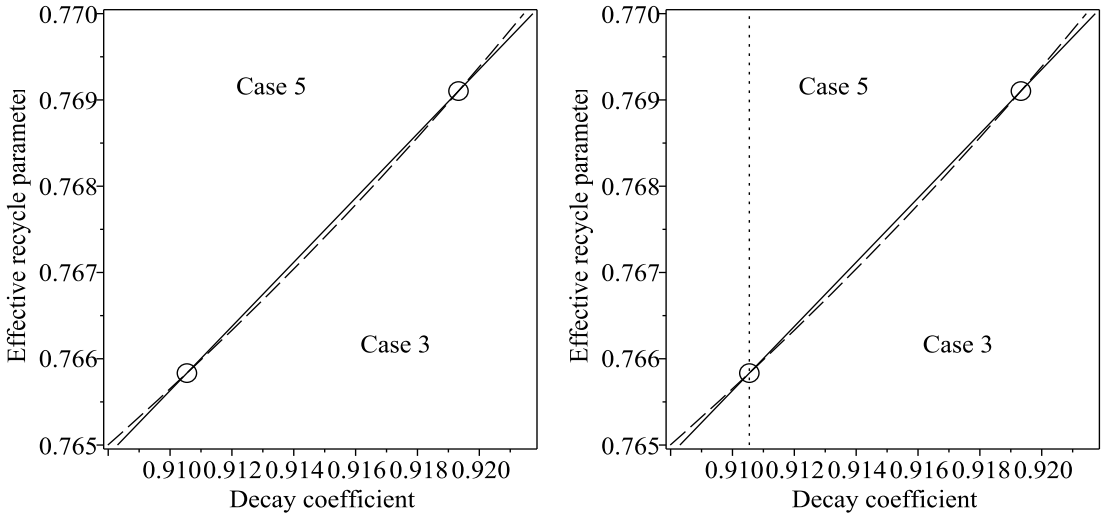

Figure 5.4: The location of the volatile suspended solids steady-state digrams in the effective recycle parameter (R^*) - decay coefficient (k_d^*) parameter plane, where A=1. The solid, dash and dotted lines represent line 2, line 3 and $k^*_{\mathrm{d,cr}}$ respectively.

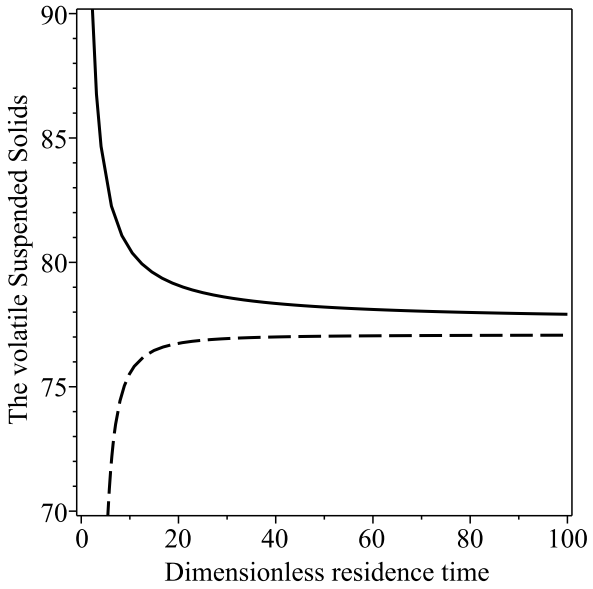

Figure 5.5: The volatile suspended solids steady-state digram as a function of the dimensionless residence time (τ^*), where k_d^*=0.9151 and R^*=0.7675. The solid and dash lines represent the the washout and no-washout branches respectively. The washout branch is always stable and the no-washout branch is always unstable.

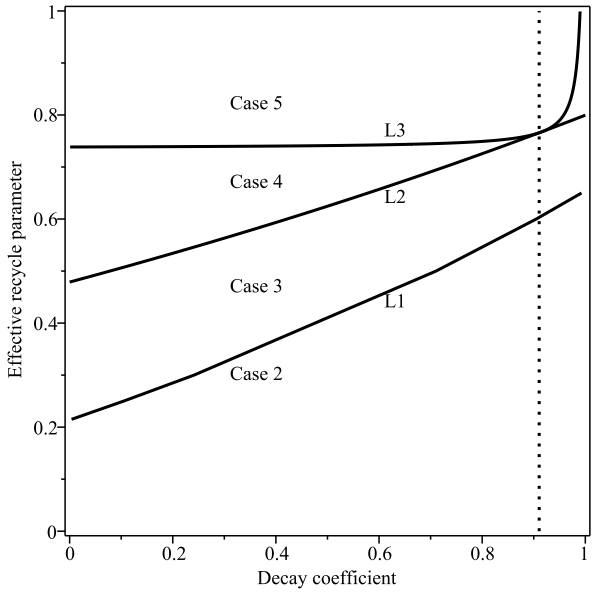

Figure 5.6: The location of the volatile suspended solids steady-state digrams in the effective recycle parameter (R^*) - decay coefficient (k_d^*) parameter plane, where A=1. The dotted vertical line shows the critical value of the decay coefficient ($k_{\mathrm{d,cr2}}^*$).

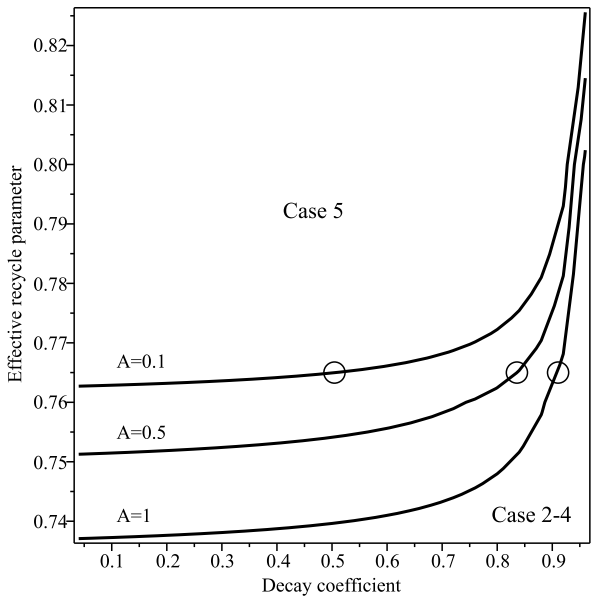

Figure 5.7: The location of line 3 (transition from case 4 to case 5) in the effective recycle parameter (R^*) - decay coefficient (k_d^*) parameter plane, where A=0.1, 0.5 and 1.

5.2.3 Conclusion

If we increase the value of the decay rate inside the bioreactor then the value of the effective recycle ratio at the transition from case 4 to case 5 increases. However, as shown in figure 5.6 it is a very small increase. If we increase the decay rate too much then the washout solution is globally stable which is undesirable. Therefore, increasing the decay rate in the bioreactor is not a promising strategy to reduce sludge formation in the bioreactor.

5.3 Model two

For the model in chapter 4 we have $S^*_{0,\text{old}}$=1.9961 and $X^*_{\text{s},0,\text{old}}$=12.2133.

5.3.1 The chemical oxygen demand

From chapter 4, equation (4.38), the chemical oxygen demand is given by

$$\text{COD}^*_{\text{nw}} = \frac{1 - R^* + k_d^*\tau^*}{(1-k_d^*)\tau^* - 1 + R^*} + \frac{\alpha_g A X^*_{\text{s},0,\text{old}} + (1-f_p)\alpha_g k_d^* X^*_{\text{b,nw}}\tau^*}{1 - R^* + k_h^*\tau^*}, \tag{5.4}$$

where X^*_{bnw} is given by (4.34).

Figure 5.8 shows the dimensionless chemical oxygen demand as a function of the residence time for three values of the decay coefficient (A=1). As the decay coefficient increases it becomes more difficult to achieve 90% removal of the chemical oxygen demand. Note that the change in the value of the trans-critical bifurcation is relatively small compared to the change in the value of residence time to remove 90% of the chemical oxygen demand. For example when k_d^*=0.005 the dimensionless residence time required to achieve a chemical oxygen demand efficiency of 90% is 3.0247 and the dimensionless residence time at the trans-critical bifurcation point is τ^*_{cr}=1.1181, when k_d^*=0.3 the dimensionless residence time required to achieve a chemical oxygen demand efficiency of 90% is 9.3408 and the value at the trans-critical bifurcation

point is $\tau^*_{\rm cr}$=1.6587 and when k^*_d=0.5 the dimensionless residence time required to achieve a chemical oxygen demand efficiency of 90% is 478.3 and the value at the trans-critical bifurcation point $\tau^*_{\rm cr}$=2.4670. The corresponding dimensional values for the residence time at 90% of the chemical oxygen demand removed are 0.6654, 2.0550 and 105.2 days for k^*_d=0.005, 0.3 and 0.5 respectively.

From equation (4.61)the minimum value for the chemical oxygen demand occurs at infinite residence time and it is given by

$$\mathrm{COD}^*(\tau^* = \infty) = \frac{k^*_d}{1 - k^*_d},$$

which is an increasing function of k^*_d. Thus we can not achieve 90% of the chemical oxygen demand removal if

$$\begin{aligned} &\mathrm{COD}^*(\tau^* = \infty) > 0.1A\mathrm{COD}^*_{\rm in,old}, \\ &\Rightarrow k^*_{\rm d,critical} = \frac{0.1A\mathrm{COD}^*_{\rm in,old}}{1 + 0.1A\mathrm{COD}^*_{\rm in,old}} = 0.5044. \end{aligned}$$

As this is the same value as for model one we include that if k^*_d>0.5044 then it is impossible to achieve a chemical oxygen demand efficiency of 90%.

In conclusion when the decay coefficient increases the chemical oxygen demand inside the bioreactor increases. For sufficiently high values of the decay coefficient it is impossible to achieve 90% chemical oxygen demand removal.

5.3.2 The volatile suspended solids

From equation (4.39) the volatile suspended solids is given by

$$\mathrm{VSS}^*_{\rm nw} = \left[1 + \frac{f_p k^*_d \tau^*}{1 - R^*} + \frac{(1 - f_p) k^*_d \tau^*}{1 - R^* + k^*_h \tau^*}\right] X^*_{\rm b,nw} + \frac{A X^*_{\rm s,0,old}}{1 - R^* + k^*_h \tau^*} + \frac{X^*_{p,0}}{1 - R^*} + \frac{X^*_{i,0}}{1 - R^*}, \tag{5.5}$$

where $X^*_{\mathrm{b,NW}}$ is given by equation (2.57).

Figure 5.9 shows how the steady state diagram for the volatile suspended solids as a function of the residence time depends upon the value of the effective recycle parameter and the decay rate. Line 1 in figure 5.9 shows the transition where the target value of the volatile suspended solids is equal to the maximum value of the volatile suspended solids along the no-washout branch ($\mathrm{VSS}^*_{\mathrm{nw}}(\tau^* = \infty) = \mathrm{VSS}^*_{\mathrm{t}}$). The line marks the transition from case three, where there are three intersection points, one along the washout branch and two along the no-washout branch, as shown in figure 5.10(a), to case six, where there are two intersection points, one along the washout branch and one along the no-washout branch, as shown in figure 5.10(b). To find this transition we set equation (4.62) equal to the target value. The transition from case three to six is given by:

$$k^*_{\mathrm{d},36} = \frac{Af_p\mathrm{COD}^*_{\mathrm{in,old}} + [(1-R^*)\mathrm{VSS}^*_{\mathrm{t}} - (X^*_{i,0} + X^*_{p,0})]\{(1-f_p)\alpha_g - 1\}}{Af_p\mathrm{COD}^*_{\mathrm{in,old}} + [(1-R^*)\mathrm{VSS}^*_{\mathrm{t}} - (X^*_{i,0} + X^*_{p,0})]\{(1-f_p)\alpha_g - 1\} + f_p}. \tag{5.6}$$

In the limiting case of perfect recycle we have

$$k^*_{\mathrm{d},36}(R^* = 1) = \frac{Af_p\mathrm{COD}^*_{\mathrm{in,old}} + [(X^*_{i,0} + X^*_{p,0})]\{(1-f_p)\alpha_g - 1\}}{Af_p\mathrm{COD}^*_{\mathrm{in,old}} + [(X^*_{i,0} + X^*_{p,0})]\{(1-f_p)\alpha_g - 1\} + f_p}.$$

Figure 5.11(a) shows a blow up of figure 5.9 showing that lines 1 and 2 intersect once. (This is different from the previous model where there are two intersection points). The intersection point is where k^*_{d}=0.9105 and R^*=0.9997. This leads to the formation of a new steady-state digram (figure 5.12). However, as before this steady state digram is not of physical interest because the washout branch is always stable for the given values of the decay rate and the effective recycle parameter. From equation (4.51) when (A=1) there is a critical value of the decay coefficient

(k_d^*) above which the biomass die out.

$$k_d^* < k_{\mathrm{d,cr}}^* = \frac{A\mathrm{COD}_{\mathrm{in,old}}^*}{1 + A\mathrm{COD}_{\mathrm{in,old}}^*} = 0.9105.$$

When (A=0.5) we have $k_{\mathrm{d,cr}}^*$=0.8358 and when (A=0.1) we have $k_{\mathrm{d,cr}}^*$=0.5044.

Figure 5.11(b) shows the location of the critical value for the decay rate coincide with the intersection point.

Figure 5.13 revises figure 5.9 to include the critical value of the decay coefficient, if the decay coefficient is larger than the critical value then the washout solution is globally stable i.e. the biomass die out which leads to process failure.

Figure 5.14 shows the location of line 1 as a function of the value for A, the washout solution is globally stable if the decay rate is larger than its value at the circles.

Rearranging equation (5.6) we have

$$R_{3,6}^* = \frac{\mathrm{VSS}_{\mathrm{t}}^* - X_{i,0}^* - f_p k_d^* a_{0,\mathrm{old}}}{\mathrm{VSS}_{\mathrm{t}}^*},$$

where

$$a_{0,\mathrm{old}} = \frac{AS_0^*(1-k_d^*) - k_d^* + \alpha_g A X_{\mathrm{s,0,old}}^*(1-k_d^*)}{k_d^*(1-k_d^*)[1-(1-f_p)\alpha_g]}.$$

We have

$$\frac{dR_{3,6}^*}{dA} = -\frac{f_p \mathrm{COD}_{\mathrm{in,old}}^*}{\mathrm{VSS}_{\mathrm{t}}^*[1-(1-f_p)\alpha_g]} < 0,$$

and

$$\frac{dR_{3,6}^*}{dk_d^*} = \frac{f_p}{\mathrm{VSS}_{\mathrm{t}}^*[1-(1-f_p)\alpha_g](1-k_d^*)^2} > 0.$$

Line 2 in figure 5.9 shows the transition where the volatile suspended solids along the no-washout branch at the critical value of the residence time is equal to the target

value of the volatile suspended solids ($\mathrm{VSS}^*_{\mathrm{nw}}(\tau^* = \tau^*_{\mathrm{cr}}) = \mathrm{VSS}^*_{\mathrm{t}}$). This line makes the transition from case six, where there are two intersection points (one along the washout and one along the no-washout branch) as shown in figure 5.10(b), to case five, where there are no intersection points, as shown in figure 5.10(c).

To find this transition we equate equation (4.32) to the target value and set the residence time equal to the critical value, equation (4.48). After some algebra the formula for the transition from case six to five is given by:

$$k^*_{\mathrm{d},65} = \frac{B_{\mathrm{m2}} + C_{\mathrm{m2}}}{D_{\mathrm{m2}}},$$

where

$$\begin{aligned}
B_{\mathrm{m2}} =& -\mathrm{VSS}^*_{\mathrm{t}}\,(1-R^*)\left\{\alpha_g A X^*_{\mathrm{s},0,\mathrm{old}} + k^*_h + \left\{A S^*_{0,\mathrm{old}} + \left[A X^*_{\mathrm{s},0,\mathrm{old}} + 2(X^*_{i,0} + X^*_{p,0})\right.\right.\right.\\
&\left.\left.\left. - (1-R^*)\,\mathrm{VSS}^*_{\mathrm{t}}\right]\alpha_g\right\}(1+k^*_h)\right\},\\
C_{\mathrm{m2}} =& (X^*_{i,0} + X^*_{p,0})\left\{\alpha_g A X^*_{\mathrm{s},0,\mathrm{old}} + k^*_h + (1+k^*_h)\left[(X^*_{i,0} + X^*_{p,0})\alpha_g + A\mathrm{COD}^*_{\mathrm{in,old}}\right]\right\}\\
&+ A^2 X^*_{\mathrm{s},0,\mathrm{old}}\mathrm{COD}^*_{\mathrm{in,old}},\\
D_{\mathrm{m2}} =& \left[A X^*_{\mathrm{s},0,\mathrm{old}} + X^*_{i,0} + X^*_{p,0} - (1-R^*)\,\mathrm{VSS}^*_{\mathrm{t}}\right]\left\{A\mathrm{COD}^*_{\mathrm{in,old}} + 1 + \left[X^*_{i,0} + X^*_{p,0}\right.\right.\\
&\left.\left. - (1-R^*)\,\mathrm{VSS}^*_{\mathrm{t}}\right]\alpha_g\right\}.
\end{aligned}$$

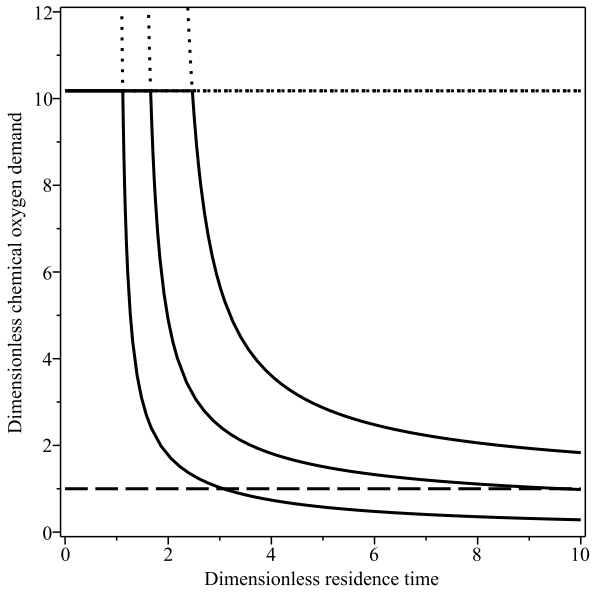

Figure 5.8: Steady state diagram for the dimensionless chemical oxygen demand. Parameter values $R^* = 0$, A=1 and k_{d}^*=0.005 (left), 0.3 and 0.5 (right) respectively. The dashed horizontal line correspond to a chemical oxygen demand removal efficiency of 90%. Model two from chapter 4.

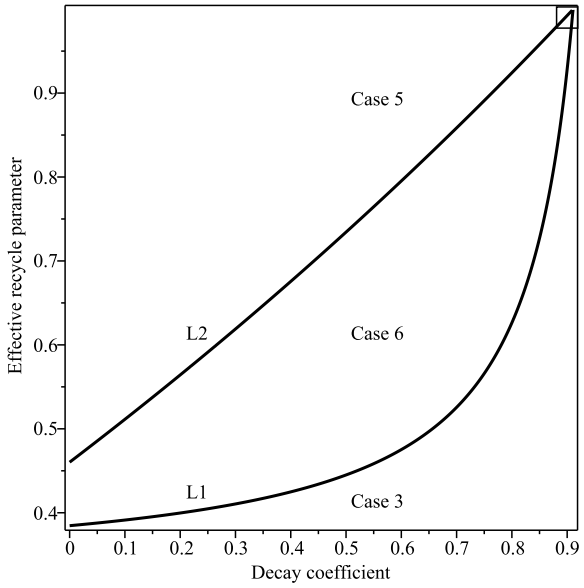

Figure 5.9: The location of the volatile suspended solids steady-state digrams in the effective recycle parameter (R^*) - decay coefficient (k_d^*) parameter plane, where A=1.

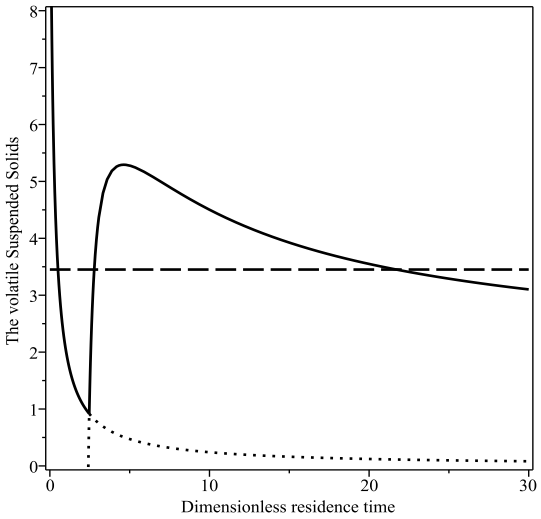

(a) Case three. Parameter values: R^*=0 and k_d^*=0.5.

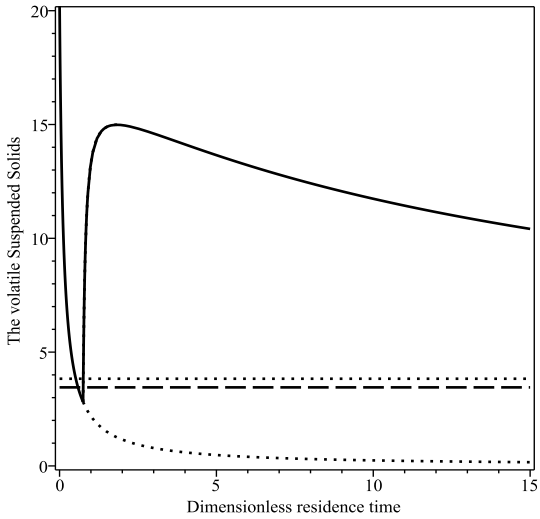

(b) Case six. Parameter values: R^*=0.4 and k_d^*=0.1.

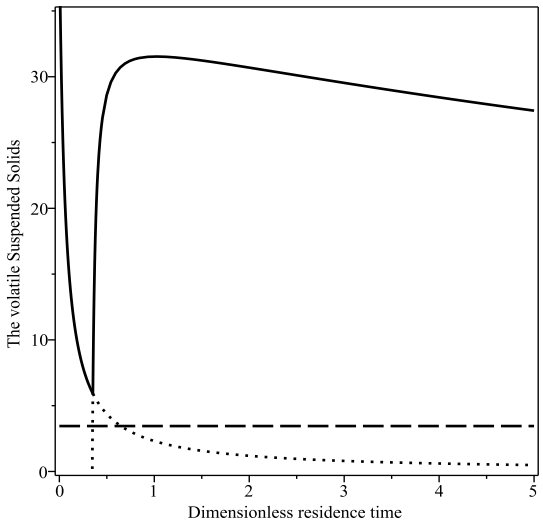

(c) Case five. Parameter values: R^*=0.7 and k_d^*=0.05.

Figure 5.10: Steady-state diagrams showing the volatile suspended solids as a function of the dimensionless residence time (τ^*). The box denotes the location of the trans-critical bifurcation. The solid and dotted lines represent stable and unstable solutions respectively.The horizontal dash line denotes the target value of the volatile suspended solids and the horizontal dotted line denotes the asymptotic value.

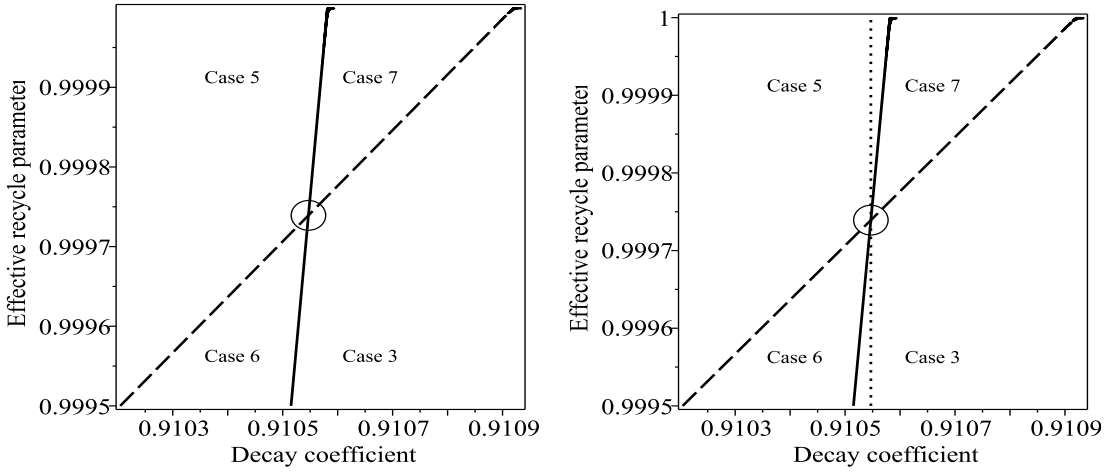

Figure 5.11: The location of the volatile suspended solids steady-state digrams in the effective recycle parameter (R^*) - decay coefficient (k_d^*) parameter plane, where A=1. The solid, dash and dotted lines represent line 1, line 2 and $k^*_{\mathrm{d,cr}}$ respectively.

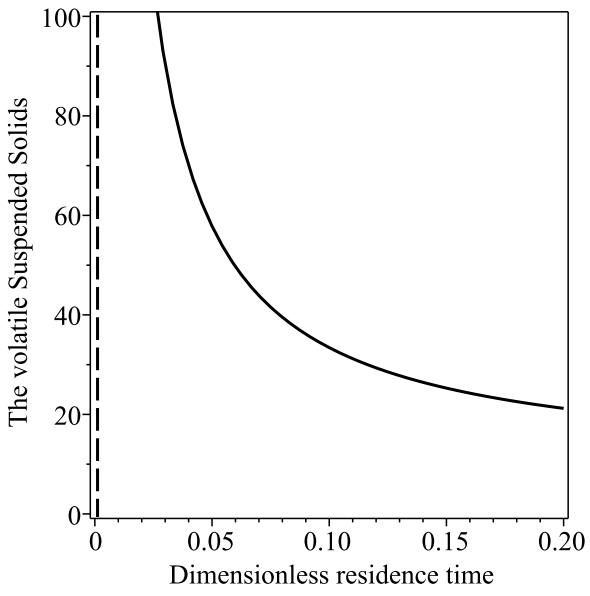

Figure 5.12: The volatile suspended solids steady-state digram as a function of the dimensionless residence time (τ^*), where k_d^*=0.9107 and R^*=0.9999. The solid and dash lines represent the the washout and no-washout branches respectively. The washout branch is always stable and the no-washout branch is always unstable.

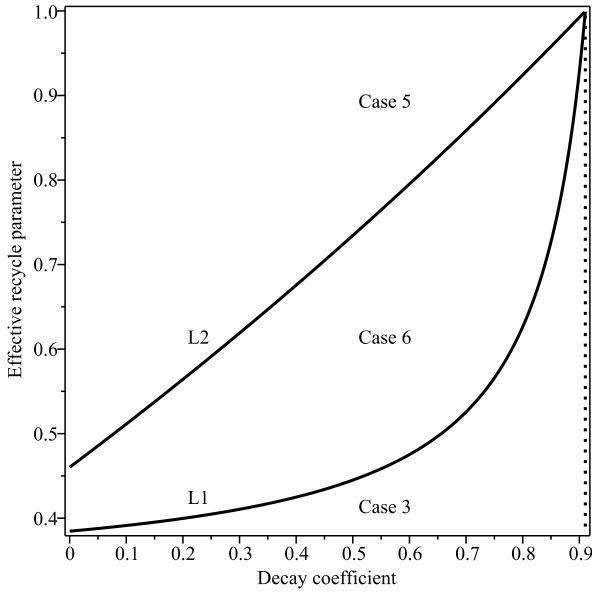

Figure 5.13: The location of the volatile suspended solids steady-state digrams in the effective recycle parameter (R^*) - decay coefficient (k_d^*) parameter plane, where A=1. The dotted vertical line shows the critical value of the decay coefficient ($k^*_{\mathrm{d,cr2}}$).

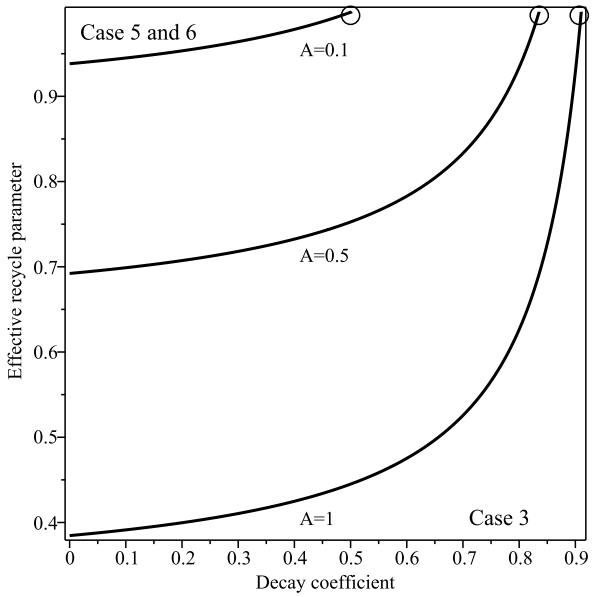

Figure 5.14: The location of line 1 (transition from case 3 to case 6) in the effective recycle parameter (R^*) - decay coefficient (k_d^*) parameter plane, where A=0.1, 0.5 and 1.

5.3.3 Conclusion

If we increase the value of the decay rate inside the bioreactor then the value of the effective recycle ratio at the transition from case 3 to case 6 increases. Although the increase is more pronounced than in model one, it remains a relatively small increase. If we increase the decay rate too much then the washout solution is globally stable which is undesirable. Therefore, we again include that increasing the decay rate in the bioreactor is not a promising strategy to reduce sludge formation in the bioreactor.

5.4 Summary

In this chapter we investigated how increasing the decay rate effected the behavior of model one and two. We also investigated changing the chemical oxygen demand in the feed by writing the feed concentrations $AS^*_{0,\text{old}}$ and $AX^*_{\text{s},0,\text{old}}$, $(0 \leq A \leq 1)$.
From previous chapters we know that there is a critical value of the decay rate, if the decay rate is larger than the critical value then the washout solution is globally stable i.e. the biomass die out which leads to process failure. We showed that increasing the death rate makes achieving 90% chemical oxygen demand removal more difficult. This is unsurprising because if we increase the death rate then the concentration of biomass decreases.
We investigated the transition of the volatile suspended solids between desirable and undesirable behavior in both models one and two. The overall behavior is very similar. In both cases if the effective recycle parameter is larger that a critical value then we have undesirable behavior. As we increase the decay rate the critical value of the effective recycle parameter increases which is good, however the increase is too small to be significant in practice.
We conclude that increasing the death rate in the bioreactor is not an effective way to reduce sludge formation.

Chapter 6

Conclusions and suggestions for future research

6.1 Conclusion

In this thesis we undertook detailed investigations of several mathematical models for the activated sludge process, which is the most commonly used process for treating sewage and industrial wastewater using air. The main aims of this thesis were to:

- Find the steady-state solutions corresponding to washout and no-washout branches. The washout branch corresponds to process failure due to removal of all the biomass (when $X_b^* = 0$). The no-washout branch is when the biomass is present in the system.
- Determine the stability of the steady-state solutions.
- Use the stable steady-state solutions to investigate how the chemical oxygen demand and the total volatile suspended solids depend upon the residence time and the operation of a settling unit.

Our results provide insight into the activated sludge process. Here, we highlight the main conclusion of each chapter and suggest possible extensions for future work.

6.2 Thesis highlights

6.2.1 Background and method

The important concepts of the activated sludge process were explained in chapter 1. Due to environmental concerns regarding wastewater management, the activated sludge process has become an increasingly popular method for treating sewage and industrial wastewater. One drawback associated with this process is the production of 'sludge'. The expense for treating excess sludge can account for 50-60% of the running costs of a plant [19, 31, 76]. We assume that a target value for the volatile suspended solids has been set to be VSS $= 12000\text{mg}\,l^{-1}$ [102].

Chapter 2 highlighted the mathematical methods that are used in this thesis. Stability and bifurcation analyses were the main analytical techniques used to investigate models. In order to simulate and plot the solutions, the software packages MAPLE and GNUPLOT were used in chapters 2-5.

6.2.2 Model one

In chapter 2 we examined a simple extension of the standard model due to Chung and Neethling[71]. This biochemical model has not previous been examined in detail. In this model for the activated sludge process the influent contains a mixture of soluble and slowly biodegradable particulate substrate. Within the bioreactor the biodegradable particulate substrate is hydrolyzed to form soluble substrate. In turn this is used for growth by the biomass which eventually decay to produce soluble substrate in addition to inert material.

The system contains four differential equations, after simplification it reduced to two different equations. We found two steady state solutions, corresponding to washout and no-washout branches, and determined their stability as a function of the residence time. The washout branch corresponds to process failure and has to be avoided.

We showed that if the decay rate is sufficiently high then the process failure is automatic. For values of the decay coefficient below this critical value there exists a critical value of the residence time, corresponding to a trans-critical bifurcation. Below this value process failure occurs, above this value the no-washout solution branch is both physically meaningful and stable. From our expression for the solutions along the no-washout branch we obtained asymptotic expressions in the limit of high residence time.

The steady-state expressions were used to investigate how the reactor performance depends upon process parameters. We examined both the chemical oxygen demand in the reactor and the volatile suspended solids. Our main interest was the latter and we investigated how it depends upon the effective recycle parameter, the total chemical oxygen demand in the feed and how the chemical oxygen demand in the feed is partitioned between its two components. From our expression for the solutions along the no-washout branch we obtained asymptotic expressions for the chemical oxygen demand and the volatile suspended solids in the limit of high residence time.

For the default parameter values we found that there are five generic response diagrams for the steady-state concentration of volatile suspended solids. In case one the target value is larger than the maximum value along the washout branch. Thus there is no intersection point because the volatile suspended solids concentration in the effluent is always below the target value; this case is not realistic. In case two the target value is larger than the maximum value along the no-washout branch. Thus there is only one intersection point, which is on the washout branch. This is a good case to have because wherever we operate on the no-washout branch the volatile suspended solid is guaranteed to be below the target value. In the third case the target value is between the volatile suspended solids concentration at the trans-critical bifurcation and the maximum value along the no-washout branch. Thus there are three intersection points: one along the washout branch and two along the

no-washout branch. The volatile suspended solids is lower than the target value if the residence time is between the intersection point on the washout branch and the first intersection point on the no-washout branch or larger than the second intersection point on the washout branch. In practice the residence time would need to be larger than the second intersection point on the no-washout branch. In case four the target value is larger than the asymptotic value along the no-washout branch and smaller than the volatile suspended solids at the trans-critical bifurcation. There is one intersection point, on the no-washout branch. We require the residence time to be larger than the intersection value. In case five the target value is smaller than both the value at the trans-critical bifurcation and the limiting value when the residence time approaches infinity. There are no intersection points. This is undesirable because in case five the volatile suspended solids can never be reduced below the target value. The final transition, from case four to case five, corresponded to the asymptotic value of the volatile suspended solids at infinity increasing through the target value

There are two non-generic cases. These are when we have two intersection points. These happen when either the target value of the volatile suspended solid is equal to the maximum value along the washout branch or it is equal to the value at the trans-critical bifurcation.

The transition between case four and five is important, because the volatile suspended solids concentration in cases one to four is either below the target value for all values of the residence time or there is a critical value of the residence time, when the residence time is larger than this critical value then the volatile suspended solids is below the target. However, in case five the sludge content is always greater than the target value. We have shown that there is a critical value of the effective recycle parameter for the transition from case four to case five. If the recycle parameter is larger than the critical value then the volatile suspended solids can not be reduced below the target value. As we have found analytical expressions for our steady-state

solutions, the critical value of the recycle parameter can be readily determined if the target value is changed. We investigated how the location of this transition depends upon the effective recycle parameter, the total chemical oxygen demand in the feed and how the chemical oxygen demand in the feed is partitioned between its two components.

6.2.3 Model one with a sludge disintegration unit

In chapter 3 we extended our model for the activated sludge process from chapter 2 to include a sludge disintegration unit. We used the extended model to investigate how the mass of sludge produced by the activated sludge process can be reduced by coupling the bioreactor used in the process to a sludge disintegration unit. This system contains eight differential equations, four in the bioreactor and four equations in the sludge disintegration unit. We assume that there are three disintegration reactions in the sludge disintegration unit because there are three components that are degraded. An important assumption is that the time scale for the sludge disintegration reactions is quicker than the time scale for the biochemical processes. This means that we can ignore the biochemistry in the sludge disintegration unit. Therefore, the model for the sludge disintegration unit becomes a linear model.
We find two steady state solutions corresponding to washout and no-washout branches and determined their stability as a function of the residence time. We showed that as the value of the disintegration rate (γ) increases, the amount of sludge in the bioreactor decreases. Following our analysis in chapter 2, we know that the transition from case four to case five is of great practical interest. Two forms of behavior are found as the disintegration rate is increased. The transition between the two types is governed by the volatile suspended solids value when the residence time is infinity. This transition is independent of the disintegration rate (γ). Instead, for a fixed value of the effective recycle parameter (R^*) there is a critical value of the sludge disintegration factor (D). If the value of (D) is below the critical value,

then the the sludge content is always above the target value. If the value of (D) is sufficiently high then the sludge content is below the target value for sufficiently large values of the residence time.

In conclusion a very important finding in this chapter is that for a fixed value of the effective recycle parameter there is a critical value of the sludge disintegration factor (D). If the sludge disintegration factor is greater than the critical value ($D>D_{\mathrm{cr}}$) then the volatile suspended solids is guaranteed to be below the target value ($\mathrm{VSS}^*<\mathrm{VSS}_t^*$) if the residence time is larger than some critical value.

6.2.4 Model two

In chapter 4 the biochemistry from chapter 2 is changed so that the biomass decay produces slowly biodegradable substrate in addition to non-biodegradable particulates. This system contains five differential equations, rather than two in the basic model. For analysis of the long term behavior the system of equations can be reduced to three.

We found two steady state solutions corresponding to washout and no-washout branches and determined their stability as a function of the residence time. We showed that if the decay rate is sufficiently high then process failure is automatic. For values of the decay coefficient below this critical value there exists a critical value of the residence time, corresponding to a trans-critical bifurcation. Below this value process failure occurs, above this value the no-washout solution branch is both physically meaningful and stable. From our expression for the solutions along the no-washout branch we obtained asymptotic expressions in the limit of high residence time.

The steady-state expressions were used to investigate how the reactor performance depends upon process parameters. We examined the chemical oxygen demand in the reactor and the volatile suspended solids. Our main interest was the latter and we investigated how it depends upon the effective recycle parameter, the total chem-

ical oxygen demand in the feed and how the chemical oxygen demand in the feed is partitioned between its two components. From our expression for the solutions along the no-washout branch we obtained asymptotic expressions for the chemical oxygen demand and the volatile suspended solids in the limit of high residence time. For the default parameter values we found that there are three generic response diagrams for the steady-state concentration of volatile suspended solids. In the first case (called case three to be consistent with our analyse of the model in chapter 2) it is possible to ensure that the suspended solids are below the target value by operating at a sufficiently high residence time. However, the required minimum value of the residence time may be unpalatable in practice. In the second case (case six), it is only possible to ensure that the suspended solids are below the target value by operating the reactor in a very restrictive range of residence times. Over this range there is effectively no removal of chemical oxygen demand. Thus this scenario is not of practical interest. In the final case (case five) for any value of the residence time the volatile suspended solids are always above the target value. The final transition, from case four to case five, corresponds to the value of the volatile suspended solids at the transcritical bifurcation increasing through the target value.

For the model considered in this chapter it seems inevitably, except for very dilute wastewaters, that for practical values of the residence time that the steady-state suspended solids will exceed the target value. When this happens plant operation must cease, so that the sludge can be removed from the reactor. Is it possible to prevent this from happening by operating a sludge disintegration unit in situ? We investigated this possibility for the original Chung and Neethling model in chapter 3. In our future research we are going to attach a sludge disintegration unit and apply the ideas used in chapter 3.

If we compare model one in chapter 2 and model two in chapter 4 we find that this small change in the assumptions results in a large change in the behaviour of the reactor. In model one when the biomass produces slowly biodegradable substrate,

the volatile suspended solids in practice is below the target value when the effective recycle parameter is smaller the the critical value for the transition from case four to case five. However, in practice for model two the volatile suspended solids is always above the target value.

6.2.5 Model one and two

In chapter 5 we investigated how increasing the decay rate effected the behavior of the models used in chapter 2 and 4. We also investigated changing the chemical oxygen demand in the feed by writing the feed concentrations in the form $AS^*_{0,\text{old}}$ and $AX^*_{s,0,\text{old}}$, $(0 \leq A \leq 1)$.

For the models used in chapter 2 and 4 we know that there is a critical value of the decay rate, if the decay rate is larger than the critical value then the washout solution is globally stable, i.e. the biomass die out which leads to process failure. Thus any benefit that is obtained in the performance of the activated sludge process by increasing the decay rate may be limited as increasing it too much produces process failure.

We showed that increasing the death rate makes achieving 90% chemical oxygen demand removal more difficult. This is unsurprising because if we increase the death rate then the concentration of biomass decreases.

We investigated the transition of the volatile suspended solids between desirable and undesirable behavior in both models one and two. The overall behavior is very similar. In both cases if the effective recycle parameter is larger that a critical value then we have undesirable behavior. As we increase the decay rate the critical value of the effective recycle parameter increases which is good, however the increase is too small to be significant in practice.

We conclude that increasing the death rate in the bioreactor is not an effective way to reduce sludge formation.

6.2.6 Final thoughts

The models investigated in this thesis are much simpler than those developed by the IWA [43]. They have the advantage that it is possible to obtain analytic expression for the steady-state expressions. In turn these allow gain considerable insight to be obtained into the generic behaviour of the models. It is hoped that these insights will be informative in the study of the various IWA models, where analytic expressions for the steady-states are unavailable and purely numerical techniques must be deployed. A start on investigating ASM-1 using continuation methods is presented in [71].

6.3 Future work

In this thesis, we have gained a better understanding of the activated sludge process through the analysis of simple models. However, there are some aspects of these models that could be studied further.

6.3.1 Model one and two

In this thesis we investigated a process model which consisted of one biological reactor connected to a settling unit which recycle material around the reactor.
A more realistic process model for future work is to have two bioreactors with three settling units, as shown in figure 6.1. Settling unit 1 goes around the first bioreactor, settling unit 2 goes around the second bioreactor and settling unit 3 goes around the cascade. This configuration is more realistic and includes reactor setups such as the Wuhrman process, which has two bioreactors and one settling unit, the Ludzack-Ettinger process, which is a semi-aerobic activated sludge process, and the Modified Ludzack-Ettinger process, which has two bioreactors and one settling unit with recycle from the second bioreactor back to the first bioreactor [56].

Another possibility is to have the feed stream entering the second bioreactor, as

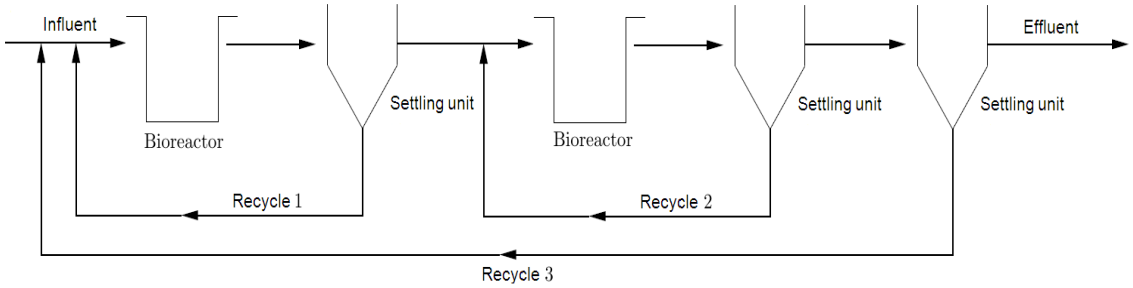

Figure 6.1: A step feed cascade reactor containing two bioreactors with three settling units.

shown in figure 6.2. (This configuration does not make sense if there is no recycle around all the cascade.)

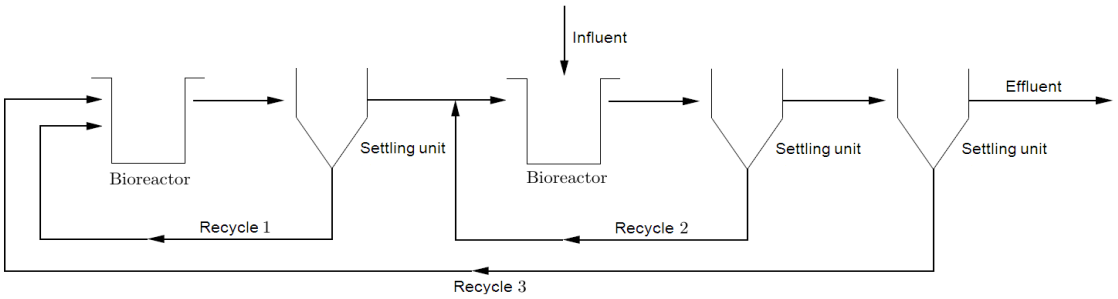

Figure 6.2: Two bioreactors with three settling units.

There are even more complicated extensions based around three bioreactors [56, page 10].

6.3.2 Model one and two with a Sludge disintegration unit

We intend to investigating model two in chapter 4 with the attached of a sludge disintegration unit. This was discussed in section 6.2.4.

After the reactor configuration in figure 6.1 has been analysed we aim to comprehensively analyse the behavior of this process when the sludge disintegration is attached either to the first bioreactor or the second bioreactor to see where it is best located. This configuration is shown in figure 6.3.

6.3.3 Further development

A simple dynamic model of a submerged membrane bioreactor has been recently developed that uses the standard model [81]. This model can be extended by replacing the Monod model with the biochemistry of the Chung and Neethling model.

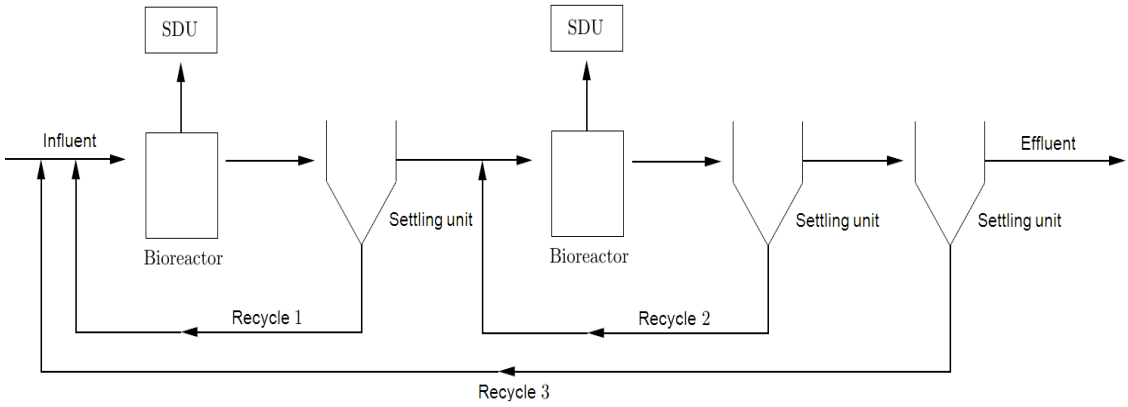

Figure 6.3: Two bioreactors with three settling units and two sludge disintegration units.

Appendix A

Appendix for Chapter 2 (model one)

A.1 Identifying when the no-washout branch is physically meaningful

The no-washout branch is physically meaningful only when the substrate and cel-mass concentrations are positive ($S^*_{\text{nw}} \geq 0$ and $X^*_{\text{b,nw}} \geq 0$). In this appendix we show that this is only true when

$$k^*_d < \frac{S^*_0 + \alpha_{g,h} X^*_{s,0}}{S^*_0 + \alpha_{g,h} X^*_{s,0} + 1} = \frac{\text{COD}^*_{\text{in}}}{1 + \text{COD}^*_{\text{in}}},$$

and

$$\tau^* > \tau^*_+ = (1 - R^*) \left[\frac{b^* + \sqrt{b^{*2} + 4ac^*}}{2a} \right] > 0.$$

A.1.1 The substrate concentration

First of all we investigate the condition for the substrate concentration to be positive, i.e.

$$S^*_{\text{nw}} = \frac{1 - R^* + k^*_d \tau^*}{(1 - k^*_d)\tau^* - 1 + R^*} > 0.$$

This requires the denominator to be positive

$$(1 - k^*_d)\tau^* - 1 + R^* > 0. \tag{A.1}$$

This is true when

$$\tau^* > \tau^*_{\text{pm},1} = \frac{1 - R^*}{1 - k^*_d},$$

and

$$0 < k^*_d < 1, \quad (0 \leq R^* < 1).$$

(Note, in section 2.4.1.2 we showed that the washout solution is globally stable when $k^*_d > 1$).

A.1.2 The biomass concentration

Now we investigate the condition for the biomass concentration to be positive, ie.

$$X^*_{\text{b,nw}} = \frac{(1 + S^*_{\text{nw}})(S^*_w - S^*_{\text{nw}})}{[S^*_{\text{nw}} - (1 + S^*_{\text{nw}}) f_s \alpha_{g,s} k^*_d]\, \tau^*} > 0.$$

First, we consider the denominator and show that it is always positive.

We have

$$\begin{aligned} S^*_{\text{nw}} - (1+S^*_{\text{nw}})f_s k^*_d \alpha_{g,s} &= (1+S^*_{\text{nw}})\left[\frac{S^*_{\text{nw}}}{1+S^*_{\text{nw}}} - f_s k^*_d \alpha_{g,s}\right], \quad \text{note } S^*_{\text{nw}}>0, \\ &= (1+S^*_{\text{nw}})\left[\frac{1-R^*+k^*_d\tau^*}{\tau^*} - f_s k^*_d \alpha_{g,s}\right], \\ &= \frac{1+S^*_{\text{nw}}}{\tau^*}\left[1-R^*+(1-f_s\alpha_{g,s})k^*_d\tau^*\right]>0, \end{aligned}$$

where we have used the relationship that

$$\frac{S^*_{\text{nw}}}{1+S^*_{\text{nw}}} = \frac{1-R^*+k^*_d\tau^*}{\tau^*}.$$

Recall that $0 \leq R^*<1$ and from equation (2.19) $0<f_s\alpha_{g,s}<1$.

Secondly, we consider the numerator. We require $S^*_w>S^*_{\text{nw}}$.

$$S^*_w = S^*_0 + \frac{\alpha_{g,h}k^*_h X^*_{s,0}\tau^*}{1-R^*+k^*_h\tau^*} > \frac{1-R^*+k^*_d\tau^*}{(1-k^*_d)\tau^*-1+R^*} = S^*_{\text{nw}}>0.$$

Note, we can assume that $(1-k^*_d)\tau^*-1+R^*>0$ as from equation (B.1) this is the condition for the substrate concentration to be positive.

Cross multiplying we obtain a quadratic inequality

$$\begin{aligned} Q(\tau^*) &= a{\tau^*}^{2*} + b\tau^* + c>0, \quad \text{where the coefficients are} \qquad \text{(A.2)} \\ a &= [(S^*_0+\alpha_g X^*_{s,0}) - (1+S^*_0+\alpha_{g,h}X^*_{s,0})k^*_d]k^*_h, \\ b &= -(1-R^*)[(1+S^*_0)(k^*_h+k^*_d) + k^*_h\alpha_{g,h}X^*_{s,0} - S^*_0], \\ c &= -(1-R^*)^2(1+S^*_0)<0. \end{aligned}$$

Note that the quadratic equation $Q(\tau^*)$ defines value of τ^* at which the washout and no-washout branches intersect, compare with equation (2.67).

We have three cases to consider depending upon the sign of the coefficient a. $a>0, a=0$ and $a<0$.

To find the values for τ^* where $Q(\tau^*)>0$, we first consider the equality

$$Q(\tau^*) = a\tau^{2*} + b\tau^* + c = 0. \tag{A.3}$$

A.1.2.1 Case one $a>0$

When $a>0$ the quadratic equation (A.3) has solutions τ^*_- and τ^*_+ with $\tau^*_-<0<\tau^*_+$, (because $c<0$).

Thus $S^*_w>S^*_{\text{nw}}$ for $\tau^*>\tau^*_+$. Hence the no-washout solution is physically meaningful when

$$\tau^* > \max(\tau^*_+, \tau^*_{\text{pm},1}).$$

The solution τ^*_+ is given by

$$\tau^*_+ = \frac{-b+\sqrt{b^2-4ac}}{2a}.$$

Note that the term b^2 and $-4ac$ both have a common factor of $(1-R^*)^2$.

Hence

$$\begin{aligned}\tau^*_+ &= \frac{-b+(1-R^*)\sqrt{b^{*2}-4ac^*}}{2a}, \\ &= (1-R^*)\left[\frac{b^*+\sqrt{b^{*2}+4ac^*}}{2a}\right],\end{aligned}$$

where

$$b^* = (1+S^*_0)(k^*_h+k^*_d) + k^*_h\alpha_{g,h}X^*_{s,0} - S^*_0,$$

$$c^* = (1 + S_0^*).$$

Note that

$$\tau_{\rm cr}^*(R^* = 0) = \frac{b^* + \sqrt{b^{*2} + 4ac^*}}{2a}.$$

Hence

$$\tau_+^* = (1 - R^*)\tau_{\rm cr}^*(R^* = 0).$$

The critical value of the residence time is a linearly decreasing function of the effective recycle parameter ($\frac{d\tau_+^*}{dR^*}$<0). It has a minimum value 0 when $R^* = 1$.

Figure A.1 shows a sketch of $Q(\tau^*)$. We now show that $0<\tau_{\rm pm,1}^*<\tau_+^*$.

By calculation we find that the value of the quadratic function $Q(\tau^*)$ at $\tau^* = \tau_{\rm pm,1}^*$ is given by

$$Q\left(\tau^* = \frac{1 - R^*}{1 - k_d^*}\right) = \frac{(1 - R^*)^2}{(1 - k_d^*)^2}\left[k_d^* - k_h^* - 1\right] <0.$$

(Recall, we can assume that $k_d^*<1$). Thus $\tau_+^*>\tau_{\rm pm,1}^*$.

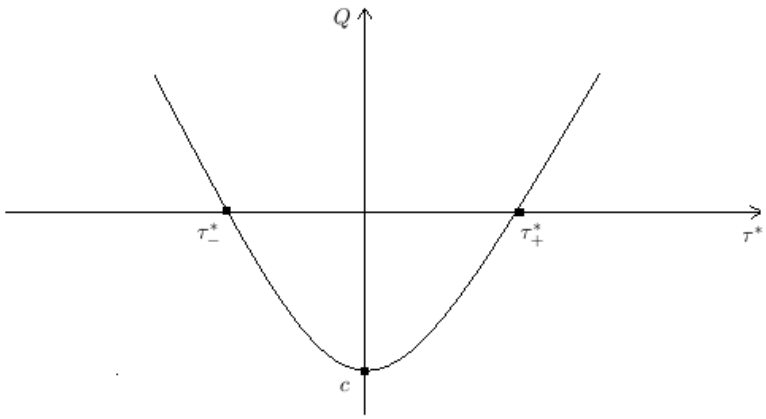

Figure A.1: Sketch of the quadratic equation $Q(\tau^*)$.

Hence we have shown for case one that the no washout solution is physically mean-

ingful when $\tau^*>\tau_+^*$ and $a>0$ i.e. when

$$k_d^*<\frac{\mathrm{COD}_{\mathrm{in}}^*}{1+\mathrm{COD}_{\mathrm{in}}^*}=k_{\mathrm{d,cr},\infty}^*.$$

This makes sense because if $k_d^*>k_{\mathrm{d,cr},\infty}^*$ then we have shown that $\lim_{t^*\to\infty} X_b^*(t^*)=0$.

A.1.2.2 Case two $a=0$

For a to be equal to zero we must have

$$S_0^*=\frac{k_d^*-(1-k_d^*)\alpha_{g,h}X_{s,0}^*}{1-k_d^*}. \tag{A.4}$$

This case is only of interest when $S_0^*>0$. This implies that

$$k_d^*>(1-k_d^*)\alpha_{g,h}X_{s,0}^*. \tag{A.5}$$

The coefficient b in equation (A.2) is

$$b=(R^*-1)[(1+S_0^*)(k_h^*+k_d^*)+k_h^*\alpha_{g,h}X_{s,0}^*-S_0^*]. \tag{A.6}$$

Substituting from (A.4) ($S_0^*(1-k_d^*)=k_d^*-(1-k_d^*)\alpha_{g,h}X_{s,0}^*$) into (A.6) we find that

$$b=-(1-R^*)\left[(1-k_d^*)\alpha_{g,h}X_{s,0}^*+(S_0^*+\alpha_{g,h}X_{s,0}^*+1)k_h^*\right]<0.$$

When $a=0$ the quadratic $Q(\tau^*)$, equation (A.2), becomes a linear function.

$$Q(\tau^*)=b\tau^*+c>0. \tag{A.7}$$

As $b<0$ and $c<0$ this gives

$$\tau^* < \frac{-c}{b} < 0.$$

As a result, when $a = 0$ the no washout solution is never physically meaningful because τ^* has to be negative.

A.1.2.3 Case three $a<0$

In this case we have

$$S_0^*(1-k_d^*) < k_d^* - (1-k_d^*)\alpha_{g,h}X_{s,0}^*.$$

From equation (A.6) we have

$$b = (1-R^*)\left[S_0^*(1-k_d^*) - S_0^*k_h^* - \alpha_{g,h}X_{s,0}^*k_h^* - k_d^* - k_h^*\right].$$
$$b < -(1-R^*)\left[(1-k_d^*)\alpha_{g,h}X_{s,0}^* + (S_0^* + \alpha_{g,h}X_{s,0}^* + 1)k_h^*\right] < 0.$$

There are two sub-cases to consider depending upon the sign of the discriminant $b^2 - 4ac$.

If $(b^2 - 4ac<0)$, then inequality (A.2) is never satisfied, as $Q(\tau^*)<0 \quad (\forall\tau^*)$ and consequently $X_{\text{b,nw}}^*$ is never physically meaningful. If the discriminant is positive $(b^2 - 4ac>0)$, then equation (A.3) has two roots with $\tau_+^*<\tau_-^*<0$ (as $a<0$ and $b<0$). Hence, $X_{\text{b,nw}}^*$ is not physically meaningful for $\tau^*>0$. This means that when $a<0$ the no washout solution is never physically meaningful.

A.2 Summary

We conclude that the no-washout solution branch is only physically meaningful when

$$k_d^* < \frac{S_0^* + \alpha_{g,h} X_{s,0}^*}{S_0^* + \alpha_{g,h} X_{s,0}^* + 1} = \frac{\mathrm{COD}_{\mathrm{in}}^*}{1 + \mathrm{COD}_{\mathrm{in}}^*},$$

and

$$\tau^* > \tau_+^* = (1 - R^*) \left[\frac{b^* + \sqrt{b^{*2} + 4ac^*}}{2a} \right] > 0.$$

Note that when $\tau^* = \tau_+^*$ then $S_W^* = S_{\mathrm{NW}}^*$ and τ_+^* is a trans-critical bifurcation point.

A.3 Values of parameters

Typical parameter values are [23]: $K_s = 5,190$ mg COD L^{-1}, $S_0 = 10,360$ mg COD L^{-1}, $X_{i,0} = 2,810$ mg VSS L^{-1}, $X_{s,0} = 22,590$ mg VSS L^{-1}, $f_s = 0.8$ g VSS (g VSS)$^{-1}$, $k_d = 0.015$ day^{-1}, $k_h = 1.1$ day^{-1}, $\alpha_g = 0.03$ mg VSS (mg COD)$^{-1}$, $\alpha_h = 1.88$ mg COD (mg VSS)$^{-1}$, $\alpha_S = 1.42$ mg COD (mg VSS)$^{-1}$, $\mu_m = 0.22$ day^{-1}.

Values of the residence time range from $5 - 40$ days.

This gives the following values for the dimensionless parameter groups:

$S_0^* = 1.996, X_{s,0}^* = 145.0857, X_{i,0}^* = 18.0475, k_d^* = 0.0682, k_h^* = 5, \alpha_{g,h} = 0.0564, \alpha_{g,s} = 0.0426,$

$\mathrm{COD}_0^* = 10.1788.$

Appendix B

Appendix for Chapter 3 (Model One with SDU)

B.1 Non-negativity of the solutions

In this appendix we show that all solution components in the model remain non negative for non-negative initial conditions.

B.1.1 Non-negativity of solutions in the bioreactor

To show that the soluble substrate concentration is non negative ($0 \leq S^*$), we consider the value for the derivative $\frac{dS^*}{dt^*}$ when $S^* = 0$. We have

$$\frac{dS^*}{dt^*}\Big|_{S^*=0} = \frac{1}{\tau^*}S_0^* + \frac{D}{\tau^*}S_s^* + \alpha_{g,h}k_h^*X_s^* + f_s\alpha_{g,s}k_d^*X_b^* > 0,$$

as by assumption $0 < S_0^*, 0 \leq S_s^*, 0 \leq X_s^*$ and $0 \leq X_b^*$ Thus the derivative is strictly positive. This means that if $S^* = 0$ then S^* is increasing, so it can not become negative.

We now consider what happens when the biomass concentration is zero ($X_b^* = 0$). We have

$$\left.\frac{dX_b^*}{dt^*}\right|_{X_b^*=0} = \frac{1}{\tau^*}X_{b,0}^* + \frac{D}{\tau^*}X_{b,s}^* \geq 0,$$

as by assumption $X_{b,0}^* \geq 0$ and $X_{b,s}^* \geq 0$. This means that $X_b^* \geq 0$. Note that

if $X_{b,0}^*>0$ then $0<\left.\frac{dX_b^*}{dt^*}\right|_{X_b^*=0} = \frac{1}{\tau^*}X_{b,0}^*$,

if $X_{b,0}^* = 0$ then $\left.\frac{dX_b^*}{dt^*}\right|_{X_b^*=0} = 0$, only if $X_{b,s}^* = 0$.

When the non-biodegradable particulates concentration is zero ($X_i^* = 0$), we have

$$\left.\frac{dX_i^*}{dt^*}\right|_{X_i^*=0} = \frac{1}{\tau^*}X_{i,0}^* + \frac{D}{\tau^*}X_{i,s}^* + f_i k_d^* X_b^* \geq 0,$$

as by assumption $X_{i,0}^* \geq 0, X_{i,s}^* \geq 0$ and $X_b^* \geq 0$.

When the biodegradable particulate substrate is zero ($X_s^* = 0$), we have

$$\left.\frac{dX_s^*}{dt^*}\right|_{X_s^*=0} = \frac{1}{\tau^*}X_{s,0}^* + \frac{D}{\tau^*}X_{s,s}^* \geq 0,$$

as by assumption $X_{s,0}^* \geq 0$ and $X_{s,s}^* \geq 0$.

B.1.2 Non-negativity of solutions in the sludge disintegration unit

We now show that the solutions in the sludge disintegration unit can never become negative.

When the soluble substrate concentration is zero ($S_s^* = 0$), we have

$$\frac{dS_s^*}{dt^*}\Big|_{S_s^*=0} = \frac{DV^*}{\tau^*}S^* + \alpha\alpha_{g,s}\gamma_b^* X_{b,s}^* + \alpha\alpha_{g,h}\gamma_s^* X_{s,s}^* + \beta_i\alpha\alpha_{\mathrm{g,SDU}}\gamma_i^* X_{i,s}^* + \chi\left[\alpha_{h,g}k_h^* X_{s,s}^* + f_s\alpha_{s,g}k_d^* X_{b,s}^*\right] \geq 0,$$

as by assumption $S^* \geq 0$, $X_{b,s}^* \geq 0$, $X_{s,s}^* \geq 0$ and $X_{i,s}^* \geq 0$.

When the biomass concentration is zero ($X_{b,s}^* = 0$), we have

$$\frac{dX_{b,s}^*}{dt^*}\Big|_{X_{b,s}^*=0} = \frac{DV^*}{\tau^*}X_b^* \geq 0,$$

as by assumption $X_b^* \geq 0$.

When the non-biodegradable particulates concentration is zero ($X_{i,s}^* = 0$), w have

$$\frac{dX_{i,s}^*}{dt^*}\Big|_{X_{i,s}^*=0} = \frac{DV^*}{\tau^*}X_i^* + f_{p,s}\gamma_b^* X_{b,s}^* + \chi\left[f_i k_d^* X_{b,s}^*\right] \geq 0,$$

as by assumption $X_i^* \geq 0$ and $X_{b,s}^* \geq 0$.

When the biodegradable particulate substrate is zero ($X_{s,s}^* = 0$), we have

$$\frac{dX_{s,s}^*}{dt^*}\Big|_{X_{s,s}^*=0} = \frac{DV^*}{\tau^*}X_s^* + (1-\alpha-f_{p,s})\gamma_b^* X_{b,s}^* \geq 0,$$

as by assumption $X_s^* \geq 0$, $X_{b,s}^* \geq 0$ and $1-\alpha-f_{p,s}>0$ from (3.2).

B.2 Physically Meaningful Solutions

The no-washout branch is physically meaningful only when the substrate and cell-mass concentrations are positive ($S^*_{nw} \geq 0$ and $X^*_{b,nw} \geq 0$).

First of all we investigate the condition for the substrate concentration to be positive, i.e.

$$S^*_{nw} = \frac{(1 - R^* + k^*_d\tau^*)P + D\gamma^*_b\tau^*}{[R^* - 1 + (1 - k^*_d)\tau^*]P - D\gamma^*_b\tau^*} > 0.$$

This requires the denominator to be positive

$$[R^* - 1 + (1 - k^*_d)\tau^*]P - D\gamma^*_b\tau^* > 0, \tag{B.1}$$

where

$$P = DV^* + \gamma^*_b\tau^*.$$

We obtain a quadratic inequality

$$\begin{aligned} Q_{S_{nw}}(\tau^*) &= a\tau^{2*} + b\tau^* + c > 0, \quad \text{where} \\ a_{Q_{S_{nw}}} &= (1 - k^*_d)\gamma^*_b > 0, \\ b_{Q_{S_{nw}}} &= (R^* - 1 - D)\gamma^*_b + (1 - k^*_d)DV^*, \\ c_{Q_{S_{nw}}} &= (R^* - 1)DV^* < 0. \end{aligned} \tag{B.2}$$

If we have

$$Q_{S_{nw}}(0) = c < 0.$$

The coefficient $a_{Q_{S_{nw}}}>0$. Therefore, the quadratic equation has solutions τ_-^* and τ_+^* with $\tau_-^*<0<\tau_+^*$.

The solution τ_+^* is given by

$$\tau_+^* = \frac{-b_{Q_{S_{nw}}} + \sqrt{{b_{Q_{S_{nw}}}}^2 - 4a_{Q_{S_{nw}}} c_{Q_{S_{nw}}}}}{2a_{Q_{S_{nw}}}} = 1.1664. \tag{B.3}$$

Figure B.1 shows a sketch of $Q_{S_{nw}}(\tau^*)$. The no washout solution is physically meaningful when $\tau^*>\tau_+^*$.

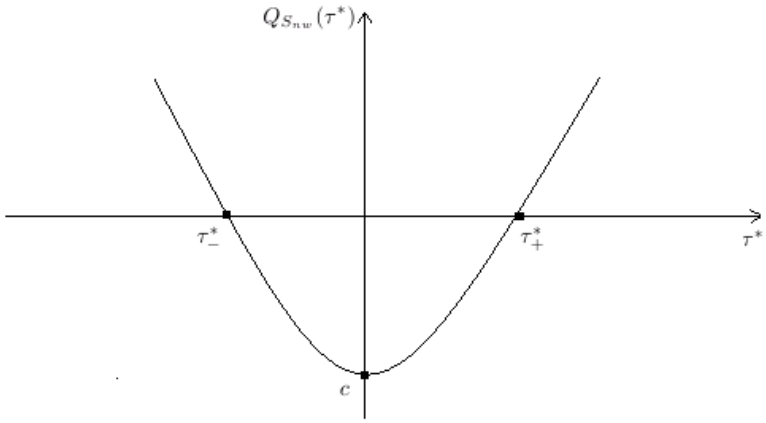

Figure B.1: Sketch of the quadratic equation $Q_{S_{nw}}(\tau^*)$.

Now we investigate the condition for the biomass concentration to be positive, i.e.

$$X_{\mathrm{b,nw}}^* = \frac{-U}{N}>0,$$

where the coefficients are

$$A = H\alpha_{\mathrm{g,h}}k_h^*>0,$$

$$B = P(1-R^*+k_d^*\tau^*) + D\gamma_{\mathrm{b}}^*\tau^*>0,$$

$$C = H(1-R^*+k_h^*\tau^*) + D\alpha\gamma_{\mathrm{s}}^*\tau^*>0,$$

$$E = P(R^*-1-(k_d^*-1)\tau^*) - D\gamma_{\mathrm{b}}^*\tau^*>0 \quad \text{provided} \quad \tau^*>\frac{P(1-R^*)}{(1-k_d^*)P - D\gamma_{\mathrm{b}}^*},$$

$$F = G(1 - R^*) + D\gamma_{\rm i}^*\beta_{\rm i}\tau^* > 0,$$

$$G = DV^* + \beta_i\gamma_i^*\tau^* > 0,$$

$$H = DV^* + \alpha\gamma_s^*\tau^* > 0,$$

$$J = (1 - \alpha - f_{\rm p,s})D^2V^*\gamma_{\rm b}^*\tau^* > 0 \quad \text{from (3.2)},$$

$$K = \{DV^*[f_{\rm i}k_d^*(\gamma_{\rm b}^*\tau^* + G) + Df_{\rm p,s}\gamma_{\rm b}^*] + f_{\rm i}k_d^*\gamma_{\rm b}^*\gamma_{\rm i}^*\beta_{\rm i}\tau^{*2}\}\tau^* > 0,$$

$$L = (1 - \alpha - f_{\rm p,s})\alpha_{\rm g,h}\gamma_{\rm s}^*\tau^* > 0,$$

$$M = \alpha_{\rm g,SDU}\gamma_{\rm i}^*\beta_{\rm i}f_{\rm p,s}\tau^* > 0,$$

$$P = DV^* + \gamma_b^*\tau^* > 0,$$

$$N = \frac{1}{CP}\left\{\frac{N1}{FGH} + \frac{N2}{\tau^*}\right\},$$

$$N1 = D\alpha\{[C\gamma_b^*(H(G\alpha_{g,s} + M) + GL) + GJ\alpha_{g,h}\gamma_s^*]F + CHK\alpha_{\rm g,SDU}\gamma_i^*\beta_i\},$$

$$N2 = \tau^*[J\alpha_{g,h}k_h^* + CPf_s\alpha_{g,s}k_d^*] - BC,$$

$$U = U1 + U2 + U3,$$

$$U1 = \frac{S_0^*E - B}{E\tau^*},$$

$$U2 = D\alpha\left(\frac{\alpha_{g,h}\gamma_s^*X_{s,0}^*}{C} + \frac{\alpha_{\rm g,SDU}\gamma_i^*\beta_iX_{i,0}^*}{F}\right),$$

$$U3 = \frac{H\alpha_{g,h}k_h^*X_{s,0}^*}{C}.$$

For the default values we have

$$X_{\rm b,nw}^*(\tau^*) = \frac{18.39584532\tau^{*2} - 21.13355289\tau^* - 1.170312500}{(0.000513145\tau^{*2} + 0.007915129\tau^* + 0.001562500)(\tau^*233 - 250)},$$

The roots of the denominator are when

$$\tau^* = 1.201759685 \quad \text{and} - 0.05293762629.$$

Thus when $\tau^* > 1.201759685$ the numerator is positive. The denominator is positive when $\tau^* > 1.0730$.

Thus the biomass concentration is physically meaningful numerically when τ^*>1.2018. We found that the soluble substrate is physically meaningful when τ^*>1.1664 and the biomass is physically meaningful when τ^*>1.2018. Thus for the default parameter values the no-washout solution is physically meaningful in chapter 3 for τ^*>1.2018. Using the default values we showed that the washout and the no-washout solution branches have a zero eigenvalue in equations (3.76) and (3.79) when τ^*=1.2018. We further showed that the soluble substrate concentration along the washout branch in equation (3.49) is equal to the soluble substrate concentration along the no-washout branch in equation (3.62) when τ^*=1.2018.

These calculations all confirm that the solutions are physically meaningful when τ^*>1.2018.

This all suggests that the critical condition for the no-washout branch to be physically meaningful is $X^*_{\text{b,nw}}$>0. However, the expression for $X^*_{\text{b,nw}}$ is too complicated to establish this analytically.

B.3 Values of parameters

Typical parameter values are [23]: $K_s = 5,190$ mg COD L^{-1}, $S_0 = 10,360$ mg COD L^{-1}, $X_{i,0} = 2,810$ mg VSS L^{-1}, $X_{s,0} = 22,590$ mg VSS L^{-1}, $f_s = 0.8$ g VSS (g VSS)$^{-1}$, $k_d = 0.015$ day^{-1}, $k_h = 1.1$ day^{-1}, $\alpha_g = 0.03$ mg VSS (mg COD)$^{-1}$, $\alpha_h = 1.88$ mg COD (mg VSS)$^{-1}$, $\alpha_S = 1.42$ mg COD (mg VSS)$^{-1}$, $\mu_m = 0.22$ day^{-1}.

Values of the residence time range from $5 - 40$ days.

This gives the following values for the dimensionless parameter groups:

$S^*_0 = 1.996, X^*_{s,0} = 145.0857, X^*_{i,0} = 18.0475, k^*_d = 0.068, k^*_h = 5, \alpha_{g,h} = 0.0564, \alpha_{g,s} = 0.0426,$

$\text{COD}^*_0 = 10.1788, V^* = 1, D = 0.1, \alpha = 0.25, \alpha_{g,SDU} = 0.0426, \beta_i = 0.2, \gamma^*_b = \gamma^*_i = \gamma^*_s = \gamma = 0.1.$

Appendix C

Appendix for Chapter 4 (model two)

C.1 Non-negativity of the solutions

In this section we show that all solution components in the model remain non negative for non-negative initial conditions.

C.1.1 Non-negativity of solutions in the bioreactor

To show that the soluble substrate concentration is non-negative ($0 \leq S^*$), we consider the value for the derivative $\frac{dS^*}{dt^*}$ when $S^* = 0$. We have

$$\frac{dS^*}{dt^*}\Big|_{S^*=0} = \frac{1}{\tau^*}S_0^* + \alpha_g k_h^* X_s^* \geq \frac{1}{\tau^*}S_0^* > 0,$$

as by assumption $0 \leq S^*$ and $0 \leq X_s^*$.

Thus the derivative is strictly positive. This means that if $S^* = 0$ then S^* is increasing, so it can not become negative.

We now consider what happens when the biomass concentration is zero ($X_b^* = 0$).

We have

$$\frac{dX_b^*}{dt^*}\Big|_{X_b^*=0} = \frac{1}{\tau^*}X_{b,0}^* \geq 0,$$

as by assumption $X_{b,0}^* \geq 0$. This means that $X_b^* \geq 0$. Note that if $X_{b,0}^*>0$ then

$$\frac{dX_b^*}{dt^*}\Big|_{X_b^*=0} = \frac{1}{\tau^*}X_{b,0}^*>0,$$

if $X_{b,0}^* = 0$ then

$$\frac{dX_b^*}{dt^*}\Big|_{X_b^*=0} = 0.$$

In the latter case the plane $X_b^*=0$ is invariant.

When the slowly biodegradable particulates concentration is zero ($X_s^* = 0$), we have

$$\frac{dX_s^*}{dt^*}\Big|_{X_s^*=0} = \frac{1}{\tau^*}X_{s,0}^* + (1-f_p)k_d^*X_b^* \geq 0,$$

as by assumption $X_{s,0}^* \geq 0$ and $X_b^* \geq 0$.

When the non-biodegradable particulates concentration is zero ($X_p^* = 0$), we have

$$\frac{dX_p^*}{dt^*}\Big|_{X_p^*=0} = \frac{1}{\tau^*}X_{p,0}^* + f_pk_d^*X_b^* \geq 0,$$

as by assumption $X_{p,0}^* \geq 0$ and $X_b^* \geq 0$.

When the particulate inert material is zero ($X_i^* = 0$), we have

$$\frac{dX_i^*}{dt^*}\Big|_{X_i^*=0} = \frac{1}{\tau^*}X_{i,0}^* \geq 0,$$

as by assumption $X_{i,0}^* \geq 0$. This means that $X_i^* \geq 0$. Note that if $X_{i,0}^*>0$ then

$$\frac{dX_i^*}{dt^*}\Big|_{X_i^*=0} = \frac{1}{\tau^*}X_{i,0}^*>0,$$

if $X^*_{i,0} = 0$ then

$$\left.\frac{dX^*_i}{dt^*}\right|_{X^*_i=0} = 0.$$

In the latter case the plane X^*_i=0 is invariant.

C.2 Global stability of the washout solution

C.2.1 The case $R^* = 0$

In this section we show that when $R^* = 0$ there is a critical value $k^*_{\mathrm{d,cr}}$<1, such that if $k^*_d \geq k^*_{\mathrm{d,cr}}$ then $\lim_{\tau^*\to\infty} X^*_b = 0$.

We first show that the value of the composite variable $(S^* + X^*_b + X^*_s)$ is bounded.

Let

$$Z^* = S^* + X^*_b + X^*_s.$$

Then

$$\begin{aligned}
\frac{dZ^*}{dt^*} &= \frac{dS^*}{dt^*} + \frac{dX^*_b}{dt^*} + \frac{dX^*_s}{dt^*}, \\
&= \frac{1}{\tau^*}(S^*_0 + X^*_{b,0} + X^*_{s,0} - Z^*) + (\alpha_g - 1)k^*_h X^*_s - f_P k^*_d X^*_b, \\
&= \frac{1}{\tau^*}(S^*_0 + X^*_{b,0} + X^*_{s,0} - Z^*) - ((1-\alpha_g)k^*_h X^*_s + f_P k^*_d X^*_b), \\
&\leq \frac{1}{\tau^*}(S^*_0 + X^*_{b,0} + X^*_{s,0} - Z^*) \quad \text{as } \alpha_g \leq 1.
\end{aligned}$$

Solving the equation we have

$$Z^* \leq \frac{B}{A} + e^{-At^*}\left(Z_0 - \frac{B}{A}\right),$$

where $A = \frac{1}{\tau^*}$ and $B = \frac{S_0^* + X_{s,0}^* + X_{b,0}^*}{\tau^*}$.

By taking $\lim_{\tau^* \to \infty}$ we deduce that

$$\begin{aligned} 0 \leq & Z^* \leq \frac{B}{A}, \\ & \leq S_0^* + X_{s,0}^* + X_{b,0}^*. \end{aligned}$$

We assume that $X_{b,0}^* = 0$. So

$$\begin{aligned} Z^* &\leq S_0^* + X_{s,0}^*, \\ \Rightarrow S^* + X_b^* + X_s^* &\leq S_0^* + X_{s,0}^*. \end{aligned}$$

In particular

$$S^* \leq S_0^* + X_{s,0}^*. \tag{C.1}$$

This gives the bound

$$\frac{S^*}{1+S^*} \leq \frac{S_0^* + X_{s,0}^*}{1 + S_0^* + X_{s,0}^*}.$$

We now consider the biomass equation.

$$\frac{dX_b^*}{dt^*} = \left[\frac{-1}{\tau^*} + \frac{S^*}{1+S^*} - k_d^*\right] X_b^*.$$

From equation (C.1) we have

$$\frac{dX_b^*}{dt^*} \leq \left[\frac{-1}{\tau^*} + \frac{S_0^* + X_{s,0}^*}{1 + S_0^* + X_{s,0}^*} - k_d^*\right] X_b^*,$$

if

$$k_d^* \geq \frac{S_0^* + X_{s,0}^*}{1 + S_0^* + X_{s,0}^*},$$

then $X_b^* \to 0$. From now on we assume that

$$k_d^* < \frac{S_0^* + X_{s,0}^*}{1 + S_0^* + X_{s,0}^*},$$

Consider the values $k_d^* < \frac{S_0^* + \alpha_g X_{s,0}^*}{1 + S_0^* + \alpha_g X_{s,0}^*}$ and $k_{d2}^* < \frac{S_0^* + X_{s,0}^*}{1 + S_0^* + X_{s,0}^*}$, with $0 < \alpha_g \leq 1$.
It follows that $k_d^* < k_{d2}^*$ because $\alpha_g X_{s,0}^* < X_{s,0}^*$.

C.3 When is the no-washout branch physically meaningful

The no-washout branch is physically meaningful only when the substrate and cell-mass concentrations are positive ($S_{\rm nw}^* \geq 0$ and $X_{\rm b,nw}^* \geq 0$). We have

$$\begin{aligned} S_{\rm nw}^* &= \frac{1 - R^* + k_d^* \tau^*}{R^* - 1 + (1 - k_d^*)\,\tau^*}, \\ X_{\rm b,nw}^* &= \frac{(a S_{\rm nw}^{*2} + b S_{\rm nw}^* + c)[R^* - 1 + (1 - k_d^*)\tau^*]}{(a_1 \tau^{*2} + b_1 \tau^* + c_1)\tau^*}, \end{aligned} \tag{C.2}$$

where the coefficients are

$$a = 1 - R^* + k_h^* \tau^* > 0, \tag{C.3}$$

$$b = (1 - R^*)(1 - S_0^*) + (1 - S_0^* - \alpha_g X_{s,0}^*) k_h^* \tau^*, \tag{C.4}$$

$$c = (R^* - 1) S_0^* - (S_0^* + \alpha_g X_{s,0}^*) k_h^* \tau^* < 0, \tag{C.5}$$

$$a_1 = ((1 - f_p)\alpha_g - 1)\, k_h^* k_d^* < 0, \tag{C.6}$$

$$b_1 = (R^* - 1)(k_h^* + k_d^*) < 0, \tag{C.7}$$

$$c_1 = -(1 - R^*)^2 < 0. \tag{C.8}$$

We first investigate the condition for the substrate concentration to be positive, i.e.

$$S^*_{\text{nw}} = \frac{1 - R^* + k^*_d\tau^*}{R^* - 1 + (1 - k^*_d)\tau^*} > 0.$$

This requires the denominator to be positive

$$R^* - 1 + (1 - k^*_d)\tau^* > 0. \tag{C.9}$$

This is true when

$$\tau^* > \tau^*_{\text{pm},1} = \frac{1 - R^*}{1 - k^*_d}, \tag{C.10}$$

where we also require

$$0 < k^*_d < 1. \quad \text{Recall that } (0 \leq R^* < 1).$$

We now investigate the condition for the biomass concentration to be positive. We write the biomass concentration in the form

$$\begin{aligned} X^*_{\text{b,nw}} &= \frac{Q(S^*_{\text{nw}})}{B(\tau^*)} \cdot \frac{A_a}{\tau^*} > 0, \\ A_a &= [R^* - 1 + (1 - k^*_d)\tau^*], \\ B(\tau^*) &= (a_1\tau^{*2} + b_1\tau^* + c_1)\tau^*, \\ Q(S^*_{\text{nw}}) &= aS^{*2}_{\text{nw}} + bS^*_{\text{nw}} + c. \end{aligned}$$

Note that inequality (C.10) establishes that $A_a > 0$.

We now note that from equations (C.6)-(C.8) the coefficients a_1, b_1 and c_1 are all negative. As we need only consider positive values for the residence time ($\tau^* > 0$) we conclude that the quadratic function $B(\tau^*)$ is negative.

Thus the condition for the biomass concentration to be positive is

$$Q(S^*_{\rm nw})<0.$$

We now consider the quadratic function

$$Q(S^*_{\rm nw}) = aS^{*2}_{\rm nw} + bS^*_{\rm nw} + c,$$

where the coefficients are defined in equations (C.3)-(C.5). We have

$$Q(S^*_{\rm nw} = 0) = c<0.$$

As a > 0 the quadratic equation Q has real solutions

$$S^*_{\rm nw} = S^*_{\rm nw,-}<0 \quad \text{and} \quad S^*_{\rm nw} = S^*_{\rm nw,+}>0.$$

As only positive values for $S^*_{\rm nw}$ are physically meaningful, the condition for the biomass concentration to be positive is given by

$$0 \leq S^*_{\rm nw} \leq S^*_{nw,+} = \frac{-b + \sqrt{b^2 - 4ac}}{2a}.$$

Substituting for the steady-state soluble substrate concentration, equation (C.2), we find, after some algebra,

$$X^*_{\rm b,nw} = \frac{-Q(\tau^*)}{B(\tau^*)A_a}>0,$$

where

$$Q(\tau^*) = a_2\tau^{*2} + b_2\tau^* + c_2, \tag{C.11}$$
$$a_2 = [(1 - k^*_d)(S^*_0 + \alpha_g X^*_{s,0}) - k^*_d]k^*_h,$$

$$b_2 = -(1-R^*)[(S_0^* + \alpha_g X_{s,0}^*)k_h^* - (1-k_d^*)S_0^* + k_d^* + k_h^*],$$
$$c_2 = -(1-R^*)^2(1+S_0^*).$$

Note that the polynomial $Q(\tau^*)$ is not identical to the polynomial $Q(S_{\text{nw}}^*)$.

The condition for the biomass concentration to be positive (as $B(\tau^*)<0$) is given by

$$Q(\tau^*) = a_2\tau^{*2} + b_2\tau^* + c_2>0.$$

Note that

$$Q(\tau^* = 0) = c_2<0. \tag{C.12}$$

Note that the quadratic equation $Q(\tau^*)$ defines value of τ^* at which the washout and no-washout branches intersect, compare with equation (4.44).

We have three cases to consider $a_2>0, a_2 = 0$ and $a_2<0$.

C.3.1 Case one $a_2>0$

When $a_2>0$ the quadratic equation has roots $\tau^* = \tau_-^*<0$ and $\tau^* = \tau_+^*>0$. We have not yet considered inequality (C.10).

Calculation shows that

$$Q(\tau^* = \tau_{\text{pm},1}^*) = Q_1 = \frac{(k_d^* - k_h^*)[1 + R^*(R^* - 2)] - (R^* - 1)^2}{(1-k_d^*)^2}.$$

Now

$$Q\left(\tau^* = \frac{1-R^*}{1-k_d^*}\right) = \frac{(1-R^*)^2}{(1-k_d^*)^2}\left[k_d^* - k_h^* - 1\right]<0.$$

(Recall, we can assume that $k_d^*<1$). Thus $\tau_+^*>\tau_{\text{pm},1}^*$.

From this we deduce that

$$0<\tau_{\text{pm},1}^*<\tau_+^*.$$

Thus the no-washout branch is physically meaningful when

$$\tau^* \geq \tau_+^* = \frac{-b_2 + \sqrt{b_2^2 - 4a_2c_2}}{2a_2},$$

$$a_2>0.$$

Note that the term b_1^2 and $-4a_2c_2$ both have a common factor of $(1-R^*)^2$.

Hence

$$\begin{aligned}\tau_+^* &= \frac{-b_2 + (1-R^*)\sqrt{b_2^{*2} - 4a_2c_2^*}}{2a_2}, \\ &= (1-R^*)\left[\frac{b_2^* + \sqrt{b_2^{*2} + 4a_2c_2^*}}{2a_2}\right],\end{aligned}$$

where

$$\begin{aligned}b_2^* &= (1+S_0^*)(k_h^*+k_d^*) + k_h^*\alpha_g X_{s,0}^* - S_0^*, \\ c_2^* &= (1+S_0^*).\end{aligned}$$

Note that

$$\tau_{\text{cr}}^*(R^*=0) = \frac{b_2^* + \sqrt{b_2^{*2} + 4a_2c_2^*}}{2a_2}.$$

Hence

$$\tau_+^* = (1-R^*)\tau_{\text{cr}}^*(R^*=0).$$

The critical value of the residence time is a linearly decreasing function of the effective recycle parameter ($\frac{d\tau_+^*}{dR^*}<0$). It has a minimum value 0 when $R^* = 1$.

Figure C.1 shows a sketch of $Q(\tau^*)$. We now show that $0<\tau_{\mathrm{pm},1}^*<\tau_+^*$.

Hence we have shown for case one that the no washout solution is physically meaningful when $\tau^*>\tau_+^*$ and $a>0$ i.e. when

$$k_d^*<\frac{\mathrm{COD}_{\mathrm{in}}^*}{1+\mathrm{COD}_{\mathrm{in}}^*} = k_{\mathrm{d,cr},\infty}^*.$$

This makes sense because if $k_d^*>k_{\mathrm{d,cr},\infty}^*$ then we have shown that $\lim_{t^*\to\infty} X_b^*(t^*) = 0$.

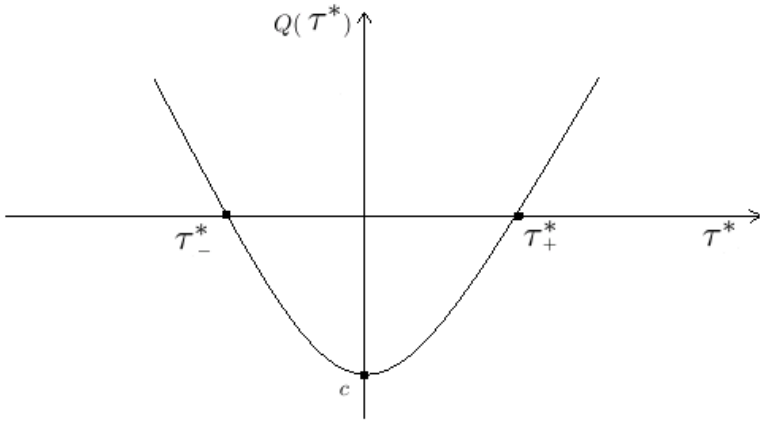

Figure C.1: Sketch of the quadratic equation $Q(\tau^*)$.

Note there is a small gap in our analysis. We have shown in this section that if

$$k_d^*>k_{d2}^* = \frac{S_0^*+X_{s,0}^*}{1+S_0^*+X_{s,0}^*},$$

then the no-washout solution is never physically meaningful. We therefore expect that we have $\lim_{t^*\to\infty} X_b^*(t^*) = 0$.

However, we only showed that the washout solution is globally stable when

$$k_d^*>k_{\mathrm{d,cr},\infty}^* = \frac{\mathrm{COD}_{\mathrm{in}}^*}{1+\mathrm{COD}_{\mathrm{in}}^*},$$

for the case when there is no recycle.

We now show that the biomass is not physically meaningful if we have cases two and three ($a_2 \leq 0$).

C.3.2 Case two $a_2 = 0$

For a_2 to be equal to zero we must have

$$S_0^* = \frac{k_d^* - (1 - k_d^*)\alpha_g X_{s,0}^*}{1 - k_d^*}. \tag{C.13}$$

This case is only of interest when $S_0^*>0$. This implies that

$$k_d^*>(1 - k_d^*)\alpha_g X_{s,0}^*. \tag{C.14}$$

The coefficient b_2 in equation (C.11) is

$$b_2 = -(1 - R^*)[(S_0^* + \alpha_g X_{s,0}^*)k_h^* - (1 - k_d^*)S_0^* + k_d^* + k_h^*], \tag{C.15}$$

Substituting from (C.13) ($S_0^*(1-k_d^*) = k_d^* - (1-k_d^*)\alpha_g X_{s,0}^*$) into (C.15) we find that

$$b_2 = -(1 - R^*)\left[(1 - k_d^*)\alpha_g X_{s,0}^* + (S_0^* + \alpha_g X_{s,0}^* + 1)k_h^*\right] <0.$$

When $a_2 = 0$ the quadratic $Q(\tau^*)$, equation (C.11), becomes a linear function.

$$Q(\tau^*) = b_2\tau^* + c_2>0. \tag{C.16}$$

As $b_2<0$ and $c_2<0$ this gives

$$\tau^*<\frac{-c_2}{b_2}<0.$$

As a result, when $a_2 = 0$ the no washout solution is never physically meaningful because the residence time (τ^*) has to be negative.

C.3.3 Case three $a_2<0$

In this case we have

$$S_0^*(1-k_d^*)<k_d^*-(1-k_d^*)\alpha_g X_{s,0}^*. \tag{C.17}$$

From equation (C.15) we have

$$b_2=(1-R^*)\left[S_0^*(1-k_d^*)-S_0^*k_h^*-\alpha_g X_{s,0}^*k_h^*-k_d^*-k_h^*\right].$$

Using equation (C.17) this gives

$$b_2<-(1-R^*)\left[(1-k_d^*)\alpha_g X_{s,0}^*+(S_0^*+\alpha_g X_{s,0}^*+1)k_h^*\right]<0.$$

There are two sub-cases to consider depending upon the sign of the discriminant $b_2^2-4a_2q_0$. If $(b_2^2-4a_2q_0<0)$, then inequality (C.11) is never satisfied as $Q(\tau^*)<0 \quad (\forall\tau^*)$. (Recall that $Q(0)<0$.)

Consequently $X_{b,nw}^*$ is never physically meaningful. If the discriminant is positive $(b_2^2-4a_2q_0>0)$, then equation (C.12) has two roots with $\tau_+^*<\tau_-^*<0$ (as $a_2<0$ and $b_2<0$). Hence, $X_{b,nw}^*$ is not physically meaningful for $\tau^*>0$. This means that when $a_2<0$ the no washout solution is never physically meaningful.

C.3.4 Summary

We conclude that the no-washout solution branch is only physically meaningful when the decay coefficient is sufficiently small

$$k_d^* < \frac{S_0^* + \alpha_g X_{s,0}^*}{S_0^* + \alpha_g X_{s,0}^* + 1} = \frac{\mathrm{COD}_{\mathrm{in}}^*}{1 + \mathrm{COD}_{\mathrm{in}}^*},$$

and the residence time is sufficiently large

$$\tau^* > \tau_+^* = (1 - R^*) \left[\frac{b_2^* + \sqrt{b_2^{*2} + 4a_2 c_2^*}}{2a_2} \right] > 0.$$

C.4 Values of parameters

Typical dimensional parameter values are [103]. Note that: $|S|$ = mg CODL^{-1}. K_s=5,190 $|S|$, S_0=10,360 $|S|$, $X_{b,0}$=0 $|S|$, $X_{i,0}$=3 $|S|$, $X_{p,0}$=0 $|S|$, $X_{s,0}$=42,469.20 $|S|$, f_p=0.08, k_d=0.015, k_h=1.1 day^{-1}, α_g=0.67, μ_m=0.22 day^{-1}.

The dimensionless parameter values are: S_0^*=1.9961, $X_{b,0}^*$=0, $X_{i,0}^*$=0.0009, $X_{p,0}^*$=0, $X_{s,0}^*$=12.2133, f_p=0.08, k_d^*=0.0682, k_h^*=5.

References

[1] F. Ahmad, A.T Jameel, M.H. Kamarudin, and M. Mel. Study of growth kinetic and modeling of ethanol production by saccharomyces cerevisae. *African Journal of Biotechnology*, 10:18842–18846, 2011.

[2] A. Ajbar and K. Alhumaizi. *Dynamics of the chemostat: a bifurcation theory approach*. Chapman and Hall/CRC, Boca Raton, Fla, 2012.

[3] A. Ajbar and Y. AlZeghayer. A fundamental analysis of dynamics of waste biodegradation in aerobic processes. *Asia-Pacific Journal of Chemical Engineering*, 9(3):423–430, 2014.

[4] A.O.M. Alharbi, M.I. Nelson, A.L. Worthy, and H.S. Sidhu. Sludge formation in the activated sludge process: Mathematical analysis. *In Proceedings of the Australian Chemical Engineering Conference*, pages 1–7, 2013. http://ro.uow.edu.au/cgi/viewcontent.cgi?article=2657&context=eispapers.

[5] A.O.M. Alharbi, M.I. Nelson, A.L. Worthy, and H.S. Sidhu. Analysis of an activated sludge model in which dead biomass is recycled into slowly biodegradable particulate substrate. *Asia-Pacific Journal of Chemical Engineering*, 2014.

[6] A.O.M. Alharbi, M.I. Nelson, A.L. Worthy, and H.S. Sidhu. Sludge formation in the activated sludge process: Mathematical analysis. *In Proceedings of the Australian Chemical Engineering Conference*, 2014. http://www.icheme.org/~/media/Documents/Conferences/CHEMECA/Chemeca%202014/

full-papers/1043_Sludge%20Formation%20In%20The%20Activated%20Sludge%20Process-%20Mathematical%20Analysis%20(2).pdf.

[7] A.O.M. Alharbi, M.I. Nelson, A.L. Worthy, and H.S. Sidhu. Sludge formation in the activated sludge process with a sludge disintegration unit. *Australian and New Zealand Industrial and Applied Mathematics Journal*, 55:348–367, 2014. http://journal.austms.org.au/ojs/index.php/ANZIAMJ/article/view/7803.

[8] J. F. Andrews. A mathematical model for the continuous culture of microorganisms utilizing inhibitory substrates. *Biotechnology and Bioengineering*, 10(6):707–723, 1968.

[9] J.F. Andrews. *Dynamics and control of the activated sludge process*, volume 6. Technomic Pub. Co, Lancaster [Pa.] U.S.A., 1992.

[10] L. Arsova. Anaerobic digestion of food waste: Current status, problems and an alternative product. Master thesis, Department of Earth and Environmental Engineering, Columbia University, May 2010. http://www.seas.columbia.edu/earth/wtert/sofos/arsova_thesis.pdf.

[11] Q. Ashraf and O. Galor. Malthusian population dynamics: Theory and evidence. 2008. http://hdl.handle.net/10419/62638S.

[12] E. Baath. Effects of heavy-metals in soil on microbial processes and populations (a review). *Water Air and Soil Pollution*, 47(3-4):335–379, 1989.

[13] N. Bacaer. *A short history of mathematical population dynamics*. London: Springer, 2011.

[14] S.K. Banerji and T.P. Regmi. Biodegradation of the chelator 2,6-pyridine dicarboxylic acid (pda) used for soil metal extraction. *Waste Management*, 18(5):331–338, 1998.

[15] A. Bjorn. Acid phase digestion at Derby STW - context and preliminary optimisation results. *Technical papers, ∧TKINS*. http://www.atkinsglobal.com/~/media/Files/A/Atkins-Global/Attachments/sectors/water/library-docs/technical-papers/acid-phase-digestion-at-derby.pdf.

[16] F. Blumensaat and J. Keller. Modelling of two-stage anaerobic digestion using the IWA anaerobic digestion model no. 1 (adm1). *Water Research*, 39(1):171–183, 2005.

[17] A. Braha and F. Hafner. Use of Monod kinetics on multi-stage bioreactors. *Water Research*, 19(10):1217–1227, 1985.

[18] J.D Bryers. Structured modeling of the anaerobic digestion of biomass particulates. *Biotechnology and Bioengineering*, 27:638–649, 1985.

[19] A.P. Canales and J.L. Poles. Decreased sludge production strategy for domestic wastewater treatment. *Water Science and Technology*, 30(8):97–106, 1994.

[20] I.S. Chang, P. Le Clech, B. Jefferson, and S. Judd. Membrane fouling in membrane bioreactors for wastewater treatment. *Journal of Environmental Engineering*, 128(11):1018–1029, 2002.

[21] K. Cheyns, J. Mertens, J. Diels, E. Smolders, and D. Springael. Monod kinetics rather than a first-order degradation model explains atrazine fate in soil mini-columns: Implications for pesticide fate modelling. *Environmental Pollution*, 158(5):1405–1411, 2010.

[22] J. Chiou and F. Wang. Estimation of monod model parameters by hybrid differential evolution. *Bioprocess and Biosystems Engineering*, 24(2):109–113, 2001.

[23] Y-C. Chung and J.B. Neethling. Viability of anaerobic digester sludge. *Journal of Environmental Engineering*, 116:330–342, 1990.

[24] D.E. Contois. Kinetics of bacterial growth: Relationship between population density and specific growth rate of continuous cultures. *Journal of General Microbiology*, 21:40–50, 1959.

[25] W.A. Coppel. *Stability and asymptotic behavior of differential equations*. Heath, Boston, 1965.

[26] H. Dette, V.B. Melas, A. Pepelyshev, and N. Strigul. Robust and efficient design of experiments for the monod model. *Journal of Theoretical Biology*, 234(4):537–550, 2005.

[27] J.H. Duranda, E.L. Iannottib, J.R. Fischerc, and J.B. Milesa. Modeling, simulating and optimizing the anaerobic digestion of swine manure. *Biological Wastes*, 24:1–15, 1988.

[28] I. Durruty, E. Okada, J.F. Gonzlez, and S.E. Murialdo. Multisubstrate Monod kinetic model for simultaneous degradation of chlorophenol mixtures. *Biotechnology and Bioprocess Engineering*, 16:908–915, 2011.

[29] J.A. Eastman and J.F. Ferguson. Solubilization of particulate organic carbon during the acid phase of anaerobic digestion. *Journal of the Water Pollution Control Federation*, 53:352–366, 1981.

[30] W.W. Eckenfelder and P. Grau. *Activated sludge process design and control: theory and practice*. Technomic Pub. Co, 1992.

[31] E. Egemen, J. Corpening, and N. Nirmalakhandan. Evaluation of an ozonation system for reduced waste sludge generation. *Water Science and Technology*, 44(2-3):445–52, 2001.

[32] P. Elefsiniotis and W.K. Oldham. Substrate degradation patterns in acid-phase anaerobic digestion of municipal primary sludge. *Environmental Technology*, 15(8):741–751, 1994.

[33] E.A. Evans, K.M. Evans, A. Ulrich, S. Ellsworth, and W. Khan. Anaerobic processes. *Water Environment Research*, 82:1235–1287, 2010.

[34] A. Fenu, G. Guglielmi, J. Jimenez, M. Sperandio, D. Saroj, B. Lesjean, C. Brepols, C. Thoeye, and I. Nopens. Activated sludge model (ASM) based modelling of membrane bioreactor (MBR) processes: a critical review with special regard to MBR specificities. *Water Research*, 44:4272–4294, 2010.

[35] J.G. Ferry. Biochemistry of methanogenesis. *Critical Reviews in Biochemistry and Molecular Biology*, 27(6):473–503, 1992.

[36] M.L. Frisk. Multifaceted microbes. *Trends in Biotechnology*, 29:51–52, 2011.

[37] J. Ganczarczyk, M.F. Hamoda, and Hong-Lit Wong. Performance of aerobic digestion at different sludge solid levels and operation patterns. *Water Research*, 14:627–633, 1980.

[38] M. Ghorbani and C. Eskicioglu. Application of the international water association activated sludge models to describe aerobic sludge digestion. *Environmental Technology*, 32:1923–1938, 2012.

[39] C. P. L. Grady Jr and R. E. Roper Jr. A model for the bio-oxidation process which incorporates the viability concept. *Water Research*, 8:471–483, 1974.

[40] A. Guisasola, S. Petzet, J.A. Baeza, J. Carrera, and J. Lafuente. Inorganic carbon limitations on nitrification: Experimental assessment and modelling. *Water Research*, 41(2):277–286, 2007.

[41] H. Guo and L. Chen. Periodic solution of a chemostat model with Monod growth rate and impulsive state feedback control. *Journal of Theoretical Biology*, 260(4):502–509, 2009.

[42] H. Hauduc, L. Rieger, A. Oehmen, M.C.M. van Loosdrecht, Y. Comeau, A. Heduit, P.A. Vanrolleghem, and S. Gillot. Critical review of activated

sludge modeling: state of process knowledge, modeling concepts, and limitations. *Biotechnology and Bioengineering*, 110:24–46, 2013.

[43] M. Henze, International Water Association. Task Group on Mathematical Modelling for Design, and Operation of Biological Wastewater Treatment. *Activated sludge models ASM1, ASM2, ASM2d and ASM3*, volume no. 9. IWA Publ, London, 2000.

[44] K.S. Hogg and J. Ganczarczyk. A performance study of aerobic sludge digestion. *Water Pollution Research*, pages 26–35, 1973.

[45] M. Hondzo and A. Wuest. Do microscopic organisms feel turbulent flows? *Environmental Science & Technology*, 43:764–768, 2009.

[46] Z.A. Irania, F. Yazdian, G. Mohebali, M. Soheili, and M. Mehrnia. Determination of growth kinetic parameters of a desulfurizing bacterium, gordonia alkanivorans RIPI90A. *Iranian Research Institute of Petroleum Industry*, 10:937–942, 2011.

[47] H. Jeswani and S. Mukherji. Degradation of phenolics, nitrogen-heterocyclics and polynuclear aromatic hydrocarbons in a rotating biological contactor. *Bioresource technology*, 111:12–20, 2012.

[48] K. K. Cheyns, J. Mertens, J. Diels, E. Smolders, and D. Springael. A Monod-based model of attached-growth anaerobic fermenter. *Biological Wastes*, 31(4):275–289, 1990.

[49] Y.C. Kim, K.H. Lee, S. Sasaki, K. Hashimoto, K. Ikebukuro, and I. Karube. Photocatalytic sensor for chemical oxygen demand determination based on oxygen electrode. *Analytical chemistry*, 72(14):3379–3382, 2000.

[50] A.R. Konak. Derivation of a generalised monod equation and its application. *Journal of Applied Chemistry and Biotechnology*, 24:453–455, 1974.

[51] A.W. Lawrence. Application of Process Kinetics to Design of Anaerobic Processes. In Pohland.F.G., editor, *Anaerobic Biological Treatment Processes*, volume 105, pages 163–190. American Chemical Society, 1971.

[52] A.W. Lawrence and P.L. McCarty. Unified basis for biological treatment design and operation. *Journal of the Sanitary Engineering Division, the American Society of Civil Engineers*, 96:757–778, 1970.

[53] P. Le-Clech, B. Jefferson, and S.J. Judd. Impact of aeration, solids concentration and membrane characteristics on the hydraulic performance of a membrane bioreactor. *Journal of Membrane Science*, 218(1):117–129, 2003.

[54] C. Liu and Y. Fang. Kinetic modeling of microbiological processes. *Petroleum and Environmental Biotechnology*, 3:e109, 2012.

[55] X. Ma, C. Chen, J. Wen, T. Ming, and W. Cui. Study on Aerobic Process Treat Auto Manufacturing Wastewater. *Advanced Materials Research*, 356-360:1967–1970, 2012.

[56] J. Makinia. *Mathematical modelling and computer simulation of activated sludge systems*. IWA Publishing, London, 2010.

[57] T.R. Malthus. *An essay on the principle of population, as it affects the future improvement of society with remarks on the speculations of Mr. Godwin, M. Condorcet, and other writers*. 1798.

[58] R. M. May. *Stability and complexity in model ecosystems*. Princeton University Press, Princeton, N.J, 1973.

[59] R.M. May. *Stability and complexity in model ecosystems*, volume 6. Princeton University Press, 2001.

[60] F. Mazenc, M. Malisoff, and J. Harmand. Stabilization and robustness analysis for a chemostat model with two species and monod

growth rates via a lyapunov approach. pages 3933–3938. IEEE, 2007. http://ieeexplore.ieee.org.ezproxy.uow.edu.au/ielx5/4433999/4434000/04434316.pdf?tp=&arnumber=4434316&isnumber=4434000.

[61] J.L. McHenry and A.G. Werker. Characterization of bioactivity in treatment wetlands utilising an enzymatic assay. *paper presented at CSCE/EWRI of ASCE Environmental Engineering Conference*, 2002. http://www.researchgate.net/profile/Alan_Werker/publication/228837829_Characterization_of_bioactivity_in_treatment_wetlands_utilising_an_enzymatic_assay/links/0912f50edcf632362a000000.pdf.

[62] J.C. Merchuk and J. A. Asenjot. Communication to the Editor The Monod Equation and Mass Transfer. *Biotechnology and Bioengineering,*, 54:91–94, 1995.

[63] L. Michaelis and M.L. Menten. Die kinetik der invertinwirkung. *Biochemische Zeitschrift*, 49:333–369, 1913.

[64] R. Moletta, D. Verrier, and G. Albagnac. Dynamic modelling of anaerobic digestion. *Water Research*, 20:427–434, 1986.

[65] F.J. Molz, M.A. Widdowson, and L.D. Benefield. Simulation of microbial growth dynamics coupled to nutrient and oxygen transport in porous media. *Water Resources Research*, 22(8):1207–1216, 1986.

[66] J. Monod. The growth of bacterial cultures. *Pasteur Institute, Paris, France*, 1949.

[67] C.J. Moretti, D. Das, B.T. Kistner, H. Gullicks, and Y.T. Hung. *Water*, 3:806–818, 2011.

[68] Y. Muslu. Application of Monod kinetics on cascade reactors-in-series. *Journal of Chemical Technology and Biotechnology*, 75(12):1151–1159, 2000.

[69] M. I. Nelson and E. Balakrishnan. An analysis of an activated sludge process containing a sludge disintegration system. Research Online, 2011.

[70] M.I. Nelson, E. Balakrishnan, and H.S. Sidhu. A fundamental analysis of continuous flow bioreactor and membrane reactor models with Tessier kinetics. *Chemical Engineering Communications*, 199(3):417–433, 2012.

[71] M.I. Nelson, T. Kerr, and X.D. Chen. A fundamental analysis of continuous flow bioreactor and membrane reactor models with death and maintenance included. *Asia Pacific Journal of Chemical Engineering*, 3:70–80, 2008.

[72] M.I. Nelson, T. Nicholls, and N. Hamzah. A biological process subject to non-competitive substrate inhibition in a generalized flow reactor. *The ANZIAM JournaL*, 54(4):273–290, 2013.

[73] M.I. Nelson and T.C.L. Yue. A mathematical analysis of a membrane bioreactor containing a sludge disintegration system. *Asia-Pacific Journal of Chemical Engineering*, 201(10):1384–1403, 2014.

[74] A.N.L. Ng and A.S. Kim. A mini-review of modeling studies on membrane bioreactor (MBR) treatment for municipal wastewaters. *Desalination*, 1:261–281, 2007.

[75] H.Y. Ng, S.W Wong, S.C. Wong, K. Krishnan, S.W. Tiew, W.O. Kwok, K.E. Ooi, Y.L. Wah, and S.L. Ong. Integrated anaerobic and aerobic processes for treatment of municipal wastewater. *Proceedings of the Water Environment Federation*, 2006(9):3205–3216, 2006.

[76] O. Nowak. Optimizing the use of sludge treatment facilities at municipal wwtps. *Journal of Environmental Science and Health, Part A*, 41(9):1807–1817, 2006.

[77] G.C. Okpokwasili and C.O. Nweke. Microbial growth and substrate utilization kinetics. *African Journal of Biotechnology*, 5:305–317, 2005.

[78] D. Orhon, F.G. Babuna, and O. Karahan. *Industrial wastewater treatment by activated sludge*. IWA Conference, London, 2009.

[79] D.W. Ostendorf, T.H. Schoenberg, E.S. Hinlein, and S.C. Long. Monod kinetics for aerobic biodegradation of petroleum hydrocarbons in unsaturated soil microcosms. *Environmental Science and Technology*, 41:2343–2349, 2007.

[80] E.A. Pearson. Kinetics of Biological Treatment. In E.F. Gloyna and W.W. Eckenfelder, editors, *Advances in Water Quality Improvement*, volume 2, pages 381–394. University of Texas Press, Austin, TX, 1968.

[81] G.A. Pimentel, A.V. Wouwer, J Harmand, and A. Rapaport. Design, analysis and validation of a simple dynamic model of a submerged membrane bioreactor. *Water Research*, 70:97–108, 2015.

[82] E.O. Powell. The growth rate of microorganisms as a function of substrate concentration. In E.O. Powell, C.G.T. Evans, R.E. Strange, and D.W. Tempest, editors, *Microbial physiology and continuous culture, third international symposium*, pages 34–36. Her Majesty's Stationery Office, London, 1967.

[83] K.L. Schulze and R.S. Lipe. Relationship between substrate concentration, growth rate, and respiration rate of escherichia coli in continuous culture. *Archives of Microbiology*, 48(1):1–20, 1964.

[84] M.J. Scott and M.N. Jones. The biodegradation of surfactants in the environment. *Biochimica et Biophysica Acta-Biomembranes*, 1508:235–251, 2000.

[85] R. Seviour and P. H. Nielsen. *Microbial Ecology of Activated Sludge*. IWA Publishing, 2010.

[86] I. Simeonov and S. Diop. Stability analysis of some nonlinear anaerobic digestion models. *International Journal Bioautomation*, 14:37–48, 2010.

[87] B. Simstich, C. Beimfohr, and H.Horn. Lab scale experiments using a submerged MBR under thermophilic aerobic conditions for the treatment of paper mill deinking wastewater. *Bioresource Technology*, 122:11–16, 2012.

[88] S. Sirianuntapiboon, P. Phothilangka, and S. Ohmomo. Decolorization of molasses wastewater by a strain no.bp103 of acetogenic bacteria. *Bioresource Technology*, 92:31–39, 2004.

[89] S. Sivaprakasam, S. Mahadevan, and M. Bhattacharya. Biocalorimetric and respirometric studies on metabolic activity of aerobically grown batch culture of pseudomonas aeruginosa. *Biotechnology and Bioprocess Engineering*, 12(4):340–347, 2007.

[90] S. Sleutel, S.D Neve, M.R.P. Roibas, and G. Hofman. The influence of model type and incubation time on the estimation of stable organic carbon in organic materials. *European Journal of Soil Science*, 56:505–514, 2005.

[91] J. Small, M. Nykyri, U. Helin, M.and Hovi, T. Sarlin, and M. Itavaara. Experimental and modelling investigations of the biogeochemistry of gas production from low and intermediate level radioactive waste. *Applied Geochemistry*, 23:1383–1418, 2008.

[92] K. Sniegowski, J. Mertens, J. Diels, E. Smolders, and D. Springael. Inverse modeling of pesticide degradation and pesticide-degrading population size dynamics in a bioremediation system: Parameterizing the monod model. *Chemosphere*, 75:726–731, 2009.

[93] D. Stanescu. Random coefficient differential equation models for monod kinetics. *Discrete and Continuous Dynamical Systems*, 54:719–728, 2009.

[94] S.W. Taylor and P.R. Jaffe. Substrate and biomass transport in a porous medium. *Environmental Technology*, 26:2181–2194, 1990.

[95] A. Tiehm, K. Nickel, and U. Neis. The use of ultrasound to accelerate the anaerobic digestion of sewage sludge. *Water Science and Technology*, 36(11):121–128, 1997.

[96] P. Turchin. *Complex Population Dynamics: A Theoretical/Empirical Synthesis*. Princeton University Press, 2003.

[97] N.V. Valeyev, C. Hundhausen, Y. Umezawa, N.V. Kotov, G. Williams, A. Clop, C. Ainali, C. Ouzounis, S. Tsoka, and F.O. Nestle. A systems model for immune cell interactions unravels the mechanism of inflammation in human skin. *PLoS computational biology*, 6(12):e1001024, 2010.

[98] J.A. Vzquez, M.P. Gonzlez, and M.A. Murado. Substrate inhibition of pediococcus acidilactici by glucose on a waste medium. simulations and experimental results. *Journal of Applied Microbiology*, 37:365–369, 2003.

[99] Y. Wei, V. Houten, R. T, A.R. Borger, D.H. Eikelboom, and Y. Fan. Minimization of excess sludge production for biological wastewater treatment. *Water Research*, 37(18):4453–4467, 2003.

[100] K. Yamamoto, M. Hiasa, T. Mahmood, and T. Matsuo. Direct solid-liquid separation using hollow fiber membrane in an activated sludge aeration tank. *Water Science and Technology*, 21(4-5):43–54, 1989.

[101] C. Yang, J. Samper, J. Molinero, and M. Bonilla. Modelling geochemical and microbial consumption of dissolved oxygen after backfilling a high level radiactive waste repository. *Journal of Contaminant Hydrology*, 93:130–148, 2007.

[102] S. Yoon. Important operational parameters of membrane bioreactor-sludge disintegration (MBR-SD) system for zero excess sludge production. *Water Research*, 37(8):1921–1931, 2003.

[103] S-H Yoon and S. Lee. Critical operational parameters for zero sludge production in biological wastewater treatment processes combined with sludge disintegration. *Water Research*, 39(15):3738–3754, 2005.

[104] M.G. Zenaitis, H. Sandhu, and S.J.B. Duff. Combined biological and ozone treatment of log yard run-off. *Water Research*, 36(8):2053–2061, 2002.

[105] G.D. Zupancic and M. Ros. Aerobic and two-stage anaerobicaerobic sludge digestion with pure oxygen and air aeration. *Bioresource Technology*, 99(1):100–109, 2008.